December 2001 • NREL/TP-500-29955

Technical Report

Unsteady Aerodynamics Experiment Phase VI: Wind Tunnel Test Configurations and Available Data Campaigns

M.M. Hand, D.A. Simms, L.J. Fingersh,
D.W. Jager, J.R. Cotrell, S. Schreck, and
S.M. Larwood

National Renewable Energy Laboratory

1617 Cole Boulevard
Golden, Colorado 80401-3393

NREL is a U.S. Department of Energy Laboratory
Operated by Midwest Research Institute • Battelle • Bechtel

Contract No. DE-AC36-99-GO10337

December 2001 • NREL/TP-500-29955

Unsteady Aerodynamics Experiment Phase VI: Wind Tunnel Test Configurations and Available Data Campaigns

M.M. Hand, D.A. Simms, L.J. Fingersh,
D.W. Jager, J.R. Cotrell, S. Schreck, and
S.M. Larwood

Prepared under Task No. WER1.1110

National Renewable Energy Laboratory

1617 Cole Boulevard
Golden, Colorado 80401-3393

NREL is a U.S. Department of Energy Laboratory
Operated by Midwest Research Institute • Battelle • Bechtel

Contract No. DE-AC36-99-GO10337

NOTICE

Available electronically at http://www.osti.gov/bridge

Available for a processing fee to U.S. Department of Energy
and its contractors, in paper, from:

U.S. Department of Energy
Office of Scientific and Technical Information
P.O. Box 62
Oak Ridge, TN 37831-0062
phone: 865.576.8401
fax: 865.576.5728
email: reports@adonis.osti.gov

Available for sale to the public, in paper, from:

U.S. Department of Commerce
National Technical Information Service
5285 Port Royal Road
Springfield, VA 22161
phone: 800.553.6847
fax: 703.605.6900
email: orders@ntis.fedworld.gov
online ordering: http://www.ntis.gov/ordering.htm

Printed on paper containing at least 50% wastepaper, including 20% postconsumer waste

Table of Contents

Table of Contents iii
List of Tables v
List of Figures vii
Acknowledgements 1
Introduction 2
Wind Tunnel Facility 3
Test Turbine 8
Test Description 13
Sequences B, C, and D: Downwind Baseline (F), Downwind Low Pitch (F), Downwind High Pitch (F) 16
Sequence E: Yaw Releases (P) 16
Sequence F: Downwind High Cone (F) 17
Sequence G: Upwind Teetered (F) 17
Sequences H, I, and J: Upwind Baseline (F), Upwind Low Pitch (F), Upwind High Pitch (F) 17
Sequence K: Step AOA, Probes (P) 17
Sequence L: Step AOA, Parked (P) 18
Sequence M: Transition Fixed (P) 18
Sequence N: Sin AOA, Rotating (P) 19
Sequence O: Sin AOA, Parked (P) 19
Sequence P: Wake Flow Visualization, Upwind (P) 19
Sequence Q: Dynamic Inflow (P) 20
Sequence R: Step AOA, No Probes (P) 20
Sequences S, T, and U: Upwind, No Probes (F); Upwind 2° Pitch (F); Upwind 4° Pitch (F) 21
Sequence V: Tip Plate (F) 21
Sequence W: Extended Blade (F) 22
Sequence X: Elevated RPM (F) 22
Sequence 3: Tower Wake Measure (P) 22
Sequence 4: Static Pressure Calibration (P) 22
Sequence 5: Sweep Wind Speed (F,P) 23
Sequence 6: Shroud Wake Measure (P) 23
Sequence 7: Shroud Operating (P) 23
Sequences 8 and 9: Downwind Sonics (F,P) and Downwind Sonics Parked (P) 23
Instrumentation 25
Atmospheric Conditions 25
Wind Tunnel Flow Speed 25
Pressure Measurements 26
Wind Tunnel Pressure System 26
Five-Hole Probes 27
Static Probe 29
Pressure Taps 29
Pressure Transducer 32
Pressure System Controller (PSC) 34

Structural Measurements 34
Strain Gauges 34
Accelerometers 35
Load Cells 35
Pitch Rate and Generator Power 36
Wind Tunnel Balance System 36
Position Encoders 37
Time 39
Data Acquisition and Reduction Systems 41
PCM System Hardware 41
Calibration Procedures 41
PCM System Software 42
Derived Channels 44
Wind Tunnel Parameters 44
Mensor Differential Pressure Transducer 44
Pressure Measurement Path (or Reference Pressure Correction) 45
Hydrostatic Pressure and Centrifugal Force Corrections 45
Dynamic Pressure 46
Pressure Coefficients 47
Pressure Measurement Considerations 47
Aerodynamic Force Coefficients 51
Estimated Aerodynamic Rotor Loads 53
Flow Angles 55
Yaw Error 57
Teeter Angle 57
Cone Angle 57
Sonic Anemometer Wind Speed 57
Rotation Parameters 57
Loads from Strain Gauge Measurements 58
Wind Tunnel Scale Forces and Moments 59
References 60
Appendix A: Machine Data for Phase VI Turbine 62
Appendix B: Instrumentation, Data Collection, and Data Processing for Phase VI 94
Appendix C: Test Matrix 171
Appendix D: NASA Software Requirements Document 218
Appendix E: NASA Instrumentation and File Format 240
Appendix F: Hydrostatic Correction 253
Appendix G: Wake Measurements: Sequences 8 and 9 260
Appendix H: Field Test 272
Appendix I: Tares for Wind Tunnel Scales 281
Appendix J: Wake Flow Visualization: Sequence P 291
Appendix K: Transition Fixed: Sequence M 294

List of Tables

Table 1. Test Matrix Overview 14
Table 2. Atmospheric Conditions 25
Table 3. Sonic Anemometer Channels 26
Table 4. Wind Tunnel Pressure Measurements 27
Table 5. Five-hole Probe Pressures 28
Table 6. Pressure Tap Channels 31
Table 7. Pressure Tap Chord Locations 31
Table 8. Nominal, Full-scale, Pressure Transducer Measurement Ranges 33
Table 9. Mensor Channels 33
Table 10. Strain Gauge Measurements 34
Table 11. Accelerometer Measurements 35
Table 12. Load Cell Measurements 36
Table 13. Pitch Rate and Generator Power 36
Table 14. Wind Tunnel Balance Forces 37
Table 15. Position Encoder Channels 39
Table 16. Time Channels 40
Table 17. PCM Decoder Board Specifications 41
Table 18. Wind Tunnel Computed Parameters 44
Table 19. Mensor Differential Pressure Transducer Channels 45
Table 20. Dynamic Pressure Measurements 47
Table 21. Aerodynamic Force Coefficients 52
Table 22. Estimated Aerodynamic Rotor Loads 54
Table 23. Five-hole Probe Offset Angles 55
Table 24. Flow Angle Measurements 56
Table 25. Miscellaneous Channels 58
Table 26. Loads from Strain Gauge Measurements 59
Table 27. Forces and Moments from Wind Tunnel Balance System 59
Table A-1. Blade chord and twist distributions 64
Table A-2. Airfoil profile coordinates 65
Table A-3. Wind tunnel profile coefficients from CSU (Re = 300,000) 69
Table A-4. Wind tunnel profile coefficients from CSU (Re = 500,000) 70
Table A-5. Wind tunnel profile coefficients from CSU (Re = 650,000) 71
Table A-6. Wind tunnel profile coefficients from OSU (Re = 750,000) 72
Table A-7. Wind tunnel profile coefficients from OSU (Re = 1,000,000) 73
Table A-8. Wind tunnel profile coefficients from DUT (Re = 1,000,000) 74
Table A-9. Estimated blade structural properties 76
Table A-10. Blade modal frequencies 79
Table A-11. Rotor inertia computation 82
Table A-12. Drivetrain inertia computation 83
Table A-13. Drivetrain damping and damped frequency 85
Table A-14. Drivetrain natural frequency and stiffness 85
Table A-15. Modes for upwind turbine at 0° yaw and 90° azimuth 91
Table A-16. Modes for turbine with blades removed, instrumentation boxes installed 92
Table A-17. Modes for tower mounted to semispan 92
Table B-1. Pressure Tap Chord Locations 138
Table B-2. Applied Load Calibration File Names 160

Table B-3. Pseudo Applied Load Calibration File Names 161
Table B-4. Electronics Path Calibration File Names and Voltage Ranges 162
Table C-1. Sequence B, Downwind Baseline (F), 197 files of 30-second duration 171
Table C-2. Sequence C, Downwind Low Pitch (F), 95 files of 30-second duration 173
Table C-3. Sequence D, Downwind High Pitch (F), 93 files of 30-second duration 175
Table C-4. Sequence E, Yaw Releases (P), 181 files of 30-second duration 177
Table C-5. Sequence F, Downwind High Cone (F), 49 files of 30-second duration 179
Table C-6. Sequence G, Upwind Teetered (F), 160 files of 30-second duration 181
Table C-7. Sequence H, Upwind Baseline (F), 161 files of 30-second duration, 2 files of 6-minute duration 183
Table C-8. Sequence I, Upwind Low Pitch (F), 49 files of 30-second duration, 2 files of 6-minute duration 184
Table C-9. Sequence J, Upwind High Pitch (F), 53 files of 30-second duration, 2 files of 6-minute duration 185
Table C-10. Sequence K, Step AOA, Probes (P), 18 files of varying duration 187
Table C-11. Sequence L, Step AOA Parked (P), 6 files of varying duration 189
Table C-12. Sequence M, Transition Fixed (P), 46 files of 30-second duration, 3 files of 90-second duration 190
Table C-13. Sequence N, Sin AOA, Rotating (P), 121 files of varying duration 192
Table C-14. Sequence O, Sin AOA, Parked (P), 131 files of varying duration 195
Table C-15. Sequence P, Wake Flow Vis. Upwind (P), 19 files of 3-minute duration 199
Table C-16. Sequence Q, Dynamic Inflow (P), 12 files of varying duration 200
Table C-17. Sequence R, Step AOA, No Probes (P), 21 files of varying duration 201
Table C-18. Sequence S, Upwind, No Probes (F), 104 files of 30-second duration, 2 files of 6-minute duration 202
Table C-19. Sequence T, Upwind, 2° Pitch (F), 21 files of 30-second duration 203
Table C-20. Sequence U, Upwind, 4° Pitch (F), 21 files of 30-second duration 204
Table C-21. Sequence V, Tip Plate (F), 21 files of 30-second duration 205
Table C-22. Sequence W, Extended Blade (F), 17 files of 30-second duration 206
Table C-23. Sequence X, Elevated RPM (F), 45 files of 30-second duration 207
Table C-24. Sequence 3, Tower Wake, 39 files of 30-second duration 208
Table C-25. Sequence 4, Static Pressure Calibration (F,P), 31 files of 30-second duration 209
Table C-26. Sequence 5, Sweep Wind Speed, 6 points of 6-minute duration 211
Table C-27. Sequence 6, Shroud Wake, 49 files of 30-second duration 212
Table C-28. Sequence 7, Shroud Operating (P), 26 files of 30-second duration 214
Table C-29. Sequence 8, Downwind Sonics (F,P),153 files of 30-second duration 215
Table C-30. Sequence 9, Sonic Validation (P), 6 files of 30-second duration 216
Table E-1. NASA Channels Other Than Wall Pressures 241
Table E-2. NASA Instrumentation Problems 243
Table E-3. Wall and Ceiling Pressure Port Locations 245
Table G-1. Wake Measurement Literature 261
Table G-2. Example Data File Listing 269
Table G-3. Sonic Anemometer Noise Quantification 270
Table F-1. Hydrostatic Corrections for Various Turbine Configurations 258
Table H-1. Summary of Data Collected and Problems Encountered During Field-Testing 276
Table I-1. Weight Tare Run 031 for Upwind Turbine Configuration, Turntable = 0º 282
Table I-2. Weight Tare Run 032 for Upwind Turbine Configuration, Turntable = 0º 283
Table I-3. Weight Tare Run 033 for Upwind Turbine Configuration, Turntable = 180º 284
Table I-4. Aerodynamic Tare Run 056 with Tower and Nacelle (Blades Removed) 286
Table I-5. Aerodynamic Tare Run 058 with Tower Only 290
Table K-1. Zigzag Tape Radial Range and Thickness 296

List of Figures

Figure 1. NASA Ames Research Center Full-Scale Aerodynamics Complex with close-up view of fan drives and (80 x 120) test section. Note people for scale....3
Figure 2. Wind tunnel scale system *T*-frame and side view of scale system (NFAC 1993) 4
Figure 3. NASA semispan mount and wind turbine tower in 24.4-m x 36.6-m test section....5
Figure 4. Inflow velocity and flow quality measurements upwind of the turbine. Total pressure and static pressure ports are located on walls, ceiling, and floor (obstructed by tower) of wind tunnel. Sonic anemometers were mounted on airfoil-shaped stands....6
Figure 5. Wind tunnel control room. Data acquisition computer, turbine control computer, and video rack shown in foreground....7
Figure 6. Turbine components, 0° cone angle....9
Figure 7. Ground view of hub in downwind, rigid configuration, 3.4° cone angle....10
Figure 8. Drivetrain configuration, top view; drivetrain and yaw drive/brake, side view....11
Figure 9. Blade planform dimensions....12
Figure 10. Gill port atmospheric pressure reference....26
Figure 11. Wind tunnel and wind turbine pressure system diagram (not to scale)....27
Figure 12. Blade-mounted five-hole probe....28
Figure 13. Upwind static probe (Sequence 4 only)....29
Figure 14. Blade surface pressure and five-hole probe locations....30
Figure 15. Frequency response for 0.457-mlong, 0.7874-mm inner diameter pressure tube from Butterfield et al. 1992. (Note linear scale on horizontal axis.)....32
Figure 16. Yaw moment measurement conventions....36
Figure 17. Yaw angle measurement convention....37
Figure 18. Rotor azimuth measurement convention....38
Figure 19. Blade pitch angle measurement convention, 0° at tip....38
Figure 20. Blade flap angle measurement convention....39
Figure 21. Schematic of boom and instrumentation enclosure wake interference....48
Figure 22. Example of blade dynamic pressure measurement affected by boom/box wake interference and 5-hole probe dynamic pressure outside probe measurement range....49
Figure 23. Example of tunnel flow angle exceeding probe range as evidenced with flow angle measurements....50
Figure 24. Region of rotor plane where pressure measurement issues must be considered....51
Figure 25. Aerodynamic force coefficient conventions....53
Figure 26. Local flow angle measurement convention....56
Figure 27. Spanwise flow angle measurement convention....56
Figure 28. Wind tunnel scale measurement conventions....59
Figure A-1. Turbine rotor, 0° cone angle shown (dimensions in meters)....63
Figure A-2. Blade root surface depiction (dimensions in meters)....66
Figure A-3. Blade planform for standard tip or smoke tip....66
Figure A-4. Attachment point at blade tip (r = 4.938 m)....67
Figure A-5. Smoke tip with smoke generator inside....67
Figure A-6. Blade extension (Sequence W)....67
Figure A-7. Tip plate dimensions for chord of 0.143 m (Sequence V)....68
Figure A-8. Tip plates installed (Sequence V)....68
Figure A-9. Cross-section of blade....77
Figure A-10. Section view of pitch shaft mounted in hub....78
Figure A-11. Top view and side view of drive train....80

Figure A-12. Startup test csstart1 82
Figure A-13. Startup test csstart2 83
Figure A-14. Rotor speed decrease during stopping test csstop2 84
Figure A-15. Tower (dimensions in meters) 87
Figure A-16. Tower shroud (Sequences 6 and 7 only) 88
Figure A-17. Rotor lock installed for parked blade sequences L and O 88
Figure A-18. Steel reaction mass suspended from gantry crane 89
Figure A-19. Shaker mounted to steel reaction mass and attached to tower 90
Figure B-1. Top view showing location of sonic anemometers relative to turbine (not shown to scale); turbine is shown in downwind orientation 104
Figure B-2. Front view looking downwind (not shown to scale). Sonic anemometers located 26.5 m upwind of the turbine tower 104
Figure B-3. East sonic anemometer wiring diagram 106
Figure B-4. West sonic anemometer wiring diagram 107
Figure B-5. Teeter link load cell location 109
Figure B-6. Teeter link load cell 109
Figure B-7. Teeter damper load cell locations 111
Figure B-8. Teeter damper load cell cross-sectional view 111
Figure B-9. Yaw moment measurement conventions 112
Figure B-10. Yaw moment load cell location 113
Figure B-11. Blade 1 flap bending strain gauge slope calibration 117
Figure B-12. Root bending gauges, side view 117
Figure B-13. Blade 1 root bending strain gauge configuration 118
Figure B-14. Blade 3 root bending strain gauge configuration 119
Figure B-15. Low-speed shaft strain gauge location (downwind configuration) 121
Figure B-16. Low-speed shaft strain gauge configuration (downwind turbine) 121
Figure B-17. Low-speed shaft strain gauge location within nacelle 122
Figure B-18. Nacelle accelerometer location within nacelle 124
Figure B-19. Blade tip accelerometer configuration 125
Figure B-20. Servo-motor signal diagram 128
Figure B-21. Power enclosure 129
Figure B-22. Blade pitch angle orientation 131
Figure B-23. Azimuth angle encoder 131
Figure B-24. Azimuth angle measurement convention 132
Figure B-25. Yaw angle measurement convention. In positive yaw, the blade advances into the wind at 180° azimuth for both configurations 132
Figure B-26. Blade flap angle encoder location 134
Figure B-27. Blade flap angle encoder close-up view 134
Figure B-28. Blade flap angle convention 135
Figure B-29. Tapered/twisted blade planform 138
Figure B-30. Pneumatic layout 142
Figure B-31. Pressure system diagram 143
Figure B-32. Mensor electrical ports 145
Figure B-33. Pressure system controller (PSC) enclosure 145
Figure B-34. Time code generator 147
Figure B-35. Rotor-based PCM enclosure 155
Figure B-36. Ground-based PCM rack 156
Figure B-37. Signal path from PCM streams to useable data 158
Figure B-38. Production of calibration and header files (calibration procedures are summarized on p. 160) 158
Figure B-39. Data processing flow chart 159

Figure E-1. NASA pressure system. 248
Figure F-1. Ideal representation of reference pressure line hydrostatic correction for pressure transducers within the instrumented blade 254
Figure F-2. Example of measured pressure and pressure corrected for hydrostatic variation obtained with turbine running in zero-wind condition 257
Figure G-1. Propeller wake visualization (Van Dyke 1988) 261
Figure G-2. Full view of UAE turbine and wake measurement tower in (80 x 120) test section 262
Figure G-3. Top view of wake measurement set-up [ft(m)] 263
Figure G-4. Front view of wake measurement set-up 263
Figure G-5. Line drawing of ATI K-probe 264
Figure G-6. Rohn 65GH tower section drawing 265
Figure G-7. Data acquisition schematic 267
Figure G-8. Wake measurement example time series graph 268
Figure H-1. Yaw error angle convention 274
Figure H-2. Barometer wiring diagram 279
Figure H-3. Yaw moment strain gauge configuration with original yaw shaft and brake mechanism 280
Figure J-1. Hollow aluminum blade tip with smoke generating cartridge installed 292
Figure J-2. Typical photo of wake flow visualization taken with digital still camera 293
Figure K-1. Turbine configuration for sequence M 294
Figure K-2. Zigzag turbulator tape geometry 295
Figure K-3. Zigzag tape installed near pressure ports 295

Acknowledgements

The authors would like to express their sincere gratitude to the staff of the 80 x 120-ft wind tunnel at NASA's Ames Research Center. It is through their cooperation and assistance that the data contained in this report was obtained. We thank Steve Nance, Ron York, and Cash Best for precisely controlling the wind tunnel speed. Mike Simundich and Ira Chandler tirelessly collected data with the NASA system. Technical assistance from Alan Wadcock, Wayne Johnson, Pete Zell, Bill Warmbrodt, and Bob Kufeld helped us understand the challenges of converting our field measurement turbine to a wind tunnel model. Thanks also to Bob Kufeld for rotating through our data collection stations to give us a break. Thanks to Janet Beegle and Joe Sacco for coordinating NASA resources. Thanks to David Nishikawa for incorporating last-minute changes to the NASA file format. Art Silva and Ben Bailey kept all the NASA instrumentation operating smoothly. Rob Fong continued to troubleshoot the balance scales until they worked. Thanks also to the crew on the first shift that initiated the walk-through process so that we could maximize our time in the tunnel. We appreciate Romy Montano for resetting the wind tunnel breakers when needed and Rusty Hunt for getting the tunnel ready to run after the motor rewind procedure.

Without our colleagues at the National Renewable Energy Laboratory (NREL), we would never have managed to prepare for the test and transport all the equipment. Jim Adams machined parts as they were designed. Scott Wilde, Andy Meiser, and Garth Johnson were instrumental in preparing the cargo container to hold all of the equipment and the turbine. Thanks also for bringing the turbine home.

Lastly, we are grateful to the visionaries of the wind industry, particularly Sandy Butterfield, whose perseverance and persistence over the past decade resulted in a coveted time slot in this busy wind tunnel. Management support from Mike Robinson was also crucial in the success of this test.

This work was done at the National Renewable Energy Laboratory in support of the U.S. Department of Energy under contract number DC-AC36-98-GO10337.

Introduction

The primary objective of the Unsteady Aerodynamics Experiment (UAE) has been to provide information needed to quantify the full-scale, three-dimensional (3-D) aerodynamic behavior of horizontal-axis wind turbines (HAWT's). Since 1987, this experiment has been conducted by the National Renewable Energy Laboratory (NREL) at the National Wind Technology Center (NWTC) near Golden, Colorado (Butterfield et al. 1992, Simms et al. 1999b, Hand et al. 2001). These field tests, as well as similar tests performed in Europe (Schepers et al. 1997), have shown that wind turbines undergo very complex aerodynamic response phenomena when operating in the field environment. All wind turbine design codes are based on aerodynamic forces derived from steady two-dimensional (2-D) wind tunnel airfoil test results. Field-testing has shown that 3-D effects are prevalent in wind turbine field operation. Additionally, field tests have shown that wind turbines are subjected to highly dynamic load conditions as a result of turbulent inflow and shear across the rotor plane. Separating the effects due to inflow anomalies from the effects due strictly to operation in a 3-D environment was impossible with the field data. However, wind tunnel testing provided this opportunity. The only wind tunnel sizeable enough to accommodate this 10-m-diameter wind turbine is owned and operated by the National Aeronautics and Space Administration (NASA) and is located at the NASA Ames Research Center at Moffett Field, California. This wind tunnel test section is 24.4 m x 36.6 m (80 ft x 120 ft).

The purpose of this wind tunnel test was to acquire accurate quantitative aerodynamic and structural measurements on a wind turbine, geometrically and dynamically representative of full-scale machines, in an environment free from pronounced inflow anomalies. These data will be exploited to develop and validate enhanced engineering models for designing and analyzing advanced wind energy machines. A Science Panel meeting was held by NREL for the purpose of identifying wind tunnel operating conditions that would yield data needed to validate the semiempirical models currently used to simulate the effects of dynamic stall and 3-D responses (Simms et al. 1999a). After completion of the wind tunnel test, another Science Panel meeting was called in which participants modeled specific wind tunnel test configurations. The model predictions were compared with the wind tunnel test measurements (Simms et al. 2001).

The UAE research turbine measures several quantities that provide the type of data required for validation of these semiempirical models. Blade surface pressures, angle-of-attack, and inflow dynamic pressure at five span locations on one blade are the heart of the measurement system. Blade root bending moments, low-speed shaft bending moments, and nacelle yaw moment are recorded, as well as blade tip and nacelle accelerations. Positional measurements, such as nacelle yaw, rotor azimuth, and blade pitch are included. Servo-motors control the blade pitch and nacelle yaw angle with a high degree of accuracy.

This report is intended to familiarize the user with the entire scope of the wind tunnel test and to support the use of these data. Appendix A describes the turbine in detail sufficient for model development. The instrumentation, signal processing, data acquisition, and data processing are presented in Appendix B along with several detailed figures and wiring diagrams. The test matrix as completed is contained in Appendix C. Appendices D and E describe the NASA-supplied instrumentation and data files. The other appendices refer to measurement corrections, corresponding field data, and specific wind tunnel test configurations.

Wind Tunnel Facility

Located in NASA Ames Research Center, the National Full-Scale Aerodynamics Complex shown in Figure 1 began in 1944 with one closed-loop test section of 12.2-m x 24.4-m (40-ft x 80-ft) dimensions. In 1987, a 24.4-m x 36.6-m (80-ft x 120-ft) test section was added. This test section is open loop and, because of its large size, necessitated a substantial increase in the power output capability of the tunnel's fans. Originally, each of the six fans was six-bladed and driven by a 4,500-kW (6,000-horsepower) electric motor. The upgraded system includes six 15-bladed fans, each driven by a 16,800-kW (22,500-horsepower) electric motor for a total electrical power consumption of 106 MW. Variable-speed control of the fans, combined with variable-pitch control of the fan blades, permits precise control of the test-section velocity. Test-section velocities are continuously variable from nearly zero to 50 m/s.

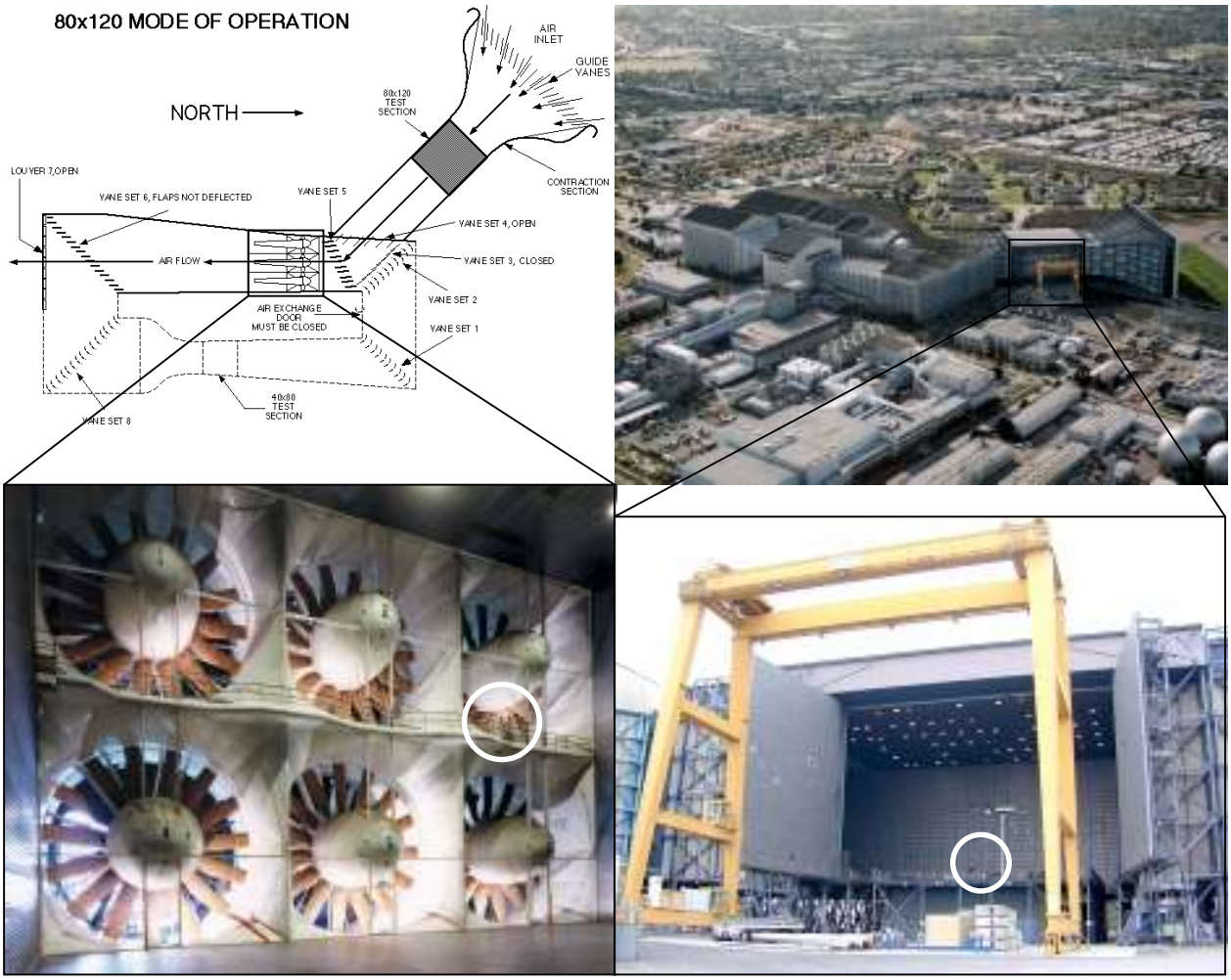

Figure 1. NASA Ames Research Center Full-Scale Aerodynamics Complex with close-up view of fan drives and (80 x 120) test section. Note people for scale.

In the 24.4-m x 36.6-m (80-ft x 120-ft) test section, the wind turbine tower is mounted to a *T*-frame, which is itself supported by the tunnel balance system illustrated in Figure 2 (NFAC 1993). The balance system has seven primary components, four lift elements placed at the corners, two side elements, and one drag element. Together, these elements can be used to resolve the three components of force and the three components of moment applied to the low-speed shaft of the wind turbine. These measurements include aerodynamic drag of the tower because aerodynamic tare coefficients were not applied. The weight of the rotor as a function of yaw angle is also included because weight tare coefficients were not applied. (The necessary equations are included in Appendix D, and the data necessary for development of weight and aero tare coefficients are contained in Appendix I). Note that the struts shown in Figure 2 were not used in the test. Instead, a tower was placed at the center of rotation of the *T*-frame on the NASA semispan mount.

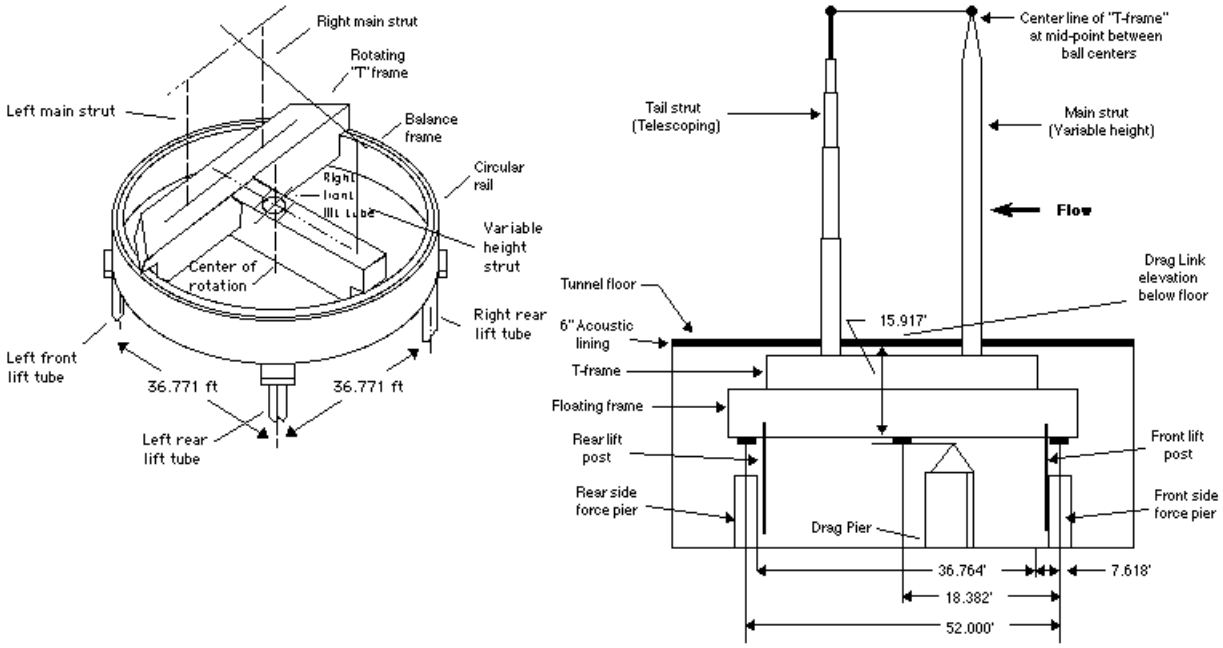

Figure 2. Wind tunnel scale system *T*-frame and side view of scale system (NFAC 1993)

This tower gave the turbine a hub height of 12.2 m, which is the tunnel centerline. The tower, shown in Figure 3, also encloses all of the control, data acquisition, and power cables from the turbine.

Figure 3. NASA semi-span mount and wind turbine tower in 24.4-m x 36.6-m test section

Upwind of the turbine are two systems for measuring the tunnel inflow velocity and quality. The first system is the tunnel Q system, which consists of four total and four static pressure ports (Zell 1993), shown in Figure 4. The four total-pressure ports are connected together pneumatically, as are the four static-pressure ports. Thus, there are only two measurements from this system. The second system is two sonic anemometers (see also Figures B-1 and B-2.). Each anemometer can measure the total velocity at its location with a bandwidth of 10 Hz. Note the positions of three of the four tunnel Q system static and total probes on the left, right, and top of the photo in Figure 4. The fourth set of static- and total-pressure probes is located on the floor of the wind tunnel and is obstructed by the wind turbine tower in the photo.

Figure 4. Inflow velocity and flow quality measurements upwind of the turbine. Total pressure and static pressure ports are located on walls, ceiling, and floor (obstructed by tower) of wind tunnel. Sonic anemometers were mounted on airfoil-shaped stands.

The wind tunnel test-section walls and ceiling are instrumented with pressure taps (Zell 1993). On each of the two walls, 21 pressure taps run longitudinally through the test section at a height of 12.2 m (tunnel centerline) from the tunnel floor. Twenty-one pressure taps in the ceiling run longitudinally through the test section aligned with the tunnel centerline. The precise location of each pressure tap is presented in Appendix E. Pressure transducers measure the pressure at each wall or ceiling tap relative to the outside atmospheric pressure. These data were provided by NASA and are described in Appendix E.

Operation of the turbine inside the test section causes some tunnel blockage. Blockage was quantified by adapting a method described by Glauert (1947) for wind tunnel testing of propellers. This method assumes that the turbine disk is orthogonal to the inflow, and is thus only applicable to unyawed operating conditions. Using this method, turbine blockage was found to be less than 2% for all conditions encountered during these tests and less than 1% for the majority of test conditions (Simms et al. 2001).

To get the cables from the turbine to the various control and data acquisition systems, the cables are passed through the tower to an area under the *T*-frame called the *balance house*. The balance house contains the nonrotating data acquisition system, the power handling electronics, and a

variable-speed drive for controlling turbine speed when other than synchronous speed is required. The power produced by the turbine is also connected to the grid in the balance house. Many of the control and data acquisition wires are passed through the balance house to the control room where the data are recorded and the turbine is controlled, as shown in Figure 5.

The NASA data acquisition system supplemented the time-series data collected with the NREL data acquisition system. Outside wind speed, wind direction, and temperature as well as wind tunnel pressures, temperatures, and scale readings were obtained by the NASA data acquisition system. Statistics over the duration of each NREL test point were provided in ASCII files as described in Appendix E. Several signals from NASA instruments were interfaced with the NREL data acquisition system. This report primarily focuses on the NREL data acquistion system and instrumentation, including the NASA signals incorporated in the NREL system. Appendix E, however, describes the NASA instrumentation, data acquisition system, calibration procedures, and data files for all NASA signals, including those not interfaced with the NREL system.

Figure 5. Wind tunnel control room. Data acquisition computer, turbine control computer, and video rack shown in foreground

Test Turbine

The Unsteady Aerodynamics Experiment test turbine was built from a Grumman Wind Stream-33. Many modifications were made to this turbine prior to the wind tunnel test. The 10-m diameter, stall-regulated turbine with full-span pitch control has a power rating of 20 kW. The turbine used during the wind tunnel test was a two-bladed turbine with twisted and tapered blades and was tested in both upwind and downwind rotor configurations. Figure 6 illustrates the various components of the turbine.

Wind tunnel testing began with the turbine operating in the downwind configuration. The transition to the upwind configuration was performed in one working day. Each blade was detached from the hub, rotated 180°, and reattached to the hub. The blade pitch angle was then recalibrated. The nacelle was rotated 180°, such that the rotor was upwind of the tower and the yaw angle calibration coefficients were adjusted accordingly. Because the blades rotated in the opposite direction with respect to the generator, wires on the generator were reversed to accommodate this. In addition, the blade azimuth-angle calibration coefficients were reversed. Note, however, that the blades rotated in the same direction as that of the downwind configuration with respect to the wind. In other words, the blades rotated counterclockwise as viewed from the inlet of the tunnel for both the upwind and downwind turbine configurations.

The measurement conventions were usually referenced to the wind direction, not the turbine tower. For instance, the blade root flap bending moment is positive due to a force in the downwind direction for both the upwind and downwind turbine configurations. The signs on the slope and offset calibration coefficients were changed from one configuration to another for the teeter link force, blade root bending moments, low-speed shaft torque, blade 3 azimuth, blade flap angles, and the yaw angle.

For Phase V, the NWTC designed and built a two-bladed hub to fit on the Grumman low-speed shaft (LSS) (Cotrell 1999). This hub can be configured in either rigid or teetering mode. A teeter link is used to link both halves of the hub together in the teetering and rigid modes. The teeter link consists of a force sensor, two lengths of hex stock, and two spherical rod ends. The two hex stock lengths are tapped at each end to serve as turnbuckles. Rotating the turnbuckles changes the blade cone angle. Data were collected in both rigid and teetering mode, and cone angles of 0°, 3.4°, and 18° were tested.

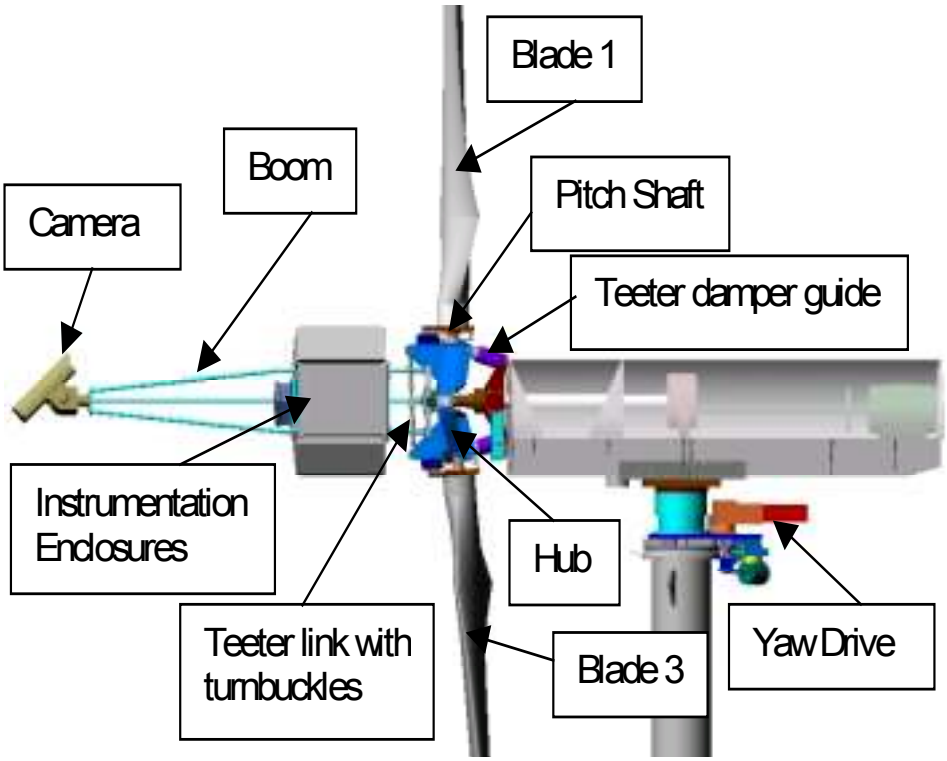

Figure 6. Turbine components, 0° cone angle

In the downwind, teetered configuration, the hub has 9° of free teeter range, or ±4.5° from the nominal 3.4° cone angle. For the upwind, teetered configuration, the free teeter range is ±1.1° from the nominal 0° cone angle. If the free teeter range is exceeded, the teeter dampers absorb the excess teeter energy. Load cells are located inside the teeter guides to record these teeter impact forces. The teeter dampers are Jarret BC1B shock absorbers, which use hydrostatic compression of elastomers.

To configure the turbine for rigid operation, the teeter dampers and guides are removed and replaced with rigid links shown in Figure 7. The links are made from one piece of hex stock, which is tapped at each end to serve as a turnbuckle. The turnbuckle allows pretensioning of the teeter link and removal of any bearing play from the teeter link rod ends. This results in a very rigid hub.

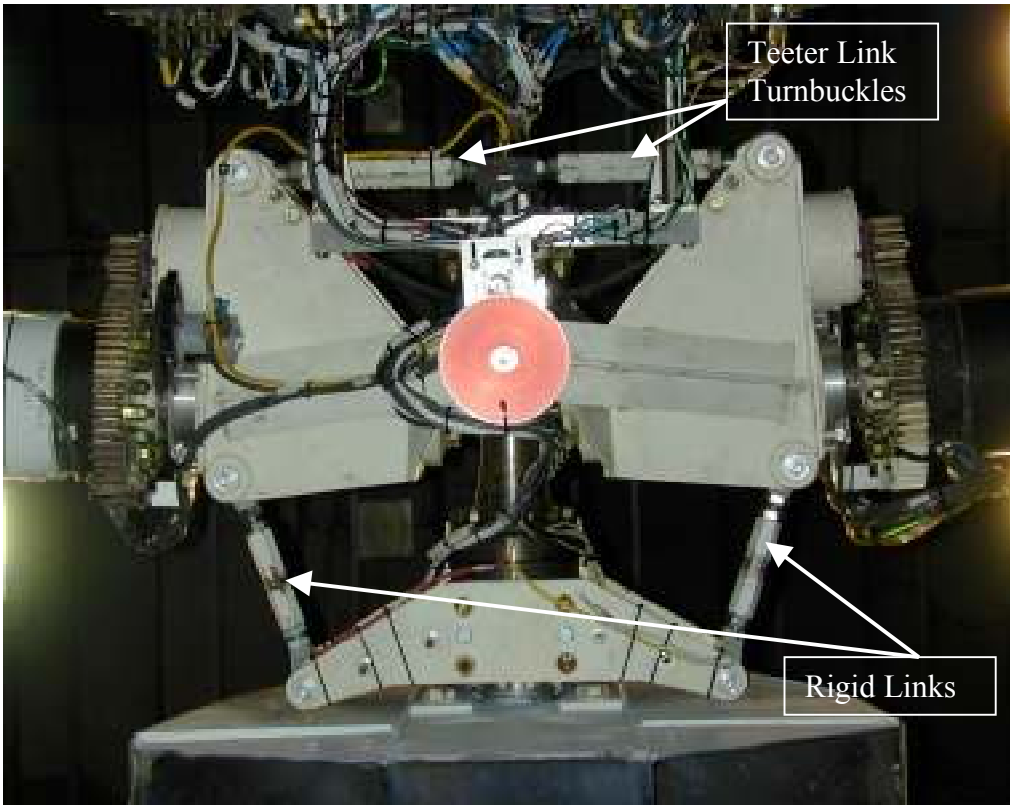

Figure 7. Ground view of hub in downwind, rigid configuration, 3.4° cone angle

The two-bladed hub has full-span pitch capability such that the blades can be pitched independently or collectively. Blade pitch control is achieved using software or an analog controller. Limit switches and hard-stops are used to limit the blade pitch angle from -15° to 95° (90° is feathered into the wind). The servomotors actively control the blades at the specified pitch angle within ±0.1°. Note that blade pitch is defined as the angle between the blade tip chord line and the plane of the turbine disk.

A new yaw support system, yaw drive, and yaw brake were designed and installed for the wind tunnel test. (Field-testing was done using the original yaw system as described in Appendix H). The yaw support system shown in Figure 8 is stronger and stiffer than the previous yaw support assembly. The yaw drive can be computer controlled or manually controlled. The manually operated yaw brake used during field-testing was redesigned. The new yaw brake uses a four-bar mechanism in conjunction with a force sensor to measure yaw moments when the yaw brake is applied. The pneumatic brake held the rotor at specified yaw angles to obtain a variety of yawed operation data points.

The drivetrain, pictured in Figure 8, is similar to the original Grumman configuration. The rotor operates at a nominal 72 RPM. Variable speed operation can also be achieved using power electronics. Low-speed shaft torque is transferred through a 25.13:1 gearbox ratio to the high-speed shaft, which is connected to the 20-kW induction generator. The drivetrain (low-speed shaft, gearbox, and high-speed shaft) inertia was determined using startup tests. An estimate of drivetrain stiffness was also obtained from this test. Data collected during operation of the instrumented turbine provided measurements of the generator slip and total efficiency of the drivetrain. The machine description in Appendix A contains these results.

A hub-mounted rotor lock was designed to obtain data with the instrumented blade parked at the top of the rotational cycle (0°). This was necessary to precisely position the rotor and to prevent damage to the gearbox from high blade loads. The rotor lock is depicted in Appendix A. The rotor brake, located on the high-speed shaft (HSS), was used to lock the rotor for testing at other azimuth positions with blade pitch angles that did not produce excessive loads.

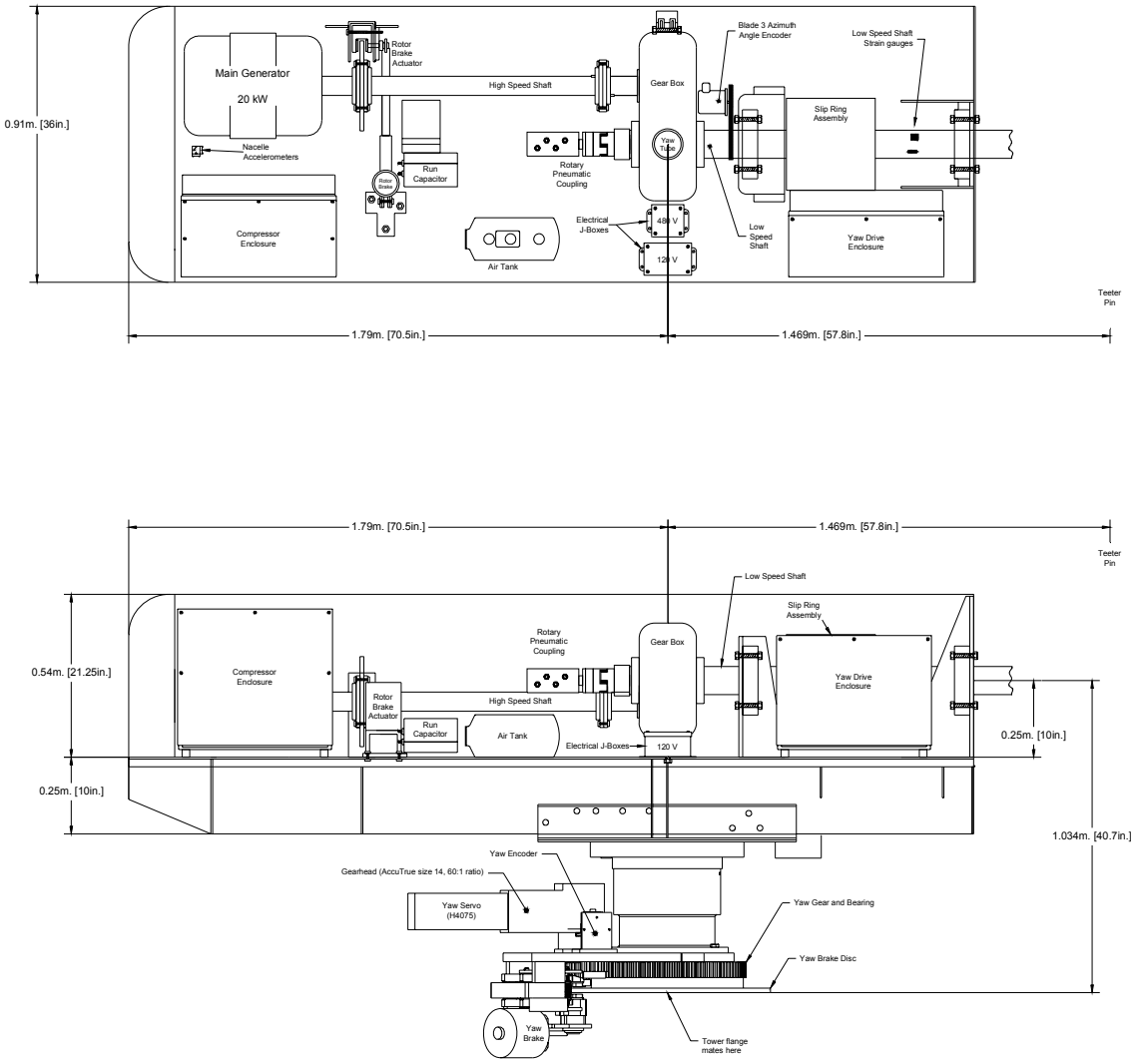

Figure 8. Drivetrain configuration, top view; drivetrain and yaw drive/brake, side view

A new tower was also designed for wind tunnel testing (Figure 3 and Appendix A). The freestanding tubular tower was designed to have the same natural frequency (with the nacelle and rotor mounted to the top) as the guyed tower used during field-testing. The tower was designed to obtain a hub height of 12.2-m (tunnel centerline), rather than the hub height of the turbine in field operation [17.03 m].

The tapered-twisted blades used during the wind tunnel test were designed and fabricated similarly to those used in previous phases of field-testing. The S809 airfoil, developed by Airfoils, Inc., under contract to NREL (Somers 1997) was used exclusively. This airfoil was optimized to improve wind energy power production and is less sensitive to leading edge roughness. The S809 has a well-documented wind tunnel database that includes pressure distributions, separation boundary locations, drag data, and flow-visualization data (Somers 1997, Butterfield et al. 1992). The primary airfoil characteristics are included in Appendix A.

The blade design was optimized on annual energy capture subject to the design constraints imposed for the instrumentation (Giguere and Selig 1999). For example, the blade chord at 80% span was specified to be 0.457 m to correspond to the constant chord blades tested in Phases I–V. Additionally, 80% span is known as the torque weighted equivalent chord location (Gessow and Myers 1967). Thus the peak power level should be the same for all three blade designs used from Phase I through Phase VI. The design process used extensive trade-off studies that considered nonlinear taper and twist, and additional airfoils, and resulted in a blade with linear taper and a nonlinear twist distribution that uses the S809 airfoil from root to tip. The blade dimensions are included in Appendix A and illustrated in Figure 9.

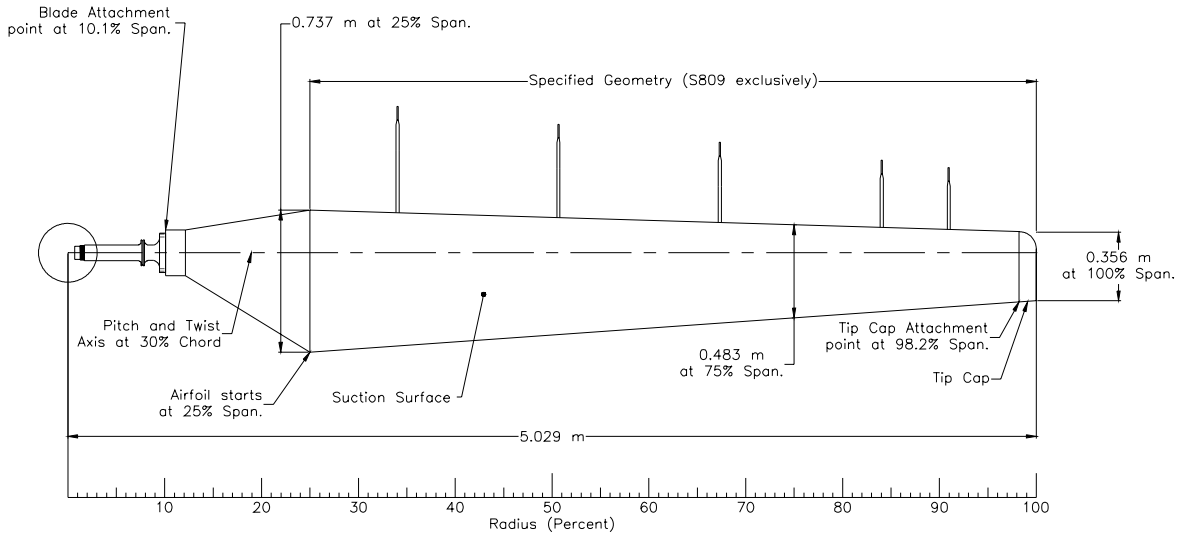

Figure 9. Blade planform dimensions

Additional hardware was designed for specific tests. For tests with the five-hole probes and stalks removed, plugs were inserted in the holes. The plugs matched the leading edge surface of the blade, and plastic tape 0.03 mm thick was used to reduce flow disturbances. Flow visualization required a custom, aluminum tip piece that would contain a smoke generator. This tip weighed more than the standard tip, so it was counterbalanced with additional weight at the tip of the opposite blade. Tip plates similar to those used as aerodynamic brake mechanisms on conventional turbines were attached to the end of each blade for one test. The purpose of this test was to gain an understanding of the tip plate's influence on performance. They were not deployable as are commercial tip plates. A blade extension was designed to attach to the end of the blade, creating an 11-m-diameter rotor. The extension used the S809 airfoil and continued the linear taper of the blade. Lastly, a symmetric airfoil-shaped shroud was installed on the tower during one test. These items are described in further detail in Appendix A.

Test Description

The test matrix was designed to accommodate two investigations of aerodynamic performance. One series of tests was designed to emulate field operation, the other to collect data to explore specific flow phenomena. These are designated by (F) and (P), respectively, in the second column of Table 1. Each test sequence was given a letter or number to differentiate it from the rest. Tests were run in both upwind and downwind turbine configurations as well as rigid and teetered. Some tests were done with the instrumented blade parked at the top of the rotor cycle or behind the tower. The five-hole probes used to measure flow angles and dynamic pressure ahead of the leading edge were installed for most tests, but they were removed for some sequences. Blade extensions, tip plates, and a tower shroud were all installed to fill out the test matrix. Test matrices in Appendix C list each condition under which data were collected for each sequence shown in Table 1.

Sequences not included in Table 1 are A, Y, Z, 1, and 2. Sequence A was used for system validation prior to the actual beginning of the test. It was also used occasionally during the test to check certain parameters. Sequences Y, Z, 1, and 2 were low-priority tests originally specified by Simms et al. (1999a), which were not completed due to time constraints.

Table 1. Test Matrix Overview

Ordinal Number	Test Sequence	Upwind/ Downwind	Rigid/ Teetered	Cone Angle (deg)	Yaw Angle (deg)	Slow Yaw Sweep	Blade Tip Pitch (deg)	Parked/ Rotating	RPM	Blade Press.	Probe Press.	Blade Tip	Day	NASA Run Number
B	Downwind Baseline (F)	Downwind	Teetered	3.4	Locked		3.0	Rotating	72.0	X	X	Baseline	1-4	11-14
C	Downwind Low Pitch (F)	Downwind	Teetered	3.4	Locked		0.0	Rotating	72.0	X	X	Baseline	1-4	11-14
D	Downwind High Pitch (F)	Downwind	Teetered	3.4	Locked		6.0	Rotating	72.0	X	X	Baseline	1-4	11-14
E	Yaw Releases (P)	Downwind	Rigid	3.4	Locked / Free		3.0	Rotating	72.0	X	X	Baseline	5	15, 16
F	Downwind High Cone (F)	Downwind	Rigid	18.0	Locked		3.0	Rotating	72.0	X	X	Baseline	6	17
G	Upwind Teetered (F)	Upwind	Teetered	0.0	Locked		3.0	Rotating	72.0	X	X	Baseline	8-9	34, 38
H	Upwind Baseline (F)	Upwind	Rigid	0.0	Locked	X	3.0	Rotating	72.0	X	X	Baseline	9,11,12,15	39, 41-43, 50
I	Upwind Low Pitch (F)	Upwind	Rigid	0.0	Locked	X	0.0	Rotating	72.0	X	X	Baseline	9,11,12	39, 41-43
J	Upwind High Pitch (F)	Upwind	Rigid	0.0	Locked	X	6.0	Rotating	72.0	X	X	Baseline	9,11,12	39, 41-43
K	Step AOA, Probes (P)	Upwind	Rigid	0.0	Locked at 0		Step & ramp	Rotating	72.0	X	X	Baseline	15	50
L	Step AOA, Parked (P)	Upwind	Rigid	0.0	Locked at 0		Step & ramp	Parked	0.0	X	X	Baseline	13	48
M	Transition Fixed (P)	Upwind	Rigid	0.0	Locked	X	3.0	Rotating	72.0	X		Baseline	16	52
N	Sin AOA, Rotating (P)	Upwind	Rigid	0.0	Locked at 0		Sinusoidal	Rotating	72.0	X	X	Baseline	14,15	49, 50
O	Sin AOA, Parked (P)	Upwind	Rigid	0.0	Locked at 0		Sinusoidal	Parked	0.0	X	X	Baseline	13	44-47
P	Wake Flow Vis. Upwind (P)	Upwind	Rigid	0.0	Locked		3.0, 12.0	Rotating	72.0			Visualize	10,11	40, 41
Q	Dynamic Inflow (P)	Upwind	Rigid	0.0	Locked at 0		Step	Rotating	72.0	X	X	Baseline	15	50
R	Step AOA, No Probes (P)	Upwind	Rigid	0.0	Locked at 0		Step & ramp	Rotating	72.0	X		Baseline	16	52
S	Upwind, No Probes (F)	Upwind	Rigid	0.0	Locked	X	3.0	Rotating	72.0	X		Baseline	16,18	52, 54
T	Upwind, 2 deg Pitch (F)	Upwind	Rigid	0.0	Locked at 0		2.0	Rotating	72.0	X		Baseline	16,18	52, 54
U	Upwind, 4 deg Pitch (F)	Upwind	Rigid	0.0	Locked at 0		4.0	Rotating	72.0	X		Baseline	16,18	52, 54
V	Tip Plate (F)	Upwind	Rigid	0.0	Locked at 0		3.0	Rotating	72.0	X		Plate	18	54
W	Extended Blade (F)	Upwind	Rigid	0.0	Locked at 0		3.0	Rotating	72.0	X		Extended	18	54
X	Elevated RPM (F)	Upwind	Rigid	0.0	Locked at 0		3.0	Rotating	90.0	X		Baseline	19	55
3	Tower Wake Measure (P)	Downwind	Rigid	3.4	Locked		53-79	Parked	0.0	X	X	Baseline	6	18
4	Static Press. Cal (P)	Downwind	Teetered	3.4	Locked at 0		3.0	Rotating	72.0	X	X	Baseline	4	14
5	Sweep Wind Speed (F,P)	Upwind	Rigid	0.0	Locked		3.0, 6.0	Rotating	72.0	X	Both	Baseline	11,19	43, 55
6	Shroud Wake Measure (P)	Downwind	Rigid	3.4	Locked		61-74	Parked	0.0	X	X	Baseline	7	19
7	Shroud Operating (P)	Downwind	Rigid	3.4	Locked		3.0	Rotating	72.0	X	X	Baseline	7	20
8	Downwind Sonics (F,P)	Upwind	Rigid	0.0	Locked		3.0	Rotating	72.0	X		Baseline	17	53
9	Sonic Validation (P)	Upwind	Rigid	0.0	Locked		3.0	Rotating	72.0			Baseline	17	53

(F) - Test conditions representative of field operation

(P) - Test conditions designed to explore specific flow physics phenomena

The test was extremely successful in that almost all data specified by the Science Panel were obtained. Occasionally, some minor problems occurred, these issues are noted in Appendix C in the tables corresponding to the affected sequences. Initially the average of the two, upwind sonic anemometers was used to set the tunnel speed. The wind velocity measured by these anemometers in the inlet contraction zone differed from the speed of the flow in the test section (97.23% of tunnel speed) because of their physical location. During Sequences B, C, and D, the nominal wind speed specified in the file name may not be representative of the actual tunnel speed. The internal software in the sonic anemometers was very sensitive to noise, such that internal settings in the devices were turned on and off sporadically. These errors have been corrected, except for those noted in Appendix C. The 5-hole probe at 67% span was plugged for a portion of Sequence O, and this is noted in Appendix C. The Mensor digital differential pressure transducer was affected by an obstruction in the reference pressure line during part of the test. This was fixed, and all affected points were repeated. In troubleshooting the problem, however, the filter settings were adjusted. These are noted in Table F-1 of Appendix F. The instrumentation malfunctions with the NASA system are noted in Table E-2 in Appendix E and the corresponding sequences in Appendix C.

The tunnel speed usually was set to a specific wind speed by converting the digital measurement of tunnel dynamic pressure and air density to wind speed. For a typical test sequence, a 30-second data point was collected at zero degrees yaw error. This file was processed and various plots and comparisons were made to ensure that all instrumentation was working properly. Meanwhile, the turbine was yawed to various angles as specified in the test matrix, and 30-second data points were collected at each yaw angle. Once all of the off-yaw conditions were collected, a second file at zero degree yaw was obtained. This file was processed, and the statistics were compared with the first point at that condition. If the measured differences were outside of the acceptable error tolerance levels, then all data between the two data sets were considered invalid, and the sequence of tests was repeated. If the differences were within acceptable error tolerances, then the data sets were considered valid. The wind speed was then adjusted for the next series of points, and the process was repeated. Some tests consisted of points with varying duration to accommodate blade pitching sequences, wind speed sweeps, or yaw sweeps. These differences are noted in the following description of each test sequence. During the sequences with special operating conditions, such as blade pitching sequences, data points under standard turbine operating conditions (0° yaw, 3° pitch) were collected to verify the functionality of the instrumentation using the method described above. On occasion, operator errors, instrumentation glitches, and optical disk drive failures required points to be repeated. These points are not contained in Appendix C, but the valid, repeated points are included.

In addition to comparing the statistics of pressure measurements from two points, the drift in calibration coefficients between pressure calibrations was considered. The pressure transducers in the blade are susceptible to temperature fluctuations. For this reason, the turbine was operated with the wind tunnel running at test conditions for at least 30 minutes before pressure calibrations were initiated and data acquisition started. This allowed turbine component temperatures to stabilize, thereby facilitating valid resulting calibrations. Pressure calibrations were repeated approximately every 30 minutes—more frequently after turbine start and less frequently after hours of data collection. The low, high, and zero point of consecutive calibrations of each pressure port were compared automatically with the *drift.exe* program. If the difference between these points exceeded 0.025%, the data collection between calibrations was repeated.

The file naming convention usually consisted of eight characters. The first letter or number specifies the specific turbine configuration according to the sequence listed in Table 1. The

following two digits represent the nominal wind speed in meters per second. The next four digits represent the yaw error angle. For negative yaw error, *M* was used. The last digit represents the numeric sequence of data collection at that specific flow condition with zero indicating the initial data point. For example, the first time the turbine was positioned at 10° yaw, 7 m/s under test configuration H, the file name was H0700100. If this point was repeated, the file name was H0700101. Some test sequences used a different file-naming convention due to the nature of the test. These conventions are explained under the description of each individual test that follows.

All sequences specified the turntable angle to be 0º unless otherwise mentioned. Also, the turbine pressure system was referenced to the outside atmospheric pressure port, the Gill port, which NASA used as a pressure reference unless otherwise mentioned. On a daily basis, both the turbine pressure system and NASA's pressure system were simultaneously checked for leaks by applying and observing a steady pressure at the reference port. Another daily task was zeroing the strain gauges and the Mensor pressure transducer. These procedures are explained in Appendix B.

Sequences B, C, and D: Downwind Baseline (F), Downwind Low Pitch (F), Downwind High Pitch (F)

This test sequence used a downwind, teetered turbine with a 3.4° cone angle. The wind speed ranged from 5 m/s to 25 m/s. Yaw angles of ±180° were achieved at low wind speeds, and yaw angles of -20° to 10° were achieved for high wind speeds. The blade tip pitch was 3° for sequence B, 0° for sequence C, and 6° for sequence D. These three sequences were interleaved during testing because the pitch angle change was easily made by the turbine operator. The rotor rotated at 72 RPM. Blade and probe pressure measurements were collected.

Sequence E: Yaw Releases (P)

This test sequence used a downwind, rigid turbine with a 3.4° cone angle. The wind speeds ranged from 7 m/s to 17 m/s. Initial yaw angles of ±90° were achieved. The blade tip pitch was 3°. The rotor rotated at 72 RPM. Blade and probe pressure measurements were collected. The teeter dampers were replaced with rigid links, and these two channels were flagged as not applicable by setting the measured values in the data file to –99999.99 Nm. The teeter link load cell was pretensioned to 40,000 N. The turbine was positioned at each specified yaw angle. A 30-second data set was collected with the yaw brake engaged. These points used a letter for the last digit beginning with *A* and proceeding through the alphabet as repeat points were needed. These points were plotted and compared to ascertain the functionality of the instrumentation. The files ending in numbers beginning with *0* and increasing with each repetition represent yaw release points.

Once the fixed-position yaw test was complete, the yaw drive was engaged to hold the turbine. The yaw brake was released, and the yaw drive was disabled allowing the turbine to yaw freely. The yaw drive was disabled about 5 seconds into the campaign, and the turbine was allowed to yaw freely for the rest of the 30-second duration. When the yaw drive is disabled, no torque is applied to the motor, and the inertia and yawing force of the nacelle and rotor overcomes the friction and inertia of the yaw gear and motor. The yaw releases were repeated five times at each condition. Four additional campaigns were collected to determine the turbine's natural yaw error by releasing the brake at 0° yaw error. These file names use the *E* designation, followed by two digits for wind speed, followed by XXXX, followed by the repetition digit.

Sequence F: Downwind High Cone (F)

This test sequence used a downwind, rigid turbine with an 18° cone angle. The wind speed ranged from 10 m/s to 20 m/s. Excessive inertial loading due to the high cone angle prevented operation at lower wind speeds. Yaw angles of ±20° were achieved. The blade tip pitch was 3°. The rotor rotated at 72 RPM. Blade and probe pressure measurements were collected. The teeter dampers were replaced with rigid links, and these two channels were flagged as not applicable by setting the measured values in the data file to –99999.99 Nm. The teeter link was replaced with a shorter bar so the load cell was not installed during this test. The teeter link load cell channel, however, was flagged as not applicable by setting the measured values in the data file to -99999.99 N.

Sequence G: Upwind Teetered (F)

Test sequence G used an upwind, teetered turbine with a 0° cone angle. The wind speeds ranged from 5 m/s to 25 m/s. Yaw angles of ±180° were achieved at low wind speeds and angles of ±10° were achieved at the high wind speeds. The blade tip pitch was 3°. The rotor rotated at 72 RPM. Blade and probe pressure measurements were collected.

Sequences H, I, and J: Upwind Baseline (F), Upwind Low Pitch (F), Upwind High Pitch (F)

This test sequence used an upwind, rigid turbine with a 0° cone angle. The wind speed ranged from 5 m/s to 25 m/s. Yaw angles of –30 to 180° were achieved at low wind speeds, and angles of ±10° were achieved for high wind speeds. The blade tip pitch was 3° for sequence H, 0° for sequence I, and 6° for sequence J. These three sequences were interleaved during testing because the pitch angle change was easily made by the turbine operator. The rotor rotated at 72 RPM. Blade and probe pressure measurements were collected. The teeter dampers were replaced with rigid links, and these two channels were flagged as not applicable by setting the measured values in the data file to –99999.99 Nm. The teeter link load cell was pretensioned to 40,000 N.

In addition to the standard 30-second campaigns, yaw sweeps were done at 7 m/s and 10 m/s. These 6-minute campaigns were collected while the yaw drive rotated the turbine 360° at a rate of 1°/s. The file names for these campaigns use the letter designation, followed by two digits for wind speed, followed by YS, followed by 000.

Sequence K: Step AOA, Probes (P)

This sequence was designed to quantify the 3-D blade static angle-of-attack response in the presence of rotational influences by varying the blade pitch angle. Sequence K used an upwind, rigid turbine with a 0° cone angle. The wind speeds ranged from 6 m/s to 20 m/s, and data were collected at yaw angles of 0° and 30°. The rotor rotated at 72 RPM. Blade and probe pressure measurements were collected. The teeter dampers were replaced with rigid links, and these two channels were flagged as not applicable by setting the measured values in the data file to -99999.99 Nm. The teeter link load cell was pretensioned to 40,000 N.

The blade pitch angle ramped continuously at 0.18°/s over a wide range of increasing and decreasing pitch angles. A step sequence was also performed. The blade pitch was stepped 5°, the flow was allowed to stabilize, and the pitch angle was held for 8 seconds. Then the pitch angle

step was repeated. Again, a wide range of pitch angles was obtained, both increasing and decreasing. The file lengths for this sequence varied from 96 seconds to 6 minutes, depending on the pitch angle range. Some short points were collected at 0° yaw and 3° pitch to verify the functionality of the instrumentation. The file name convention used the initial letter *K*, followed by two digits specifying wind speed, followed by two digits for yaw angle, followed by RU, RD, or ST, followed by the repetition digit. The angle of attack motion was differentiated by RU (ramp up), RD (ramp down), and ST (step down then step up). This sequence is related to sequences L and R.

Sequence L: Step AOA, Parked (P)

This sequence was designed to quantify the 3-D blade static angle-of-attack response in the absence of rotational influences by varying the blade pitch angle. This test sequence used an upwind, rigid turbine with a 0° cone angle. Wind speeds of 20 m/s and 30 m/s were used, and all data were collected at a yaw angle of 0°. The rotor was parked with the instrumented blade fixed at 0° azimuth, and the rotor lock was installed (see Appendix A). Blade and probe pressure measurements were collected. The teeter dampers were replaced with rigid links, and these two channels were flagged as not applicable by setting the measured values in the data file to -99999.99 Nm. The teeter link load cell was pretensioned to 40,000 N.

The blade pitch angle ramped continuously at 0.18°/s over a wide range of increasing and decreasing pitch angles. A step sequence was also performed. The blade pitch was stepped 5°, the flow was allowed to stabilize, and the pitch angle was held for 8 seconds. Then the pitch angle step was repeated. Again, a wide range of pitch angles was obtained, both increasing and decreasing. The file lengths for this sequence varied from 5 to 10 minutes, depending on the pitch angle range. The file name convention used the initial letter *L* followed by two digits specifying wind speed, followed by 00 for yaw angle, followed by RU, RD, or ST, followed by the repetition digit. The angle of attack motion was differentiated by RU (ramp up), RD (ramp down), and ST (step down, then step up). This sequence is related to sequences K and R.

Sequence M: Transition Fixed (P)

Test sequence M used an upwind, rigid turbine with a 0° cone angle. The wind speed ranged from 5 m/s to 15 m/s. Yaw angles ranged from 0° to 90°. The blade tip pitch was 3°. The rotor rotated at 72 RPM. Blade pressure measurements were collected. The five-hole probes were removed and the plugs were installed. Plastic tape 0.03 mm thick was used to smooth the interface between the plugs and the blade. The teeter dampers were replaced with rigid links, and these two channels were flagged as not applicable by setting the measured values in the data file to –99999.99 Nm. The teeter link load cell was pretensioned to 40,000 N. During post-processing, the probe channels were set to read –99999.99. Zigzag tape was installed near the leading edge of the instrumented blade on both the upper and lower surfaces as described in Appendix K.

In addition to the standard 30-second campaigns, yaw sweeps were done at 7 m/s and 10 m/s. These 90-second campaigns were collected while the yaw drive rotated the turbine 90° at a rate of 1°/s. The file names for these campaigns use the letter designation, followed by two digits for wind speed, followed by YSU, followed by 00.

Sequence N: Sin AOA, Rotating (P)

This sequence was designed to quantify the blade 3-D unsteady aerodynamic response in the presence of rotational influences by varying blade pitch angle. Test sequence N used an upwind, rigid turbine with a 0° cone angle. The wind speed was 15 m/s, and the yaw angle was 0° throughout the sequence. The rotor rotated at 72 RPM. Blade and probe pressure measurements were collected. The teeter dampers were replaced with rigid links, and these two channels were flagged as not applicable by setting the measured values in the data file to –99999.99 Nm. The teeter link load cell was pretensioned to 40,000 N.

Sinusoidal angle-of-attack histories were designed to emulate 2-D S809 dynamic data obtained at the Ohio State University (OSU) wind tunnel (Reuss Ramsey et al. 1995) and the 1P yawed flow angle-of-attack variations the turbine could be expected to encounter in routine operation. The reduced frequency (K), mean angle-of-attack (α_m), and oscillation amplitude (α_ω) were computed for each of the five primary span locations. The file lengths varied according to the time required to complete 40 oscillations at the specified frequency. The file name convention used the sequence designation N, followed by two digits for the span location (30, 47, 63, 80, or 95), followed by two digits representing the condition specified in the test matrix, followed by the repetition digit. Due to time constraints, most of the test conditions corresponding to the 63% span location were eliminated. In order to ascertain instrumentation fidelity, test points with a static pitch angle of 3° were collected throughout the sequence.

Sequence O: Sin AOA, Parked (P)

This sequence was designed to quantify the blade 3-D unsteady aerodynamic response in the absence of rotational influences by varying blade pitch angle. This test sequence used an upwind, rigid turbine with a 0° cone angle. The wind speed ranged from 18.9 m/s to 39.3 m/s, and the yaw angle was 0° throughout the sequence. The rotor was parked with the instrumented blade fixed at 0° azimuth, and the rotor lock was installed (see Appendix A). Blade and probe pressure measurements were collected. The teeter dampers were replaced with rigid links, and these two channels were flagged as not applicable by setting the measured values in the data file to -99999.99 Nm. The teeter link load cell was pretensioned to 40,000 N.

Sinusoidal angle-of-attack histories were designed to emulate 2-D S809 dynamic data obtained at the OSU wind tunnel (Reuss Ramsey et al. 1995) as well as 1P yawed flow angle-of-attack variations the turbine could be expected to encounter in routine operation. The reduced frequency (K), mean angle-of-attack (α_m), and oscillation amplitude (α_ω) were computed for each of the five primary span locations. The file lengths varied according to the time required to complete 40 oscillations at the specified frequency. The file name convention used the sequence designation O, followed by two digits for the span location (30, 47, 80, or 95), followed by two digits representing the condition specified in the test matrix, followed by the repetition digit. Due to time constraints, the test conditions corresponding to the 63% span location were eliminated. In order to ascertain instrumentation fidelity, test points with a static pitch angle of 3° were collected throughout the sequence.

Sequence P: Wake Flow Visualization, Upwind (P)

This test sequence used an upwind, rigid turbine with a 0° cone angle. The wind speed ranged from 5 m/s to 15 m/s. Yaw angles of 0° to –60° were achieved. The blade tip pitch was 3°. The

rotor rotated at 72 RPM. Blade and probe pressure measurements were collected. The teeter dampers were replaced with rigid links, and these two channels were flagged as not applicable by setting the measured values in the data file to –99999.99 Nm. The teeter link load cell was pretensioned to 40,000 N.

The aluminum blade tip designed to contain a smoke generator was installed, and counterweights were installed in the non-instrumented blade tip to compensate. The turbine was positioned at the appropriate yaw angle, and the smoke generator was ignited remotely. The campaign duration was 3 minutes for all tests except P1000000, which was 2 minutes. The file name convention was the standard format except for P10000A0, which indicated a 3° pitch angle. File P1000000 used a 12° pitch angle. After these two campaigns were collected, it was determined that all subsequent data should be collected with a 3° pitch angle. Pressure data were not acquired during this sequence, so all associated data values were flagged as not applicable by setting the measured values in the data file to 0.000 Pa. Corresponding pressure data are available from Sequence H for the 3° pitch angle test points. Flow visualization data obtained from wall- and ceiling-mounted video cameras were recorded to videotape. The camera locations and calibration procedures are described in Appendix J.

Sequence Q: Dynamic Inflow (P)

This sequence was designed to characterize the dynamic inflow variation using the five-hole probes that extend upwind of the leading edge of the blade. This test sequence used an upwind, rigid turbine with a 0° cone angle. The wind speeds ranged from 5 m/s to 15 m/s, and data were collected at a 0° yaw angle. The rotor rotated at 72 RPM. Blade and probe pressure measurements were collected. The teeter dampers were replaced with rigid links, and these two channels were flagged as not applicable by setting the measured values in the data file to -99999.99 Nm. The teeter link load cell was pretensioned to 40,000 N.

The blade pitch angle was changed from the initial tip pitch angle to the final tip pitch angle at the maximum rate of 67°/s. This angle was maintained for the specified delay time duration. Then the blade was pitched back to the initial pitch angle and held for the specified hold time. This was repeated 20 times. The campaign at 15 m/s was aborted early due to excessive low-speed shaft torque loads. The file length varied depending on the time required to obtain 20 pitch cycles for the specified range of angles. The name convention was the standard format, except for the short campaigns collected to ascertain the functionality of the instrumentation. These points were collected at a 3° pitch angle and use the characters *REF* in the four digits that normally represent yaw angle.

Sequence R: Step AOA, No Probes (P)

This sequence was designed to quantify the effect of the five-hole probes on the 3-D blade static angle-of-attack response in the presence of rotational influences by repeating Sequence K without five-hole probes. This test sequence used an upwind, rigid turbine with a 0° cone angle. The wind speeds ranged from 6 m/s to 20 m/s, and data were collected at yaw angles of 0° and 30°. The rotor rotated at 72 RPM. Blade pressure measurements were collected. The five-hole probes were removed and the plugs were installed. Plastic tape 0.03 mm thick was used to smooth the interface between the plugs and the blade. The teeter dampers were replaced with rigid links, and these two channels were flagged as not applicable by setting the measured values in the data file to –99999.99 Nm. The teeter link load cell was pre-tensioned to 40,000 N. During post-processing, the probe channels were set to read –99999.99.

The blade pitch angle ramped continuously at 0.18°/s over a wide range of increasing and decreasing pitch angles. A step sequence was also performed. The blade pitch was stepped 5°; the flow was allowed to stabilize; and the pitch angle was held for 5 seconds. Then the pitch angle step was repeated. Again, a wide range of pitch angles was obtained, both increasing and decreasing. The file lengths for this sequence varied from 96 seconds to 6 minutes depending on the pitch angle range. Some short points were collected at 0° yaw and 3° pitch to ascertain the functionality of the instrumentation and repeatability over time. The file name convention used the initial letter *R*, followed by two digits specifying wind speed, followed by two digits for yaw angle, followed by RU, RD, or ST, followed by the repetition digit. The angle of attack motion was differentiated by RU (ramp up), RD (ramp down), and ST (step down, then step up). This sequence is related to Sequences K and L.

Sequences S, T, and U: Upwind, No Probes (F); Upwind 2° Pitch (F); Upwind 4° Pitch (F)

This test sequence used an upwind, rigid turbine with a 0° cone angle. The wind speed ranged from 5 m/s to 25 m/s. Yaw angles of 0° to 180° were achieved for Sequence S, but the yaw angle remained at 0° for Sequences T and U. The blade tip pitch was 3° for Sequence S, 2° for Sequence T, and 4° for Sequence U. These three sequences were interleaved during testing because the pitch angle change was easily made by the turbine operator. The rotor rotated at 72 RPM. Blade pressure measurements were collected. The five-hole probes were removed and the plugs were installed. Plastic tape 0.03 mm thick was used to smooth the interface between the plugs and the blade. The teeter dampers were replaced with rigid links, and these two channels were flagged as not applicable by setting the measured values in the data file to -99999.99 Nm. The teeter link load cell was pretensioned to 40,000 N. During post-processing, the probe channels were set to read -99999.99.

In addition to the standard 30-second campaigns, yaw sweeps were done at 7 m/s and 10 m/s for the Sequence S configuration. These 6-minute campaigns were collected while the yaw drive rotated the turbine 360° at a rate of 1°/s. The file names for these campaigns use the letter designation, followed by two digits for wind speed, followed by YSU, followed by 00.

Sequence V: Tip Plate (F)

This test sequence used an upwind, rigid turbine with a 0° cone angle. The wind speed ranged from 5 m/s to 25 m/s, and the yaw angle was held at 0°. The blade pitch angle was 3°. The rotor rotated at 72 RPM. Blade pressure measurements were collected. The five-hole probes were removed and the plugs were installed. Plastic tape 0.03 mm thick was used to smooth the interface between the plugs and the blade. The teeter dampers were replaced with rigid links, and these two channels were flagged as not applicable by setting the measured values in the data file to –99999.99 Nm. The teeter link load cell was pretensioned to 40,000 N. During post-processing, the probe channels were set to read -99999.99. The standard tip blocks were replaced with a tip plate to simulate the effect of an undeployed tip-mounted aerodynamic brake as shown in Appendix A. Note that the blade radius was not changed during post-processing so the pressure tap locations are at the same radial location, but the reference to 30% represents 30% of 5.029 m not 4.943 m. Throughout this report, references to the blade span are made for the 5.029-m radius, not the 4.943-m radius.

Sequence W: Extended Blade (F)

This test sequence used an upwind, rigid turbine with a 0° cone angle. The wind speed ranged from 5 m/s to 21 m/s, and the yaw angle was held at 0°. The blade pitch angle was 3°. The rotor rotated at 72 RPM. Blade pressure measurements were collected. The five-hole probes were removed and the plugs were installed. Plastic tape 0.03 mm thick was used to smooth the interface between the plugs and the blade. The teeter dampers were replaced with rigid links, and these two channels were flagged as not applicable by setting the measured values in the data file to –99999.99 Nm. The teeter link load cell was pretensioned to 40,000 N. During post-processing, the probe channels were set to read –99999.99. The standard tip blocks were replaced with blade extensions that created a 5.532-m radius rotor as shown in Appendix A. The extension used the S809 airfoil throughout, and the linear taper of the blade continued along the extension. Note that the blade radius was not changed during post-processing so the pressure tap locations are at the same radial location, but the reference to 30% represents 30% of 5.029 m not 5.532 m. Throughout this report, references to the blade span are made for the 5.029-m radius, not the 5.532-m radius.

Sequence X: Elevated RPM (F)

This test sequence used an upwind, rigid turbine with a 0° cone angle. The wind speed ranged from 5 m/s to 12 m/s, and yaw angles of ±30° were obtained. The blade pitch angle was 3°. The rotor rotated at 90 RPM. Blade pressure measurements were collected. The five-hole probes were removed and the plugs were installed. Plastic tape 0.03 mm thick was used to smooth the interface between the plugs and the blade. The teeter dampers were replaced with rigid links, and these two channels were flagged as not applicable by setting the measured values in the data file to –99999.99 Nm. The teeter link load cell was pretensioned to 40,000 N. During post-processing, the probe channels were set to read -99999.99. The hydrostatic correction derived for operation at 72 RPM as described in Appendix F was applied to these data.

Sequence 3: Tower Wake Measure (P)

Sequence 3 used a downwind, rigid turbine with a 3.4° cone angle. The wind speeds for this sequence corresponded to subcritical [7 m/s], transitional [15 m/s], and supercritical [20 m/s] Reynolds number regimes for the circular cross-section tower. The yaw angle and blade tip pitch angles were selected to traverse the probe tip across the tower wake, while keeping the probe axis approximately parallel to the tunnel centerline. The rotor was parked with the instrumented blade at 180° azimuth. Blade and probe pressure measurements were collected.

Sequence 4: Static Pressure Calibration (P)

This test sequence used a downwind, teetered turbine with a 3.4° cone angle. The wind speed ranged from 5 m/s to 25 m/s. Yaw angles of 0° to 30° were achieved. The blade tip pitch was 3°. The rotor rotated at 72 RPM. Blade and probe pressure measurements were collected. A static pitot probe was installed on a boom 2.3 m upwind of the nacelle at hub height and connected to the reference side of the Mensor digital differential pressure transducer through the pneumatic rotary coupling. This provided the reference pressure for all blade-mounted pressure transducers, as opposed to the NASA atmospheric pressure reference that was used for all other test sequences. This simulates the pressure system connections used in field measurements where the static pressure was unknown.

Sequence 5: Sweep Wind Speed (F,P)

This test sequence used an upwind, rigid turbine with a 0° cone angle. The wind speed was ramped from 5 m/s to 25 m/s by the wind tunnel operator. This was repeated with a decreasing ramp. The yaw angle was maintained at 0°. The blade tip pitch was 3° or 6°. The rotor rotated at 72 RPM. Blade pressure and probe measurements were collected for both pitch angles. The five-hole probes were removed and the plugs were installed for another 3° pitch case. Plastic tape 0.03 mm thick was used to smooth the interface between the plugs and the blade. The teeter dampers were replaced with rigid links, and these two channels were flagged as not applicable by setting the measured values in the data file to –99999.99 Nm. The teeter link load cell was pretensioned to 40,000 N. During post-processing, the probe channels were set to read -99999.99. The 6-minute campaigns were named using the sequence designation 5, followed by DN or UP, which indicates the wind speed ramp direction. The next four digits are 0000, and the sequence digit is at the end.

Sequence 6: Shroud Wake Measure (P)

This test sequence used a downwind, rigid turbine with a 3.4° cone angle. The wind speeds for this sequence corresponded to subcritical [7 m/s], transitional [15 m/s], and supercritical [20 m/s] Reynolds number regimes for the circular cross-section tower. The yaw angle and blade tip pitch angles were selected to traverse the probe tip across the tower wake while keeping the probe axis approximately parallel to the tunnel centerline. The rotor was parked with the instrumented blade at 180° azimuth. Blade and probe pressure measurements were collected.

An airfoil-shaped aluminum shroud was placed on the tower below the 34% span 5-hole probe. It extended below the 91% span 5-hole probe. The turntable angle was adjusted to position the shroud at various angles relative to the flow.

Sequence 7: Shroud Operating (P)

This test sequence used a downwind, rigid turbine with a 3.4° cone angle. The wind speed ranged from 5 m/s to 25 m/s. Turntable angles from 0° to 30° were achieved, but the yaw error angle was maintained at 0° by adjusting the nacelle yaw. The blade tip pitch was 3°. The rotor rotated at 72 RPM. Blade and probe pressure measurements were collected. The teeter dampers were replaced with rigid links, and these two channels were flagged as not applicable by setting the measured values in the data file to –99999.99 Nm. The teeter link load cell was pretensioned to 40,000 N.

An airfoil-shaped aluminum shroud was placed on the tower below the 34% span 5-hole probe. It extended below the 91% span 5-hole probe. The turntable angle was adjusted to position the shroud at various angles relative to the flow, but the turbine yaw error angle was maintained at 0°. Two additional points were collected where the turntable angle was 0°, and the turbine yaw angle was 20° (71000200) or -20° (710M0200).

Sequences 8 and 9: Downwind Sonics (F,P) and Downwind Sonics Parked (P)

This test sequence used an upwind, rigid turbine with a 0° cone angle. The wind speed ranged from 5 m/s to 25 m/s. Yaw angles of 0° to 60° were achieved. The blade tip pitch was 3°. The rotor rotated at 72 RPM during Sequence 8, but it was parked during Sequence 9. Blade pressure

measurements were collected. The five-hole probes were removed and the plugs were installed. Plastic tape 0.03 mm thick was used to smooth the interface between the plugs and the blade. The teeter dampers were replaced with rigid links, and these two channels were flagged as not applicable by setting the measured values in the data file to –99999.99 Nm. The teeter link load cell was pretensioned to 40,000 N. During post-processing, the probe channels were set to read -99999.99.

Sonic anemometers were mounted on a strut downwind of the turbine. The strut was mounted to the *T*-frame, which was rotated to align the anemometers aft of the 9% and 49% radius locations at hub height. Because of this configuration, the tunnel balance data are considered invalid. Sequence 9 was designed to compare the downwind sonic anemometer readings with the upwind sonic anemometers without interference from the turbine. The rotor was parked with the instrumented blade at 0° azimuth. All pressure measurements obtained in Sequence 9 are invalid because sufficient time for temperature stabilization did not occur, thus all associated data values were flagged as not applicable by setting the measured values in the data file to 0.0000 Pa. This test is further described in Appendix G.

Instrumentation

The NREL data system acquired the time-series measurements for which this test was designed. The NASA data system, however, was used to acquire statistical, corroborating measurements. The NREL data system architecture could only incorporate analog signals provided by NASA, and these signals were incorporated into the NREL data stream as described in this section. NASA used several digital differential pressure transducers with higher resolution and better accuracy than the corresponding analog transducers. Statistical values for all NASA channels, both digital and analog, were supplied by NASA in ASCII files. The description of the NASA data system and file format is included in Appendix E. Further details regarding the NREL instrumentation, calibration procedures, signal conditioning, and filtering are included in Appendix B.

Atmospheric Conditions

The outdoor atmospheric conditions were measured with instrumentation provided by NASA. Wind speed and direction at two elevations were obtained with anemometers mounted on a tower 213.4 m from the tunnel inlet aligned with the tunnel centerline. The outdoor temperature was measured at the base of this met tower. The tunnel air temperature was measured with a device mounted to the center strut in the tunnel inlet at a height that corresponds to the test-section centerline. The dew point temperature was measured with a device mounted to the wind tunnel wall adjacent to the turntable center at a height of 3.048 m. These channels are listed in Table 2.

Table 2. Atmospheric Conditions

Channel	Channel ID	Description	Units
300	OMWS18M	Outside met wind speed 18.29 m	m/s
302	OMWS32M	Outside met wind speed 32.81m	m/s
304	OMWD18M	Outside met wind direction 18.29 m	deg
306	OMWD32M	Outside met wind direction 32.81m	deg
308	OMT4M	Outside met air temperature 4.57 m	degC
316	WTDPT	Wind tunnel dew point temperature	degC
318	WTATEMP	Wind tunnel air temperature	degC

Wind Tunnel Flow Speed

In order to duplicate the wind tunnel pressure measurement system with an independent measure of wind tunnel speed, two sonic anemometers were installed upwind of the turbine (Figure 4 and Appendix B). The anemometers were mounted on airfoil-shaped microphone stands to minimize the downwind flow disturbance. The sonic anemometers were oriented at 45° angles with respect to the inflow as suggested by the manufacturer to improve their performance in the wind tunnel setting. Because the sonic anemometers were located near the contraction cone of the wind tunnel, they did not measure the test-section flow speed accurately (97.23% of the test-section speed). To accurately measure the test-section speed, model predictions located the wind tunnel pressure measurement system in the contraction zone of the inlet. These predictions were verified experimentally by Zell (2000). Each of the three flow components of the sonic anemometers was recorded as listed in Table 3. The wind speed was computed during post-processing.

To obtain preliminary measurements of the wake of the turbine, two sonic anemometers were mounted on a strut downwind of the turbine for Tests 8 and 9 only. These anemometers were not included in the data stream. This portion of testing and associated file formats are described in Appendix G.

Table 3. Sonic Anemometer Channels

Channel	Channel ID	Description	Units
320	LESU8M	Local East sonic channel U 8 m	m/s
322	LESV8M	Local East sonic channel V 8 m	m/s
324	LESW8M	Local East sonic channel W 8 m	m/s
326	LWSU8M	Local West sonic channel U 8 m	m/s
328	LWSV8M	Local West sonic channel V 8 m	m/s
330	LWSW8M	Local West sonic channel W 8 m	m/s

Pressure Measurements

A variety of pressure measurements yield aerodynamic information. The wind tunnel employs a pressure system to measure the total and static pressures used to compute the tunnel speed (Zell 1993). This system is referenced to a Gill port outside the wind tunnel, which is at atmospheric pressure, shown in Figure 10. The wind turbine has one blade instrumented with pressure taps and five-hole probes to measure the blade surface pressures and impinging flow angles. The pressure transducers within the blade were all referenced to the pressure inside one of the rotating instrumentation boxes, the Pressure System Controller (PSC) enclosure. A digital differential pressure transducer was used to measure the difference between the pressure in the PSC Enclosure and the outside atmospheric pressure port, the Gill port. Using the common pressure reference of the Gill port permits addition of each pressure measurement resulting in all measurements referenced to free-stream static pressure.

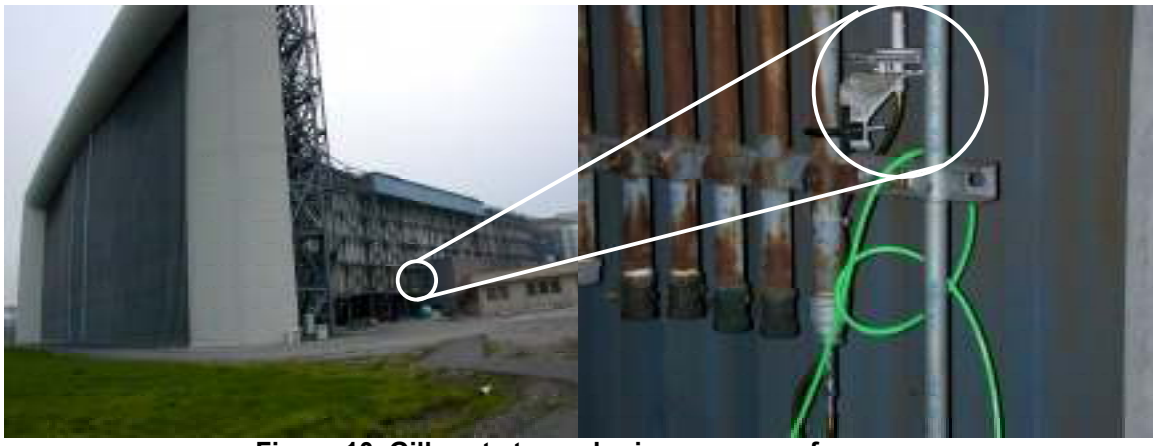

Figure 10. Gill port atmospheric pressure reference

Wind Tunnel Pressure System

Total and static pressure ports were installed in the wind tunnel inlet on each wall, the floor, and the ceiling (Zell 1993). These ports were connected to both analog and digital pressure transducers. The analog transducers were incorporated in the NREL data system and are listed in

Table 4. The digital pressure transducers' output was included in the statistical data files provided by NASA and described in Appendix E. Ambient pressure was also measured both by analog and digital barometers. Each of these pressure transducers was referenced to the Gill port located outside of the wind tunnel. A diagram of the NASA pressure instrumentation path is shown in Figure 11.

Table 4. Wind Tunnel Pressure Measurements

Channel	Channel ID	Description	Units
310	WTBARO	Wind tunnel barometric pressure	Pa
312	WTSTAT	Wind tunnel static pressure	Pa
314	WTTOTAL	Wind tunnel total pressure	Pa

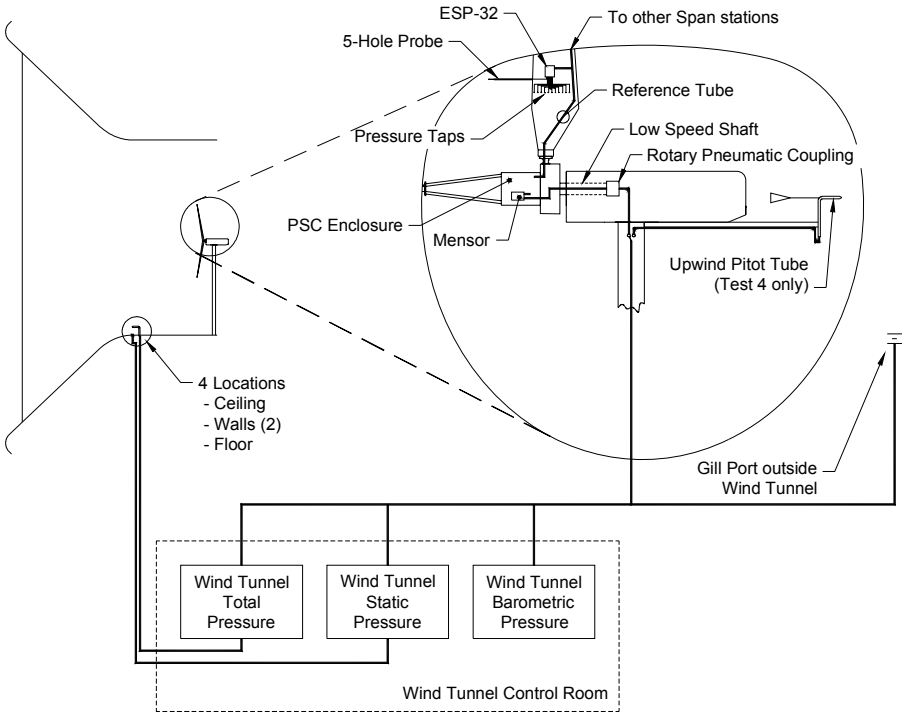

Figure 11. Wind tunnel and wind turbine pressure system diagram (not to scale)

Five-Hole Probes

The spherical-tip 5-hole probe shown in Figure 12 provided dynamic pressure, local flow angle, and spanwise flow angle measurements ahead of the blade at a distance of 80% chord (Sequences B, C, D, E, F, G, H, I, J, K, L, N, O, Q, 3, 4, 5, 6, and 7). Probes were mounted at five span locations, 34%, 51%, 67%, 84%, and 91% span. The probes were positioned at an angle nominally 20° below the chord line to align the probe with the flow under normal operating conditions. The pressure channels associated with each of the five ports are contained in Table 5. Stainless-steel tubes with an outer diameter of 1.6 mm and inner diameter of 0.7874 mm, carried the probe pressures to the pressure transducer. A short piece of plastic tubing [1.6 mm inner diameter] joined the tubes to the transducers, which were mounted inside the blade near the full-chord pressure tap stations.

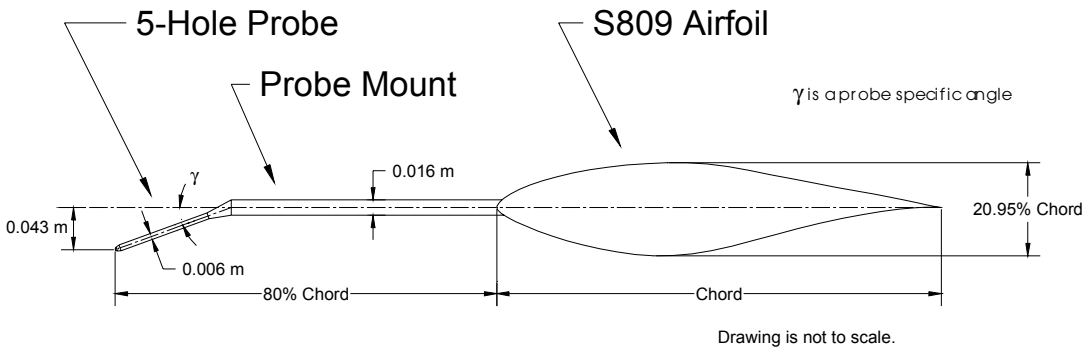

Figure 12. Blade-mounted five-hole probe

The probe manufacturer, Aeroprobe, supplied calibration information obtained in their wind tunnel facility. The difference between the inboard and outboard pressures was normalized with the tunnel dynamic pressure to correspond with the spanwise flow angle. The difference in pressure between the upper (towards upper surface of the airfoil) and lower port measurements was normalized with the tunnel dynamic pressure in order to calibrate the local flow angle. The center port pressure normalized with the tunnel dynamic pressure provided the total pressure. These wind tunnel data provided by Aeroprobe were input to a neural network model to create surfaces for each of the three probe measurements for all five probes (Fingersh and Robinson 1997). The surfaces were implemented as look-up tables in the post-processing code. The spanwise flow angle and local flow angle channels appear in Table 24, and the dynamic pressure measurements appear in Table 20.

The individual five-hole probe channels are listed in Table 5. The raw measured pressure was not stored in each of these channels. In order to obtain pressure measurements relative to the static pressure, hydrostatic pressure corrections, centrifugal force corrections, and reference pressure corrections were applied to each channel. These corrections are described later in this report in the derived channel section (p. 44).

Table 5. Five-hole Probe Pressures

Channel	Channel ID	Description	Units
052, 053, 152, 153, 252	5HC34, 5HC51, 5HC67, 5HC84, 5HC91	5-hole Center Port 1 (34%, 51%, 67%, 84%, and 91% span)	Pa
054, 055, 154, 155, 254	5HL34, 5HL51, 5HL67, 5HL84, 5HL91	5-hole Lower Port 2 (34%, 51%, 67%, 84%, and 91% span)	Pa
056, 057, 156, 157, 256	5HU34, 5HU51, 5HU67, 5HU84, 5HU91	5-hole Upper Port 3 (34%, 51%, 67%, 84%, and 91% span)	Pa
058, 059, 158, 159, 258	5HO34, 5HO51, 5HO67, 5HO84, 5HO91	5-hole Outboard Port 4 (34%, 51%, 67%, 84%, and 91% span)	Pa
060, 061, 160, 161, 260	5HI34, 5HI51, 5HI67, 5HI84, 5HI91	5-hole Inboard Port 5 (34%, 51%, 67%, 84%, and 91% span)	Pa

Static Probe

During field-testing, the static port of a Dwyer 160-U pitot static probe was used to reference all pressure measurements to nominal free stream static pressure. This probe was mounted 2.3 m upwind of the nacelle at hub height when the turbine was operating in a downwind condition. The probe was attached to a vane that aligned itself with the wind as shown in Figure 13. It was installed on the wind turbine during the wind tunnel test for Sequence 4 only in order to replicate field data. Pressure tubing with 1.6-mm inner diameter connected the static probe to a rotary pneumatic coupling on the low-speed shaft. The other end of the coupling transferred this pressure to the Mensor digital differential pressure transducer, which was open to the PSC enclosure.

Figure 13. Upwind static probe (Sequence 4 only)

Pressure Taps

The most important, yet most difficult, measurements were the blade surface tap pressures. The quality of the aerodynamic performance coefficients depends on the accuracy of individual pressure tap measurements. Aerodynamic coefficients for a particular radial station resulted from the integrated value of the measured pressure distribution. The measurement approach was to install small pressure taps in the surface of the blade skin. Each opening was mounted flush to the airfoil surface. The flush profile was necessary to prevent the taps themselves from disturbing the flow. Stainless-steel tubes with an outer diameter of 1.6 mm [0.7874-mm inner diameter], were installed inside the blade's skin during manufacturing to carry surface pressures to the pressure transducer. A short piece of plastic tubing [1.6 mm] inner diameter joined the tubes to the transducers. To mitigate potential dynamic effects, total tubing length was kept less than 0.45 m by mounting the pressure transducers inside the blade near the pressure tap locations. The taps were aligned along the chord (instead of being staggered) so that spanwise variations in pressure

distributions would not distort measured chordwise distributions. As illustrated in Figure 14, the taps were concentrated toward the leading edge to achieve increased resolution in the more active regions of the pressure distributions.

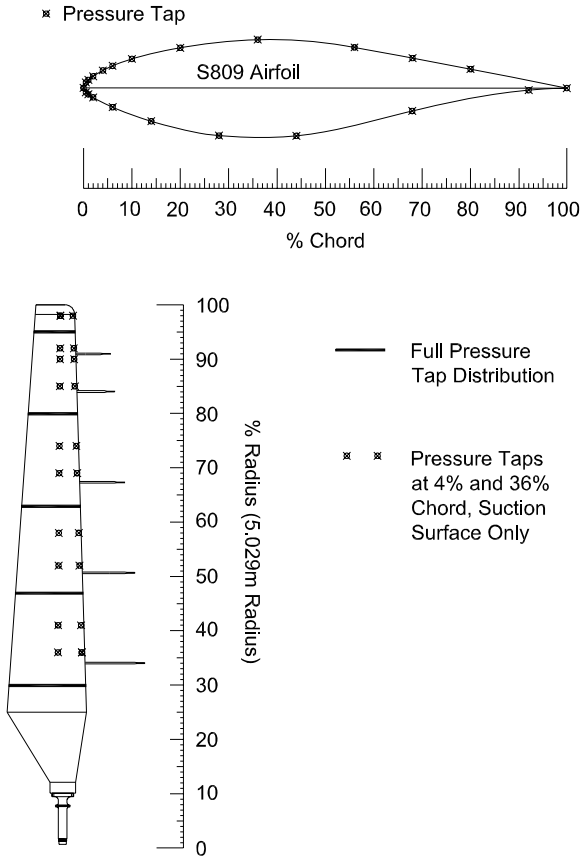

Figure 14. Blade surface pressure and five-hole probe locations

Twenty-two taps were instrumented at five primary spanwise locations: 30%, 46.6%, 63.3%, 80%, and 95% span. Pairs of taps at 4% chord and 36% chord were installed at various other intermediate span locations (36%, 41%, 52%, 58%, 69%, 74%, 85%, 90%, 92%, and 98%) on the suction surface. These channels are listed in Table 6. The correlation between pressure tap number and airfoil chord location is shown in Table 7. The raw, measured pressure was not stored in each of these channels. Normalized pressure coefficients relative to static pressure were stored in these channels instead. The normalization scheme, reference pressure correction, hydrostatic pressure correction, and centrifugal force correction are presented in the section about derived channels (p. 44).

Table 6. Pressure Tap Channels

Channel	Channel ID	Description	Units
000-042 (even)	Ptt30ccc	Surface Pressure Coefficients at 30% Span tt = Pressure Tap Number (1, 4, 6, 8, 11, 13, 15, 17, 18, 19, 20, 21, 22, 23, 24, 25, 27, 31, 32, 34, 36,	Cp
001-043 (odd)	Ptt47ccc	Surface Pressure Coefficients at 47% Span tt = Pressure Tap Number (1, 4, 6, 8, 11, 13, 15, 17, 18, 19, 20, 21, 22, 23, 24, 25, 27, 31, 32, 34, 36,	Cp
100-142 (even)	Ptt63ccc	Surface Pressure Coefficients at 63% Span tt = Pressure Tap Number (1, 4, 6, 8, 11, 13, 15, 17, 18, 19, 20, 21, 22, 23, 24, 25, 27, 30, 32, 34, 36,	Cp
101-143 (odd)	Ptt80ccc	Surface Pressure Coefficients at 80% Span tt = Pressure Tap Number (1, 4, 6, 8, 11, 13, 15, 17, 18, 19, 20, 21, 22, 23, 24, 25, 27, 30, 32, 34, 36,	Cp
200-250 (even)	Ptt95ccc	Surface Pressure Coefficients at 95% Span tt = Pressure Tap Number (1, 4, 6, 8, 11, 13, 15, 17, 18, 19, 20, 21, 22, 23, 24, 25, 27, 30, 32, 34, 36,	Cp
44-51, 144-151, 244-250 (even)	P18ss04U P11ss36U	Intermediate surface Pressure Coefficients at 36%, 41%, 52%, 58%, 69%, 74%, 85%, 90%, 92%, and 98% Span	Cp

Table 7. Pressure Tap Chord Locations

Pressure Tap Number	% chord	Surface	tt*	ccc*
1	100%	Trailing edge	01	100
4	80%	Upper	04	80U
6	68%	Upper	06	68U
8	56%	Upper	08	56U
11	36%	Upper	11	36U
13	20%	Upper	13	20U
15	10%	Upper	15	10U
17	6%	Upper	17	06U
18	4%	Upper	18	04U
19	2%	Upper	19	02U
20	1%	Upper	20	01U
21	0.5%	Upper	21	.5U
22	0%	Leading edge	22	000
23	0.5%	Lower	23	.5L
24	1%	Lower	24	01L
25	2%	Lower	25	02L
27	6%	Lower	27	06L
30	14%	Lower	30	14L
32	28%	Lower	32	28L
34	44%	Lower	34	44L
36	68%	Lower	36	68L
38	92%	Lower	38	92L

* See Table 6.

Based on tests performed in Phase I of the experiment, corrections to compensate for dynamic effects on pressure measurements caused by the pressure tap tubing were not applied to measured data sets (Butterfield et al. 1992). An effort was made to mitigate needed corrections by keeping the tubing length as short as possible [less than 0.457 m for most pressure tap tubes]. Gain amplifications and phase effects that occur in 0.457-m lengths of the stainless-steel tubes were measured during Phase I (Butterfield et al. 1992) and are reproduced in Figure 15. Results indicated that these effects were not significant up to a frequency of 50 Hz. The five-hole probe tubes and some of the intermediate pressure tap tubes were longer than 0.457 m. At the 34% span five-hole probe, the tubes could be twice the length of tubing tested in Figure 15. Thus, dynamic effects may be evident below 50 Hz for the 5-hole probes and intermediate tap pressure measurements.

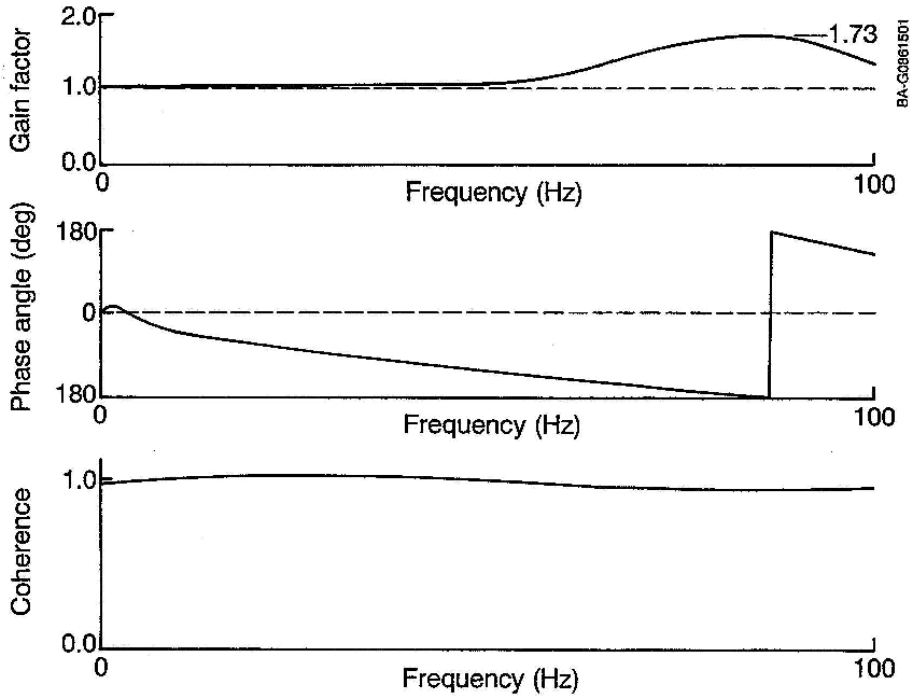

Figure 15. Frequency response for 0.457-m long, 0.7874-mm inner diameter pressure tube from Butterfield et al. 1992. (Note linear scale on horizontal axis.)

Pressure Transducer

The dynamic pressure varied significantly along the span of the blade due to rotational effects, so transducers with different measurement ranges were used. The nominal transducer ranges are listed below in Table 8. The transducers, Pressure Systems Inc. (PSI) model ESP-32, scanned port to port at 16,666 Hz and completed a scan of all pressure taps at 520.83 Hz. One transducer was used at each primary span location to measure 26 differential pressures at the blade surface pressure taps and each of the five ports of a five-hole probe. These measurements were referenced to the pressure in one of the hub-mounted instrumentation boxes, the PSC enclosure. Each transducer was installed inside the blade as close to the pressure taps as possible (see Figure 11). These electronic scanner-type transducers provided remote calibration capability through a

pneumatically operated valve. The capacity to purge all of the pressure taps with dry air was used periodically to prevent moisture or small particles from affecting the pressure measurements.

Table 8. Nominal, Full-scale, Pressure Transducer Measurement Ranges

30% Span	± 2488 Pa (±10 in. H_2O)
47% Span	± 2488 Pa (±10 in. H_2O)
63% Span	± 4977 Pa (±20 in. H_2O)
80% Span	± 6894 Pa (±1 psi)
95% Span	± 10,342 Pa (±1.5 psi)

For all blade surface and probe pressure measurements, the common reference pressure source was the pressure inside one of the rotating instrumentation boxes on the hub, the PSC enclosure. Each transducer located in the blade was connected to the reference source via a plastic 1.6-mm inner diameter tube between the hub and the transducer. The hub-mounted instrumentation box was vented to the atmosphere through an orifice on the upwind side of the box. This resulted in a time constant of about 5–10 seconds and provided a relatively stable pressure reference.

Because of the rotation of the reference pressure line, centrifugal forces acting on the column of air contained in the tube change the pressure along the radius of the blade. Each measurement was corrected for centrifugal force effects and normalized with the blade stagnation pressure, as described later in the derived channel section (p. 44). In addition, a correction was applied to account for the hydrostatic pressure changes as the transducers inside the blade moved up and down in the local atmosphere because of blade rotation. This is also discussed in the derived channel section, and the derivation is contained in Appendix F.

Integral with the rotating pressure measurement system, a highly accurate differential pressure measurement transducer (Mensor model 4010) was used for two purposes. During pressure calibrations, it was used to measure the pressure difference between the stable rotating (PSC enclosure) reference pressure and the calibration pressure applied by a motorized syringe. During operation, it was used to measure the pressure difference between the stable rotating (PSC enclosure) reference pressure and the atmospheric pressure at the Gill port. A rotary, pneumatic coupling was installed on the generator side of the low-speed shaft with one end connected to the Mensor in the PSC enclosure. The other end was connected to a 6.35-mm inner diameter tube that extended down the tower, through the balance room, to the control room where it joined the NASA pressure system and ultimately was connected to the Gill port outside the wind tunnel. This provided the same pressure reference for both the NASA pressure measurements and the turbine pressure measurements. Pressure was applied to this leg of the system daily in order to verify system integrity. Only during Test 4 was the upwind static probe installed to reference all turbine pressure measurements to the static pressure upwind of the turbine. Figure 11 illustrates the various pressure measurement paths.

Table 9 shows the channels corresponding to the digital signal from the Mensor. These are converted into one pressure measurement during post-processing. Two channels are required because the Mensor output is 16 bits, and the data acquisition system is a 12-bit system.

Table 9. Mensor Channels

Channel	Channel ID	Description	Units
259	MENS1	Digital First 12 bits from D pressure	Pa
261	MENS2	Digital Last 12 bits from D pressure	Pa

Pressure System Controller (PSC)

Remote control of ESP-32 pressure transducer calibration, scanner addressing, and demultiplexing of the analog multiplexed signals were performed by the PSC, a hub-mounted microprocessor control unit designed by NREL (Butterfield et al. 1992). The PSC was completely redesigned in subsequent phases to improve the accuracy and the user interface. Currently up to 155 pressure channels may be processed simultaneously. All pressure ports were scanned at 520.83 Hz.

Once the PSC scanned the pressure transducers, the samples were digitized, synchronized, and passed to the pulse code modulation (PCM) encoder. The PCM system multiplexed 62 channels of data into one digital data stream, which was conducted through a single coaxial cable. Rotor data were encoded into three PCM streams, which were passed over slip rings to the control room and were recorded on optical disk for subsequent processing.

Structural Measurements

Strain Gauges

Bending moments were measured at the root of each blade and on the low-speed shaft with strain gauges. The strain gauges measuring root flap and edge loads were applied to the steel pitch shaft adjacent to the blade attachment location. The pitch shaft was reduced to a uniform cylinder, 80 mm in diameter at 8.6% span [0.432 m], the location where the strain gauges were applied. The uniform, cylindrical region eliminates geometry effects to facilitate accurate measurement of flap and edge bending moments. The pitch shaft rotates with the blade when the blade pitch changes to maintain alignment of the strain gauges with the blade chord at the tip of the blade. This cylindrical section of the blade root is illustrated in Figure 9 and in Appendix B. The low-speed shaft was instrumented with strain gauges to measure bending about two axes and torque. Diagrams of the strain gauge orientation are included in Appendix B. The measurement conventions were such that positive blade root flap bending occurred because of a force in the downwind direction for both the upwind and downwind turbine configurations. Blade root edge bending and low-speed shaft torque were positive because of a force in the direction of rotation for both the upwind and downwind turbine configurations. The low-speed shaft bending gauges were originally applied to correspond to blade positioning for a three-blade rotor, thus the measurement conventions are somewhat complicated. The conventions are specified in Appendix B. Table 10 lists all of the strain gauge measurement channels.

Table 10. Strain Gauge Measurements

Channel	Channel ID	Description	Units
225	B1RFB	Strain Blade 1 Root Flap Bending	N-m
227	B1REB	Strain Blade 1 Root Edge Bending	N-m
233	B3RFB	Strain Blade 3 Root Flap Bending	N-m
235	B3REB	Strain Blade 3 Root Edge Bending	N-m
237	LSSXXB	Strain X-X LSS Bending	N-m
239	LSSYYB	Strain Y-Y LSS Bending	N-m
241	LSSTQ	Strain LSS Torque	N-m

Accelerometers

Accelerometers in the blade tips and the nacelle bedplate provide information regarding the motion of the turbine. Acceleration in both the flap and edge directions was measured with pairs of accelerometers in the tips of each blade. Positive flap acceleration occurred when the blade accelerated downwind, perpendicular to the tip chord, for both upwind and downwind turbine configurations. Positive edge acceleration occurred when the blade accelerated in the direction of rotation, parallel to the tip chord, for both upwind and downwind configurations. A triaxial accelerometer construction on the nacelle bedplate opposite the hub provided fore-and-aft, pitch, and yaw acceleration of the nacelle. If the nacelle accelerated in the negative yaw direction, the nacelle yaw accelerometer measured a positive value. Positive fore-and-aft acceleration occurred if the nacelle accelerated toward the hub. The pitch acceleration was positive in the vertical direction. The nacelle accelerometer calibration coefficients were not changed between the upwind and downwind turbine configurations. Accelerometer specifications are contained in Appendix B, and the channels corresponding to accelerometer measurements are listed in Table 11.

Table 11. Accelerometer Measurements

Channel	Channel ID	Description	Units
201	B1ACFL	Accelerometer Blade 1-Flap	m/s^2
203	B1ACED	Accelerometer Blade 1-Edge	m/s^2
209	B3ACFL	Accelerometer Blade 3-Flap	m/s^2
211	B3ACED	Accelerometer Blade 3-Edge	m/s^2
336	NAACYW	Nacelle Accelerometer Yaw	m/s^2
338	NAACFA	Nacelle Accelerometer Fore-Aft	m/s^2
340	NAACPI	Nacelle Accelerometer Pitch	m/s^2

Load Cells

Load cells were used to measure the teeter damper impact forces, the yaw moment, and the force imparted by the blades on the link mechanism between them. Load cells placed inside the teeter dampers recorded the forces applied during teeter impact (Sequences B, C, D, G, and 4). A tension/compression load cell in the link between the blades measured the force between the blades for the teetered turbine configurations (Sequences B, C, D, G, and 4). This link was pretensioned to 40,000 N when the turbine configuration used a rigid hub. The measurement convention was such that positive link force corresponded to positive blade root flap bending moment. Another tension/compression load cell was placed adjacent to the yaw brake caliper. The load cell constrains the motion of a four-bar linkage where the brake caliper is one bar. Yaw moment was a positive moment in the direction required to restore the turbine from a negative yaw error to zero yaw error for both the upwind and downwind turbine configurations shown in Figure 16. These load cell measurements are listed in Table 12, and a description of the instrumentation as well as measurement conventions are presented in Appendix B.

Table 12. Load Cell Measurements

Channel	Channel ID	Description	Units
223	TLINKF	Strain Teeter Link Force	N
229	B1TDAMPF	Strain Blade 1 Teeter Damper Force	N
231	B3TDAMPF	Strain Blade 3 Teeter Damper Force	N
342	NAYM	Nacelle Yaw Moment	N-m

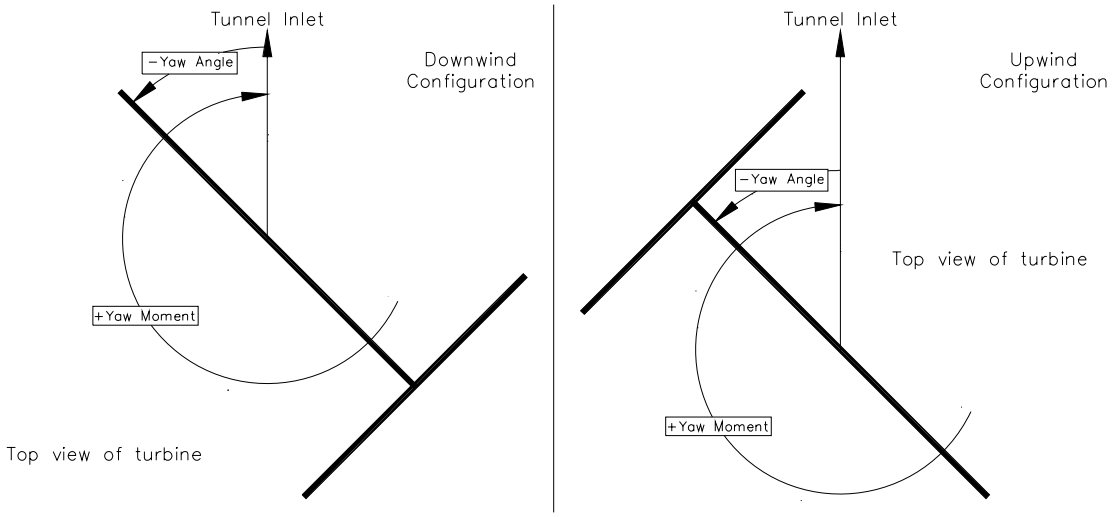

Figure 16. Yaw moment measurement conventions

Pitch Rate and Generator Power

The servomotors that pitch the blades produce an output signal corresponding to the pitch rate. This was incorporated into the data stream shown in Table 13. The generator power was also measured as a data channel using an Ohio Semitronics, Inc., (OSI) power watt transducer. These instruments are described further in Appendix B.

Table 13. Pitch Rate and Generator Power

Channel	Channel ID	Description	Units
243	B1PRATE	Blade 1 pitch rate	deg/s
247	B3PRATE	Blade 3 pitch rate	deg/s
332	GENPOW	Generator power	kW

Wind Tunnel Balance System

The wind tunnel was equipped with seven load cells that measure forces applied by the model to the *T*-frame on which the turntable rests. The location of the scales is shown in Figure 2. These channels are listed in Table 14. The lift forces are positive up; the side forces are positive starboard; the drag force is positive downstream. These forces were resolved into three forces and moments at the low-speed shaft during post-processing. For various reasons noted in Appendix E, these measurements were not reliable during most of the wind tunnel test.

Table 14. Wind Tunnel Balance Forces

Channel	Channel ID	Description	Units
344	WTLFLIFT	Wind tunnel left front lift (#1)	N
346	WTRFLIFT	Wind tunnel right front lift (#2)	N
348	WTLRLIFT	Wind tunnel left rear lift (#3)	N
350	WTRRLIFT	Wind tunnel right rear lift (#4)	N
352	WTFSFORC	Wind tunnel front side force (#5)	N
354	WTRSFORC	Wind tunnel rear side force (#6)	N
356	WTDRAG	Wind tunnel drag (#7)	N

Position Encoders

Gear-driven, BEI model R-25 and RAS-25 optical absolute position encoders were used to measure yaw position, blade pitch angle, blade flap angle, and rotor azimuth position. The yaw position encoder was located near the yaw brake. The rotor azimuth encoder was located in the nacelle on the low-speed shaft. Each blade was provided with an encoder for pitch angle measurement and flap angle measurement. Figures 17–19 illustrate the measurement conventions, and Table 15 contains the channel descriptions.

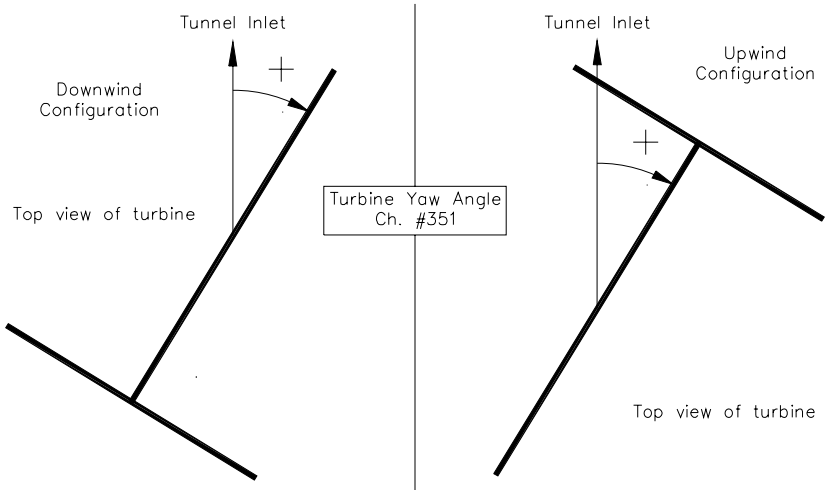

Figure 17. Yaw angle measurement convention

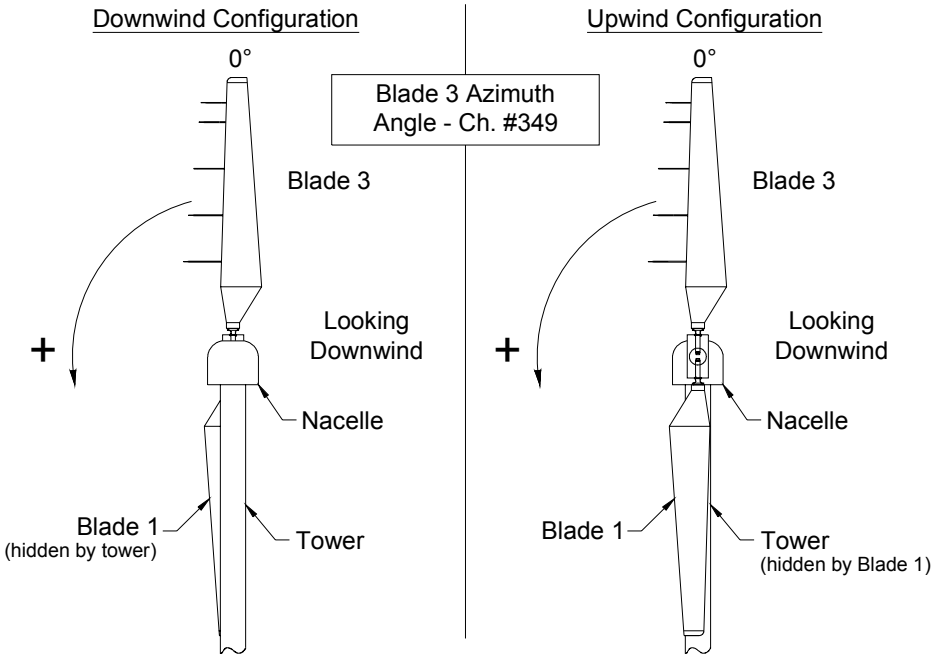

Figure 18. Rotor azimuth measurement convention

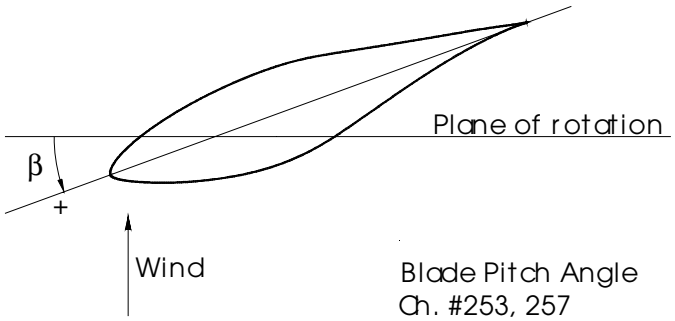

Figure 19. Blade pitch angle measurement convention, 0° at tip

Individual blade flap angles were obtained with an encoder on either side of the teeter pin with an 8:1 gear ratio to improve the accuracy of the small angle measurements. Although the blade cone angle was set at a nominal value, flexibility in the linkage permits slight fluctuation of approximately 0.02°. Figure 20 illustrates the measurement conventions used.

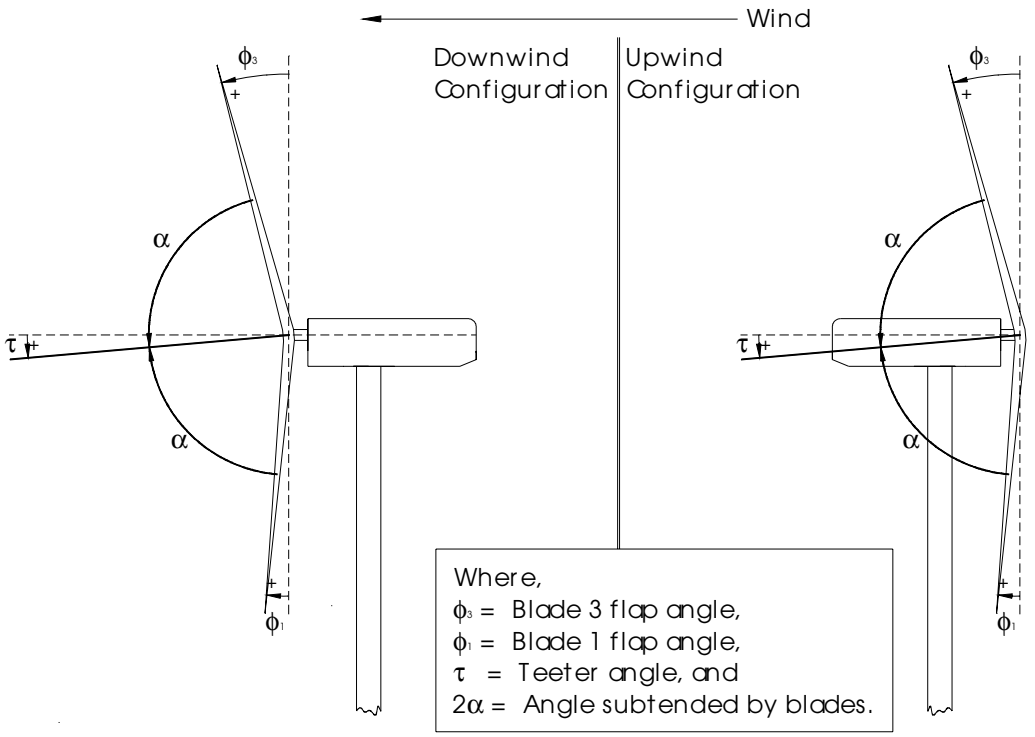

Figure 20. Blade flap angle measurement convention

The wind tunnel turntable angle was measured with a single-turn absolute resolver. Because the turntable did not move while data were collected, this channel was not actually measured in order to eliminate the small fluctuations due to noise in the system. The slope was set to zero, and the offset was set to duplicate the reading shown on the wind tunnel operator's screen. The turntable remained at zero for the majority of tests. It was positioned at different angles for Tests 6, 7, 8, and 9 only. The turntable measurement was positive clockwise when viewed from the top.

Table 15. Position Encoder Channels

Channel	Channel ID	Description	Units
251	B1FLAP	Digital Blade 1 Teeter Angle	deg
253	B1PITCH	Digital Blade 1 Pitch	deg
255	B3FLAP	Digital Blade 3 Teeter Angle	deg
257	B3PITCH	Digital Blade 3 Pitch	deg
349	B3AZI	Blade 3 Azimuth Angle	deg
351	YAW	Yaw Angle	deg
358	YAWTABLE	Turntable angle	deg

Time

A time code generator provided a signal that was recorded in the channels shown Table 16.

Table 16. Time Channels

Channel	Channel ID	Description	Units
353	DAY	Clock - Day	day
355	HOUR	Clock - Hour	hour
357	MINUTE	Clock - Minute	minute
359	SECOND	Clock - Second	second
361	MILLISEC	Clock - Millisecond	msec

Data Acquisition and Reduction Systems

PCM System Hardware

To increase accuracy, simplify instrumentation, and reduce noise, digital and analog data signals are sampled and encoded into PCM streams as close to the transducer as possible. For this reason, three PCM streams originate in the instrumentation boxes mounted on the hub, and one PCM stream originates in the ground-based PCM rack below the base of the turbine in the balance house. The rotor streams are conducted through slip rings and cables to the wind tunnel control room where all four streams are then decommutated and stored on optical disk. A customized digital PCM-based hardware system for data acquisition was developed and tested throughout Phase I of the Unsteady Aerodynamics Experiment (UAE) (Butterfield et al. 1992). This hardware has been upgraded through each phase of the experiment. All of the channels were sampled at 520.83 Hz and stored directly to optical disk. Copies of the optical disks and the processed engineering unit files were recorded on compact discs for dissemination.

The PCM encoders convert conditioned analog-input voltages into digital counts. The digital signals are also encoded into PCM streams. The digital conversion code limits the overall accuracy to 12-bit resolution for count values ranging from 0 to 4095. Therefore, quantization errors are limited to 0.024% of full scale, and the peak signal-to-noise ratio (S/N) is 83 dB. Signal conditioning the analog signals before PCM encoding allows the channels to use as much of the quantization range as possible. Also, filtering the analog signals before PCM encoding reduces the potential for aliasing, or the 'folding back' of high frequency components of the signal into a lower frequency range. The pressure signals were not filtered due to the filtering effect of the pressure tubes and the difficulty in filtering analog multiplex signals.

The decoder boards are printed circuit boards mounted inside the chassis of a personal computer (PC). The specifications listed in Table 17 are taken from Butterfield et al. (1992) but still reflect the current specifications. Software that controls the decoder boards was written in C for DOS. Upon receiving a capture command, a direct memory access (DMA) controller moves decoded data from the PCM board to computer memory in variable buffer sizes from 0–64 kilobytes. Each word is tagged with its corresponding PCM board number, and custom software was developed to facilitate conversion of the PCM data to binary files.

Table 17. PCM Decoder Board Specifications

Bit Rate	1-800 Kbits/second
Input Streams	4 (only one processed at a time)
Input Polarity	Negative or positive
Input Resistance	>10 Kohms
Codes	Bi-phase L, NRZ
Bit Sync Type	Phase-locked loop (PLL)
Input Data Format	8-12 bits/word, most significant bit (MSB) first
Words Per Frame	2-64 (including sync)
Sync Words Per Frame	1-3 (maximum 32 bits)

(Source: Butterfield et al. 1992)

Calibration Procedures

The most desirable calibration is to apply a known load and measure the response with the instrumentation system, i.e., a full-path calibration. Several points provide data for linear

interpolation, and the slope and offset values of a linear transducer can then be determined. This form of calibration is used for the pressure transducers, strain gauges, and load cells, but it is not feasible for a number of instruments because the manufacturer's calibrations are required (as in the case of accelerometers). In this situation, calibration coefficients are obtained through the manufacturer. The analog instruments output values in units of volts, but the data acquisition system converts all measurements into digital counts. Known reference voltages were inserted in place of the transducer signal to separately calibrate the system electronics path. These values were used to convert the manufacturer-supplied calibration coefficients to units of counts. Lastly, the digital position encoders must be oriented with a known position to obtain the offset, although the slope is prescribed by the instrument. Detailed descriptions of the calibration procedures for each channel are included in Appendix B.

Calibrations of the pressure channels were performed in the manner described in Simms and Butterfield (1991) by using a motorized syringe to apply positive and negative pressure to all scanning transducers simultaneously over their full measurement range. This was done approximately every half-hour by remote control while the turbine was operating. Calibration coefficients were derived by performing a least-squares linear regression on each of the pressure channels referenced to the PSC enclosure. In order to verify lack of zero-drift and slope-drift in the pressure transducers, comparisons were made between the current calibration and the one performed one half hour before. The Mensor digital differential pressure transducer was zeroed daily during testing according to manufacturer specifications.

The strain gauges were also calibrated by applying a known load. A saddle was attached to each blade to isolate loads in both flap and edge directions. Weights were used to apply a moment that was measured by the strain gauges. A least-squares regression analysis provided slope calibration coefficients. The zero offsets were determined by positioning each blade in zero-load locations of the rotational cycle. The slopes were calibrated before the wind tunnel test, and the strain gauges were zeroed daily throughout wind tunnel testing.

A custom jig was built to apply loads to load cells in series. One of the load cells is considered the calibration load cell, and the others are the teeter link load cell, the yaw moment load cell, or the button force sensors used to measure teeter impact. The jig is loosened or tightened over the range of the load cell being calibrated. The calibration load cell provides the known load. Linear regression provides slope and offset coefficients. The load cells were calibrated on the ground prior to installing the hub on the turbine. The data acquisition system was used to obtain the load measurements, and only the length of cable from the load cell to the system differed from field application. The load cells were zeroed by noting the count values under zero-load conditions. The slope calibration was performed in July 1999. The teeter link load cell was zeroed before wind tunnel testing. The damper load cells and yaw moment load cell were zeroed daily during testing.

A database of the resulting calibration coefficients was maintained and applied to raw data values to produce engineering unit data files. Because all of the measured channels were linear, only slope and offset calibration coefficients were applied.

PCM System Software

A diagram of the signal path from PCM streams to useable data along with the possible viewing options is shown in Figure B-37. It was possible to view a bar graph showing all channels within each of the four PCM streams. The count value of a user-selected channel was noted on the bottom of the screen. The most powerful real-time viewing program displayed nearly all

measured channels on one screen. Each of the five pressure distributions, angles of attack, and dynamic pressures were displayed graphically in real time. Inflow conditions, such as wind speed, azimuth angle, yaw angle, and yaw error were displayed as well. A bar graph tracked power, root flap bending moment, damper load cells, teeter link force, yaw moment, low-speed shaft bending, and low-speed shaft torque. Other parameters, such as time, pitch angles, and rotational speed appeared as text. A modified version of this program could also be used to review recorded data at adjustable speeds. Time histories of user selected channels could be displayed by selecting an averaging value. Each point average was updated graphically in real time. This software provided a means of determining inoperable channels quickly and easily.

The flow charts presented in Figures B-38 and B-39, (pp. 158 and 159), illustrate the process of creating the engineering unit files that are stored on compact disc. Pressure calibrations were initiated with *psc.exe* that controls the syringe in the PSC package. The resulting measurements were fit to a linear curve with the corresponding slope and offset values entered in the *prescal.hdr* file. A similar process was performed using the *gencal.exe* program to determine slope and offset values for the strain gauges, load cells, and electronic path calibrations. All of the other calibration coefficients for anemometers, accelerometers, optical absolute position encoders, the NASA-supplied channels, and the power transducer were determined using manufacturer specifications and/or single-point offset determination that were entered in the spreadsheet *calconst.xls*. The *buildhdr.exe* program converted the manufacturer-supplied calibration coefficients in units of volts to engineering units created by the electronic path calibrations. Production of the *master.hdr* file resulted in one file containing all slope and offset values for each measured channel. This file, in conjunction with the recorded data file, (**.dat*), was input to the main processing program called *munch.exe*. This program requires additional input files that explain the pressure profiles (*cexp.prf*), the blade shape (*cexp.bsh*), the record format (*cexp.rft*), and the ID codes for the data channels (*chanid.txt*).

The *munch.exe* program created two files: the header file and the engineering unit file. The header file is an ASCII file that contains a description of each channel, calibration coefficients, and statistics for the 10-minute campaign (mean, standard deviation, maximum, record location of maximum, minimum, record location of minimum, and number of errors). An example of the header file is attached in Appendix B, p. 169. The engineering unit file is a binary file that contains the time series of each channel converted from digital counts to engineering units. Additionally the time series of several derived channels, such as normal and tangential force coefficients, were included. An example of the format of the engineering unit file appears in Appendix B, p. 170. All of these files were stored on compact disc along with the calibration files, the recorded data file, and *munch.exe* input files.

While creating the engineering unit file, a byte is attached to each record to indicate whether or not channels exceeded the measurement ranges. This “error byte” contains 8 bits representing each of the 5 span locations, one bit for the 4% chord and one bit for the 36% chord spanwise distributed taps, and one bit for all other channels (including 5-hole probe pressure measurements). If the bit is turned on, the maximum value of the transducer was exceeded for at least one of the channels associated with that measurement source. For example, if the pressure at any tap at 30% span exceeded the transducer measurement range, the error bit representing the 30% span station was incremented. If the 4% chord tap at 30% span exceeded the transducer measurement range, the bit representing the 30% span taps was incremented as well as the bit representing the 4% chord spanwise pressure tap distribution.

Derived Channels

Wind Tunnel Parameters

NASA provided equations to correct the measured total and static pressures from inlet pressures to test-section pressures and to compute the dynamic pressure, wind speed, and air density. These equations are included in Appendix D, the NASA Software Requirements Document (Equations 401A-407). Although all output parameters are in International System of Units (SI) , the equations provided by NASA assume U.S. Customary System (USCS) units. The measured parameters were converted to USCS units with *munch.exe*. The calculated values were obtained in USCS units and subsequently converted to metric units for output. Table 18 lists the output channels computed using the measurements provided with NASA instrumentation.

Table 18. Wind Tunnel Computed Parameters

Channel	Channel ID	Description	Units
880	VTUN	Tunnel velocity	m/s
881	QTUN	Tunnel dynamic pressure	Pa
882	RHOTUN	Tunnel air density	kg/m^3
883	PTTUN	Tunnel total pressure	Pa
884	PSTUN	Tunnel static pressure	Pa
885	PATUN	Tunnel centerline pressure	Pa

The equations in Appendix D are summarized as follows. The tunnel centerline absolute pressure was computed by correcting the measured atmospheric pressure with the height differential between the Gill port and the tunnel centerline. Although the equations in Appendix D indicate that the static pressure at the inlet must be corrected to obtain the test-section static pressure, this was deemed unnecessary after a NASA calibration performed in December 1999 (Zell 2000). The measured total and static pressures were added to the corrected tunnel centerline pressure to obtain absolute pressures. The air density was computed using the measured dew point temperature (WTDPT), the measured tunnel air temperature (WTATEMP), the corrected atmospheric pressure, and the tunnel static pressure. The tunnel dynamic pressure was computed using the total and static pressures. The tunnel velocity is computed using the air density and dynamic pressure.

Mensor Differential Pressure Transducer

The Mensor differential pressure transducer generates a 16-bit signal, but each channel in the data system is 12 bits. Thus, two channels were used to transmit the 16-bit, digital signal output from the Mensor. These two channels were combined in *munch.exe* to obtain the measured pressure in engineering units. A 1-per-revolution fluctuation was evident in the Mensor pressure measurement. This has been attributed to dynamic effects related to the tubing connecting the three instrumentation enclosures, the pressure tubing between the Mensor and the pneumatic coupling on the low-speed shaft, and the filters internal to the Mensor. The hydrostatic pressure correction described in Appendix F was applied to the Mensor measurement as shown in Equation 1 to eliminate this pressure fluctuation. Table 19 contains the engineering unit channel computed by *munch.exe* from the two data channels with the hydrostatic correction applied.

$$M_{corr} = M_{meas} + A\cos(B3AZI - \phi), \qquad \text{(Eq. 1)}$$

where
M_{corr} = corrected pressure from Mensor, Pa
M_{meas} = measured pressure from Mensor, Pa
A = hydrostatic pressure correction amplitude, Pa
B3AZI = Blade 3 azimuth angle, converted to radians
ϕ = hydrostatic pressure correction phase angle, radians.

Table 19. Mensor Differential Pressure Transducer Channels

Channel	Channel ID	Description	Units
823	MENSOR	Static pressure - instrumentation box presure	Pa

The Mensor pressure transducer measured differential pressure between the PSC Enclosure and one of two other ports: the upwind static probe (Test 4) or the NASA Gill port pressure reference (all other tests). The Mensor is programmable with several different filter and window settings. Hydrostatic corrections for each filter and window combination were developed. Also, the correction differs between the upwind and downwind turbine configuration because the rotation direction changes. Lastly, corrections depend on whether or not the Mensor was connected to the NASA Gill port pressure reference or to the upwind static probe. The various corrections and corresponding test sequences are presented in Appendix F.

Pressure Measurement Path (or Reference Pressure Correction)

All of the ESP-32 pressure transducers located inside the instrumented blade were referenced to the PSC Enclosure. These transducers measured the differential pressure between a pressure tap (P_{tap}) and the PSC enclosure (P_{PSC}) or one port of the five-hole probe and the PSC enclosure. The Mensor measured either the differential pressure between the Gill port atmospheric pressure (P_{atm}) and the PSC enclosure or the upwind static probe (P_{statpr}) and the PSC enclosure. The wind tunnel inlet was instrumented to measure the pressure differential between the tunnel centerline static pressure (P_{∞}) and the Gill port atmospheric pressure. Recall that the recent calibration performed by NASA confirmed that the static pressure at the inlet was also the test-section static pressure. Combining these pressure differentials as follows, all pressure measurements were made in reference to static pressure.

$$P_{tap} - P_{\infty} = [P_{tap} - P_{PSC}] - [P_{atm} - P_{PSC}] - [P_{\infty} - P_{atm}] \quad \text{(Eq. 2)}$$

$$P_{tap} - P_{statpr} = [P_{tap} - P_{PSC}] - [P_{statpr} - P_{PSC}] \quad \text{(Eq. 3)}$$

Equation 3 represents the pressure measurements obtained with the upwind static pressure probe installed, Test 4 only. All other tests used the pressure system path described in Equation 2. These equations were implemented in *munch.exe* for each pressure tap measurement and each port of the five-hole probes.

Hydrostatic Pressure and Centrifugal Force Corrections

The hydrostatic pressure variation in the reference pressure tube that occurs as a result of blade rotation was removed per Equation 4 for both 5-hole probe and pressure tap channels. The derivation of this correction is explained in Appendix F.

The differential pressure transducers located in the blade actually measure a pressure difference between the tubes at the location of the transducer. When the blade is rotating, this pressure measurement is not the desired pressure measurement between the tap and the PSC enclosure because of the centrifugal force acting on the air in the tubes. This force was added to each measured pressure data value per Equations 5 and 6. Each of the probe pressures was also corrected in this manner, but the radius was defined from the center of rotation to the probe tip instead of along the span of the blade.

$$P_{meas} = [P_{tap} - P_{\infty}] + P_{cent} + A\cos(B3AZI - \phi), \quad \text{(Eq. 4)}$$

$$P_{cent} = \frac{1}{2} RHOTUN\left(r * \cos(cone) * RPM * \frac{\pi}{30}\right)^2 \text{ for pressure taps, and} \quad \text{(Eq. 5)}$$

$$P_{cent} = \frac{1}{2} RHOTUN\left(\sqrt{(r\cos(cone))^2 + (1.1 * chord)^2} * RPM * \frac{\pi}{30}\right)^2 \text{ for 5-hole probes.} \quad \text{(Eq. 6)}$$

where
P_{meas} = differential pressure corrected for centrifugal force, Pa
P_{cent} = centrifugal force correction, Pa
r = radial distance along blade span to surface pressure tap or 5-hole probe, m
chord = chord at 5-hole pressure probe mount, m
cone = nominal blade cone angle, rad
A = hydrostatic pressure correction amplitude, Pa
ϕ = hydrostatic pressure correction phase, rad
RHOTUN = air density, kg/m^3
RPM = rotational speed, rev/min
B3AZI = blade 3 azimuth angle, converted to radians.

Dynamic Pressure

Because all pressure measurements were referenced to test-section centerline static pressure, direct measurement of approximate dynamic pressure was possible. Two measurements of dynamic pressure at the turbine were obtained: five-hole probe dynamic pressure and stagnation point dynamic pressure. These measurements were compared to the wind tunnel dynamic pressure for parked blade conditions by Simms et al. (2001).

The pressure measured with the 5-hole probes and corrected for centrifugal and hydrostatic effects was one measure of dynamic pressure, and these channels are listed in Table 14. The difference between the inboard and outboard ports was normalized with the center port pressure after the reference pressure, hydrostatic pressure, and centrifugal force corrections were applied. The difference between the upper and lower ports was normalized similarly. The probe dynamic pressure was then extracted from the look-up table using these two numbers. An algorithm using a spherical coordinate system was developed to determine the probe total pressure measurement, and bilinear interpolation was used to obtain the probe measurements from their respective surfaces (Freeman and Robinson 1998). During the sequences when the 5-hole probes were removed, "dummy" channels were created containing values of –9999.99 to maintain a consistent file size. The numbers referring to the span location in the ID codes were replaced with DP to signify "dummy probes."

Another measure of dynamic pressure used the stagnation point pressure at each of the full-chord pressure tap locations. The pressure tap at each primary span location where the measured

pressure attains a maximum was considered to be the stagnation point, and the corresponding pressure at that location was used as the stagnation pressure. The resolution of the pressure taps on the lower surface was assumed sufficient to extract the maximum positive surface pressure, especially at lower angles of attack. According to Shipley et al. (1995), the stagnation point method is the preferred method of estimating dynamic pressure on the blade. This measurement of dynamic pressure was used to normalize each of the blade surface pressures and is thus referred to as the *normalization pressure*. Table 20 also includes these dynamic pressure measurements.

Table 20. Dynamic Pressure Measurements

Channel	Channel ID	Description	Units
822	QNORM30	Normalization Factor at 30% Span	Pa
828	QNORM47	Normalization Factor at 47% Span	Pa
834	QNORM63	Normalization Factor at 63% Span	Pa
840	QNORM80	Normalization Factor at 80% Span	Pa
846	QNORM95	Normalization Factor at 95% Span	Pa
863	5HP34P	5-hole Probe 34% Pressure	Pa
866	5HP51P	5-hole Probe 51% Pressure	Pa
869	5HP67P	5-hole Probe 67% Pressure	Pa
872	5HP84P	5-hole Probe 84% Pressure	Pa
875	5HP91P	5-hole Probe 91% Pressure	Pa

Pressure Coefficients

Each of the corrected blade surface pressure values was normalized by the corrected stagnation pressure at the corresponding span location as shown in Equation 7. These values were recorded in the engineering unit files for each pressure tap (see Tables 6 and 7).

$$C_p = \frac{P_{meas}}{Q_{norm}}, \qquad \text{(Eq. 7)}$$

where
C_p = pressure coefficient, dimensionless
P_{meas} = differential pressure corrected for centrifugal force, Pa
Q_{norm} = stagnation point dynamic pressure corrected for centrifugal force, Pa.

The intermediate taps were normalized with a dynamic pressure that was linearly interpolated or extrapolated from the two, nearest, full-chord pressure tap locations. This estimation can both overestimate and underestimate the actual dynamic pressure at the intermediate taps.

Pressure Measurement Considerations

Pressure distributions occasionally indicated that the magnitude of the C_p at the 0.5% chord upper surface pressure tap was approximately 10% less than that of the adjacent pressure taps. This could be attributed to a slight radial displacement (5–6 mm at 47%, 63%, and 80% span stations) of the leading edge tap or to interference from adjacent taps. This has very little effect on the integrated aerodynamic force coefficients, however, because the slight reduction in pressure is applied over a small area (0.5% chord).

The pressure measurements were affected by the wake of the instrumentation boom and enclosures during the upwind configurations in yawed conditions. A schematic of the wake

interaction is shown in Figure 21 as a top view of the turbine at a 60° yaw angle. Figure 22 illustrates the effect of the boom wake on the stagnation point pressure measurement as a function of blade 3 azimuth angle for a 10 m/s, 60º yaw case. The interaction of the instrumentation boom and enclosures is evident in the scatter at azimuth angles near 90º.

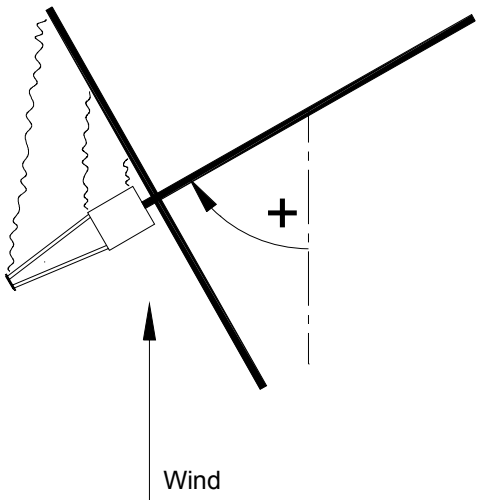

Figure 21. Schematic of boom and instrumentation enclosure wake interference

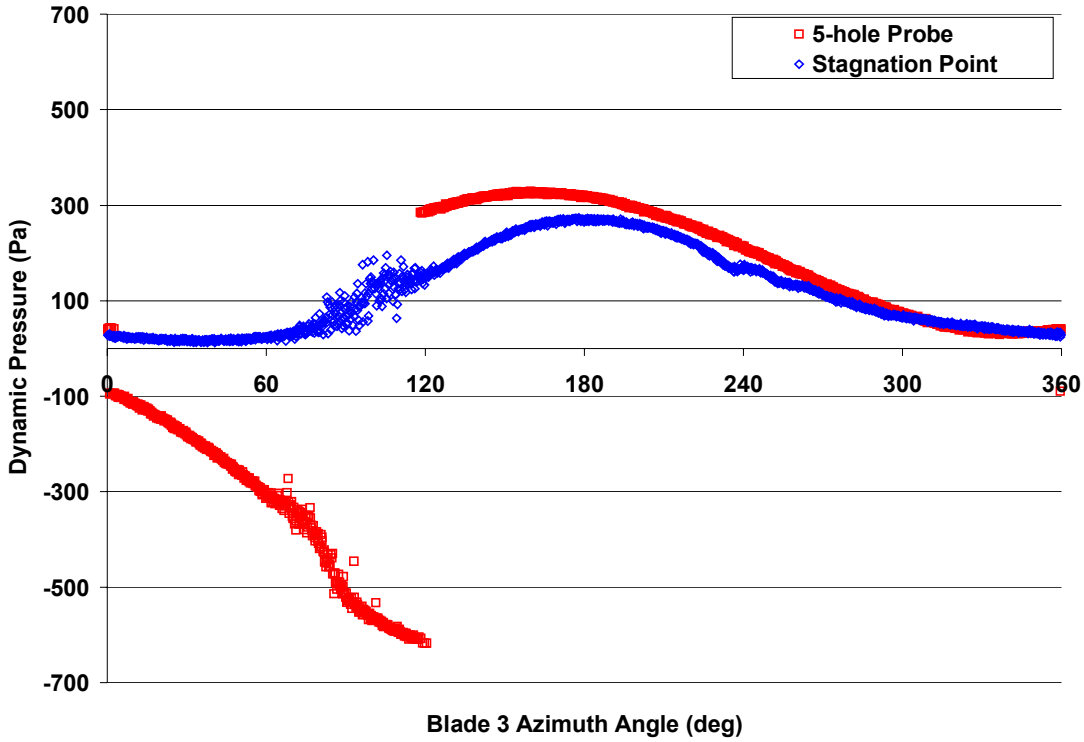

Figure 22. Example of blade dynamic pressure measurement affected by boom/box wake interference and 5-hole probe dynamic pressure outside probe measurement range

In yawed conditions, the angle of the tunnel flow with respect to the five-hole probes can exceed the design range for the probes. The inflow acceptance angle for the probes is ±35º according to the manufacturer. The 5-hole probe dynamic pressure measurement shown in Figure 22 is obviously invalid for azimuth angles from 0º to 120º. Figure 23 provides an example of the local flow angle and spanwise flow angle measurements for the same inflow condition. The obvious discontinuities occur when the flow angle trend exceeds 35º. Note that the magnitude of the measurement alone is not sufficient to determine whether the probe acceptance angle was exceeded. The measurement trend over the entire rotational cycle is necessary to determine the regions of the plane where the range of the probe was exceeded.

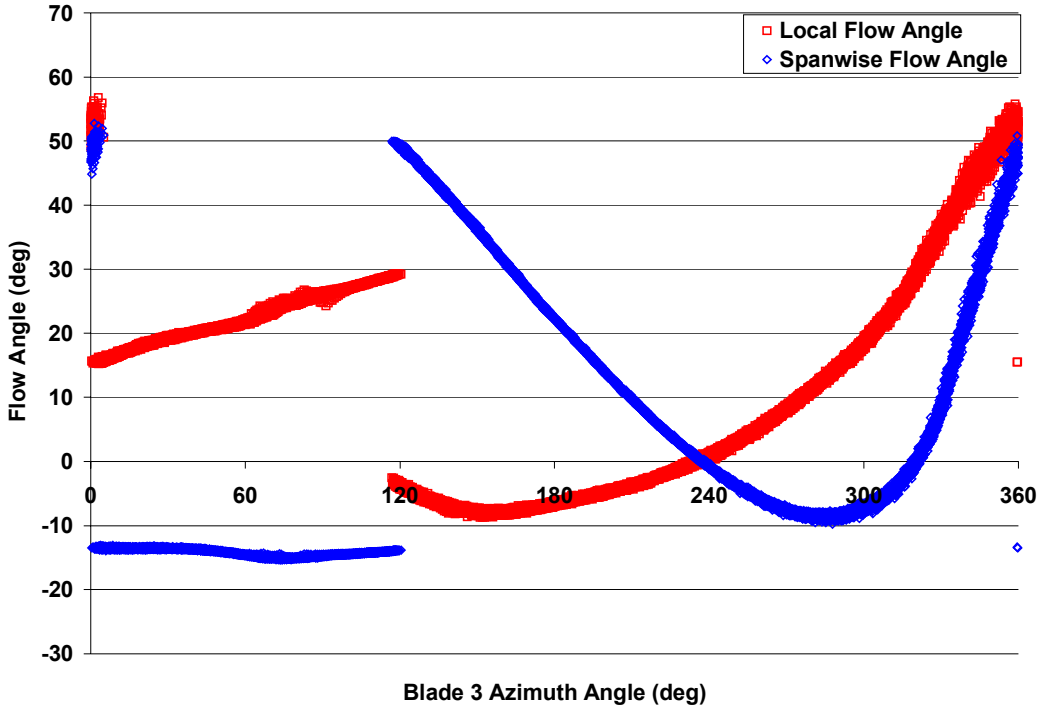

Figure 23. Example of tunnel flow angle exceeding probe range as evidenced with flow angle measurements

The shaded area in Figure 24 approximates the region of the rotational cycle where pressure measurements may be affected by the wake of the boom and instrumentation boxes or the tunnel flow with respect to the probe. These instances are evident in time-traces of dynamic pressure measurements from the blade stagnation pressure (wake interaction) and the five-hole probe dynamic pressure and flow angles (probe range). The user must be aware of these issues when studying yawed conditions.

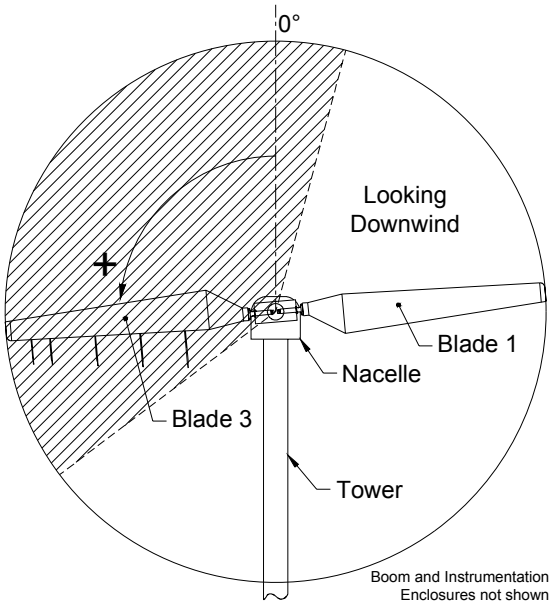

Figure 24. Region of rotor plane where pressure measurement issues must be considered

Aerodynamic Force Coefficients

The pressure distributions for rotating-blade data were integrated to compute normal force coefficients (C_N) and tangential force coefficients (C_T). They represent the forces acting perpendicular and parallel to the airfoil chord, respectively. The average pressure between two adjacent taps was first projected onto the chord line, integrated to determine the C_N values, and then projected onto an axis orthogonal to the chord and integrated to compute C_T values. IEquations 8 and 9 give the integration procedure used to determine C_N and C_T. The x and y values begin at the trailing edge (x = 1), proceed forward over the upper surface of the blade, and then aft along the bottom surface, ending at the starting point, the trailing edge.

$$C_N = \sum_{i=1}^{\#oftaps} \left(\frac{C_{p_i} + C_{p_{i+1}}}{2} \right) \left(x_{i+1} - x_i \right), \text{ and} \qquad \text{(Eq. 8)}$$

$$C_T = \sum_{i=1}^{\#oftaps} \left(\frac{C_{p_i} + C_{p_{i+1}}}{2} \right) \left(y_{i+1} - y_i \right); \qquad \text{(Eq. 9)}$$

where
C_p = normalized pressure coefficient
x_i = normalized distance along chord line from leading edge to i^{th} pressure tap
y_i = normalized distance from chord line along axis orthogonal to chord to i^{th} pressure tap.

In a similar integral procedure, pitching moment coefficients (C_M) were determined. The pitching moment represents the total moment about the 1/4 chord due to the normal and tangential forces at a pressure tap with the vertical or horizontal distance from the pitch axis as the moment arm. Note that the pitch and twist axis is at 30% chord. This equation follows:

$$C_M = -\sum_{i=1}^{\#oftaps} \left[\left(\frac{C_{p_i} + C_{p_{i+1}}}{2} \right) \left[\left(x_{i+1} - x_i \right) \left(\frac{x_{i+1} - x_i}{2} + x_i - 0.25 \right) + \left(y_{i+1} - y_i \right) \left(\frac{y_{i+1} - y_i}{2} + y_i \right) \right] \right] \qquad \text{(Eq. 10)}$$

All other airfoil performance coefficients, such as torque (C_{TQ}) and thrust (C_{TH}), were computed using the C_N and C_T values in conjunction with their reference angles. Torque and thrust coefficients were calculated as a function of blade pitch angle (β) and local twist angle (ϕ), both of which were easily measured. To maintain the convention of thrust coefficient positive perpendicular to the plane of rotation, the cone angle must be included. The torque coefficient includes cone angle such that multiplication by a moment arm along the blade span would result in torque due to a force at the radial distance in the plane of rotation.

$$C_{TQ} = (C_N \sin(\phi + \beta) + C_T \cos(\phi + \beta)) * \cos(cone), \quad \text{(Eq. 11)}$$

$$C_{TH} = (C_N \cos(\phi + \beta) - C_T \sin(\phi + \beta)) * \cos(cone). \quad \text{(Eq. 12)}$$

All of the aerodynamic force coefficients are listed in Table 21 and illustrated in Figure 24.

Table 21. Aerodynamic Force Coefficients

Channel	Channel ID	Description	Units
825	CN30	Normal force coefficient at 30% span	Cn
826	CT30	Tangent force coefficient at 30% span	Ct
827	CTH30	Thrust coefficient at 30% span	Cth
828	CTQ30	Torque coefficient at 30% span	Ctq
829	CM30	Pitch moment coefficient at 30% span	Cm
831	CN47	Normal force coefficient at 47% span	Cn
832	CT47	Tangent force coefficient at 47% span	Ct
833	CTH47	Thrust coefficient at 47% span	Cth
834	CTQ47	Torque coefficient at 47% span	Ctq
835	CM47	Pitch moment coefficient at 47% span	Cm
837	CN63	Normal force coefficient at 63% span	Cn
838	CT63	Tangent force coefficient at 63% span	Ct
839	CTH63	Thrust coefficient at 63% span	Cth
840	CTQ63	Torque coefficient at 63% span	Ctq
841	CM63	Pitch moment coefficient at 63% span	Cm
843	CN80	Normal force coefficient at 80% span	Cn
844	CT80	Tangent force coefficient at 80% span	Ct
845	CTH80	Thrust coefficient at 80% span	Cth
846	CTQ80	Torque coefficient at 80% span	Ctq
847	CM80	Pitch moment coefficient at 80% span	Cm
849	CN95	Normal force coefficient at 91% span	Cn
850	CT95	Tangent force coefficient at 91% span	Ct
851	CTH95	Thrust coefficient at 91% span	Cth
852	CTQ95	Torque coefficient at 91% span	Ctq
853	CM95	Pitch moment coefficient at 91% span	Cm

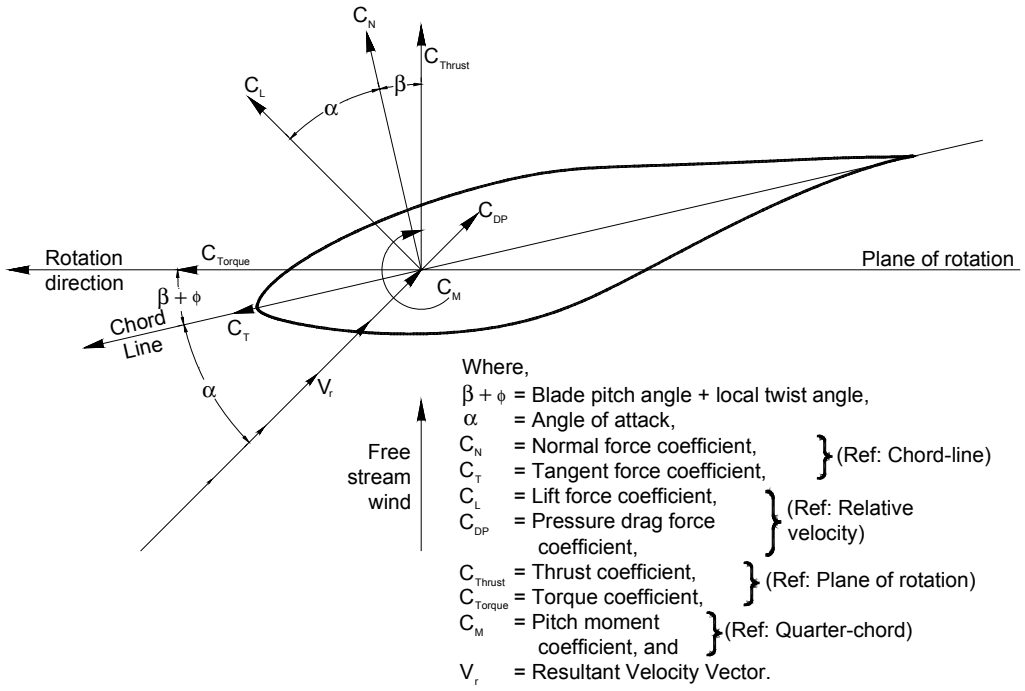

Figure 25. Aerodynamic force coefficient conventions

Estimated Aerodynamic Rotor Loads

Torque and thrust coefficients were integrated along the span of the blade and multiplied by the number of blades (2) to provide a rough estimate of the total aerodynamic thrust and torque applied to the entire rotor. This integration divided the blade into panels that extend halfway between full-chord pressure tap locations. It was assumed that the pressure at the pressure tap location was applied evenly over the corresponding panel. The panel at the root began at 25% span and extended to halfway between the 30% and 47% span stations. The panel at the tip began halfway between the 80% and 95% stations and extended to the tip. There is no tip loss model applied. Because the thrust and torque coefficients are relative to the plane of rotation, the cone angle does not appear in these equations. In highly yawed conditions, the assumption that each blade is enduring the same load is clearly incorrect. These estimates are provided primarily for the purpose of rough measurement crosschecking and estimating general trends in uniform flow conditions. They are not intended to be valid under yawed conditions. Thrust is positive downwind and torque is positive in the direction of rotation. These derived channels appear in Table 22, and the equations follow:

$$EAEROTH = 2 * \sum_{n=1}^{5} C_{TH\,n} * QNORM_n * area_n \qquad \text{(Eq. 13)}$$

$$EAEROTQ = 2 * \sum_{n=1}^{5} C_{TQ\,n} * QNORM_n * area_n * r_n \qquad \text{(Eq. 14)}$$

where
n = index for each panel
QNORM = blade stagnation pressure at full-chord pressure tap location, Pa
area = area of each trapezoidal panel, m^2
r = radial location to full-chord pressure tap location along the blade span, m.

The blade root flap bending moment was measured with strain gauges, but it was also estimated using the pressure measurements and the teeter link force. The root flap bending moment was estimated by integrating the normal and tangential coefficients in the plane of the tip chord to correspond with the alignment of the root flap strain gauges. This integration used the same panels as the thrust and torque integrals. The strain gauges were located 0.432 m from the center of rotation, and the moment arm was adjusted accordingly. When the blade is coned, there is a contribution to the measured root flap moment from the blade inertia (B_M) in addition to the aerodynamic contribution. This contribution was estimated using the blade mass and center of gravity (r_{CG}) from Appendix A as follows. Estimated aerodynamic root flap bending moment is positive due to a downwind force applied at the tip of the blade.

$$B_M = mass * r_{CG} * \left(RPM * \frac{\pi}{30} \right)^2 * \cos(cone) * (r_{CG} - 0.432) * \sin(cone) \quad \text{(Eq. 15)}$$

$$EAERORFB = -B_M + \sum_{n=1}^{5} (C_N * \cos(Twist) + C_T * \sin(Twist)) * QNORM_n * area_n * (r_n - 0.432) \quad \text{(Eq. 16)}$$

Another estimate of the root flap bending moment was obtained using the estimated thrust and the teeter link force. A free-body diagram of the hub and blade root results in (1) the measured strain gauge moment at the blade root, (2) the blade thrust applied as a shear force at the strain gauge location, (3) the teeter link force applied 0.249 m from the teeter pin, and (4) the mass momentum of the hub itself at a distance from the teeter pin. Summation of the moments about the teeter pin is zero, and solving for the measured strain gauge moment yields an estimate of that measurement. There are two equations, one for the upwind configuration and one for the downwind configuration. This is necessary to maintain the convention of the measured root flap bending moment regardless of the rotor configuration. Note that this channel only contains relevant data for the teetered rotor sequences (B, C, D, G, and 4). The teeter link was pretensioned in order to maintain rigidity in the hub for all other sequences.

Downwind: $$ETEEMRFB = TLINKF * D_{TL} - \frac{EAEROTH}{2} * D_{SG} - F_{hub} D_{hub} \quad \text{(Eq. 17)}$$

Upwind: $$ETEEMRFB = TLINKF * D_{TL} - \frac{EAEROTH}{2} * D_{SG} + F_{hub} D_{hub} \quad \text{(Eq. 18)}$$

where
D_{TL} = 0.249, m
D_{SG} = 0.432*cos(B3FLAP), m
F_{HUB} = ½ (**237**)*(RPM*π/30)^2*(0.282)*cos(B3FLAP), N
D_{HUB} = 0.029-0.282*sin(B3FLAP), m.

Table 22. Estimated Aerodynamic Rotor Loads

Channel	Channel ID	Description	Units
815	EAEROTH	Estimated aerodynamic thrust	N
816	EAEROTQ	Estimated aerodynamic torque	Nm
817	EAERORFB	Estimated aerodynamic root flap bending moment	Nm
818	ETEEMRFB	Estimated root flap bending moment from teeter	Nm

Flow Angles

The 5-hole probes measure the local flow angle and the spanwise flow angle as shown in Figures 25 and 26 and listed in Table 24. The angular values are extracted from tables based upon the neural network surfaces. The normalized difference between opposing ports in each five-hole probe is used to locate the resulting angle in each table. Tables exist for each probe for both the local flow angle and the spanwise flow angle. During the sequences when the 5-hole probes were removed, "dummy" channels were created containing values of –9999.99 to maintain a consistent file size. The numbers referring to the span location in the ID codes were replaced with DP to signify "dummy probes."

The probe stalks were designed to be aligned with the chord and perpendicular with the pitch and twist axis. The probes were then attached to the stalk at a nominal 20° angle to place the probe in better alignment with the flow when the turbine is operating. The actual angle between the chord and the probe (γ) was measured at each span location. The angle between the probe and the plane perpendicular to the pitch and twist axis (ε) was also measured. Table 23 contains these measured angles between each probe and the chord. The local flow angle and spanwise flow angle channels contain the angles of the flow relative to the chord. The transformation equations to obtain the angle relative to the blade chord instead of the probe follow:

$$LFA = \tan^{-1}\left(\frac{\cos\alpha * \cos(\theta+\varepsilon) * \sin\gamma + \sin\alpha\cos\gamma}{\cos\alpha * \cos(\theta+\varepsilon) * \cos\gamma - \sin\alpha\sin\gamma}\right) \quad \text{(Eq. 19)}$$

$$SFA = \tan^{-1}\left(\frac{\cos\alpha\sin(\theta+\varepsilon)}{\cos\alpha\cos(\theta+\varepsilon)\cos\gamma - \sin\alpha\sin\gamma}\right) \quad \text{(Eq. 20)}$$

where
α = local flow angle with respect to probe, deg
θ = spanwise flow angle with respect to probe, deg
ε = spanwise probe angle offset, deg
γ = local flow probe angle offset, deg.

Table 23. Five-hole Probe Offset Angles

Span Location	Local flow angle (γ), degrees	Spanwise flow angle (ε), degrees
34%	22.4	-0.9
51%	19.9	-1.0
67%	22.1	0.7
84%	21.3	-0.7
91%	20.3	-0.4

Table 24. Flow Angle Measurements

Channel	Channel ID	Description	Units
866	5HP34A	5 hole probe 34% span local flow angle	deg
869	5HP51A	5 hole probe 51% span local flow angle	deg
872	5HP67A	5 hole probe 67% span local flow angle	deg
875	5HP84A	5 hole probe 84% span local flow angle	deg
878	5HP91A	5 hole probe 91% span local flow angle	deg
867	5HP34F	5 hole probe 34% span spanwise flow angle	deg
870	5HP51F	5 hole probe 51% span spanwise flow angle	deg
873	5HP67F	5 hole probe 67% span spanwise flow angle	deg
876	5HP84F	5 hole probe 84% span spanwise flow angle	deg
879	5HP91F	5 hole probe 91% span spanwise flow angle	deg

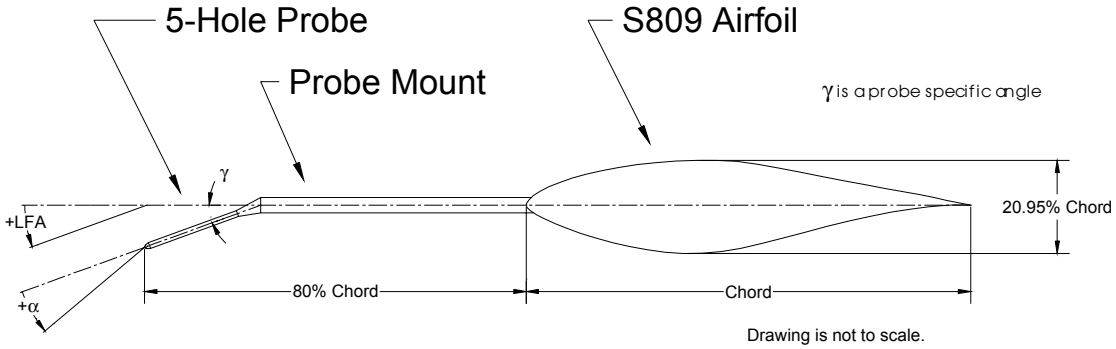

Figure 26. Local flow angle measurement convention

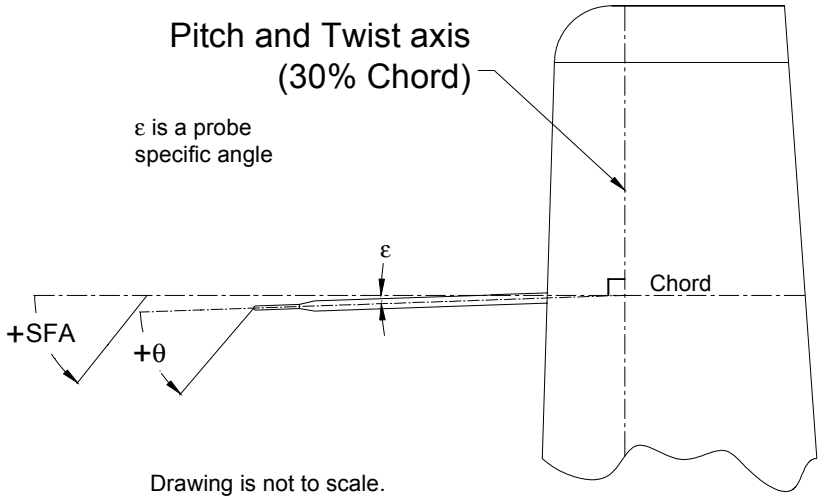

Figure 27. Spanwise flow angle measurement convention

Yaw Error

The yaw error angle was computed using the measured turbine yaw angle and the turntable angle. For all tests, with the exception of Tests 6, 7, 8, and 9, the turntable was at zero degrees. Thus, the measurement convention for yaw angle depicted in Appendix B corresponds to the measurement convention for yaw error. The following equation illustrates the computation of yaw error using the ID codes for the measured channels.

$$YAWERR = YAW + YAWTABLE \quad \text{(Eq. 21)}$$

Teeter Angle

The teeter angle was computed according to Equation 22 using each blade flap angle. The measurement convention is shown in Figure 20. Although this angle only pertains to teetered rotor tests (Sequences B, C, D, G, and 4), it is included in all data files.

$$TEETER = \frac{B3FLAP - B1FLAP}{2} \quad \text{(Eq. 22)}$$

Cone Angle

The cone angle was computed according to Equation 23 using each blade flap angle. The measurement convention is shown in Figure 20. The nominal cone angle was used in the equations above rather than the instantaneous cone angle contained here.

$$CONE = \frac{B3FLAP + B1FLAP}{2} \quad \text{(Eq. 23)}$$

Sonic Anemometer Wind Speed

The wind speed computed from the sonic anemometers is simply the vector sum of the U and V components for each anemometer. The following equation illustrates this computation for the east sonic anemometer.

$$LMSWS1 = \sqrt{LESU8M^2 + LESV8M^2} \quad \text{(Eq. 24)}$$

The wind direction is usually obtained from the vector components of the sonic anemometer readings. However, the microphone stands upon which the sonic anemometers were mounted were not stiff. The sonic anemometers themselves moved angularly in the flow as the stands moved. Thus, computation of wind direction would be contaminated with the anemometer motion, and it is not included in the data files.

Rotation Parameters

The rotor speed was computed using a 150-sample buffer, the known sample rate of 520.83 Hz, and the rotor azimuth position (B3AZI). This equates to a resolution of roughly 0.05 rpm. A counter was also activated at each zero crossing of the blade 3 azimuth angle to count the number of blade rotations throughout a campaign. These channels are listed in Table 25. During parked

blade tests (L, O, 3, and 6), these channels are included in the engineering unit files, and they read "0."

Table 25. Miscellaneous Channels

Channel	Channel ID	Description	Units
810	YAWERR	Yaw error angle	deg
811	TEETER	Teeter angle	deg
812	CONE	Cone angle	deg
813	RPM	Rotational speed	rpm
814	CYCLECNT	Cycle count	rev
858	LMSWS1	Sonic #1 wind speed (East)	m/s
863	LMSWS2	Sonic #2 wind speed (West)	m/s

Loads from Strain Gauge Measurements

The low-speed shaft torque strain gauge measures some bending due to gravity as the rotor rotates. To compensate for this, a static, non-rotating data point was collected at 5º azimuth increments throughout a complete rotation. The torque measurement was fit with a sine wave. This sine wave was subtracted from the measured torque as a function of azimuth angle to eliminate the effect of gravity only. This correction does not compensate for dynamic effects. The correction differs between upwind and downwind configuration because the rotor turns in the opposite direction relative to the nacelle. For the high cone angle test, Sequence F, the strain gauge zero calibration data at 30º azimuth increments was used to develop a sinusoidal correction to accommodate the increased gravitational effect because of the high cone angle. The following equations illustrate the correction as a function of measured low-speed shaft torque (LSSTQ) and blade 3 azimuth angle (B3AZI).

Downwind: $$LSSTQCOR = LSSTQ - 252.82 * \cos(B3AZI - 182.65) \quad \text{(Eq. 25)}$$

Downwind, High Cone Angle:

$$LSSTQCOR = LSSTQ - 315.34 * \cos(B3AZI - 182.65) \quad \text{(Eq. 26)}$$

Upwind: $$LSSTQCOR = LSSTQ + 252.82 * \cos(B3AZI - 177.35) \quad \text{(Eq. 27)}$$

The two, low-speed shaft bending measurements were broken into horizontal and vertical vector components as shown in the following equations. The horizontal component is positive due to a force in the direction that will cause positive yaw moment. The vertical component is positive in the direction because of the gravitational force. There are two pairs of equations, one for the upwind configuration and one for the downwind configuration. This accounts for the different rotational direction with respect to the nacelle.

Downwind: $$\begin{aligned} LSSVB &= LSSXXB * \cos(B3AZI + 120) + LSSYYB * \cos(B3AZI + 210) \\ LSSHB &= LSSXXB * \sin(B3AZI + 120) + LSSYYB * \sin(B3AZI + 210) \end{aligned} \quad \text{(Eq. 28)}$$

Upwind: $$\begin{aligned} LSSVB &= LSSXXB * \cos(B3AZI + 240) + LSSYYB * \cos(B3AZI + 150) \\ LSSHB &= -(LSSXXB * \sin(B3AZI + 240) + LSSYYB * \sin(B3AZI + 150)) \end{aligned} \quad \text{(Eq. 29)}$$

The aerodynamic power produced by the rotor was computed using the corrected low-speed shaft torque measurement and the rotational speed computation. Note that this quantity differs from the power produced by the generator (because of generator and drivetrain losses), which was measured with a watt transducer (GENPOW).

$$ROTPOW = LSSTQCOR * RPM * \frac{\pi}{30{,}000} \qquad \text{(Eq. 30)}$$

Table 26. Loads from Strain Gauge Measurements

Channel	Channel ID	Description	Units
819	LSSTQCOR	Low-speed shaft torque, corrected	Nm
820	LSSHB	Low-speed shaft bending-horizontal	Nm
821	LSSVB	Low-speed shaft bending-vertical	Nm
822	ROTPOW	Aerodynamic power from rotor	kW

Wind Tunnel Scale Forces and Moments

The seven scale measurements were used to compute three forces and three moments about the low-speed shaft at hub height. The equations are contained in Appendix D, the NASA Software Requirements Document (Equations 605–610). These equations assume that the distances are in feet and the scale measurements are in pounds. The *munch.exe* processing software outputs these forces and moments in SI units. Because no weight or aerodynamic tares were applied to the load cell measurements, the drag force is measured directly by the load cell, WTDRAG. The measurement conventions are shown in Figure 27.

Table 27. Forces and Moments from Wind Tunnel Balance System

Channel	Channel ID	Description	Units
886	WTLIFTF	Wind tunnel lift force	N
356	WTDRAG	Wind tunnel drag (#7)	N
888	WTPITCHM	Wind tunnel pitch moment	N
889	WTSIDEF	Wind tunnel side force	Nm
890	WTYAWM	Wind tunnel yaw moment	Nm
891	WTROLLM	Wind tunnel roll moment	Nm

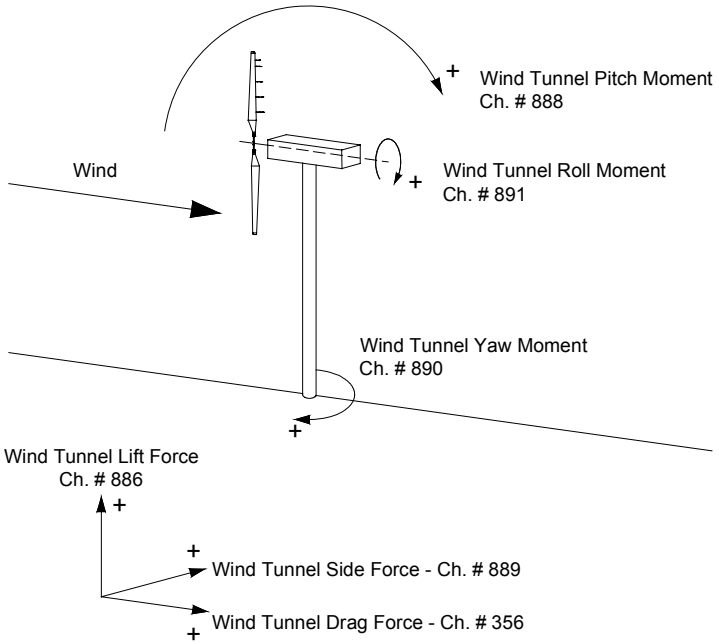

Figure 28. Wind tunnel scale measurement conventions

References

Butterfield, C.P.; Musial, W.P.; Simms, D.A. (1992). *Combined Experiment Phase I Final Report.* NREL/TP-257-4655. Golden, CO: National Renewable Energy Laboratory.

Cotrell, J.R. (1999). *The Mechanical Design, Analysis, and Testing of a Two-Bladed Wind Turbine Hub*. NREL/TP-500-26645. Golden, CO: National Renewable Energy Laboratory.

Fingersh, L.J; Robinson, M.C. (1997). "Wind Tunnel Calibration of 5-hole Pressure Probes for Application to Wind Turbines." *Proceedings of 16th ASME Wind Energy Symposium, January 6-9, Reno, NV*. New York: American Institute for Aeronautics and Astronautics.

Freeman, J.B.; Robinson, M.C. (1998). "Algorithm Using Spherical Coordinates to Calculate Dynamic Pressure from 5-Hole Pressure Probe Data." *Proceedings of 1998 ASME Wind Energy Symposium, January 12-15, Reno, NV*. New York: American Institute for Aeronautics and Astronautics.

Gessow, A.; Myers, G. (1967). *Aerodynamics of the Helicopter*. New York, New York: Frederick Ungar Publishing Co.

Giguere, P.; Selig, M.S. (1999). *Design of a Tapered and Twisted Blade for the NREL Combined Experiment Rotor.* NREL/SR-500-26173. Golden, CO: National Renewable Energy Laboratory.

Glauert. H. (1947). *The Elements of Aerofoil and Wing Theory* (2nd. ed.), Cambridge University Press.

Hand, M.M.; Simms, D.A.; Fingersh, L.J.; Jager, D.W.; Cotrell. J.R. (2001). *Unsteady Aerodynamics Experiment Phase V: Test Configurations and Available Data Campaigns.* NREL/TP-500-29491. Golden, CO: National Renewable Energy Laboratory.

National Full-Scale Aerodynamic Complex (NFAC). (Revised Summer 1993). *NFAC Operations Manual Part 4A -Test Planning Guide.* Moffett Field, CA: NASA Ames Research Center, National Full-Scale Aerodynamics Division.

Reuss Ramsay, R.; Hoffman, M.J.; Gregorek, G.M. (1995). *Effects of Grit Roughness and Pitch Oscillations on the S809 Airfoil*. NREL/TP-442-7817. Golden, CO: National Renewable Energy Laboratory.

Schepers, J.G.; Brand, A.J.; Bruining, A.; Graham, J.M.R.; Hand, M.M.; Infield, D.G.; Madsen, H.A.; Paynter, R.J.H.; Simms, D.A. (1997). *Final Report of IEA Annex XIV: Field Rotor Aerodynamics*. ECN-C-97-027. Petten, the Netherlands: Netherlands Energy Research Foundation ECN.

Shipley, D.E.; Miller, M.S.; Robinson, M.C.; Luttges, M.W.; Simms, D.A. (1995). *Techniques for the Determination of Local Dynamic Pressure and Angle-of-attack on a Horizontal Axis Wind Turbine*. NREL/TP-442-7393. Golden, CO: National Renewable Energy Laboratory.

Simms, D.; Schreck, S.; Hand, M.; Fingersh, L.J. (2001). *NREL Unsteady Aerodynamics Experiment in the NASA-Ames Wind Tunnel: A Comparison of Predictions to Measurements*. NREL/TP–500-29494. Golden, CO: National Renewable Energy Laboratory.

Simms, D.; Schreck, S.; Hand, M.; Fingersh, L.; Cotrell, J.; Pierce, K.; Robinson, M. (1999a). *Plans for Testing the NREL Unsteady Aerodynamics Experiment 10m Diameter HAWT in the NASA Ames Wind Tunnel*. NREL/TP-500-27599. Golden, CO: National Renewable Energy Laboratory.

Simms, D.A.; Hand, M.M.; Fingersh, L.J.; Jager, D.W. (1999b). *Unsteady Aerodynamics Experiment Phases II-IV: Test Configurations and Available Data Campaigns.* NREL/TP-500-25950. Golden, CO: National Renewable Energy Laboratory.

Simms, D.A.; Butterfield, C.P. (1991). *A PC-Based Telemetry System for Acquiring and Reducing Data from Multiple PCM Streams*. SERI/TP-257-4123. Golden, CO: Solar Energy Research Institute (now known as National Renewable Energy Laboratory).

Somers, D.M. (1997). *Design and Experimental Results for the S809 Airfoil*. NREL/SR-440-6918. Golden, Colorado: National Renewable Energy Laboratory.

Zell, P.T. (1993). *Performance and Test Section Flow Characteristics of the National Full-Scale Aerodynamics Complex 80- by 120-Foot Wind Tunnel.* NASA TM 103920.

Zell, P.T. (24 August 2000). Internal memorandum. NASA Ames Research Center.

Appendix A: Machine Data for Phase VI Turbine

Basic Machine Parameters

- Number of blades: 2
  - Rotor diameter: varies with tip attachment
  - 10.058 m with standard tip or smoke tip (all sequences except V and W)
  - 9.886 m with tip plate (Sequence V)
  - 11.064 m with tip extension (Sequence W)
- Hub height: 12.192 m
- Type of rotor: teetered (Sequences B, C, D, G, and 4) or rigid
- Rotational speed: 71.63 RPM synchronous speed, 90 RPM (Sequence X only) using Square D, variable-speed drive
- Cut-in wind speed: 6 m/s some tests were run at 5 m/s
- Power regulation: stall
- Rated power: 19.8 kW
- Tilt: 0°
- Cone angle: 0°, 3.4°, or 18°
- Location of rotor: upwind or downwind
- Rotational direction: counterclockwise (viewed from upwind)
- Rotor overhang: 1.401 m (yaw-axis to blade-axis); 1.469 m (yaw-axis to teeter pin)

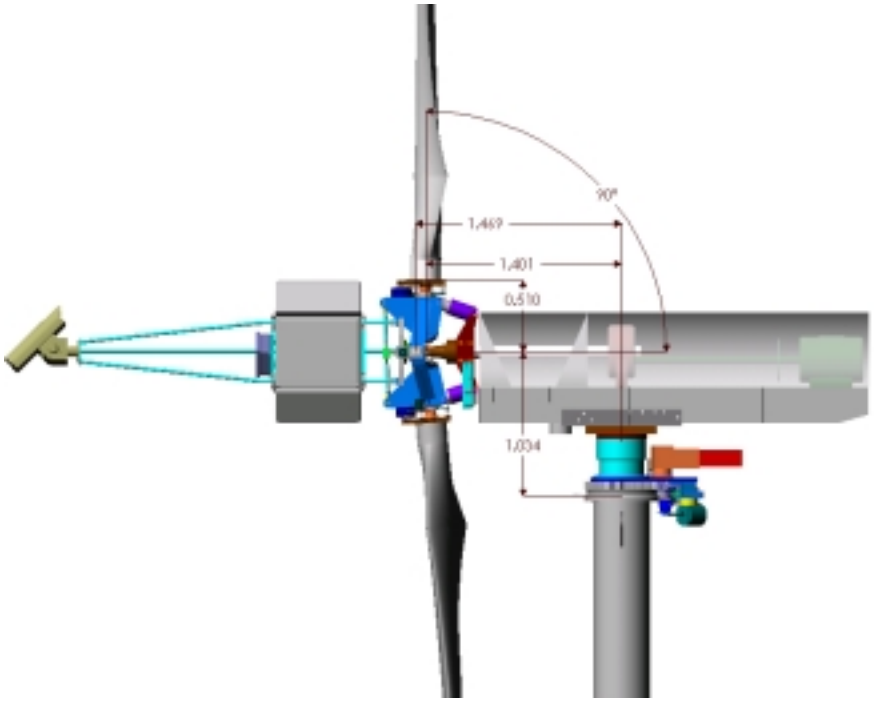

Figure A-1. Turbine rotor, 0° cone angle shown (dimensions in meters)

Rotor

Geometry

- Blade cross section and planform: NREL S809, tapered and twisted
- Root extension from center of rotation to airfoil transition: 0.883 m
- Blade tip pitch angle (manually set by turbine operator): 0°, 2°, 3°, 4°, 6°, cycling, ramping, (see each data file).
- Blade profile: NREL S809
- Blade chord: see Table A-1.
- Blade twist: see Table A-1.

Table A-1. Blade chord and twist distributions

Radial Distance r (m)	Span Station[1] (r/5.532 m)	Span Station[1] (r/5.029 m)	Chord Length (m)	Twist[2] (degrees)	Thickness (m)	Twist Axis (% chord)
0.0	0.0	0.0	Hub - center of rotation	Hub – center of rotation	Hub – center of rotation	Hub - center of rotation
0.508[3]	0.092	0.101	0.218 (root hub adapter)	0.0 (root hub adapter)	0.218	50 (root hub adapter)
0.660[4]	0.120	0.131	0.218	0.0	0.218	50
0.883[5]	0.160	0.176	0.183	0.0	0.183	50
1.008[5]	0.183	0.200	0.349	6.7	0.163	35.9
1.067[5]	0.193	0.212	0.441	9.9	0.154	33.5
1.133[5]	0.205	0.225	0.544	13.4	0.154	31.9
1.257[5]	0.227	0.250	0.737	20.040	0.154	30
1.343	0.243	0.267	0.728	18.074	20.95% chord	30
1.510	0.273	0.300	0.711	14.292	20.95% chord	30
1.648	0.298	0.328	0.697	11.909	20.95% chord	30
1.952	0.353	0.388	0.666	7.979	20.95% chord	30
2.257	0.408	0.449	0.636	5.308	20.95% chord	30
2.343	0.424	0.466	0.627	4.715	20.95% chord	30
2.562	0.463	0.509	0.605	3.425	20.95% chord	30
2.867	0.518	0.570	0.574	2.083	20.95% chord	30
3.172	0.573	0.631	0.543	1.150	20.95% chord	30
3.185	0.576	0.633	0.542	1.115	20.95% chord	30
3.476	0.628	0.691	0.512	0.494	20.95% chord	30
3.781	0.683	0.752	0.482	-0.015	20.95% chord	30
4.023	0.727	0.800	0.457	-0.381	20.95% chord	30
4.086	0.739	0.812	0.451	-0.475	20.95% chord	30
4.391	0.794	0.873	0.420	-0.920	20.95% chord	30
4.696	0.849	0.934	0.389	-1.352	20.95% chord	30
4.780	0.864	0.950	0.381	-1.469	20.95% chord	30
5.000	0.904	0.994	0.358	-1.775	20.95% chord	30
5.305	0.959	1.055	0.328	-2.191	20.95% chord	30
5.532	1.000	1.100	0.305	-2.500	20.95% chord	30

[1.] The blade radius is modified by changing the tip piece.

[2.] Twist convention is positive towards feather. Values listed are relative to zero twist at the 3.772-m station [75% span on a 5.029-m blade]. Twist is 2.5 degrees toward stall at the tip [on a 5.532-m blade].

[3.] Each blade attaches to the hub at a point 0.508 m from the center of rotation.

[4.] There is a cylindrical section at the root that extends from 0.508 to 0.883 m. The airfoil transition begins at approximately the 0.883-m radial station.

[5.] There is a transition from the cylindrical section to the S809 airfoil along the 0.883- to 1.257-m region. The transition ends with a 0.737-m chord S809 airfoil at the 1.257-m span station.

- Airfoil distribution: Except for the root [0 to 1.257 m, the blade uses the S809 at all span locations. The airfoil coordinates are shown in Table A-2, and the root is depicted in Figure A-2.

Table A-2. Airfoil profile coordinates

Upper Surface		Lower Surface	
x/c	y/c	x/c	y/c
0.00037	0.00275	0.00140	-0.00498
0.00575	0.01166	0.00933	-0.01272
0.01626	0.02133	0.02321	-0.02162
0.03158	0.03136	0.04223	-0.03144
0.05147	0.04143	0.06579	-0.04199
0.07568	0.05132	0.09325	-0.05301
0.10390	0.06082	0.12397	-0.06408
0.13580	0.06972	0.15752	-0.07467
0.17103	0.07786	0.19362	-0.08447
0.20920	0.08505	0.23175	-0.09326
0.24987	0.09113	0.27129	-0.10060
0.29259	0.09594	0.31188	-0.10589
0.33689	0.09933	0.35328	-0.10866
0.38223	0.10109	0.39541	-0.10842
0.42809	0.10101	0.43832	-0.10484
0.47384	0.09843	0.48234	-0.09756
0.52005	0.09237	0.52837	-0.08697
0.56801	0.08356	0.57663	-0.07442
0.61747	0.07379	0.62649	-0.06112
0.66718	0.06403	0.67710	-0.04792
0.71606	0.05462	0.72752	-0.03558
0.76314	0.04578	0.77668	-0.02466
0.80756	0.03761	0.82348	-0.01559
0.84854	0.03017	0.86677	-0.00859
0.88537	0.02335	0.90545	-0.00370
0.91763	0.01694	0.93852	-0.00075
0.94523	0.01101	0.96509	0.00054
0.96799	0.00600	0.98446	0.00065
0.98528	0.00245	0.99612	0.00024
0.99623	0.00054	1.00000	0.00000
1.00000	0.00000	0.00000	0.00000

(Source: Butterfield et. al, 1992)

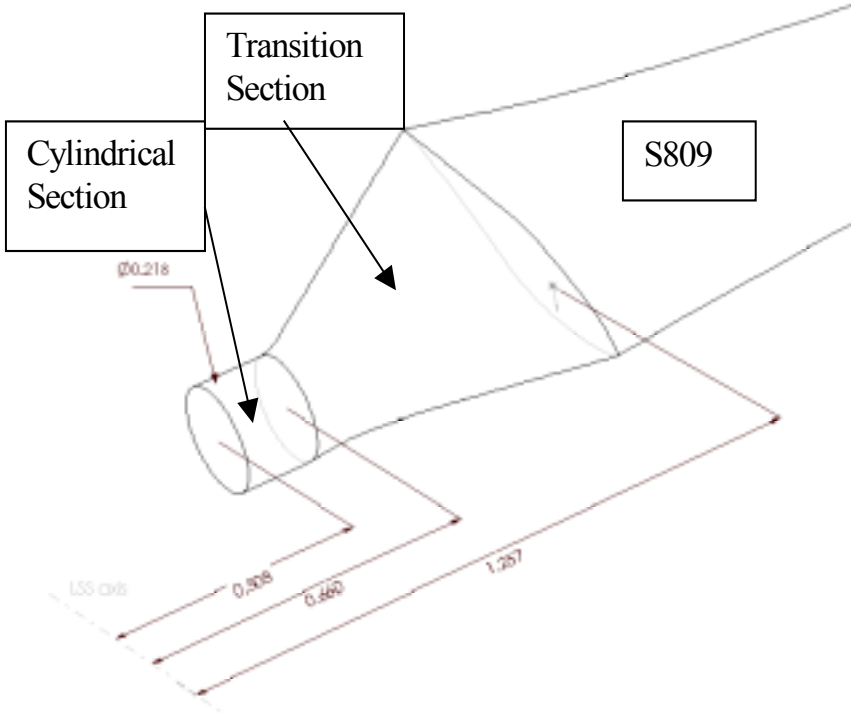

Figure A-2. Blade root surface depiction (dimensions in meters)

Blade tip attachment:

- All tip pieces attach at a radius of 4.938 m (Figures A-3 and A-4). Plastic tape, 0.03 mm (7 mil) thick was used to smooth the transition from the blade to the tip attachment.
- Standard and smoke tips are same dimensions, resulting in 5.029-m radius (Figure A-5).
- Tip plate: 0.005-m thick 5052-H32 aluminum, edges machined to 2.4-mm radius (Figures A-7 and A-8).
- Blade extension: S809 airfoil (see Table A-1, Figure A-6).

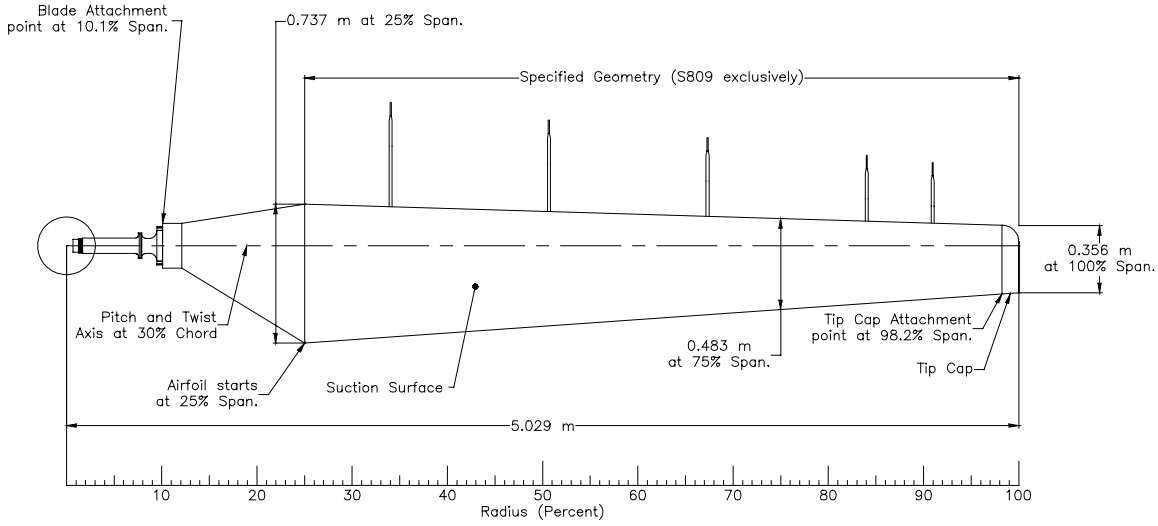

Figure A-3. Blade planform for standard tip or smoke tip

Figure A-4. Attachment point at blade tip (r = 4.938 m)

Figure A-5. Smoke tip with smoke generator inside

Figure A-6. Blade extension (Sequence W)

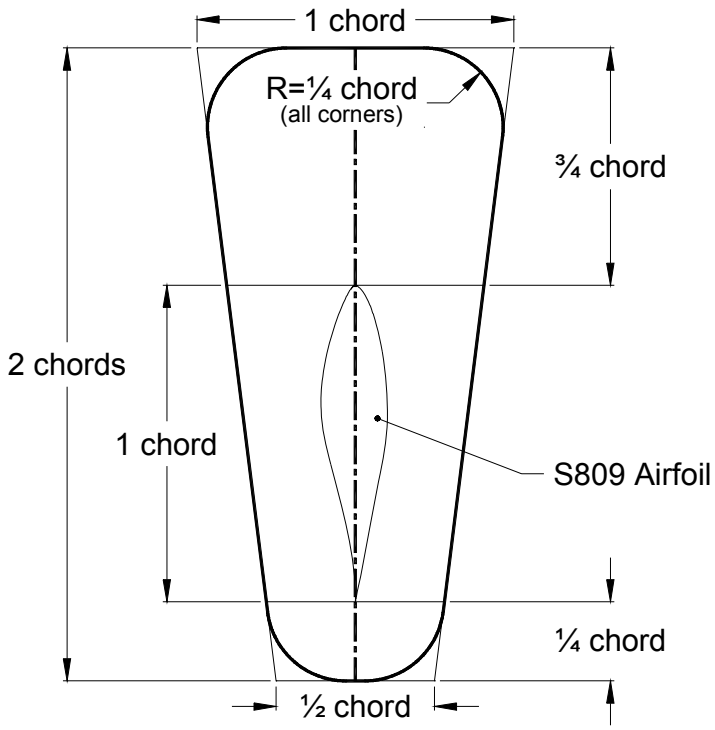

Figure A-7. Tip plate dimensions for chord of 0.143 m (Sequence V)

Figure A-8. Tip plates installed (Sequence V)

Aerodynamic Coefficients for S809 Airfoil

Aerodynamic coefficients (α = angle of attack, C_l = lift coefficient, C_{dp} = pressure drag coefficient) obtained at the Colorado State University (CSU) wind tunnel with a Reynolds number of 300,000 are shown in Table A-3 (Butterfield et al. 1992).

Table A-3. Wind tunnel profile coefficients from CSU (Re = 300,000)

α	C_l	C_{dp}
0	0.105	0.0117
1.99	0.307	0.0116
4.08	0.545	0.0139
6.11	0.748	0.0135
8.14	0.88	0.0198
10.2	0.878	0.036
11.2	0.87	0.0446
12.2	0.854	0.0496
13.1	0.877	0.0619
14.1	0.894	0.0731
15.2	0.891	0.0865
16.3	0.745	0.22
17.2	0.591	0.248
18.1	0.592	0.265
19.2	0.58	0.279
20.2	0.604	0.298
22.1	0.588	0.323
26.2	0.669	0.412
30.2	0.946	0.633
35.2	1.02	0.799
40.3	1.08	0.983
45.2	1.23	1.31
45.1	1.13	1.21
50	1.21	1.51
60	1.05	1.86
69.9	0.805	2.27
80	0.456	2.16
90	0.128	2.24

- Aerodynamic coefficients (α = angle of attack, C_l = lift coefficient, C_{dp} = pressure drag coefficient) obtained at the CSU wind tunnel with a Reynolds number of 500,000 are shown in Table A-4 (Butterfield et al. 1992).

Table A-4. Wind tunnel profile coefficients from CSU (Re = 500,000)

α	C_l	C_{dp}
-2.23	-6.00E-02	6.00E-03
-1.61E-01	1.56E-01	4.00E-03
1.84	3.69E-01	6.00E-03
3.88	5.71E-01	8.00E-03
5.89	7.55E-01	9.00E-03
7.89	8.60E-01	1.70E-02
8.95	8.87E-01	2.40E-02
9.91	8.69E-01	3.50E-02
10.9	8.68E-01	3.90E-02
12	8.94E-01	4.80E-02
12.9	9.38E-01	6.10E-02
14	9.29E-01	7.40E-02
14.9	9.08E-01	8.00E-02
16	9.12E-01	1.06E-01
17	6.55E-01	2.71E-01
18	5.88E-01	2.65E-01
19	5.87E-01	2.81E-01
20	5.97E-01	2.99E-01
22	6.03E-01	3.26E-01
24	6.47E-01	3.75E-01
26	6.83E-01	4.19E-01
28.1	7.45E-01	4.82E-01
30	8.24E-01	5.60E-01
35	1.05	8.17E-01
40	1.14	1.03
45	1.2	1.26
50	1.12	1.38
55	1.17	1.7
60	1.08	1.87
65	9.40E-01	1.98
70	8.57E-01	2.19
74.9	6.66E-01	2.17
79.9	4.72E-01	2.21
84.8	3.56E-01	2.32
89.9	1.42E-01	2.09

- Aerodynamic coefficients (α = angle of attack, C_l = lift coefficient, C_{dp} = pressure drag coefficient) obtained at the CSU wind tunnel with a Reynolds number of 650,000 are shown in Table A-5 (Butterfield et al. 1992).

Table A-5 Wind tunnel profile coefficients from CSU (Re = 650,000)

α	C_l	C_{dp}
-0.25	0.151	0.002
1.75	0.354	0.001
3.81	0.561	0.002
5.92	0.765	0.006
7.94	0.86	0.015
9.98	0.848	0.031
11	0.892	0.043
12	0.888	0.049
13	0.927	0.043
14	0.91	0.075
15	0.91	0.075
16	0.928	0.107
17	0.686	0.278
18	0.639	0.276
19	0.576	0.273
20	0.552	0.275
22	0.596	0.323
23.9	0.649	0.37
26	0.68	0.417
30	0.851	0.576
35	1.01	0.789
40	1.12	1.03
45	1.12	1.19
50	1.1	1.36
55.3	1.08	1.58
60.2	0.931	1.62
65.2	0.968	2
70.2	0.776	2.04
75.2	0.63	2.13
80.2	0.485	2.32
85.1	0.289	2.14
90.2	0.109	2.27

- Aerodynamic coefficients (α = angle of attack, C_l = lift coefficient, C_{dp} = pressure drag coefficient; C_{dw} = total drag coefficient from wake traverse, C_m = moment coefficient) obtained at the Ohio State University (OSU) wind tunnel with a Reynolds number from 730,000 to 770,000 are shown in Table A-6.

Table A-6. Wind tunnel profile coefficients from OSU (Re = 750,000)

α	C_l	C_{dp}	C_{dw}	C_m	Re x 10^6
-20.1	-0.56	0.3027		0.0612	0.76
-18.1	-0.67	0.3069		0.0904	0.75
-16.1	-0.79	0.1928		0.0293	0.75
-14.2	-0.84	0.0898		-0.009	0.75
-12.2	-0.7	0.0553		-0.0045	0.75
-10.1	-0.63	0.039		-0.0044	0.73
-8.2	-0.56	0.0233	0.0639	-0.0051	0.74
-6.1	-0.64	0.0112	0.0119	0.0018	0.74
-4.1	-0.42	-0.0004	0.0121	-0.0216	0.76
-2.1	-0.21	-0.0003	0.011	-0.0282	0.75
0.1	0.05	0.0029	0.0113	-0.0346	0.75
2	0.3	0.0056	0.0107	-0.0405	0.74
4.1	0.54	0.0067	0.0121	-0.0455	0.75
6.2	0.79	0.0085	0.0131	-0.0507	0.74
8.1	0.9	0.0127	0.0139	-0.0404	0.75
10.2	0.93	0.0274	0.0436	-0.0321	0.75
11.3	0.92	0.0303		-0.0281	0.74
12.1	0.95	0.0369		-0.0284	0.74
13.2	0.99	0.0509		-0.0322	0.74
14.2	1.01	0.0648		-0.0361	0.74
15.3	1.02	0.0776		-0.0363	0.74
16.3	1	0.0917		-0.0393	0.74
17.1	0.94	0.0994		-0.0398	0.73
18.1	0.85	0.2306		-0.0983	0.77
19.1	0.7	0.3142		-0.1242	0.76
20.1	0.66	0.3186		-0.1155	0.76
22	0.7	0.3694		-0.1265	0.76
24.1	0.79	0.4457		-0.1488	0.77
26.2	0.88	0.526		-0.1723	0.76

- Aerodynamic coefficients (α = angle of attack, C_l = lift coefficient, C_{dp} = pressure drag coefficient; C_{dw} = total drag coefficient from wake traverse, C_m = moment coefficient) obtained at the OSU wind tunnel with a Reynolds number from 990,000 to 1,040,000 are shown in Table A-7.

Table A-7. Wind tunnel profile coefficients from OSU (Re = 1,000,000)

α	C_l	C_{dp}	C_{dw}	C_m	Re x 10^6
-20.1	-0.55	0.2983		0.0590	1.01
-18.2	-0.65	0.2955		0.0797	1.02
-16.2	-0.80	0.1826		0.0244	1.01
-14.1	-0.79	0.0793		0.0060	0.99
-12.1	-0.70	0.0547		-0.0043	1.01
-10.2	-0.63	0.0401	0.0750	-0.0035	1.00
-8.2	-0.58	0.0266		-0.0032	1.00
-6.2	-0.61	0.0183	0.0193	0.0088	1.00
-4.1	-0.40	0.0004	0.0127	-0.0245	0.99
-2.1	-0.16	0.0009	0.0090	-0.0308	1.00
0	0.07	0.0022	0.0085	-0.0356	1.01
2.1	0.30	0.0037	0.0088	-0.0394	1.00
4.1	0.55	0.0050	0.0088	-0.0461	1.00
6.1	0.79	0.0063	0.0090	-0.0499	1.00
8.2	0.90	0.0096	0.0167	-0.0364	1.00
10.1	0.94	0.0231	0.0487	-0.0396	1.00
11.2	0.93	0.0236		-0.0280	1.00
12.2	0.97	0.0368		-0.0307	1.00
13.3	1.00	0.0551		-0.0362	0.99
14.2	1.02	0.0618		-0.0365	0.99
15.2	1.03	0.0705		-0.0375	0.99
16.2	1.01	0.0880		-0.0430	1.00
17.2	0.95	0.1043		-0.0456	0.99
18.1	0.90	0.1325		-0.0581	1.00
19.2	0.78	0.3474		-0.1464	1.02
20	0.67	0.3211		-0.1171	1.02
22.1	0.70	0.3699		-0.1253	1.02
24	0.77	0.4348		-0.1430	1.03
26.1	0.91	0.5356		-0.1783	1.04

- Aerodynamic coefficients (α = angle of attack, C_l = lift coefficient, C_{dw} = total drag coefficient, C_m = moment coefficient) obtained at the Delft University of Technology (DUT) Low Speed Laboratory low-turbulence wind tunnel with a Reynolds number of 1,000,000 are shown in Table A-8 (Somers 1997).

Table A-8. Wind tunnel profile coefficients from DUT (Re = 1,000,000)

α	C_l	C_{dw}	C_m
-1.04	0.019	0.0095	-0.0408
-0.01	0.139	0.0094	-0.0435
1.02	0.258	0.0096	-0.0462
2.05	0.378	0.0099	-0.0487
3.07	0.497	0.0100	-0.0514
4.10	0.617	0.0100	-0.0538
5.13	0.736	0.0097	-0.0560
6.16	0.851	0.0095	-0.0571
7.18	0.913	0.0127	-0.0506
8.20	0.952	0.0169	-0.0439
9.21	0.973	0.0247	-0.0374
10.20	0.952	0.0375	-0.0397
11.21	0.947	0.0725	-0.0345
12.23	1.007	0.0636	-0.0420
13.22	1.031	0.0703	-0.0420
14.23	1.055	0.0828	-0.0419
15.23	1.062	0.1081	-0.0418
16.22	1.043	0.1425	-0.0452
17.21	0.969	0.1853	-0.0458
18.19	0.938	0.1853	-0.0544
19.18	0.929	0.1853	-0.0658
20.16	0.923	0.1853	-0.0783

Structural Properties for 10.058-m-Diameter Rotor, No 5-hole Probes, Standard Tip Attachment

- Rotor mass: 577.3 kg

  There is a slight imbalance attributed to the instrumentation enclosures, hub, boom, wiring, and camera. A sine wave was fit to the measured generator power as a function of the blade 3 azimuth angle. The zero to peak torque offset is 60 Nm above the mean with the peak located at a blade 3 azimuth angle of 159°.
- Pitch shaft, bull gear, instrumentation, bearings, nut, spacers: 38.6 kg (for one blade)
- Hub mass: 237.8 kg
- Boom, instrumentation enclosures, and camera mass: 141.9 kg
- Blade mass with standard tip (without five-hole probes but with probe plugs inserted):
  - Blade 1: Balanced to match Blade 3
  - Blade 3: 60.2 kg
  - Difference between 5-hole probe mounts and 5-hole probe plugs: 0.454 kg
  - Difference between smoke tip with smoke generator and regular tip: 1.089 kg (Blade 1 balanced with counterweight)
  - Difference between tip plate and standard tip: 2.41 kg
  - Difference between blade extension and standard tip: 2.47 kg
- Blade center of gravity with standard tip, probe plugs inserted (from center of rotation):
  - Blade 1: Balanced to match Blade 3
  - Blade 3: 2.266 m
- Blade mass and stiffness distributions:

  Estimates of mass and stiffness distributions were made with an experimental code that computes blade properties using the material properties shown in Table A-9. The blade pressure transducers and polyvinyl chloride (PVC) tubing that carries instrumentation wires were included. These estimates have been validated with hand calculations for the blade portion. A satisfactory match between blade frequencies predicted with the structural estimates and the measured frequencies has not been achieved. The complex geometry and boundary conditions of the pitch shaft have not been modeled sufficiently. The elastic axis and center of gravity positions are positive toward the leading edge referenced to the pitch and twist axis of 30% chord. The *y*-axis is out-of-plane, or positive downwind, and the *x*-axis is positive toward the leading edge, or in the direction of rotation.

Table A-9. Estimated blade structural properties

Distance from Center of Rotation (m)	Sectional Mass Per Unit Length (kg/m)	Mass Moment of Inertia about *Y*-axis (kgm^4)	Mass Moment of Inertia about *X*-axis (kgm^4)	Distance to Section Center of Gravity (m)	Distance to Section Elastic Axis (m)	Torsional Stiffness (Nm^2)	Axial Stiffness (Nm)	Edgewise Stiffness (Nm^2)	Flapwise Stiffness (Nm^2)
5	6.440	4.16E-02	2.68E-03	-0.046	-0.011	2.73E+05	9.36E+07	6.71E+05	6.80E+04
4.78	6.882	5.16E-02	3.37E-03	-0.046	-0.009	3.34E+05	1.09E+08	8.45E+05	9.05E+04
4.696	7.043	5.54E-02	3.64E-03	-0.046	-0.009	3.57E+05	1.15E+08	9.14E+05	9.97E+04
4.391	7.672	7.21E-02	4.81E-03	-0.047	-0.006	4.57E+05	1.38E+08	1.21E+06	1.40E+05
4.086	8.291	9.15E-02	6.20E-03	-0.048	-0.004	5.73E+05	1.61E+08	1.56E+06	1.89E+05
4.023	8.416	9.56E-02	6.50E-03	-0.048	-0.004	5.97E+05	1.66E+08	1.63E+06	2.00E+05
3.781	8.935	1.14E-01	7.85E-03	-0.048	-0.002	7.07E+05	1.85E+08	1.97E+06	2.49E+05
3.476	9.585	1.40E-01	9.74E-03	-0.049	-0.001	8.56E+05	2.10E+08	2.44E+06	3.20E+05
3.185	10.253	1.69E-01	1.19E-02	-0.049	0.001	1.03E+06	2.35E+08	2.97E+06	4.03E+05
3.172	10.279	1.70E-01	1.20E-02	-0.049	0.001	1.03E+06	2.36E+08	2.99E+06	4.07E+05
2.867	10.853	2.04E-01	1.41E-02	-0.049	0.005	1.22E+06	2.56E+08	3.59E+06	4.79E+05
2.562	11.705	2.45E-01	1.72E-02	-0.048	0.008	1.45E+06	2.92E+08	4.38E+06	6.08E+05
2.343	12.380	2.77E-01	1.99E-02	-0.047	0.01	1.63E+06	3.21E+08	5.02E+06	7.20E+05
2.257	14.379	3.59E-01	2.44E-02	-0.057	0.004	2.19E+06	3.52E+08	6.23E+06	8.05E+05
1.952	14.741	3.94E-01	2.77E-02	-0.064	-0.002	2.45E+06	3.57E+08	6.49E+06	9.16E+05
1.648	15.210	4.29E-01	3.17E-02	-0.073	-0.013	2.74E+06	3.67E+08	6.69E+06	1.07E+06
1.51	15.623	4.51E-01	3.40E-02	-0.075	-0.016	2.89E+06	3.84E+08	6.92E+06	1.17E+06
1.343	16.134	4.78E-01	3.68E-02	-0.078	-0.019	3.09E+06	4.04E+08	7.20E+06	1.30E+06
1.257	16.265	4.88E-01	3.80E-02	-0.081	-0.023	3.18E+06	4.07E+08	7.22E+06	1.35E+06
0.883	9.973	3.98E-02	3.98E-02	0	0	4.02E+05	3.95E+08	1.65E+06	1.65E+06
0.66	33.797	6.73E-02	6.73E-02	0	0	2.14E+06	1.03E+09	4.77E+06	4.77E+06
0.61	44.797	6.73E-02	6.73E-02	0	0	3.12E+06	1.33E+09	6.10E+06	6.10E+06
0.559	50.797	6.73E-02	6.73E-02	0	0	3.68E+06	1.48E+09	6.85E+06	6.85E+06
0.508	39.557	6.26E-04	6.26E-04	0	0	3.00E+06	1.01E+09	4.06E+06	4.06E+06
0.483	223.973	1.87E-02	1.87E-02	0	0	1.31E+07	6.69E+09	1.72E+07	1.72E+07
0.369	34.784	6.99E-05	6.99E-05	0	0	3.16E+05	1.04E+09	4.16E+05	4.16E+05

- Load is carried by a carbon fiber D-spar that tapers in thickness from root to tip, shown in Figure A-9. The carbon is primarily unidirectional with ±45° S-glass fibers interwoven. The non-load-carrying skin is fiberglass.

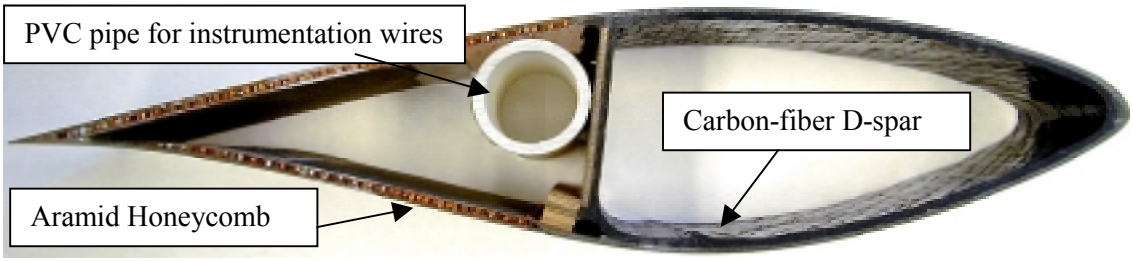

Figure A-9. Cross-section of blade

- A modal test was performed with each blade attached to a dummy pitch shaft that was clamped at the bearing locations and mounted to a concrete block. The blade orientation was with the trailing edge down. Driving point measurements were made at two locations: 1.702 m from the blade mounting flange at 30% chord (center of gravity), and at 4.243 m from the blade mounting flange at 30% chord (inboard of tip mounting sleeve). The blade modes were excited with a PCB modally tuned impact hammer (model number 086C05, serial number 3804). The accelerations were measured with a PCB three-axis accelerometer (model number 356A18, serial number 4155). The measurements were recorded on an HP35670A spectrum analyzer. Figure A-10 illustrates the bearing locations and dimensions of the pitch shaft mount.

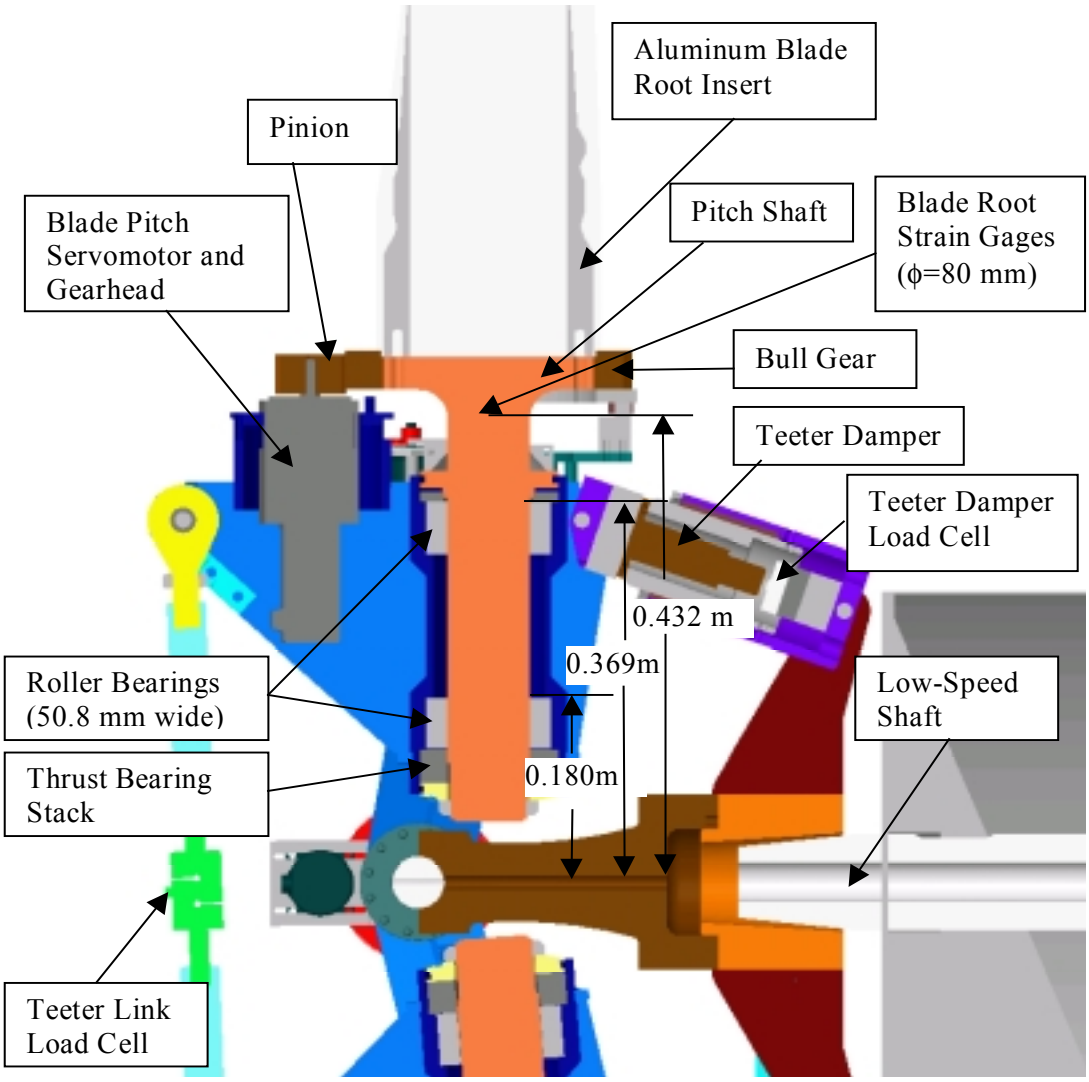

Figure A-10. Section view of pitch shaft mounted in hub

Table A-10. Blade modal frequencies

First edgewise eigenfrequency	
Non-instrumented blade	9.062 Hz
Instrumented blade	8.9 Hz
First flapwise eigenfrequency	
Non-instrumented blade	7.313 Hz
Instrumented blade	7.25 Hz
Second flapwise eigenfrequency	
Non-instrumented blade	30.062 Hz
Instrumented blade	29.438 Hz

Power Train

Layout

- The power train consists of the rotor mounted on a low-speed shaft coupled to a high-speed shaft via a gearbox. The high-speed shaft couples directly to an induction generator. The mechanical brake is positioned on the high-speed shaft. The low-speed shaft is 94-mm outer diameter and approximately 38-mm inner diameter. The mainframe thickness is approximately 5 mm. The box beam, which supports the mainframe above the tower, has outer dimensions of 0.254 m vertically by 0.3048 m horizontally. The distance from the tower top flange to the yaw bearing is 50.17 mm. The yaw column is 0.2794-m inner diameter with outer diameters of 0.3556 m and 0.3175 m. Additional dimensions of the mainframe are shown in Figure A-11.

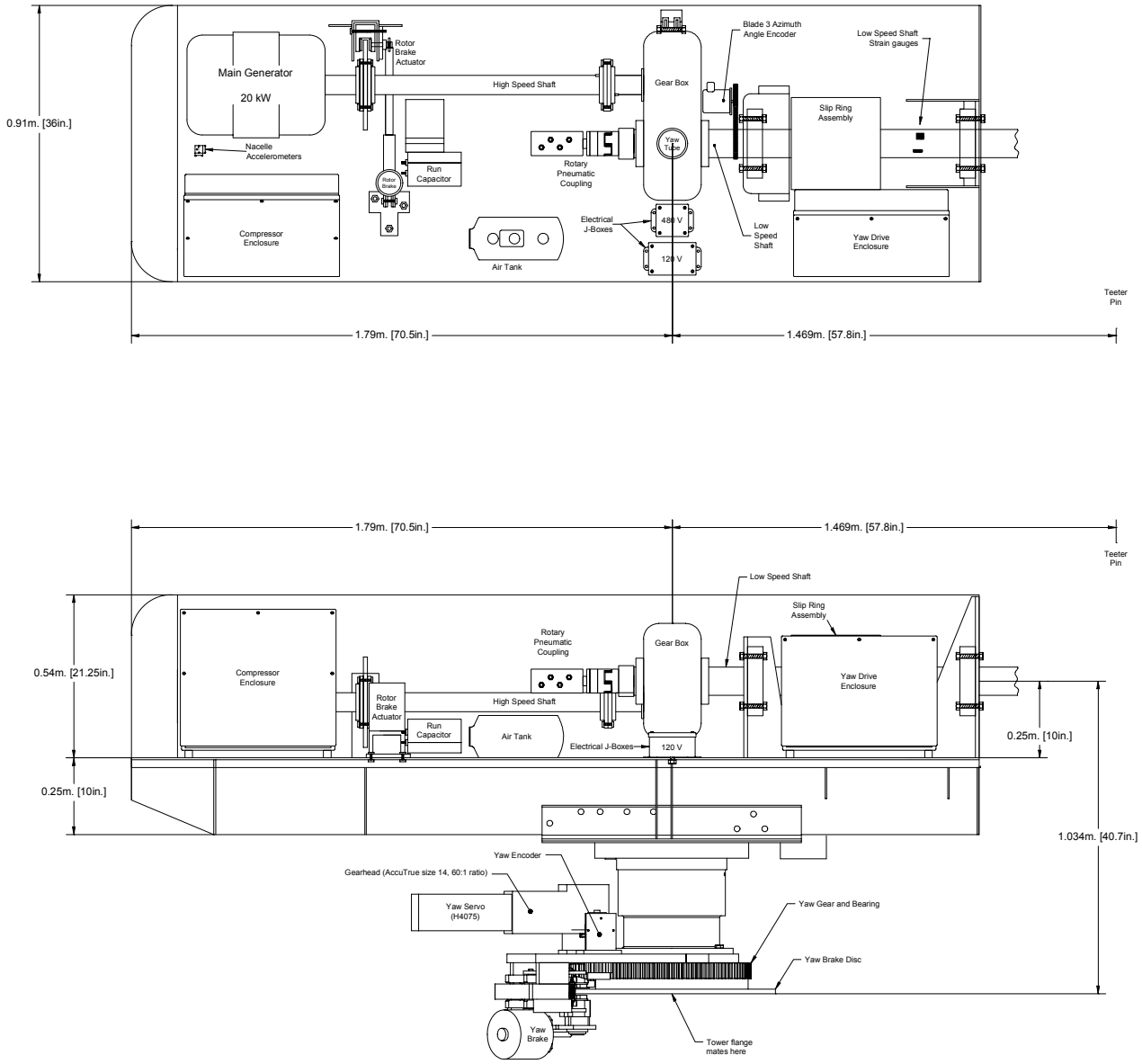

Figure A-11. Top view and side view of drivetrain

Characteristics

- Rotor inertia with respect to (w.r.t.) the low-speed shaft, includes boom and instrumentation boxes: 949 kg m^2
- Power train inertia w.r.t. the low-speed shaft (low-speed shaft, gearbox, high-speed shaft, generator): 144–179 kg m^2

- Power train stiffness (low-speed shaft, gearbox, and high-speed shaft as a lumped parameter): $1.99 \cdot 10^5$ Nm/rad.
- Power train natural frequency: 5.78 Hz
- Power train damping: 0.06 to 0.08
- Gearbox ratio: 25.13:1
- Gearbox mounted on end of low-speed shaft. It is attached to the bedplate with a torque arm.
- High-speed shaft inertia: Not available
- High-speed shaft damping: 0.5% to 1.0%
- High-speed shaft stiffness: Not available
- Generator inertia: 143-kg m^2 w.r.t. low-speed shaft
- Generator slip: 1.69% at 20 kW
- Generator time constant: <0.025 seconds (electromechanical time constant, for generator only)
- Power train efficiency:
  - Gearbox: 97% (from Grumman design documents)
  - Windage, couplings, main shaft bearings: 98% (from Grumman design documents)
  - Generator: The efficiency curve (in %) of the combined system (gearbox + generator) versus generator power (kW) is as follows:
  - $Eff = P_{gen}/[(1.698641 \cdot 10^{-3}) \cdot P_{gen}^2 + (1.1270445 \cdot 10^0) \cdot P_{gen} + (1.391369 \cdot 10^0)] * 100$.
  - Thus, the efficiency is constant at about 78%.
- Maximum brake torque: 115 Nm

Power Train Computations

Rotor Inertia Computation

The inertia of the rotor itself was calculated using low-speed shaft torque and rate of change of rotor speed during startup of the turbine. The rotor was initially at rest. Then generator power was supplied initiating rotor rotation. Torque, azimuth angle, and generator power were recorded for 30 seconds. The data captured included initial ringing of the low-speed shaft as the rotation began. The data was processed with the MUNCH program, which computed RPM from the rate of change of the azimuth angle.

The portion of the 30-second data file used in calculation of the rotor inertia was approximately one revolution of the instrumented blade in the region where the torque measurement was relatively constant. The sinusoidal correction for low-speed shaft torque was applied to the measured torque. The rotor speed at the endpoints of this region along with the average torque over this region provided the mass moment of inertia of the rotor about the low-speed shaft as follows:

$$T = J\dot{\omega}$$

The test was performed two times, and the average inertia computed. All related charts are attached.

Table A-11. Rotor inertia computation

Test Name	Dw/dt (rad/s^2)	Ave. Torque (Nm)	Standard Deviation	Rotor Inertia (kgm^2)
csstart1	2.34	-2210	81	946
csstart2	2.38	-2261	152	951
			Average:	949

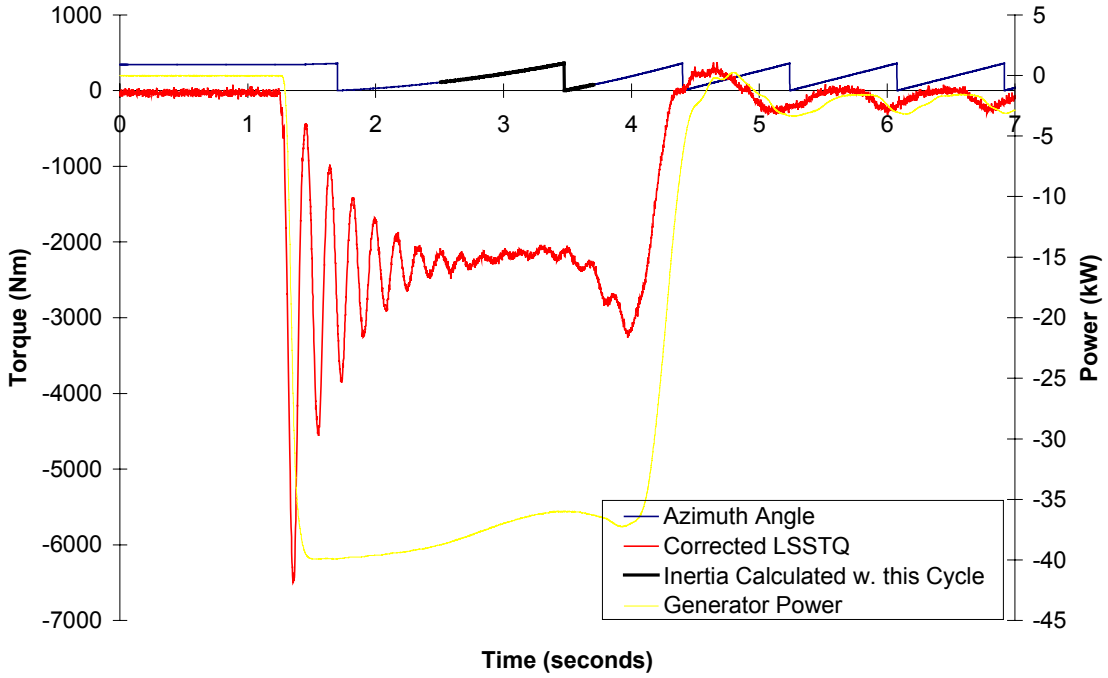

Figure A-12. Startup test csstart1

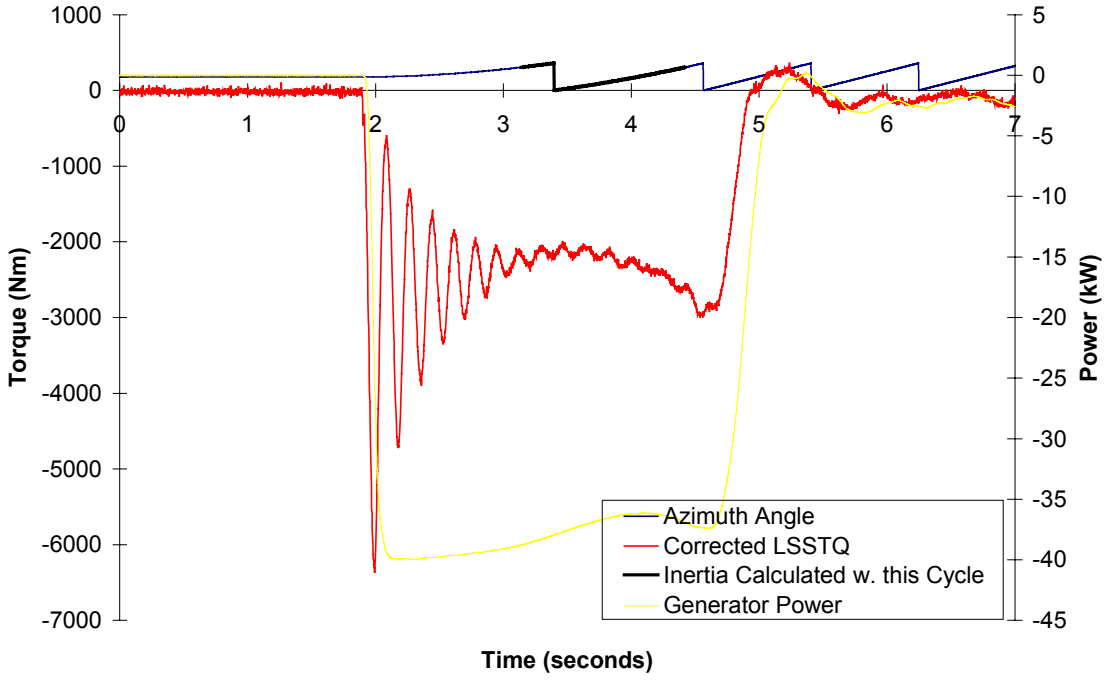

Figure A-13. Startup test csstart2

Drivetrain Inertia Computation

The inertia of the drivetrain was obtained by using the corrected low-speed shaft torque and rotational speed as the rotor slowed after disconnecting the generator power. Data was collected for 30 seconds while the rotor slowed. By pitching the blades toward feather after the generator is disconnected, aerodynamic friction slows the rotor quickly, reducing the effect of gearbox friction. Friction from the gearbox also slows the rotor and causes the inertia to be underestimated. The blades were pitched during one of the two stopping tests. The region with the fastest decrease in rotor speed over the shortest time was selected to compute the drivetrain inertia, Figure A-14. The rotational speed change during the rotor slow-down and the corresponding average torque provided the mass moment of inertia of the drivetrain with respect to the low-speed shaft as follows:

$$T = J\dot{\omega}$$

Table A-12. Drivetrain inertia computation

Test Name	dw/dt (rad/s^2)	Ave. Torque (Nm)	Standard Deviation	Drive Train Inertia (kgm^2)
csstop2	-1.98	-285	93	144

Due to the gearbox friction, this value underestimates the actual drivetrain inertia. During the Phase IV portion of testing, a pendulum test was performed on the three-blade turbine to

determine the full-system inertia, and start-up tests were performed to determine the rotor inertia. The pendulum test consisted of placing a weight on the end of one blade and allowing the rotor to swing back and forth. The frequency of pendulum swings is used to compute the full-system inertia. In this test, the gearbox friction reduces the frequency of oscillations, which causes the inertia to be overestimated. The difference between the rotor inertia obtained from startup tests and the full-system inertia obtained from the pendulum test is the drivetrain inertia, 179 kg m^2. The true drivetrain inertia should be bounded by these two tests.

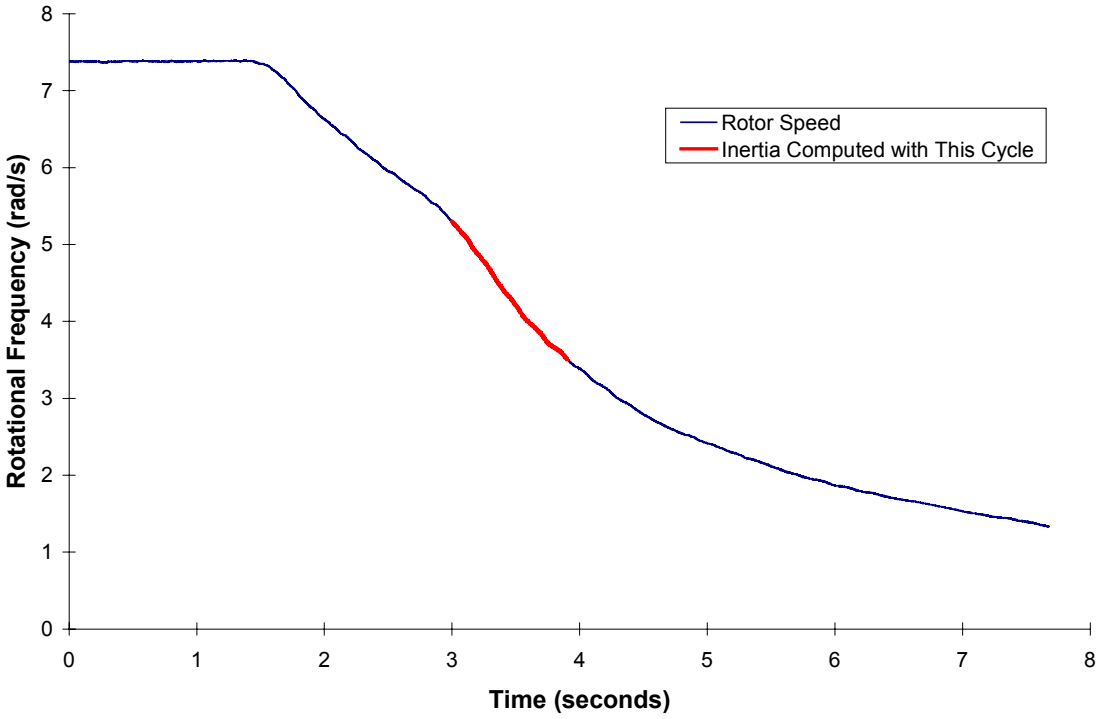

Figure A-14. Rotor speed decrease during stopping test csstop2

Drivetrain Damping and Frequency Computation

The startup tests were used to estimate the drivetrain damping and natural frequency. As the generator power was initiated, the torque measurement showed the drivetrain dynamics. Determination of the damped frequency was made using the corrected torque measurement. The first cycle was neglected, but the time required for the next five complete cycles was calculated. The damped frequency was the quotient. The peaks for the torque cycles and the corresponding time were extracted from each of the startup tests. The mean of each half-cycle was computed and a polynomial curve fit as a function of time was determined. This mean torque was then subtracted from each of the peak values. The amplitude of successive peaks was used in the following formula to compute the damping:

$$\ln \frac{x_i}{x_{i+1}} \cong 2\pi\xi$$

The average and standard deviation of the first six consecutive pairs is shown in Table A-13. In addition, an exponential curve fit was applied to the mean-adjusted torque peaks. The damping and natural frequency values resulting from the equation solver are also included in the table.

Table A-13. Drivetrain damping and damped frequency

Test Name	Damping (measured)	Damping Standard Deviation	Damped Frequency, Hz (measured)	Damping (Exponential Curve Fit)	Natural Frequency, Hz (Exponential Curve Fit)
csstart1	0.07	0.01	5.70	0.06	5.70
csstart2	0.07	0.01	5.84	0.06	5.85
Average:	0.07	0.01	5.77	0.06	5.78

Drivetrain Stiffness Computation

Knowledge of the rotor inertia and the generator inertia with respect to the low-speed shaft facilitate computation of the stiffness of all components in between if the natural frequency of these components is known. The stiffness of the low-speed shaft, gearbox, and high-speed shaft were thus determined:

$$K = \frac{\left(2\pi f_n\right)^2}{\frac{1}{I_r} + \frac{1}{I_g}}$$

where I_r is the rotor inertia, I_g is the generator inertia, f_n is the measured natural frequency, and K is the stiffness of the lumped components between the rotor and the generator.

The natural frequency was computed from the measured damping and damped frequency resulting from the startup tests as follows:

$$\omega_d = \omega_n \sqrt{1-\xi^2}$$

This was determined for both startup tests, and the stiffness was calculated using the corresponding rotor inertia determined for each test. The average stiffness was then calculated and is presented in Table A-14.

Table A-14. Drivetrain natural frequency and stiffness

Test Name	Drivetrain Natural Freq. (Hz)	Drivetrain Stiffness (Nm/rad)
csstart1	5.71	1.94E+05
csstart2	5.85	2.04E+05
Average:	5.78	1.99E+05

Tower and Nacelle

Description

- Basic description: two different diameter cylinders connected by a short conical section. The conical section base is 3.4 m above the tower base. The conical section top is 3.9 m above the tower base. The base of the tower is a 1.829-m-diameter flange that mounts to the semispan mount below the floor of the wind tunnel. The wind tunnel floor is 0.356 m above the base of the tower (Figure A-15).

Characteristics

- Tower material: ASTM A106 schedule 40 (bottom) and schedule 80 (top) Type B pipe, A36 19-mm (0.75-in.) plate
- Tower height: 11.5 m, 11.14 m above tunnel floor
- Tower diameter (base): 0.6096-m outer diameter, 0.0175-m thickness (design values)
- Tower diameter (top): 0.4064-m outer diameter, 0.0214-m thickness (design values)
- Tower mass: 3,317 kg (provided by manufacturer's model; includes paint, flanges, welds and webs; does not include bolts)
- Position of tower head center of gravity: Not available
- Nacelle, hub, pitch shafts (2), and boom mass: 1,712 kg
- Nacelle, hub, pitch shafts (2), and boom inertia about the yaw axis: 3,789 kg m^2

  The inertia was obtained by performing a bi-filar pendulum test on the nacelle, hub, pitch shafts, and boom assembly. Using a spreader bar, the nacelle was hung from the upwind and downwind ends. The nacelle was perturbed about the yaw axis, and the time required to swing through 10 cycles was recorded. The inertia (assuming that the nacelle, hub, pitch shafts, and boom structure was axisymmetric) was then computed about the center of the nacelle. This inertia was translated to the yaw axis.
- Yaw drive motor and gearhead inertia w.r.t yaw axis: 122 kg m^2 (computed)
- Yaw drive gearhead and motor backdrive start-up friction: 53 Nm (computed)
- Distance from top of tower flange to low-speed shaft: 1.034 m (3.398 ft)
- Tower shroud (Sequences 6 and 7 only): symmetric airfoil-shaped shroud with thickness 0.46 m and chord 0.89 m as shown in Figure A-16.
- Rotor lock (Sequences L and O only): Aluminum block designed to lock rotor in vertical position for parked blade tests shown in Figure A-17.

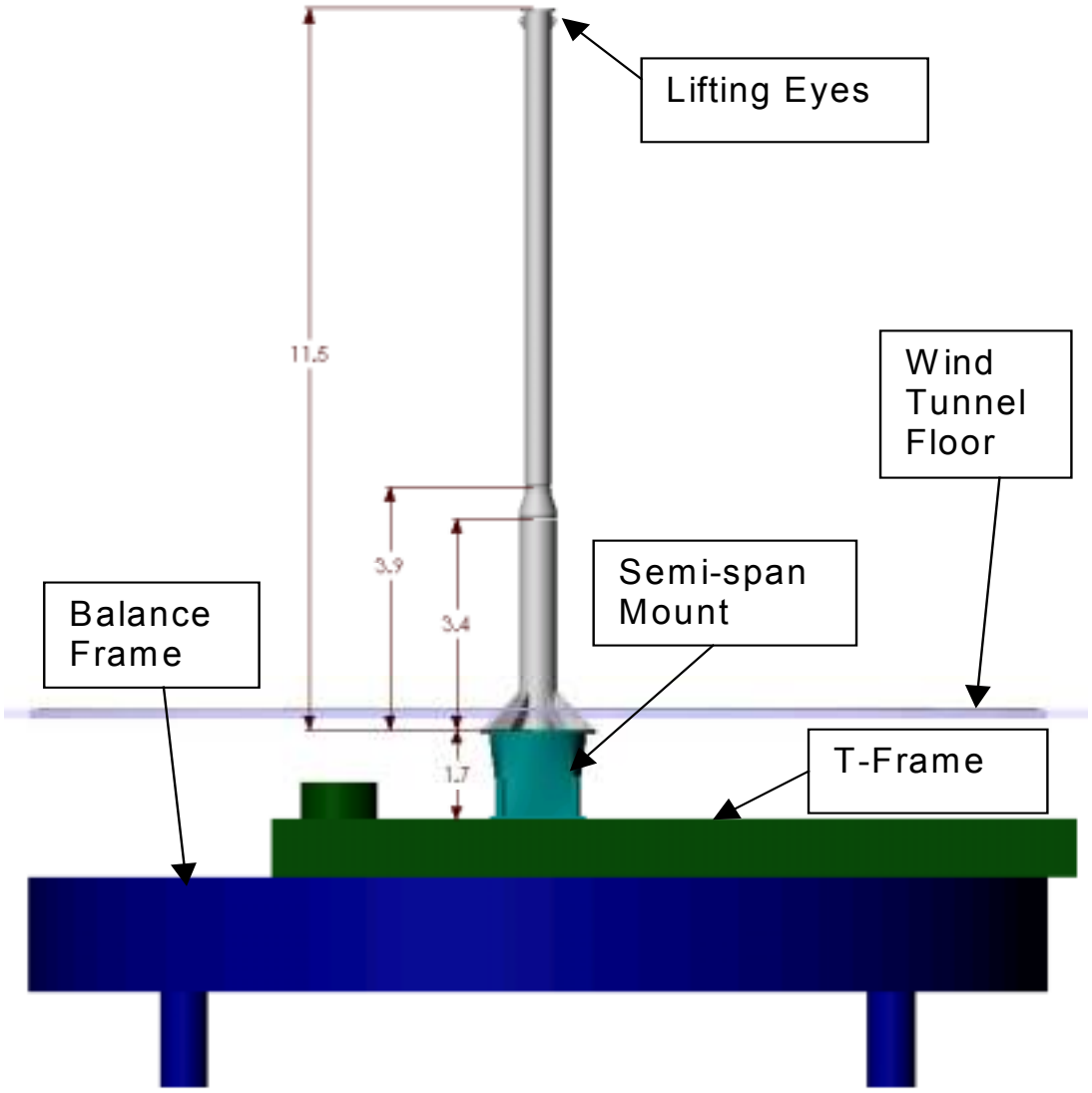

Figure A-15. Tower (dimensions in meters)

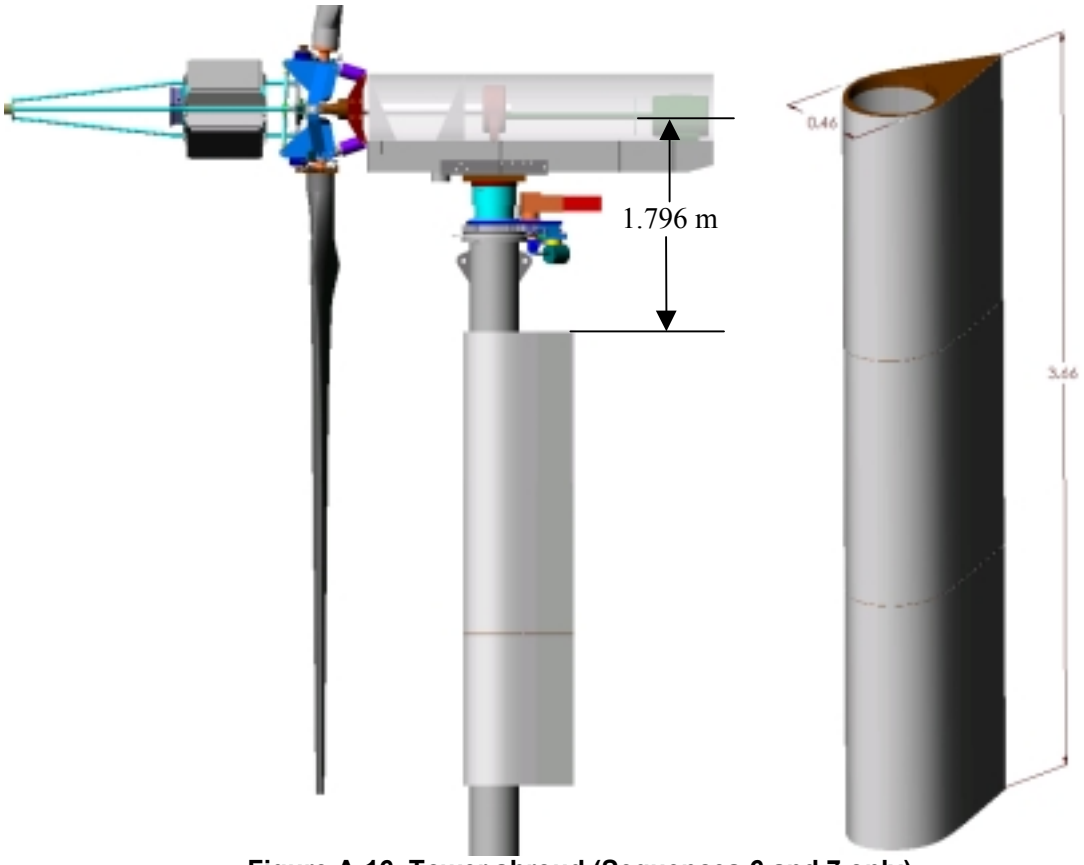

Figure A-16. Tower shroud (Sequences 6 and 7 only)

Figure A-17. Rotor lock installed for parked blade sequences L and O

Modal Test Summary

- The full system modal test was performed by Navcon Engineering Network while the turbine was installed in the wind tunnel (Navcon Engineering Network 2000). Three turbine configurations were measured: operational turbine (Blade 3 at 90º, upwind turbine configuration), upwind turbine with blades removed, and tower alone. An electronic shaker was used to excite the modes. It was mounted to a 2869 kg steel reaction mass that was

suspended from the main gantry crane shown in Figure A-18. A load cell was screwed to an aluminum block which was bolted to the top of the tower. The shaker was attached to the load cell with a 0.305-m steel threaded rod shown in Figure A-19. Summaries of the resonant frequencies and damping values for each of the three configurations are included in Tables A-15 through A-17.

Figure A-18. Steel reaction mass suspended from gantry crane

Figure A-19. Shaker mounted to steel reaction mass and attached to tower

Operational Turbine

Table A-15. Modes for upwind turbine at 0° yaw and 90° azimuth

Mode No.	Frequency [Hz]	Damping [Hz]	Damping %Cr
1	1.67	0.1	4.8
2	1.75	0.1	3.5
3	2.47	0.1	5.5
4	5.86	0.1	1.9
5	5.90	0.0	0.5
6	7.17	0.2	2.6
7	7.30	0.1	1.0
8	8.74	0.1	0.7
9	11.84	0.1	0.6
10	11.88	0.1	0.6
11	13.02	0.2	1.4
12	14.53	0.1	0.9
13	14.97	0.2	1.5
14	18.09	0.2	1.1
15	18.18	0.2	1.0
16	18.05	0.3	1.5
17	18.17	0.2	1.2
18	20.29	0.3	1.5
19	22.76	0.2	0.8
20	23.75	0.3	1.1
21	25.26	0.4	1.5

Turbine with Blades Removed

Table A-16. Modes for turbine with blades removed, instrumentation boxes installed

Mode No.	Frequency [Hz]	Damping [Hz]	Damping %Cr
1	1.34	0.1	8.0
2	1.79	0.0	2.4
3	1.85	0.1	3.3
4	5.92	0.0	0.6
5	7.10	0.2	2.6
6	8.55	0.2	1.8
7	11.01	0.3	2.5
8	11.62	0.1	0.6
9	12.68	0.6	4.9
10	14.56	0.1	0.8
11	15.02	0.3	1.7
12	18.12	0.2	1.1
13	20.45	0.3	1.7
14	23.83	0.3	1.2
15	24.91	0.5	2.1

Tower Alone

Table A-17. Modes for tower mounted to semi-span

Mode No.	Frequency [Hz]	Damping [Hz]	Damping %Cr
1	1.74	0.1	6.3
2	2.36	0.2	6.5
3	2.73	0.1	3.2
4	3.91	0.0	0.5
5	4.03	0.0	0.6
6	8.14	0.1	1.2
7	10.38	0.2	2.0
8	10.66	0.2	1.6
9	11.93	0.1	0.5
10	14.01	0.3	2.2
11	14.75	0.1	0.6
12	18.07	0.3	1.8
13	19.50	0.2	0.9
14	19.91	0.1	0.7
15	21.03	0.1	0.3
16	22.04	0.3	1.3
17	24.80	0.2	1.0

References

Butterfield, C.P.; Musial, W.P.; Simms, D.A. (1992). *Combined Experiment Phase I Final Report.* NREL/TP-257-4655. Golden, CO: National Renewable Energy Laboratory.

Navcon Engineering Network. (2000). *Modal Test of the Unsteady Aerodynamics Experiment*. Unpublished.

Somers, D.M. (1997). *Design and Experimental Results for the S809 Airfoil*. NREL/SR-440-6918. Golden, Colorado: National Renewable Energy Laboratory.

Appendix B: Instrumentation, Data Collection, and Data Processing for Phase VI

NASA Anemometers

Channel	ID Code	Description
300	OMWS18M	Outside met wind speed 18.29 m
302	OMWS32M	Outside met wind speed 32.81 m
304	OMWD18M	Outside met wind direction 18.29 m
306	OMWD32M	Outside met wind direction 32.81 m

Location	Meteorological tower 213.4 m (700') from tunnel inlet
Measurement type and units	Wind speed, m/s; wind direction, degrees
Range	0–64.3 m/s, 0–360º
Resolution	4.47 m/s / V; 36º/V
Calibration Method	Manufacturer specifications (M1) and electronic path calibration (E1)
Sensor Description	Handar sonic anemometer 14-25A

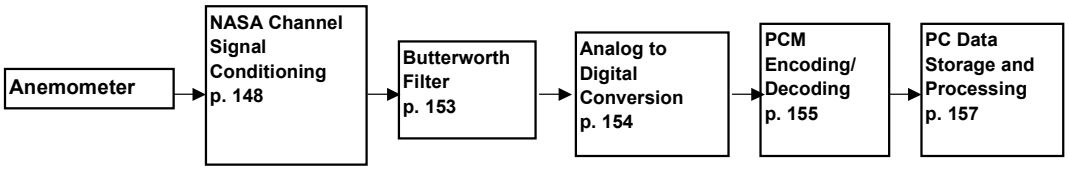

Note: Wind direction is positive clockwise from magnetic North.

Calibration Procedure

Manufacturer specifications – (M1)

1. NASA personnel arranged a calibration with the appropriate manufacturers.
2. Enter the slope and the offset in the appropriate columns of *calconst.xls*. The slope and offset provided by NASA were in (U.S. Customary System) USCS units. These were converted to metric units in *calconst.xls*.

Electronic path calibration – (E1)

1. Modify *vbl.lst* so the NASA anemometer channels are listed at the top of the file. Set NV (number of variables) in the first line to the number of channels to be calibrated, and insure that the correct PCM stream is specified in *gencal.cap* (PCM stream 3).
2. Connect the precision voltage generator to the ground-based PCM rack NASA channel connector.
3. Run the *gc.bat* batch file, which invokes both *gencal.exe* and *genfit.exe*. Collect samples for voltages ranging from 0.0 to 9.0 V in 1-V increments with two repetitions at each voltage level. The recorded input and output values are stored in the **.cao* input file. *Genfit.exe* computes slopes and offsets of the electronic path from the processor output to the computer

in units of V/count and V, respectively. These values are stored in a temporary header file, **.hdr*. These slope and offset values are combined with the manufacturer-provided slope and offset during the *buildhdr.bat* process to obtain units of engineering unit/count and counts, respectively.

Calibration frequency

The anemometers were calibrated in February 1999 prior to installation on the tower. The electronic path calibration was performed prior to wind tunnel testing.

Channel	ID Code	Description
310	WTBARO	Wind tunnel barometric pressure
312	WTSTAT	Wind tunnel static pressure
314	WTTOTAL	Wind tunnel total pressure

Location	Control room
Measurement type and units	Pressure, Pa
Range	75,800-103,400 Pa (WTBARO); 2,490 Pa (WTSTAT); 1,000 Pa (WTTOTAL)
Resolution	68,948 Pa/V (WTBARO); 249 Pa/V (WTSTAT); 100 Pa/V (WTTOTAL)
Calibration Method	Manufacturer specifications (M1) and electronic path calibration (E1)
Sensor description	Edwards 590DF (WTSTAT, WTTOTAL) Edwards 590A (WTBARO)

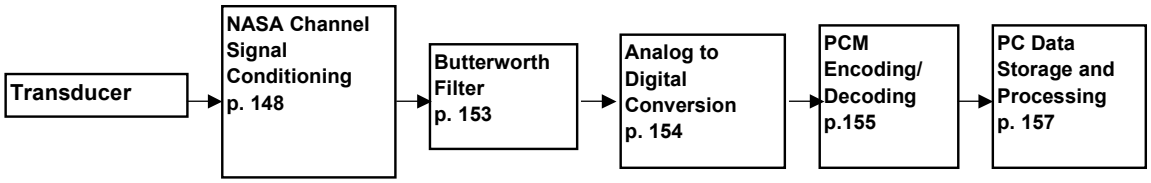

Calibration Procedure

Manufacturer specifications - (M1)

1. NASA personnel arranged a calibration at the NASA calibration laboratory.

Enter the slope and the offset in the appropriate columns of *calconst.xls*. The slope and offset provided by NASA were in USCS units. These were converted to metric units in *calconst.xls*.

Electronic path calibration - (E1)

1. Modify *vbl.lst* so the NASA pressure channels are listed at the top of the file. Set NV (number of variables) in the first line to the number of channels to be calibrated, and insure that the correct PCM stream is specified in *gencal.cap* (PCM stream 3).
2. Connect the precision voltage generator to the ground-based PCM rack NASA channel connector.
3. Run the *gc.bat* batch file, which invokes both *gencal.exe* and *genfit.exe*. Collect samples for voltages ranging from 0.0 to 9.0 V in 1-V increments with two repetitions at each voltage level. The recorded input and output values are stored in the **.cao* input file. *Genfit.exe* computes slopes and offsets of the electronic path from the processor output to the computer in units of V/count and V, respectively. These values are stored in a temporary header file, **.hdr*. These slope and offset values are combined with the manufacturer-provided slope and offset during the *buildhdr.bat* process to obtain units of engineering unit/count and counts, respectively.

Calibration frequency

The transducers were calibrated in November 1999 with an expiration date of November 2000. The electronic path calibration was performed prior to wind tunnel testing.

NASA Turntable Angle

Channel	ID Code	Description
347	YAWTABLE	Turntable angle
Location		Turntable
Measurement type and units		Angular position, degrees
Sensor description		Kearfott 2R982-004

Note: The slope and offset were input in *ang.hdr* to match the turntable angle reading at the wind tunnel controller's station. The turntable was used for Tests 6, 7, 8, and 9 only. The measurement convention is such that positive turntable angle results from clockwise rotation.

Channel	ID Code	Description
344	WTLFLIFT	Tunnel balance left front lift (#1)
346	WTRFLIFT	Tunnel balance right front lift (#2)
348	WTLRLIFT	Tunnel balance left rear lift (#3)
350	WTRRLIFT	Tunnel balance right rear lift (#4)
352	WTFSFORC	Tunnel balance front side force (#5)
354	WTRSFORC	Tunnel balance rear side force (#6)
356	WTDRAG	Tunnel balance drag force (#7)

Location	Lift tubes below *T*-frame
Measurement type and units	Force, N
Range	-222,411 to 444,822 N (#1–#4); -222,411 to 222,411 N (#5–#7)
Resolution	52,507 N/V (#1, #3); 52,520 N/V (#2); 52,912 N/V (#4); 53,201 N/V (#5); 53,000 N/V (#6); 54,282 N/V (#7)
Calibration Method	Manufacturer specifications (M1) and electronic path calibration (E1)
Sensor description	ACME custom-designed system

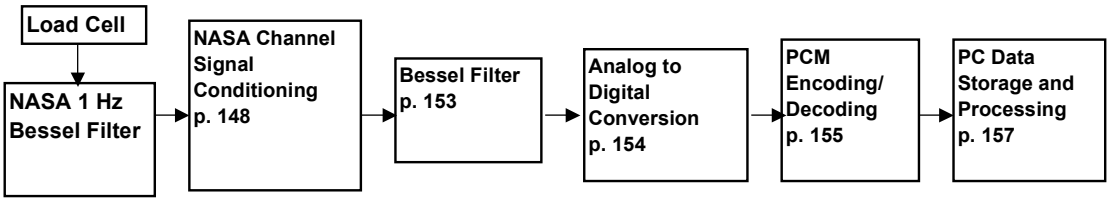

Calibration Procedure

Manufacturer specifications - (M1)

1. NASA personnel arranged a calibration with the manufacturer.
2. Enter the slope and the offset in the appropriate columns of *calconst.xls*. The slope and offset provided by NASA were in USCS units. These were converted to metric units in *calconst.xls*.

Electronic path calibration - (E1)

1. Modify *vbl.lst* so the NASA turntable force channels are listed at the top of the file. Set NV (number of variables) in the first line to the number of channels to be calibrated, and insure that the correct PCM stream is specified in *gencal.cap* (PCM stream 3).
2. Connect the precision voltage generator to the ground-based PCM rack NASA channel connector.
3. Run the *gc.bat* batch file, which invokes both *gencal.exe* and *genfit.exe*. Collect samples for voltages ranging from 0.0 to 9.0 V in 1-V increments with two repetitions at each voltage level. The recorded input and output values are stored in the **.cao* input file. *Genfit.exe* computes slopes and offsets of the electronic path from the processor output to the computer in units of V/count and V, respectively. These values are stored in a temporary header file, **.hdr*. These slope and offset values are combined with the manufacturer-provided slope and

offset during the *buildhdr.bat* process to obtain units of engineering unit/count and counts, respectively.

Calibration frequency

The transducers were calibrated in April 2000. The electronic path calibration was performed prior to wind tunnel testing.

Channel	ID Code	Description
308	OMT4M	Outside met air temperature 4.57 m
318	WTATEMP	Wind tunnel air temperature
316	WTDPT	Wind tunnel dew point temperature

Location	Meteorological tower 213.36 m (700') from inlet (OMT4M); Tunnel inlet, 30.48 m (100') from ground level (WTATEMP); Tunnel wall adjacent to turntable center, 3.048 m (10') from floor (WTDPT)
Measurement type and units	Ambient temperature, °C
Range	-18–149ºC (OMT4M); 0–38ºC (WTATEMP); -40–27ºC within 45ºC to 65ºC depression at 25ºC (WTDPT)
Resolution	5.6ºC/V (OMT4M); 5.51ºC/V (WTATEMP); 3.49ºC/V (WTDPT)
Calibration Method	Manufacturer specifications (M1) and electronic path calibration (E1)
Sensor description	Handar 435A (OMT4M) Hart Scientific thermistor 5610 (WTATEMP) Protimeter RSO (WTDPT)

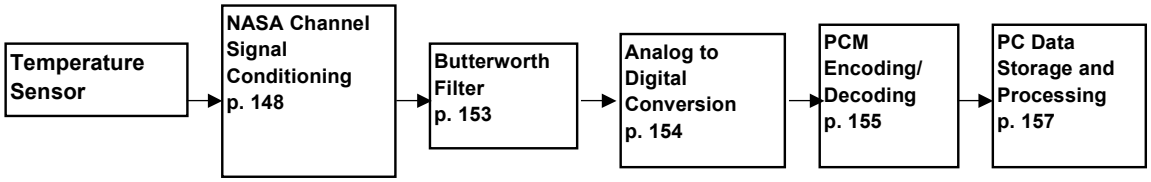

Calibration Procedure

Manufacturer specifications - (M1)

1. NASA personnel arranged a calibration with the manufacturer.
2. Enter the slope and the offset in the appropriate columns of *calconst.xls*. The slope and offset provided by NASA were in USCS units. These were converted to metric units in *calconst.xls*.

Electronic path calibration - (E1)

1. Modify *vbl.lst* so the NASA temperature channels are listed at the top of the file. Set NV (number of variables) in the first line to the number of channels to be calibrated, and insure that the correct PCM stream is specified in *gencal.cap* (PCM stream 3).
2. Connect the precision voltage generator to the ground-based PCM rack NASA channel connector.
3. Run the *gc.bat* batch file, which invokes both *gencal.exe* and *genfit.exe*. Collect samples for voltages ranging from 0.0 to 9.0 V in 1-V increments with two repetitions at each voltage level. The recorded input and output values are stored in the **.cao* input file. *Genfit.exe* computes slopes and offsets of the electronic path from the processor output to the computer in units of V/count and V, respectively. These values are stored in a temporary header file,

*.*hdr*. These slope and offset values are combined with the manufacturer-provided slope and offset during the *buildhdr.bat* process to obtain units of engineering unit/count and counts, respectively.

Calibration frequency

The wind tunnel temperature transducer was calibrated July 1999, with an expiration date of July 2000. The dew point transducer was calibrated November 1999, with an expiration date of August 2000. The outside temperature transducer was calibrated in 1997 prior to installation. The electronic path calibration was performed prior to wind tunnel testing.

Channel	ID Code	Description
320	LESU8M	Local East sonic channel U 8 m
322	LESV8M	Local East sonic channel V 8 m
324	LESW8M	Local East sonic channel W 8 m
326	LWSU8M	Local West sonic channel U 8 m
328	LWSV8M	Local West sonic channel V 8 m
330	LWSW8M	Local West sonic channel W 8 m

Location	Microphone stands located 24 m upwind of turbine
Measurement type and units	3-D, orthogonal components of wind speed and direction, m/s and degrees
Sensor description	3-axis sonic anemometer Accuracy: Wind speed, ±1% or ±0.05 m/s Wind direction, ±0.1° Temperature, ± 1% (not recorded) Applied Technologies, Inc. Model: SATI/3K

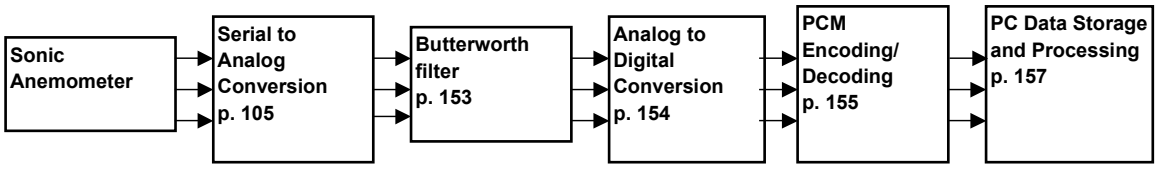

Note: Each of the three wind velocity components is contained in the PCM streams and recorded. Wind speed is determined using these components during post-processing. The sonic anemometer's determination of wind speed, wind direction, and temperature is not used.

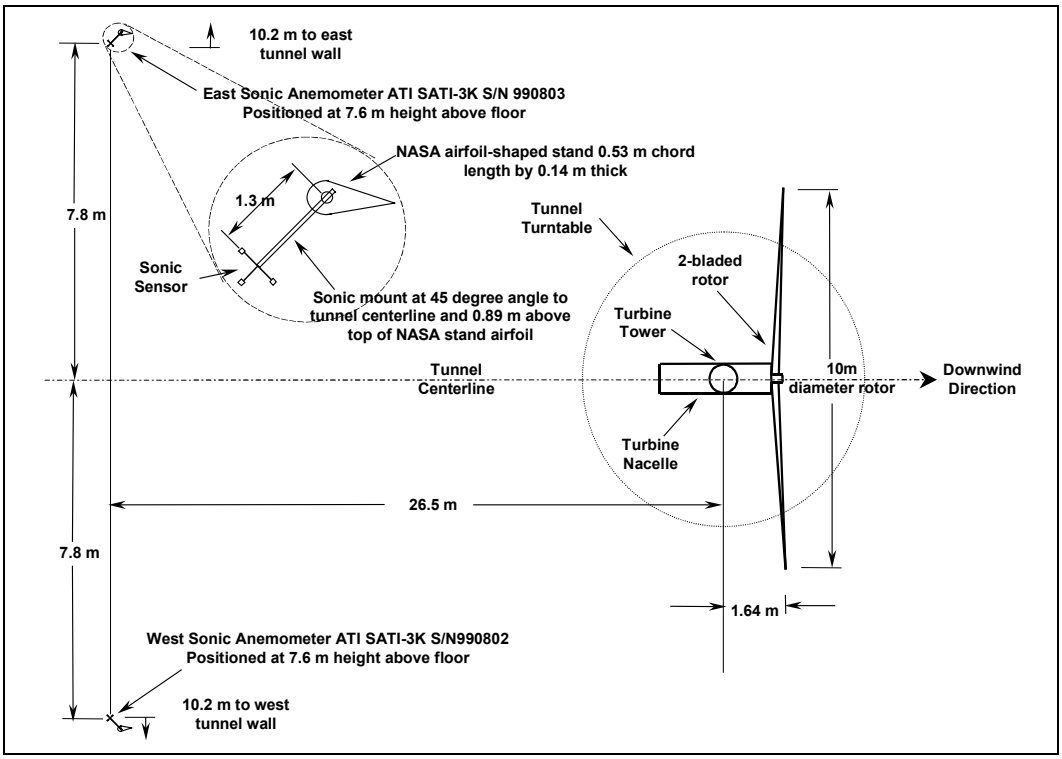

Figure B-1. Top view showing location of sonic anemometers relative to turbine (not shown to scale); turbine is shown in downwind orientation

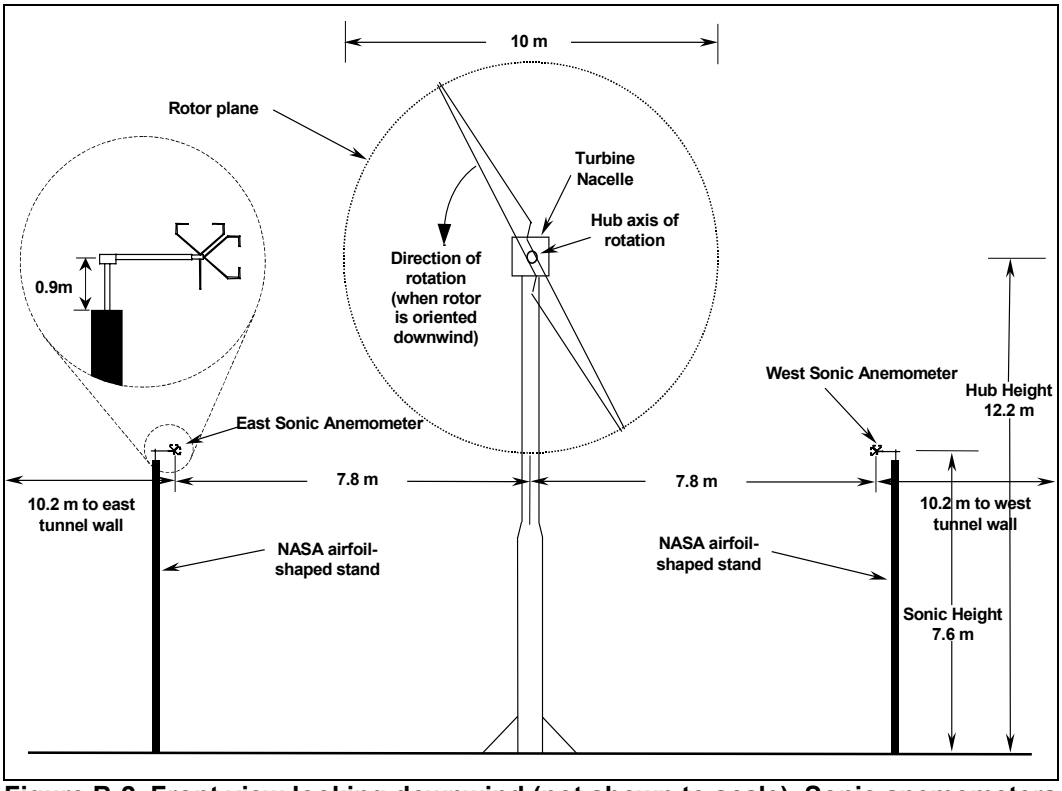

Figure B-2. Front view looking downwind (not shown to scale). Sonic anemometers located 26.5 m upwind of the turbine tower

Channel	ID Code	Description
320	LESU8M	Local East sonic channel U 8 m
322	LESV8M	Local East sonic channel V 8 m
324	LESW8M	Local East sonic channel W 8 m
326	LWSU8M	Local West sonic channel U 8 m
328	LWSV8M	Local West sonic channel V 8 m
330	LWSW8M	Local West sonic channel W 8 m

Location	PCM rack
Range	±50 m/s at ±5 V (U,V); ±15 m/s at ±5 V (W)
Resolution	10 m/s / Volt (U,V); 3 m/s / Volt (W)
Calibration method	Pseudo applied load calibration (A4)
Input Signal	Serial RS-232C
Output Signal	±5 Vdc
Description	Serial to analog converter
	Applied Technologies, Inc. Model: SA-4

Calibration Procedure

Pseudo applied load calibration - (A4)

1. Modify *vbl.lst* so the sonic anemometer channels are listed at the top of the file. The U and V channels are calibrated together, and the W channel is calibrated by itself. Each anemometer must be calibrated separately. Set NV (number of variables) in the first line to the number of channels to be calibrated, and insure that the correct PCM stream is specified in *gencal.cap* (all meteorological channels are on PCM stream 3).
2. Connect the laptop computer to the serial-to-analog converter input.
3. Run the *gc.bat* batch file, which invokes both *gencal.exe* and *genfit.exe*. Using the laptop computer, input serial signals corresponding to specific wind speeds. Collect samples for wind speed signals ranging from –45 to 45 m/s in 10-m/s increments with two repetitions at each signal level for the U and V channels. Collect samples for wind speed signals ranging from –13.5 to 13.5 m/s in 2.5-m/s increments. The recorded input and output values are stored in the **.cao* input file. *Genfit.exe* computes slopes and offsets of the electronic path from the converter input to the computer in units of m/s/count and m/s, respectively. These values are stored in a temporary header file, **.hdr*. This file is read during the *buildhdr* process, and the values are placed in the *master.hdr* file.

Calibration frequency

The transducers were calibrated according to manufacturer specifications (ATI Operator's Manual), and an electronic path calibration was performed prior to wind tunnel testing. The manufacturer-specified calibration consists of placing a 'zero-air chamber' over each axis of the anemometer. A laptop computer is used to communicate the ambient air temperature and relative humidity to the sonic anemometer, and internal calibrations are completed.

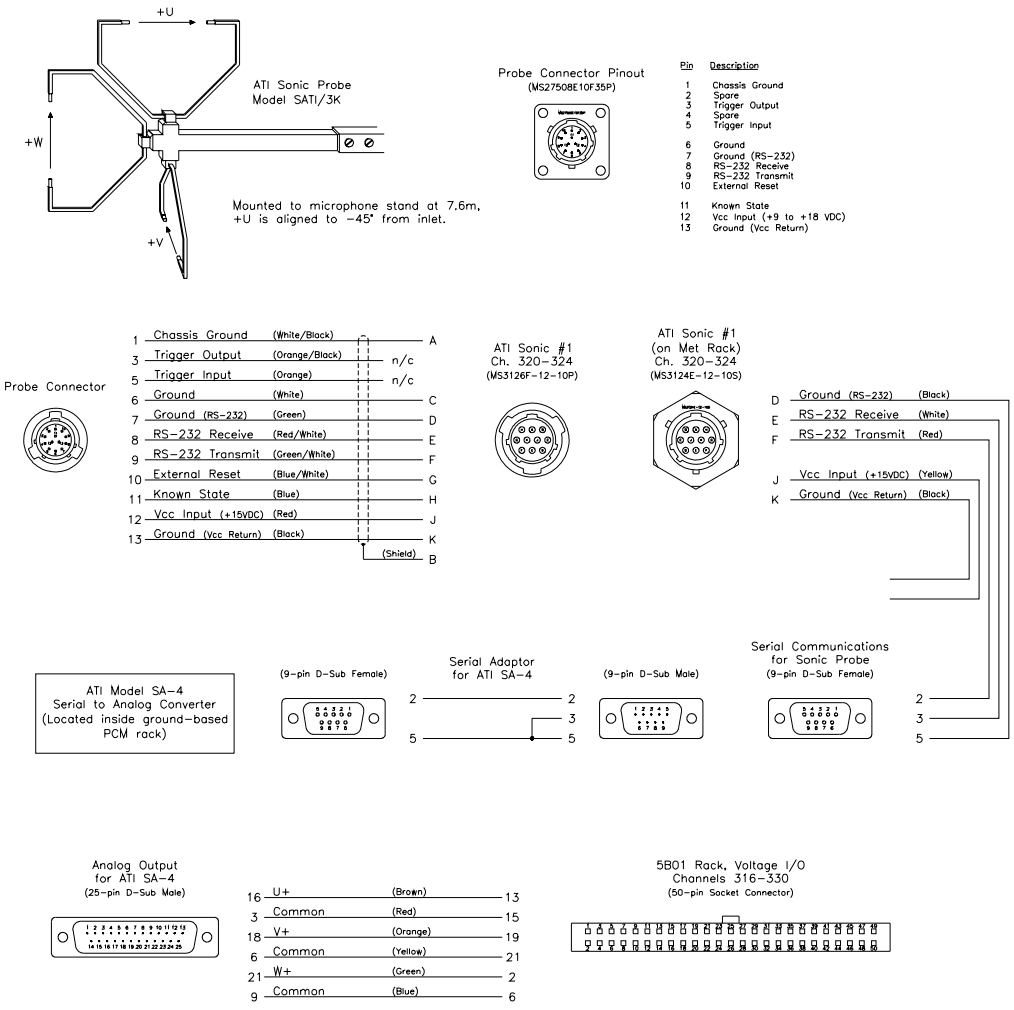

Figure B-3. East sonic anemometer wiring diagram

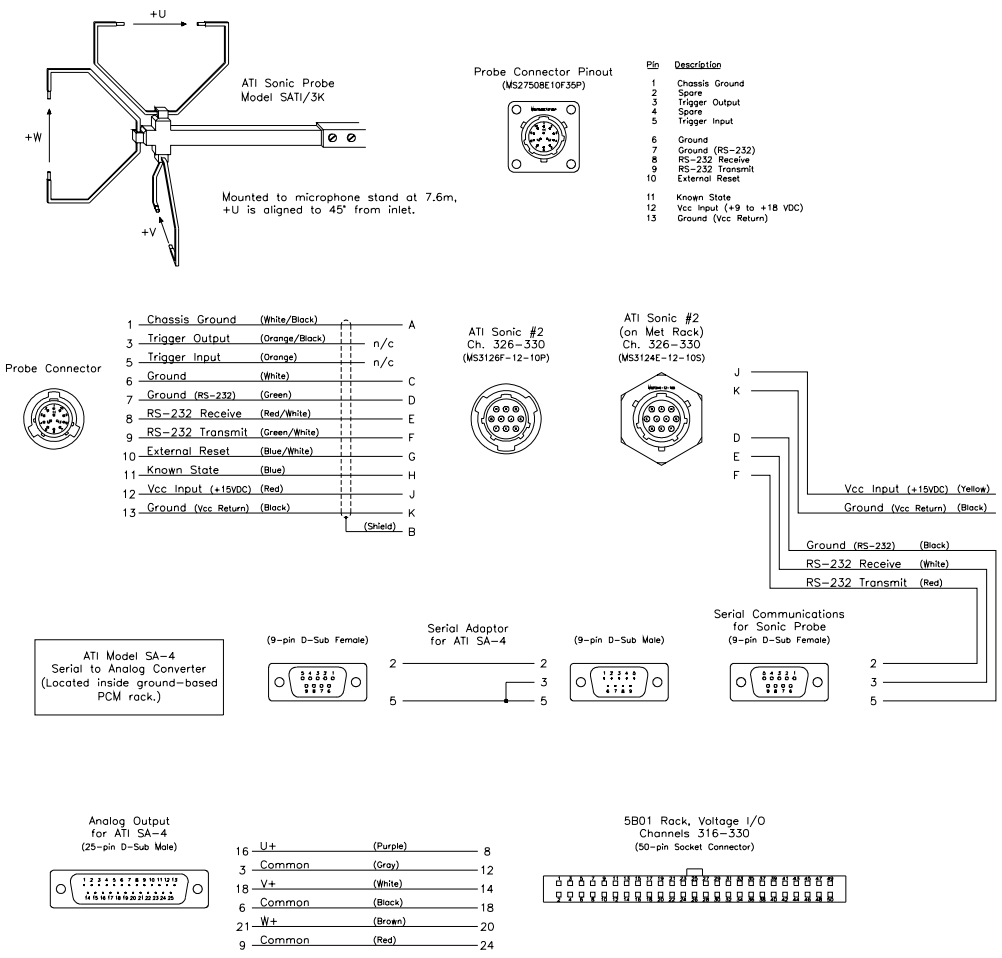

Figure B-4. West sonic anemometer wiring diagram

Channel	ID Code	Description
223	TLINKF	Strain Teeter link force
Location		Teeter link, hub
Measurement type and units		Tensile and compressive load, N
Excitation		10 Vdc
Range		±10,000 lbs.
Resolution		32 N/bit
Calibration method		Application of known loads (A3) and single point offset (S1)
Sensor description		Hermetically sealed, universal tension and compression force sensor Transducer Techniques Model: HSW-10K

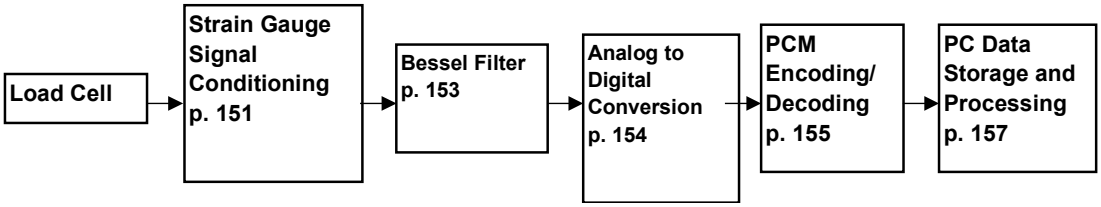

Note: The sign convention is such that positive teeter link force coincides with positive flap bending moment. Thus, compressive forces are positive in the downwind configuration, and tensile forces are positive for the upwind configuration. During rigid rotor operation, the teeter link force was pre-tensioned to approximately 40,000 Nm to prevent backlash from the hub joints.

Calibration Procedure

Application of known loads - (A3)

1. A custom jig was built to align two load cells in series and apply a load mechanically. The calibration load cell (Transducer Techniques Model SW-10K) was connected to a digital meter, and the other load cell was placed in the data acquisition system to get a full-path calibration. This calibration was performed when the rotor was assembled on the ground. Only the length of cable between the sensor and the data acquisition system differed from that used to collect data in the field.
2. Using the digital meter, loads were applied from –10,000 lbs to 10,000 lbs in 2500-lb increments and the count values noted. A linear regression analysis provided the slope and offset coefficients, which were entered manually in the *strains.hdr* file.

Single point offset - (S1)

1. The offset was determined by placing the rotor at a 90°-azimuth angle and disconnecting one pin on the hard link. The load on the load cell should be zero. The count values were noted and the offset computed as the multiple of slope*counts. This value was manually entered in the *strains.hdr* file.

Calibration frequency

The slope was calibrated July 1999. The offset was determined prior to testing.

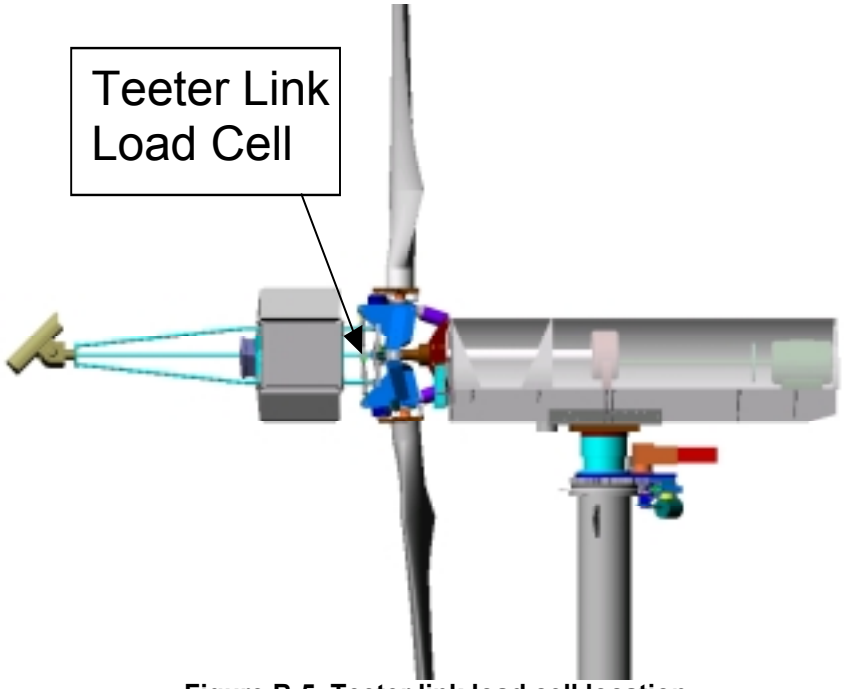

Figure B-5. Teeter link load cell location

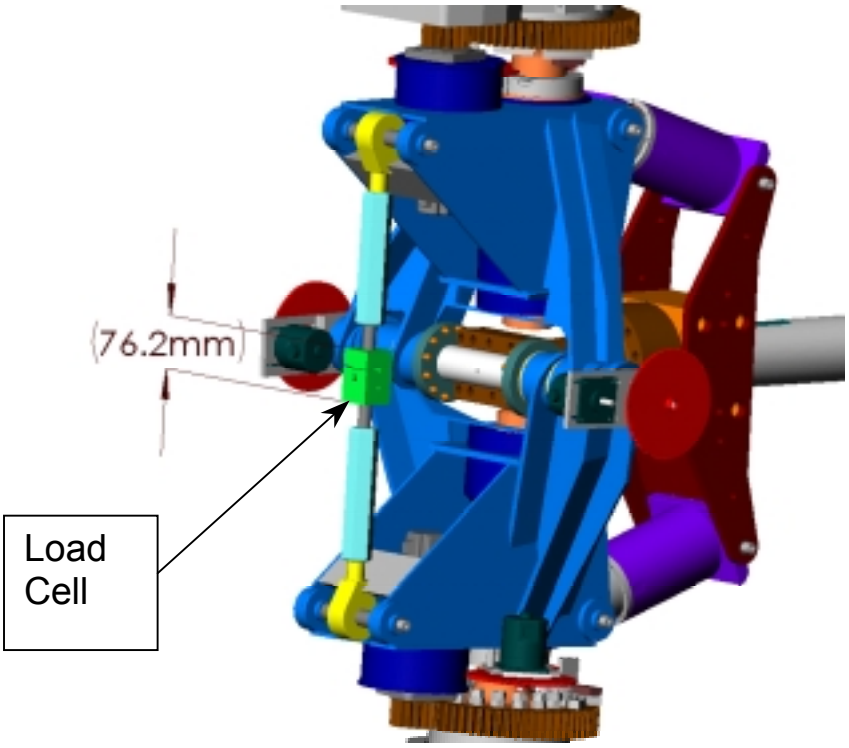

Figure B-6. Teeter link load cell

Channel	ID Code	Description
229	B1TDAMPF	Strain Blade 1 Teeter damper force
231	B3TDAMPF	Strain Blade 3 Teeter damper force

Location	Teeter damper, one for each blade
Measurement type and units	Compressive load, N
Excitation	10 Vdc
Range	10,000 lbs.
Resolution	30 N/bit
Calibration method	Application of known loads (A3); Single point offset (S1)
Sensor description	Button force sensor
	Sensotec Model: 53/0239-08

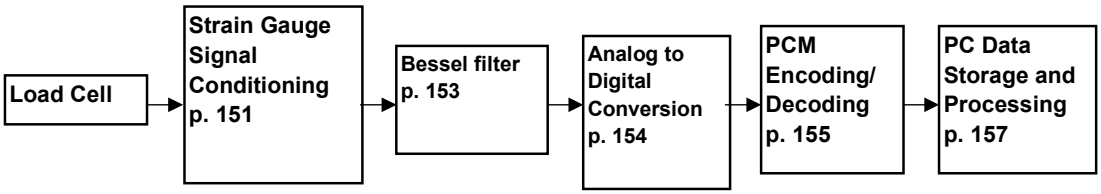

Note: When the dampers were disconnected for rigid-hub operation, the slope and offset were adjusted such that the channel would always report –99999.99N.

Calibration Procedure

Application of known loads - (A3)

1. A custom jig was built to align both of the button sensors with the calibration load cell in series. A mechanical load was then applied. The calibration load cell (Transducer Techniques Model SW-10K) was connected to a digital meter, and the button load cells were placed in the data acquisition system to get a full-path calibration. This calibration was performed when the rotor was assembled on the ground. Only the length of cable between the sensor and the data acquisition system differed from that used to collect data in the field.
2. Using the digital meter, loads were applied from 0 lbs to 8,000 lbs in 2,000-lb increments, and the count values noted. A linear regression analysis provided the slope and offset coefficients, which were entered manually in the *strains.hdr* file.

Single point offset - (S1)

1. The offset was determined by placing the rotor at 0° teeter angle, which corresponds to zero load on the teeter dampers. The count values were noted and manually entered in the *strains.hdr* file.

Calibration frequency

The slope was calibrated in July 1999. The offset was determined daily during testing.

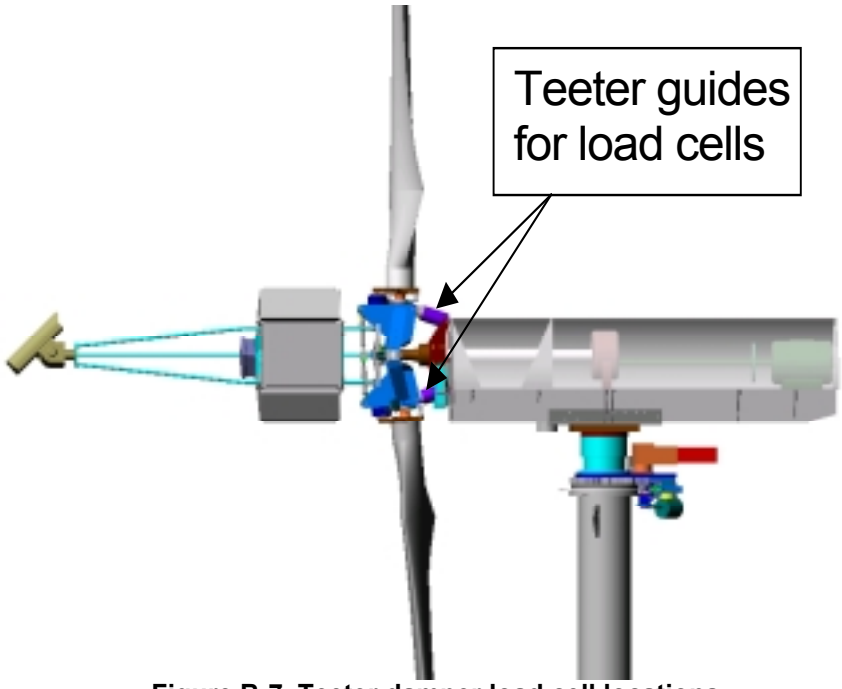

Figure B-7. Teeter damper load cell locations

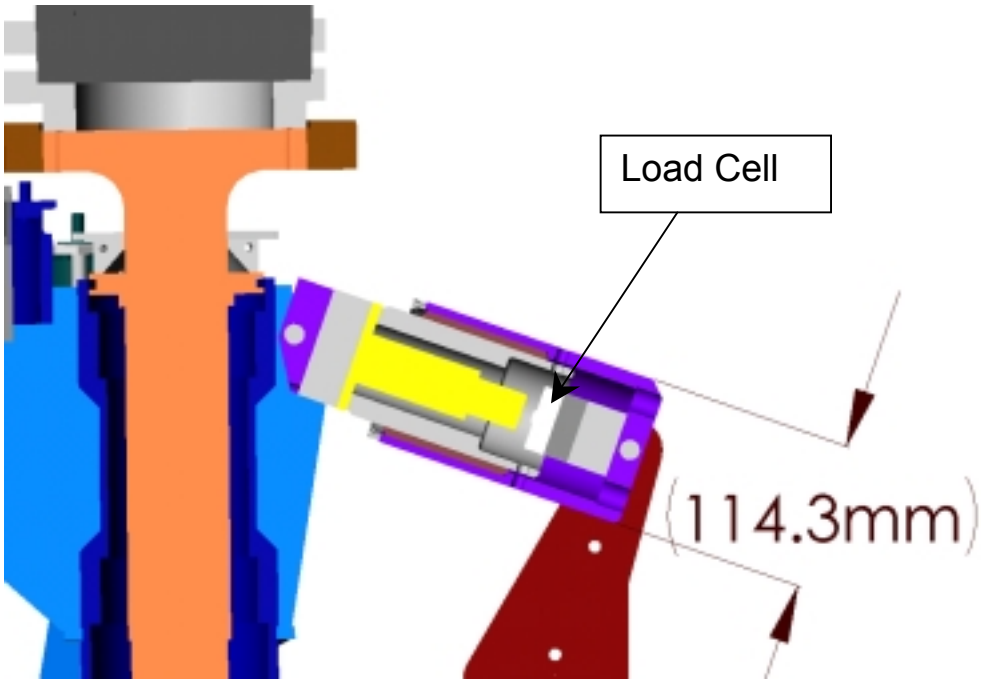

Figure B-8. Teeter damper load cell cross-sectional view

Channel	ID Code	Description
342	NAYM	Nacelle yaw moment
Location		Adjacent to yaw brake caliper; constrains motion of four-bar linkage where brake caliper is one bar.
Measurement type and units		Tensile and compressive load, N
Excitation		10 Vdc
Range		±10,000 lbs.
Resolution		32 N/bit
Calibration method		Application of known loads (A1)
Sensor description		Hermetically sealed, universal tension and compression force sensor
		Transducer Techniques Model: HSW-10K

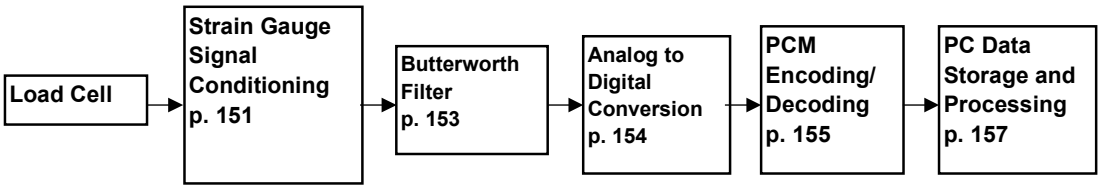

Note: The sign convention is such that positive yaw moment is in the direction of a moment restoring the turbine from negative yaw error to zero degrees yaw error.

Calibration Procedures (See p. 110)

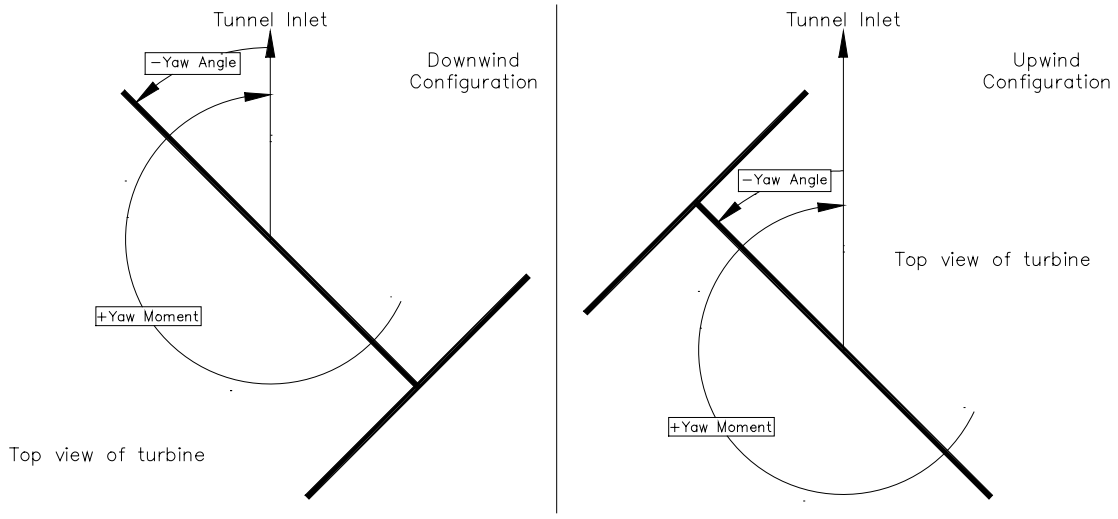

Figure B-9. Yaw moment measurement conventions

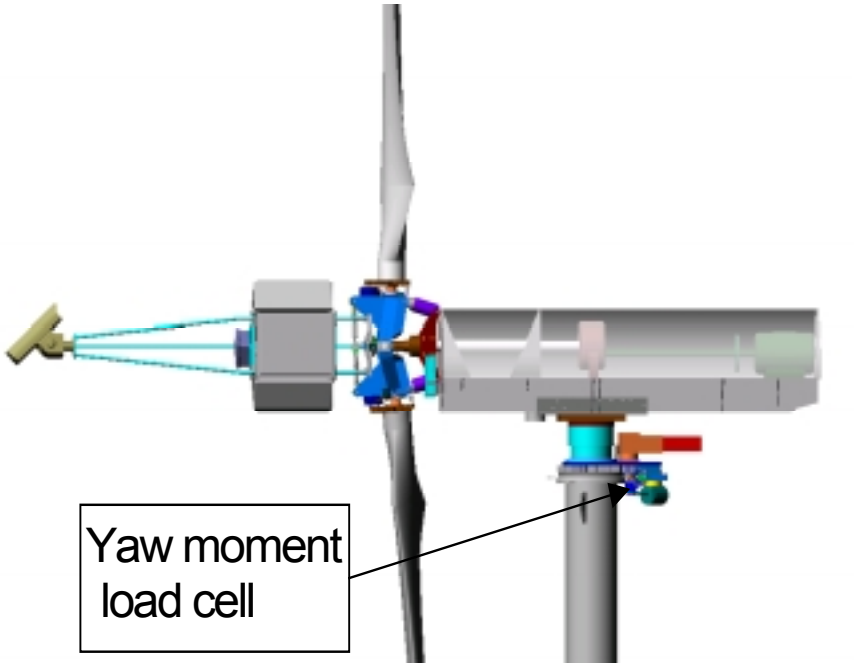

Figure B-10. Yaw moment load cell location

Channel	ID Code	Description
225	B1RFB	Blade 1 root flap bending moment
227	B1REB	Blade 1 root edge bending moment
233	B3RFB	Blade 3 root flap bending moment
235	B3REB	Blade 3 root edge bending moment

Location	Pitch shaft (8.6% span), 8360 Steel
Measurement type and units	Bending moment, Nm
Excitation	5Vdc
Range	± 5000με
Resolution	2000 με / V
Calibration method	Application of known loads (A1)
Sensor description	Resistance = 350.0 ± 0.4% Ω Measurements Group, Inc. Model: LWK-09-W250B-350

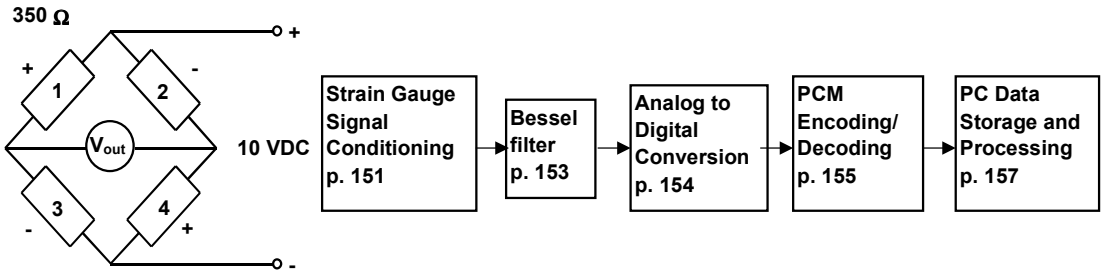

Note: Flap bending moment is positive when a force acts in the downwind direction; the flap moment vector is parallel to the tip chord. Edge bending moment is positive when a force acts in the direction of rotation; the edge moment vector is perpendicular to the tip chord. The physical direction changes from the downwind configuration to the upwind configuration, and the signs of the slope and offset coefficients were adjusted accordingly to maintain the measurement conventions relative to the wind direction.

Calibration Procedures

Application of known loads (A1)

A custom jig was used for strain gauge calibrations to isolate load conditions to one direction only (flap or edge). The jig mounts on the blade at 80% span (1 m inboard of the tip), and the blade is pitched to 1.4°, which corresponds to 0° at 80% span (Note: the strain gauges rotate with the blade). A cord is attached to the jig and runs over a pulley to the ground where weights are applied. One person in the man-lift mounts the jig on the blade and positions the man-lift so the pulley is level and square with the cord attachment to the jig. To calibrate the flap gauges, the cord is attached to the jig at a 90° angle to the blade chord. The edge gauges are calibrated by attaching the cord to the jig at a point aligned with the blade chord. Another person applies the weights in 20-lb increments from 0 to 120 lb. A third person operates the computer to collect samples at each load condition. The low-speed shaft bending gauges were calibrated by hanging

weights from the boom in a similar manner. These procedures produce new slope values for the strain gauge measurements. The pitch encoder gear must be separated from the pitch shaft for the load to be transferred solely through the pitch shaft. Loosening the gear may be necessary if hysteresis is apparent.

Determination of the offset values was performed as in previous phases of the experiment. Essentially, the root flap and edge offsets were determined by placing each blade in a position where the respective load is zero. The offset for the low-speed shaft and hub shaft gauges was determined by recording cyclic bending moments and torque. The average over one complete rotation was equivalent to the offset under zero load.

The slope and offset values were inserted in a temporary header file called *strains.hdr*. This file is read during the *buildhdr* process, and the values are placed in the *master.hdr* file.

Slope coefficient calibration:

1. The man-lift person notifies the ground people which blade and which direction (flap or edge) will be calibrated first. The computer person selects the appropriate channel(s) in *vbl.lst* to place at the top of the file. The number of channels to be collected is specified in the first line with NV, and the PCM stream on which the channels are contained is selected in *gencal.cap*. All of the strain gauges are on PCM stream 2 except the yaw moment load cell (NAYM) which is on PCM stream 3. The yaw moment channel (NAYM) is calibrated separately because it is on a different PCM stream than the other strain gauges. The low-speed shaft torque (LSSTQ) is included with each of the edge bending channels (B1REB, B3REB). The flap bending gauges (B1RFB, B3RFB) are each calibrated alone. The low-speed shaft bending gauges are calibrated separately (LSSXXB, LSSYYB) by suspending weights directly from the hub side of the camera mount at rotor positions corresponding to pure bending for each gauge.
2. The *gencal* program is run while the weights are applied from 0 to 120 lbs in 20-lb increments with two repetitions at each level. When suspending weights from the boom, they are applied from 0 to 100 lbs in 20-lb increments with three repetitions at each level. *Gencal* is run again while the weights are removed. The recorded weight and count values are stored in the **.cao* input files. A few seconds between applying the weight and collecting the data allows any vibrations of the turbine to damp. This is done for both flap and edge directions for each of the blades to calibrate flap bending, edge bending, and low-speed shaft torque strain gauges as well as the yaw moment load cell. The weights are applied again in each of the above configurations to load the blades in both positive and negative directions. The weights are applied to the boom at rotor positions of 60°, 150°, 240°, and 340° to load the low-speed shaft bending gauges in both positive and negative directions.
3. Compute moments in Nm using the following formula:

$$M = \left(\frac{w * \left(R * 39.37 \frac{in}{m} - r \right)}{12 \frac{in}{ft}} \right) 1.35582 \frac{Nm}{ft \cdot lb}$$ where M = Bending moment (Nm),

w=weight applied (0 to 120 lb), R=Blade radius (5 m), and r=radial distance to strain gauge (0.43 m from low-speed shaft to blade root gauges). The moment arm from the low-speed shaft gauges to the point on the boom at which the load was applied is 3.11 m. This replaces the term in parentheses in the numerator of the above equation. Plot each curve in Excel, and perform a linear curve fit to determine the slope for both the positive and negative bending

conditions for each strain gauge. Enter the average of the magnitude of the two slope values in the temporary header file, *strains.hdr*.

Offset coefficient calibration

1. All of the strain gauges were listed in *vbl.lst* for input to *gencal*. The instrumented blade was positioned at 30° increments over one complete rotational cycle. Three samples were obtained at each position. The blade flap angles were positioned to be equal corresponding to zero teeter angle.
2. The offset for flap bending channels was determined by averaging the count value of each blade at 90° and at 270°, where the flap load is 0 Nm. This number may be compared with the value obtained by averaging the loads at 0° and at 180°, where the average load should be 0 Nm.
3. A similar procedure provided the offset values of the edge bending channels. The average load at 0° and at 180° provided the zero offset, while a comparison of the average load at 90° and 270° indicated whether or not the procedure worked properly.
4. The low-speed shaft bending for both X-X and Y-Y axes and the low-speed shaft torque average to zero over the complete rotational cycle. This average count value was used to determine the offset.
5. The yaw moment offset was determined by recording the count value when the yaw brake was released in zero wind conditions.
6. The count values obtained under zero-load conditions for each channel were multiplied by the corresponding slope value and entered in *strains.hdr*.

Note: The calibration pins must be installed during the blade flap pulls to maintain a zero-degree flap angle.

Calibration frequency

The strain gauge slopes were calibrated prior to wind tunnel testing. The offsets were determined daily during wind tunnel testing.

Figure B-11. Blade 1 flap bending strain gauge slope calibration

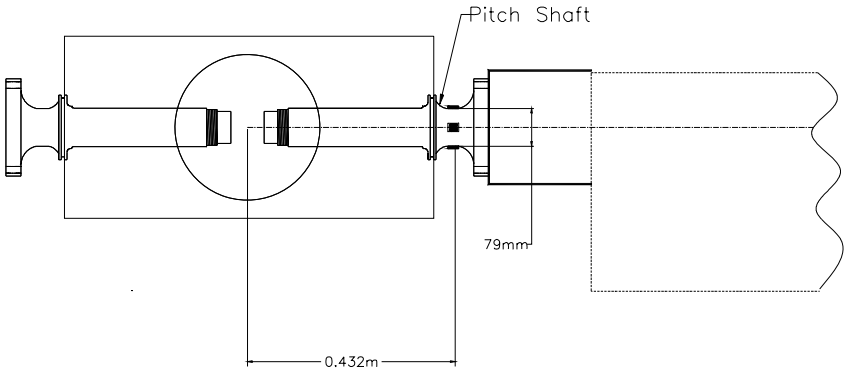

Figure B-12. Root bending gauges, side view

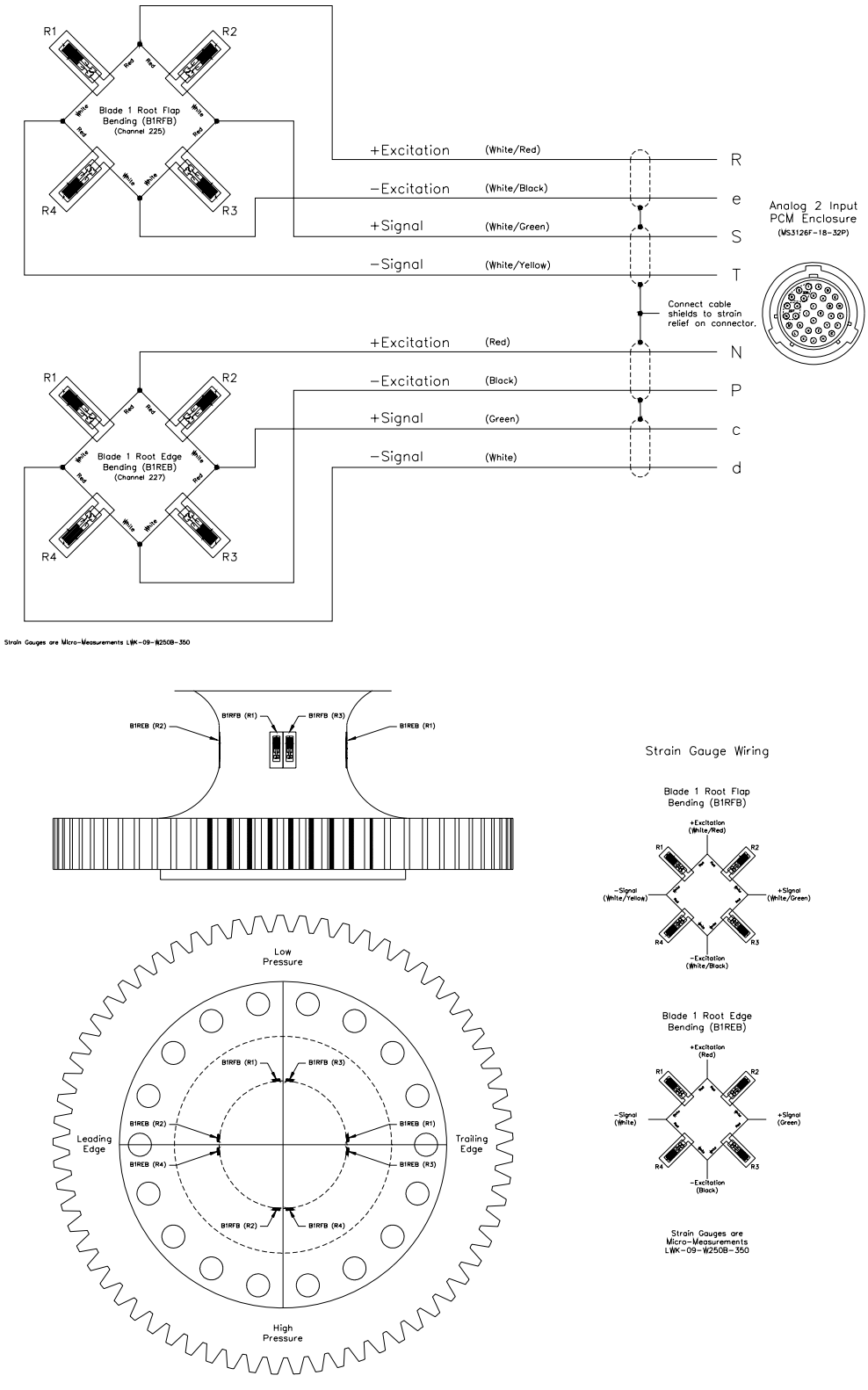

Figure B-13. Blade 1 root bending strain gauge configuration

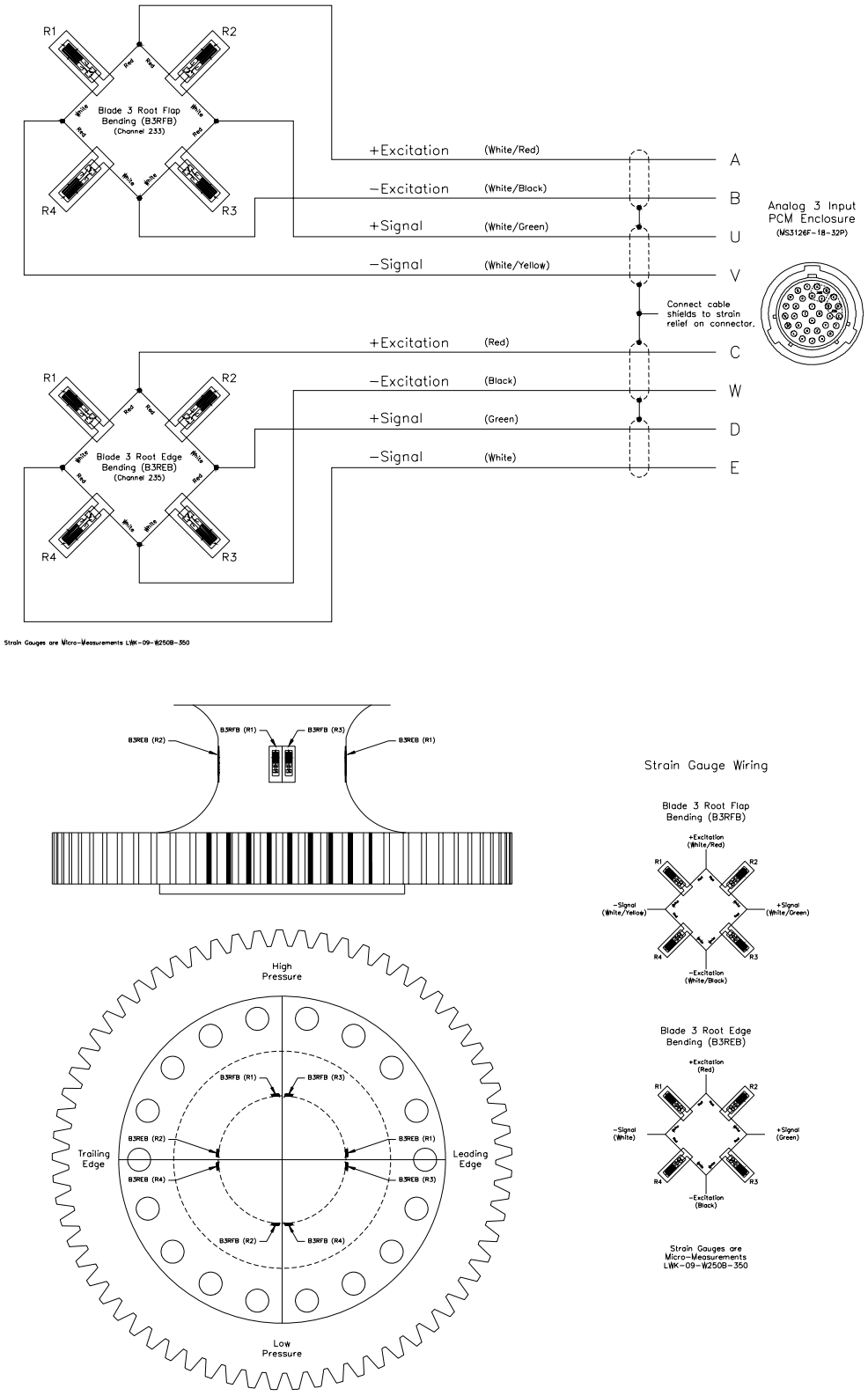

Figure B-14. Blade 3 root bending strain gauge configuration

Strain Gauges (Low-speed shaft)

Channel	ID Code	Description
237	LSSXXB	X-X low-speed shaft bending moment
239	LSSYYB	Y-Y low-speed shaft bending moment
241	LSSTQ	Low-speed shaft torque

Location	Low-speed shaft
Measurement type and units	Bending moment, Nm; torque, Nm
Excitation	10 Vdc
Range	± 50,000 με
Resolution	10,000 με / V
Calibration method	Application of known loads (A1)
Sensor description	Resistance = 350.0 ± 0.4% Ω
	Measurements Group, Inc.
	Model: CEA-06-250UW-350 (LSS Bending)
	CEA-06-250US-350 (LSS Torque)

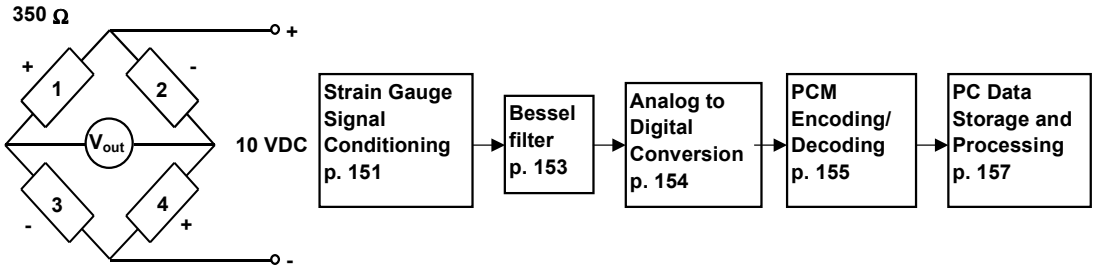

Note: The low-speed shaft XX bending gauge has a positive peak when blade 3 is at 240° azimuth and a negative peak when blade 3 is at 60° azimuth for the downwind turbine configuration. The low-speed shaft YY bending gauge has a positive peak when blade 3 is at 150° azimuth and a negative peak when blade 3 is at 330° azimuth for the downwind turbine configuration. For the upwind configuration, the low-speed shaft XX bending gauge has a positive peak when blade 3 is at 120° azimuth and a negative peak when blade 3 is at 300° azimuth. The YY bending gauge reaches a positive peak at blade 3 azimuth 210° and a negative peak at blade 3 azimuth 30° in the upwind configuration. The low-speed shaft torque is positive in the direction of rotation for both upwind and downwind configurations.

Calibration Procedures (See p. 110)

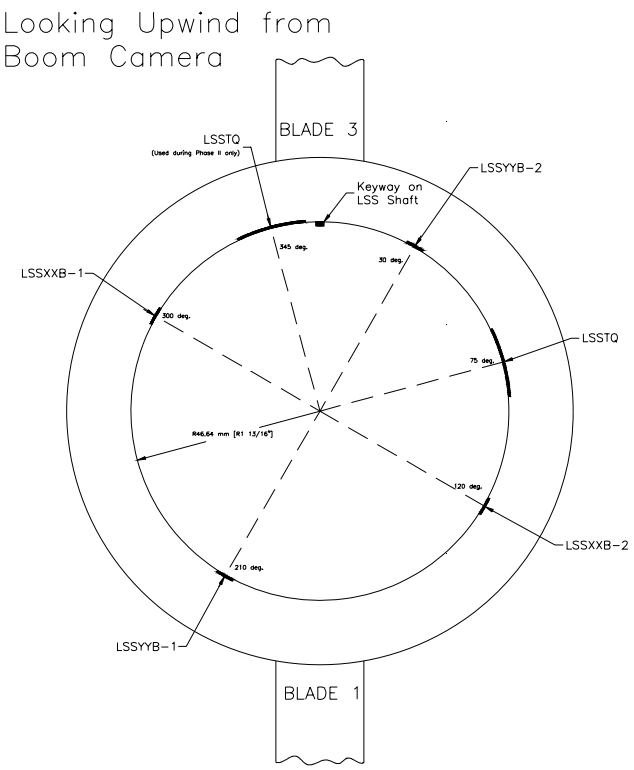

Figure B-15. Low-speed shaft strain gauge location (downwind configuration)

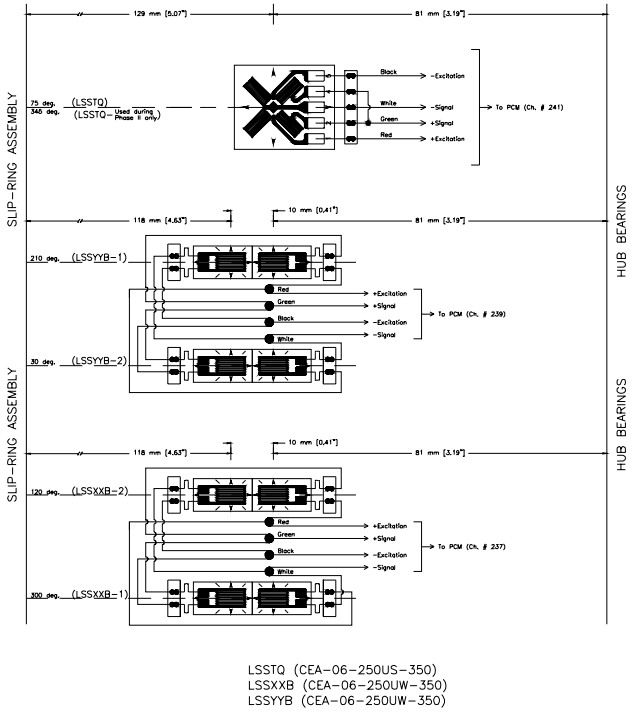

Figure B-16. Low-speed shaft strain gauge configuration (downwind turbine)

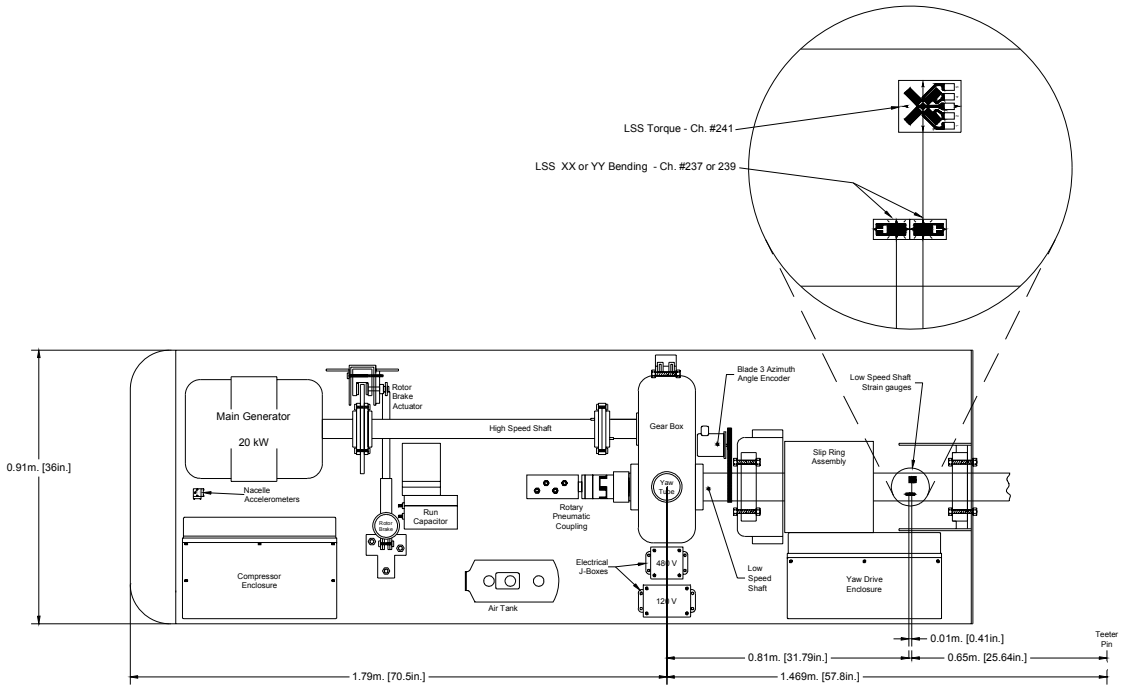

Figure B-17. Low-speed shaft strain gauge location within nacelle

Channel	ID Code	Description
201	B1ACFL	Blade 1 tip accelerometer – flap
203	B1ACED	Blade 1 tip accelerometer – edge
209	B3ACFL	Blade 3 tip accelerometer – flap
211	B3ACED	Blade 3 tip accelerometer – edge
336	NAACYW	Nacelle accelerometer – yaw
338	NAACFA	Nacelle accelerometer – fore-aft sway
340	NAACPI	Nacelle accelerometer – pitch

Location	Blade tip, inside tip block; nacelle bedplate near generator
Measurement type and units	linear acceleration, m/s^2
Excitation	15 Vdc
Range	±2 V = ±10 g
Sensitivity	200 mV / g
Calibration method	Manufacturer specifications (M8) and electronic path calibration (E1)
Sensor description	Variable capacitance accelerometer
	Endevco Corporation Model: 7290A-10

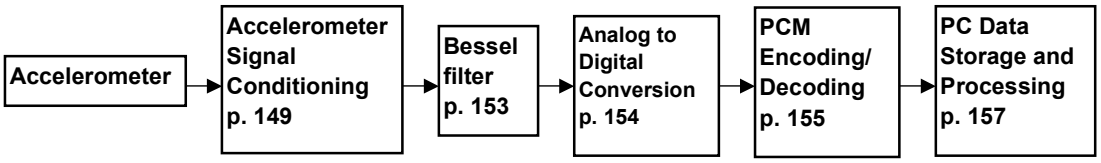

Note: Flap acceleration is positive due to acceleration in the downwind direction, perpendicular to the tip chord; edge acceleration is positive due to acceleration in the direction of rotation, parallel to the tip chord. If the nacelle accelerated in the negative yaw direction, the nacelle yaw accelerometer measured a positive value. Positive fore-aft acceleration occurred if the nacelle accelerated toward the hub. The pitch acceleration was positive in the vertical direction.

Calibration Procedure

Manufacturer specifications - (M8)

1. Endevco Corporation calibrated the accelerometers before installation.
2. Enter the sensitivity as recorded by Endevco and the offset (0 g) in the appropriate columns of *calconst.xls*.

Electronic path calibration (E1)

1. Modify *vbl.lst* so the accelerometer channels are listed at the top of the file. Set NV (number of variables) in the first line to the number of channels to be calibrated, and insure that the correct PCM stream is specified in *gencal.cap* (PCM stream 2 for blade accelerometers and PCM stream 3 for nacelle accelerometers). Because the nacelle accelerometers and the blade tip accelerometers are on different PCM streams, they must be separated into two **.cao* files.

2. Connect the precision voltage generator to the accelerometer output prior to the signal conditioners.
3. Run the *gc* batch file, which invokes both *gencal* and *genfit*. Collect samples for voltages ranging from –0.9 to 0.9 V in 0.2-V increments for nacelle accelerometers (-0.8 to 0.8 in 0.2-V increments for blade accelerometers) with two repetitions at each voltage level. The recorded input and output values are stored in the **.cao* input file. *Genfit* computes slopes and offsets of the electronic path from the processor output to the computer in units of V/count and V, respectively. These values are stored in a temporary header file, **.hdr*. These slope and offset values are combined with the manufacturer provided slope and offset during the *buildhdr* process to obtain units of engineering unit/count and counts, respectively.

Calibration frequency

The accelerometers were calibrated prior to installation. An electronic path calibration was performed prior to wind tunnel testing.

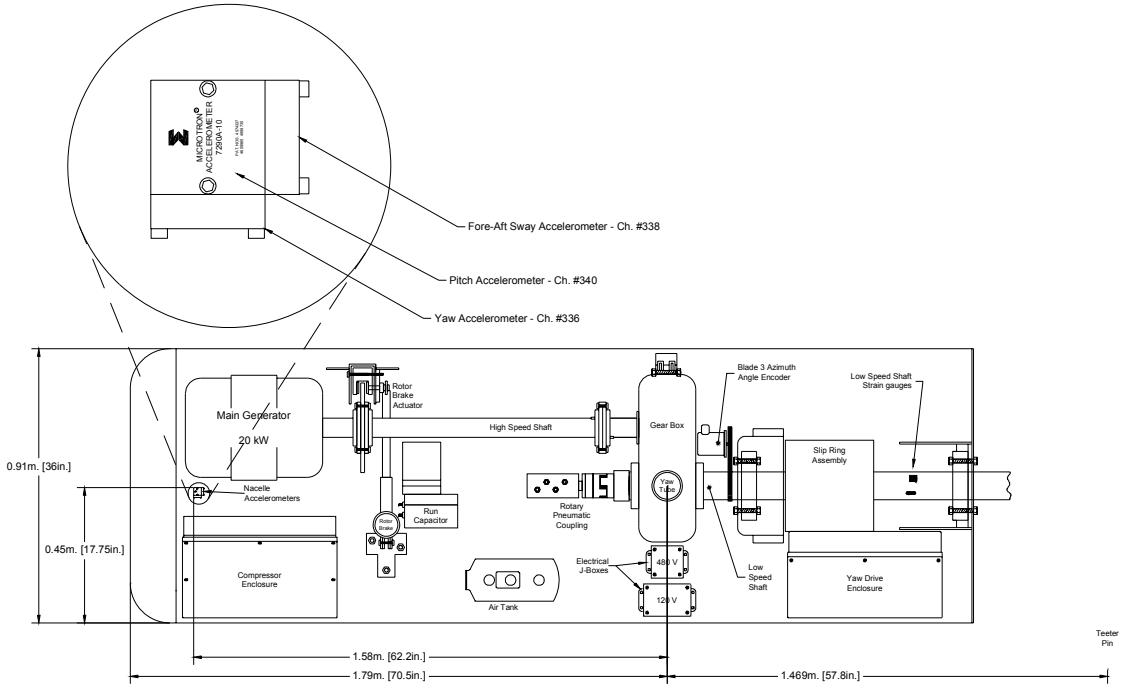

Figure B-18. Nacelle accelerometer location within nacelle

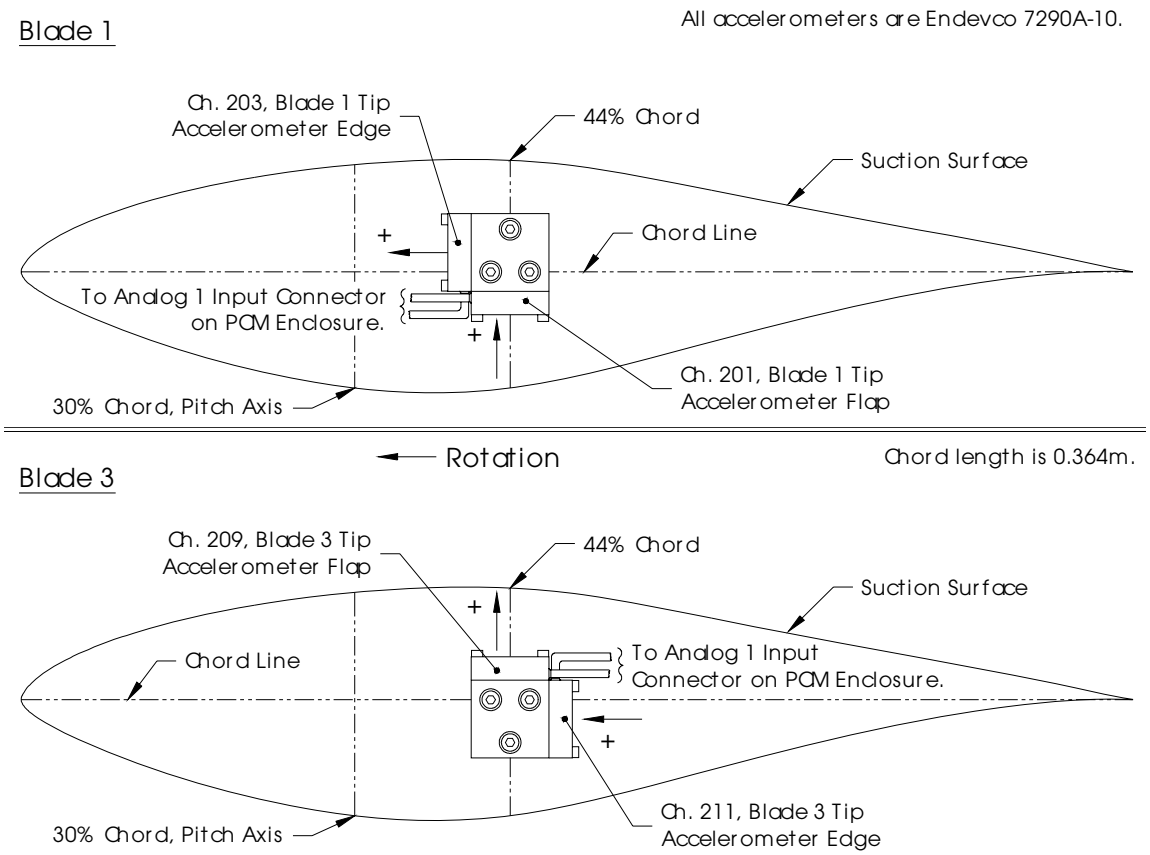

Figure B-19. Blade tip accelerometer configuration

Channel	ID Code	Description
332	GENPOW	Generator power

Location	Power handling cabinet inside data shed
Measurement type and units	Electrical power, kW
Range	-40 kW to 40 kW = -5V to 5V
Resolution	8 kW/V
Calibration method	Manufacturer specifications (M7) and electronic path calibration (E1)
Sensor description	AC Watt Transducer 3 phase, 3 wire 50/60 Hz Ohio Semitronics, Inc. Model: PC5-63C (DOE#: 00502C)

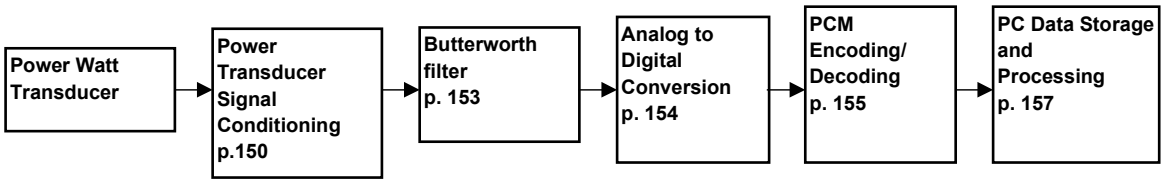

Calibration Procedure

Manufacturer specifications - (M7)

1. The NREL Calibration Laboratory performed a calibration before installing the power Watt transducer.
2. Enter the slope (8 kW/V) and the offset (0 kW) in the appropriate columns of *calconst.xls*.

Electronic path calibration - (E1)

1. Modify *vbl.lst* so the power channel is listed at the top of the file. Set NV (number of variables) in the first line to the number of channels to be calibrated, and insure that the correct PCM stream is specified in *gencal.cap* (PCM stream 3).
2. Connect the precision voltage generator to the power transducer output.
3. Run the *gc.bat* batch file, which invokes both *gencal.exe* and *genfit.exe*. Collect samples for voltages ranging from –4.5 to 4.5 V in 1-V increments with two repetitions at each voltage level. The recorded input and output values are stored in the **.cao* input file. *Genfit.exe* computes slopes and offsets of the electronic path from the processor output to the computer in units of V/count and V, respectively. These values are stored in a temporary header file, **.hdr*. These slope and offset values are combined with the manufacturer provided slope and offset during the *buildhdr.bat* process to obtain units of engineering unit/count and counts, respectively.

Calibration frequency

The transducer was calibrated in the laboratory prior to installation. The electronic path calibration was performed prior to wind tunnel testing.

Channel	ID Code	Description
243	B1PRATE	Blade 1 pitch rate
247	B3PRATE	Blade 3 pitch rate

Location	Root attachment of each blade
Measurement type and units	Rate of rotation, deg/s
Power Requirement	120 V
Range	0 to 66.6 deg/s = 0V to 6.6V
Resolution	10 deg/s/V
Calibration method	Manufacturer specifications (M6) and electronic path calibration (E1)
Sensor description	Programmable microdrive
	ElectroCraft motor: LD2003 ElectroCraft microdrive: DDM005

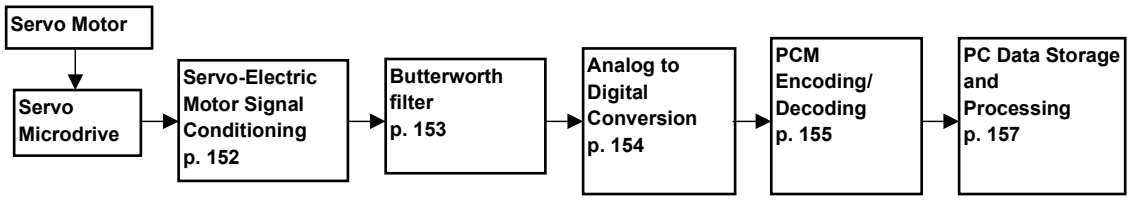

Calibration Procedures

Manufacturer specifications (M6)

1. Because the range is adjustable, it was set to prevent railing at full speed (66.6°/s). The range selected was 0 to 10 V corresponds to 0°/s to 100°/s.
2. Enter the slope (10°/s/V) and offset (0°/s) in the appropriate columns of *calconst.xls*.

Electronic path calibration - (E1)

1. Modify *vbl.lst* so the pitch rate channels are listed at the top of the file. Set NV (number of variables) in the first line to the number of channels to be calibrated, and insure that the correct PCM stream is specified in *gencal.cap* (PCM stream 2).
2. Connect the precision voltage generator to the microdrive output.
3. Run the *gc.bat* batch file, which invokes both *gencal.exe* and *genfit.exe*. Collect samples for voltages ranging from –9 to 9 V in 2-V increments with two repetitions at each voltage level. The recorded input and output values are stored in the **.cao* input file. *Genfit.exe* computes slopes and offsets of the electronic path from the processor output to the computer in units of V/count and V, respectively. These values are stored in a temporary header file, **.hdr*. These slope and offset values are combined with the manufacturer-provided slope and offset during the *buildhdr.bat* process to obtain units of engineering unit/count and counts, respectively.

Calibration Frequency

The electronic path calibration was performed prior to wind tunnel testing.

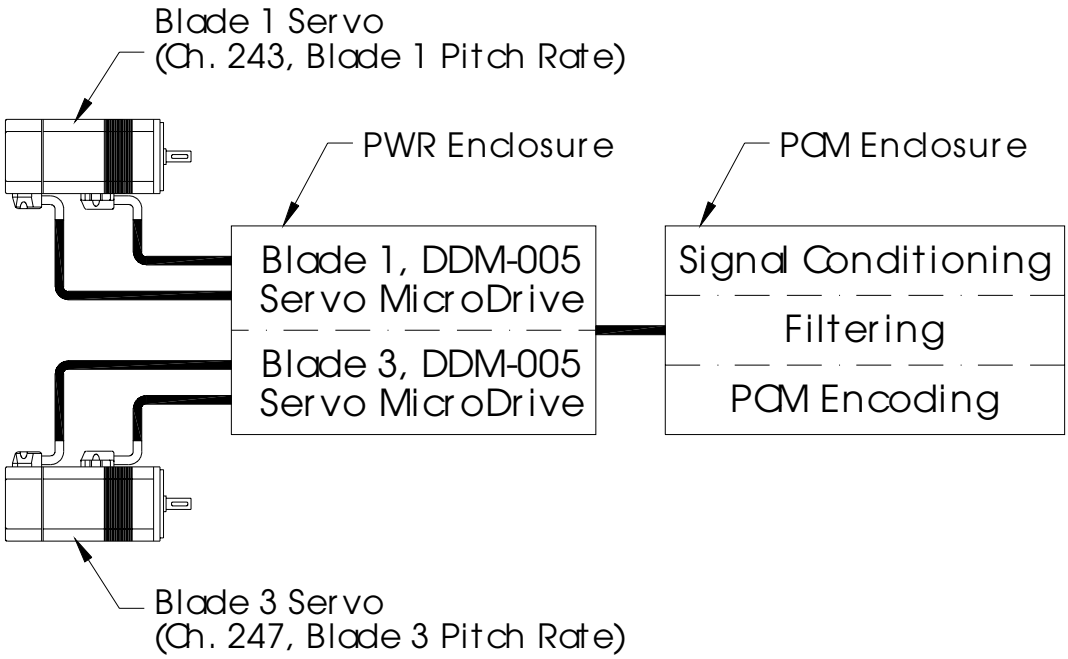

Figure B-20. Servo-motor signal diagram

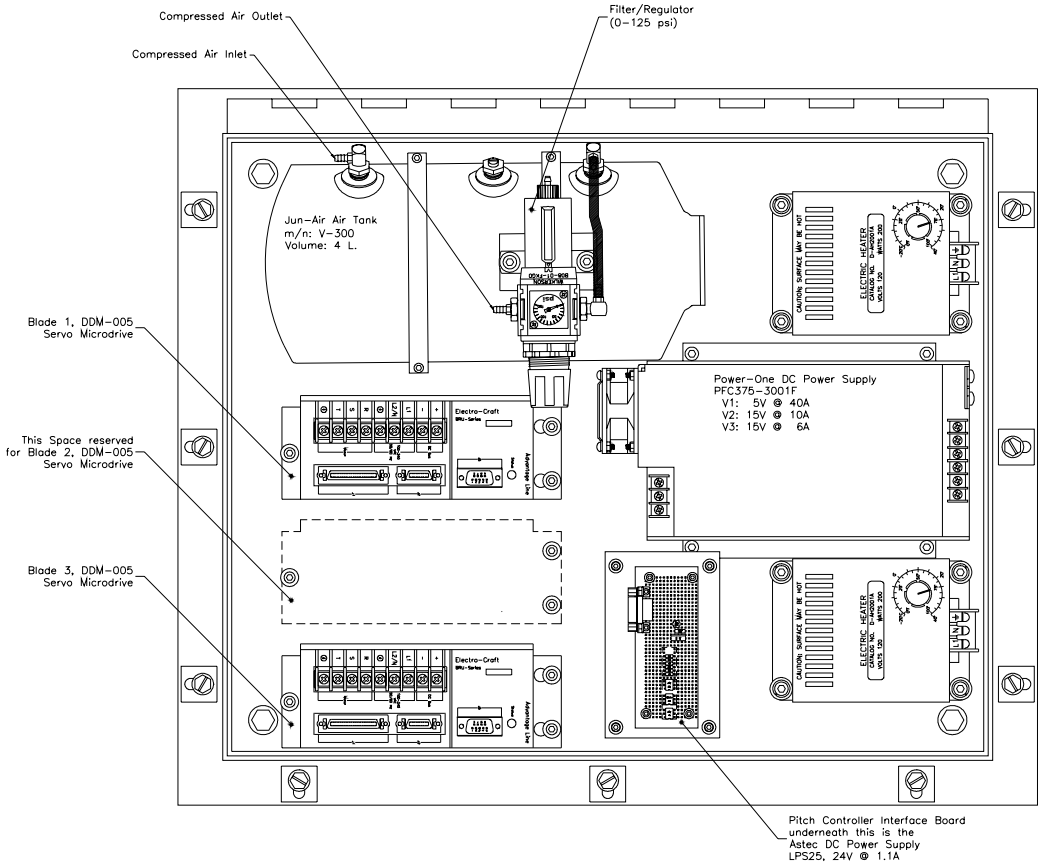

Figure B-21. Power enclosure

Channel	ID Code	Description
253	B1PITCH	Blade 1 pitch angle
257	B3PITCH	Blade 3 pitch angle
349	B3AZI	Blade 3 azimuth angle
351	YAW	Turbine yaw angle

Location	Root attachment of each blade; low-speed shaft in nacelle; yaw axis.
Measurement type and units	Angular position, degrees
Power Requirement	15 Vdc
Range	360° = 4,096 counts
Resolution	0.08789 °/count
Calibration method	Manufacturer specifications (M5) and single point offset determination (S3)
Sensor description	Digital, gray code resolver Accuracy: ±1/2 Count (LSB), worst case BEI Motion Systems Company Model: R25-4096-24 (azimuth only); RAS-25

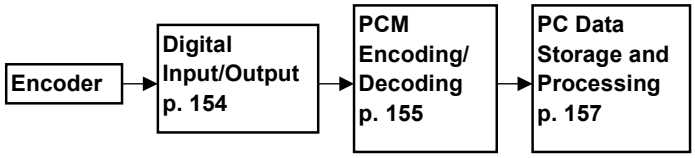

Calibration Procedure

Manufacturer specifications - (M5)

1. BEI Motion Systems performed a calibration before installation of all digital position encoders.
2. Enter the slope (0.08789°/count) in the appropriate columns of *calconst.xls*.

Single point offset determination - (S3)

1. (This is a two-person operation requiring one person in the man-lift to position the blades or turbine and one person on the ground to operate the computer.)
2. The man-lift person notifies the ground person which encoder is to be calibrated. A reference point is used to determine the offset for each encoder as follows:
3. Each blade is individually pitched to 0°, and an Angle-star is used to measure the exact pitch angle. The jig is placed on both the upwind and downwind side of the blade, and the rotor is positioned at both 90° and 270°. The four pitch measurements, in counts, are averaged together.
4. The nacelle is aligned by eye with the wind tunnel inlet center strut to determine the yaw angle offset.

5. The instrumented blade is aligned by eye with the tower (180°) to determine the azimuth angle offset.
6. The difference between the data acquisition system angle and the known angle is determined in counts. This value is added to the current count value listed in *calconst.xls*. A new *master.hdr* file is created using the macros *Write ang.hdr* and *Write convert.v2u* along with the program *vupdate.exe*. The angle is then repositioned and the difference obtained. If the difference is greater than 2-3 counts, the process is repeated.

Calibration frequency

The blade pitch, yaw angle, and azimuth angle offsets were determined prior to wind tunnel testing.

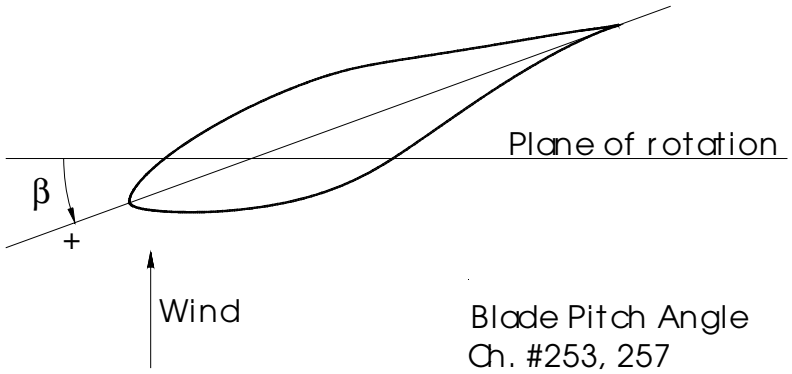

Figure B-22. Blade pitch angle orientation

Figure B-23. Azimuth angle encoder

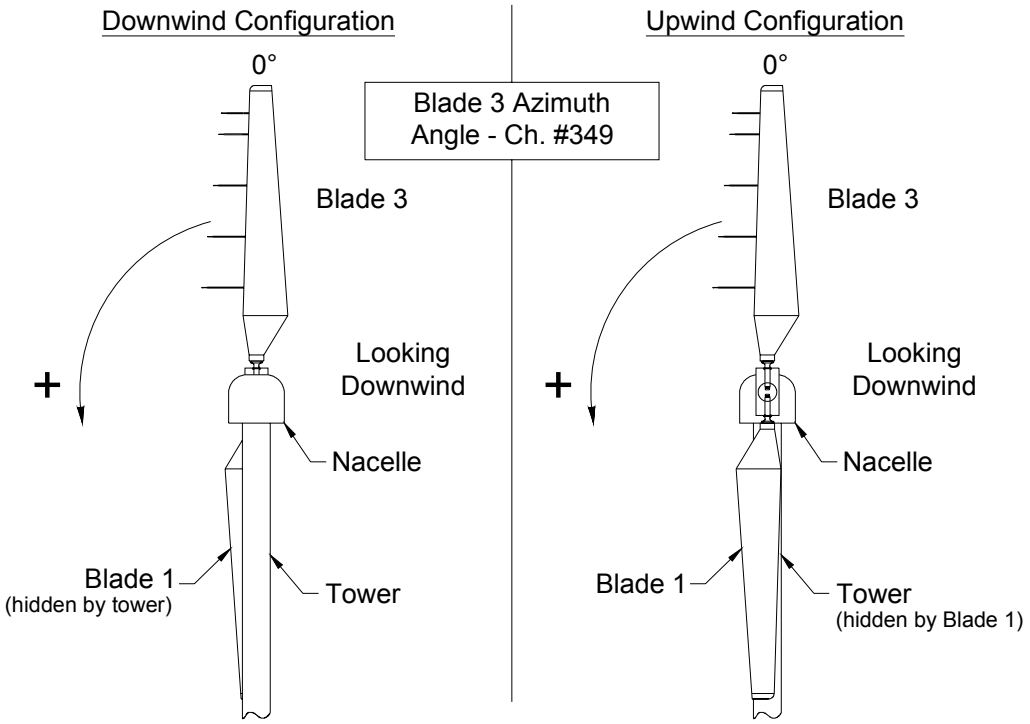

Figure B-24. Azimuth angle measurement convention

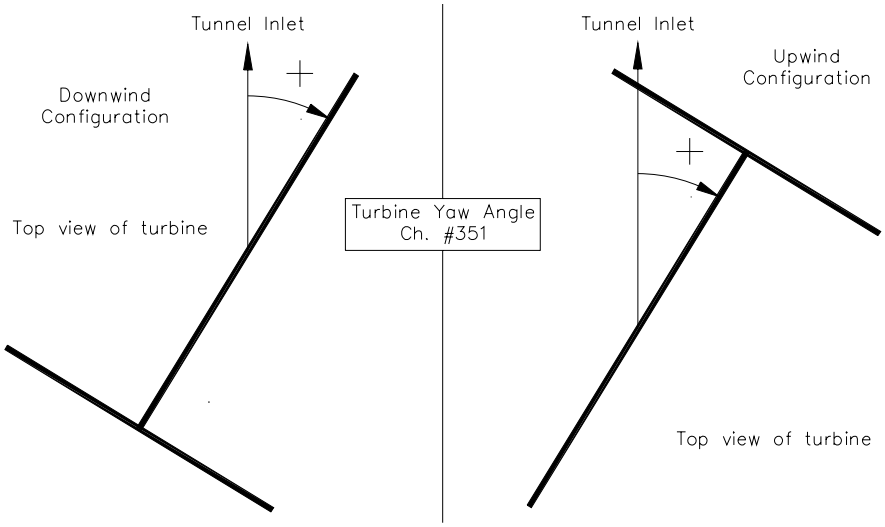

Figure B-25. Yaw angle measurement convention. In positive yaw, the blade advances into the wind at 180° azimuth for both configurations

Channel	ID Code	Description
251	B1FLAP	Blade 1 flap angle
255	B3FLAP	Blade 3 flap angle

Location	Mounted on hub outboard of teeter bearing
Measurement type and units	angular position, degrees
Power Requirement	15 Vdc
Range	45° (restricted by damper)
Resolution	0.0110°/count (with 8:1 anti-backlash gearing)
Calibration method	Manufacturer specifications (M4) and single point offset determination (S2)
Sensor description	Digital, gray code resolver Accuracy: ±1/2 Count (LSB), worst case BEI Motion Systems Company Model: RAS-25

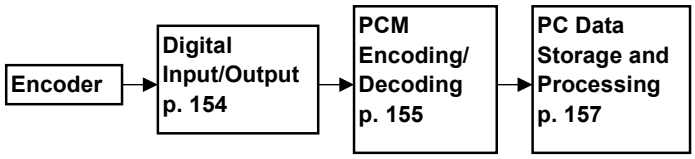

Calibration Procedure

Manufacturer specifications - (M4)

1. BEI Motion Systems performed a calibration before installation of all digital position encoders.
2. Enter the slope (360 °/(4,096 counts*(8 gear-ratio))) in the appropriate columns of *calconst.xls*.

Single point offset determination - (S2)

(This is a two-person operation requiring one person in the man-lift to insert the calibration pins and one person on the ground to operate the computer.)

1. Calibration pins are inserted in each teeter damper individually to position the blades at 0° flap angle.
2. The difference between the data acquisition system angle and the known angle is determined in counts. This value is added to the current count value listed in *calconst.xls*. A new *master.hdr* file is created using the macros *Write ang.hdr* and *Write convert.v2u* along with the program *vupdate*. The angle is then repositioned and the difference obtained. If the difference is greater than 2-3 counts, the process is repeated.

Calibration frequency

The single point-offset determination was done prior to wind tunnel testing.

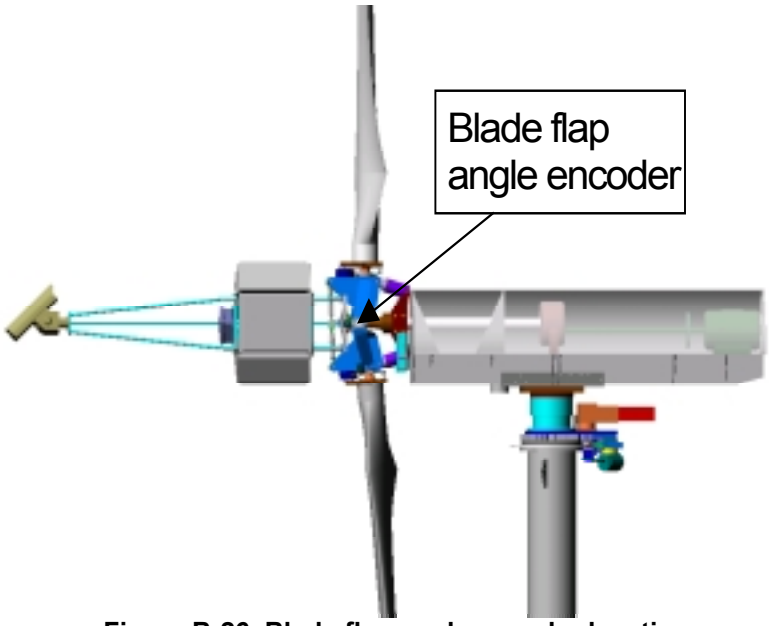

Figure B-26. Blade flap angle encoder location

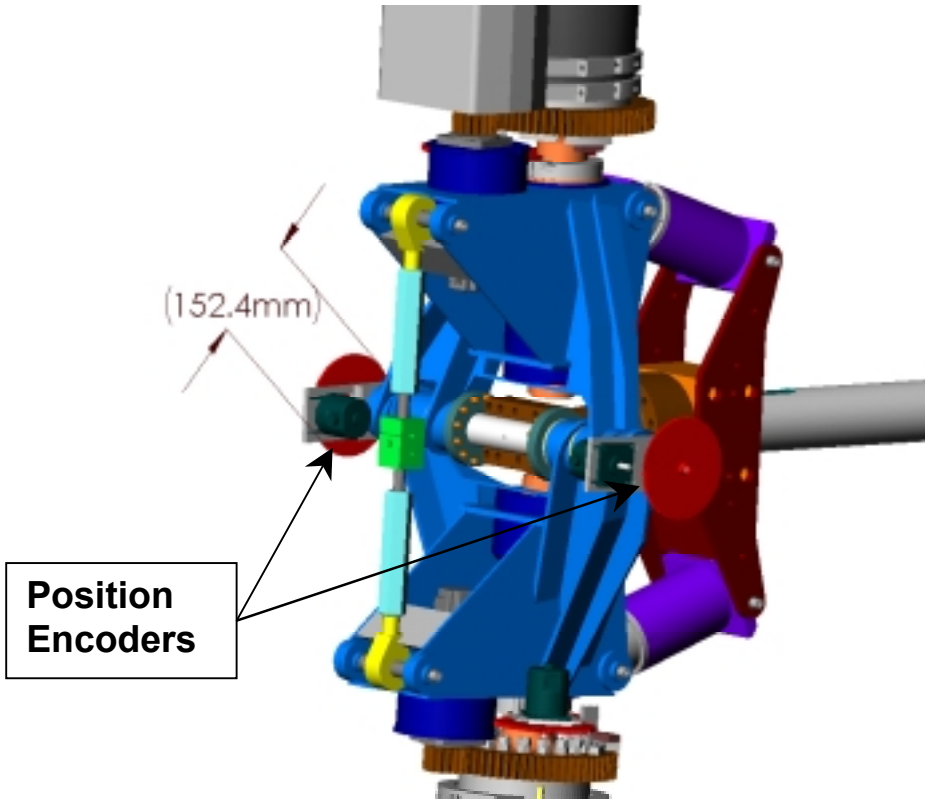

Figure B-27. Blade flap angle encoder close-up view

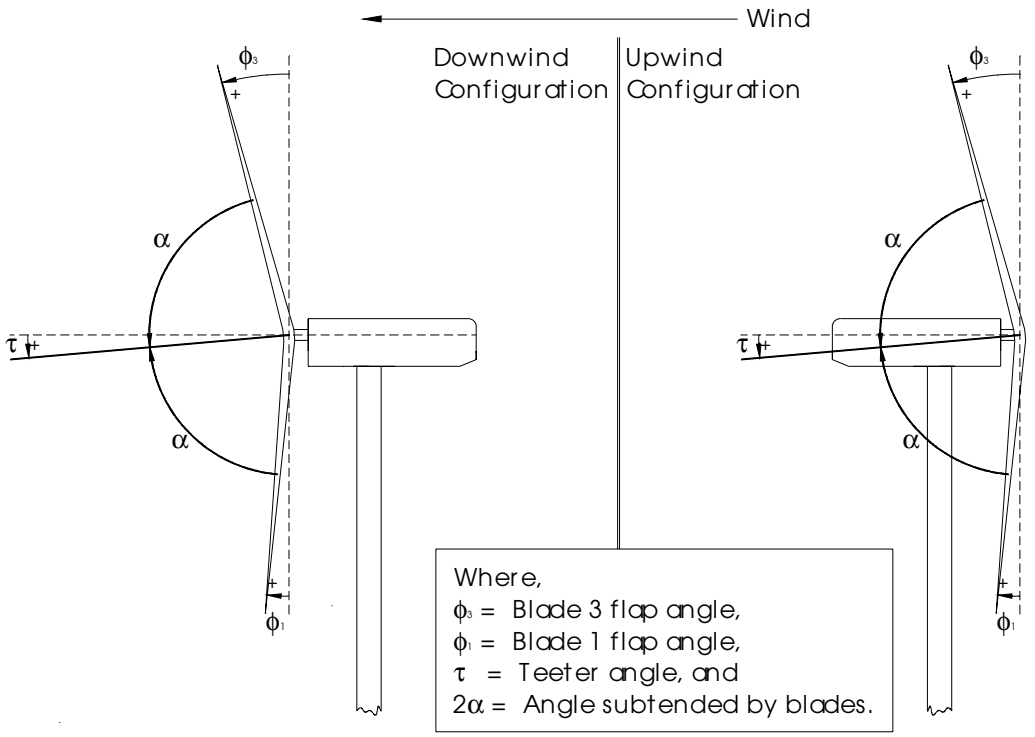

Figure B-28. Blade flap angle convention

Pressure Transducers (30% and 47% span)

Channel	ID Code	Description
000-050 (even)	Ptt30ccc Ptt36ccc Ptt41ccc	Surface pressures at 30%, 36%, and 41% span tt = transducer tap number ccc = % chord pressure tap location
001-051 (odd)	Ptt47ccc Ptt52ccc Ptt58ccc	Surface pressures at 47%, 52%, and 58% span tt = transducer tap number ccc = % chord pressure tap location
052-060 (even)	5Hx34	5-hole probe at 34% span x = designation of hole in 5-hole probe
053-061 (odd)	5Hx51	5-hole probe at 51% span x = designation of hole in 5-hole probe

Location	Within blade 3 at approximately 30% span and 47% span
Measurement type and units	Pressure difference between surface or probe and hub
Power Requirement	5 Vdc, ±12 Vdc
Range	±2,500 Pa (10" H_2O) = ±5 V
Resolution	500 Pa/V
Calibration method	Application of known pressures (A2)
Sensor description	32 channel electronic pressure scanner Scan rate: up to 20,000 readings/second Pressure Systems Model: ESP-32SL

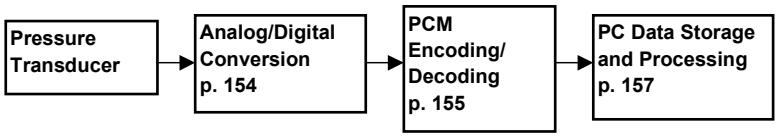

Note:

1. Small pressure taps were installed in the surface of the blade skin during manufacturing. Each opening was mounted flush to the airfoil surface and was 0.7874 mm inner diameter.
2. Stainless steel tubes, 0.45 m in length, were installed inside the blade's skin during manufacturing to carry surface pressures to the pressure transducer. A short piece of plastic tubing joined the tubes to the transducers.

Five-hole probe positions

The five-hole probes were mounted to a stalk that was aligned with the blade chord. The probes were angled approximately 20° to position the tip in the flow. These angles were measured using a custom jig and the Angle Star. Both the relative local flow angle offset and the spanwise flow angles were measured. A machined jig was used to align the holes of the five-hole probe parallel and perpendicular to the leading edge of the blade. This was done by eye.

For the local flow angle offset measurement, the blade was placed horizontal to the ground. The jig was placed immediately inboard and outboard of the probe stalk. The angle of the chord relative to the ground was recorded as the local blade angle. A machined surface jig was placed on the five-hole probe, and another Angle Star was used to measure the angle of the probe

relative to the ground. The difference is the angle of the probe relative to the chord of the blade. This was done for all five span locations. The probes were removed and replaced to determine repeatability.

The spanwise flow angle offsets were calibrated similarly. The blade was positioned straight down with 0° cone angle. The Angle Star was then used to measure the stalk angle and the probe angle relative to the ground. The probe angle is positive inboard of the probe. These angles are shown in Table 23.

Calibration Procedures

Application of known pressures - (A2)

This calibration is designed to provide an accurate slope calibration of the complete pressure system. The pressure system controller is invoked to provide NIST-traceable reference pressures at all pressure ports. The pressures ramp up and down across the measurement range. Linear regression provides calibration coefficients that are automatically updated in *master.hdr* before data acquisition. This calibration is performed approximately every 30 minutes.

1. After the turbine has been rotating for 30 minutes, the temperature variations are minimized. A batch file initiates a pressure calibration. The syringe in a hub-mounted instrumentation box (PSC Enclosure, p. 145) applies a pressure to each transducer at once. Pressures were applied at -0.9, -0.7, -0.5, -0.3, -0.2, -0.1, 0.1, and 0.2 psi. The actual pressure applied to the transducers is measured with the Mensor digital differential pressure transducer. A linear regression analysis provides slope and offset values, which are incorporated in *master.hdr*. During consecutive runs, the post-calibration of one data segment may also serve as the pre-calibration for the next data segment.

Table B-1. Pressure Tap Chord Locations

Pressure Tap Number	% chord	Surface	tt	ccc
1	100%	Trailing edge	01	100
4	80%	Upper	04	80U
6	68%	Upper	06	68U
8	56%	Upper	08	56U
11	36%	Upper	11	36U
13	20%	Upper	13	20U
15	10%	Upper	15	10U
17	6%	Upper	17	06U
18	4%	Upper	18	04U
19	2%	Upper	19	02U
20	1%	Upper	20	01U
21	0.5%	Upper	21	.5U
22	0%	Leading edge	22	000
23	0.5%	Lower	23	.5L
24	1%	Lower	24	01L
25	2%	Lower	25	02L
27	6%	Lower	27	06L
30	14%	Lower	30	14L
32	28%	Lower	32	28L
34	44%	Lower	34	44L
36	68%	Lower	36	68L
38	92%	Lower	38	92L

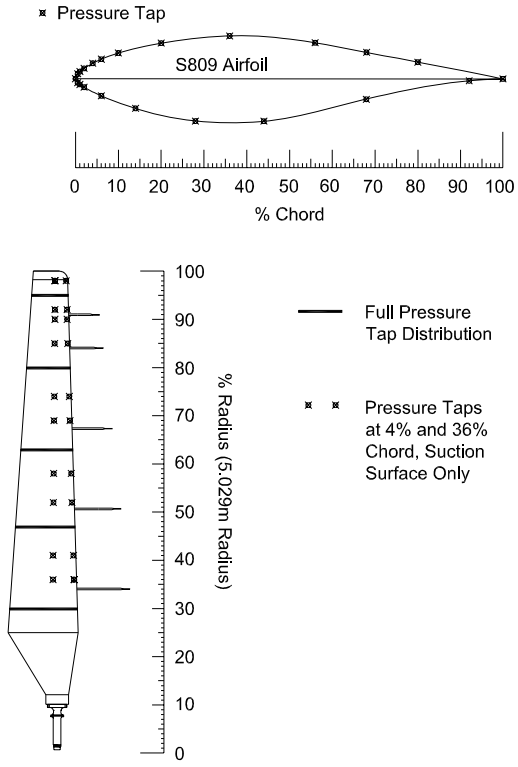

Figure B-29. Tapered/twisted blade planform

Pressure Transducers (63% span)

Channel	ID Code	Description
100-150 (even)	Ptt63ccc Ptt69ccc Ptt74ccc	Surface pressures at 63%, 69%, and 74% span tt = transducer tap number ccc = % chord pressure tap location
152-160 (even)	5Hx67	Five-hole probe at 67% span x = designation of hole in five-hole probe

Location	Within blade 3 at approximately 63% span
Measurement type and units	Pressure difference between surface or probe and hub
Power Requirement	5 Vdc, ±12 Vdc
Range	±5,000 Pa (20" H_2O) = ±5 V
Resolution	1,000 Pa / V
Calibration method	Application of known pressures (A2)
Sensor description	32 channel electronic pressure scanner Scan rate: up to 20,000 readings/second Pressure Systems Model: ESP-32SL

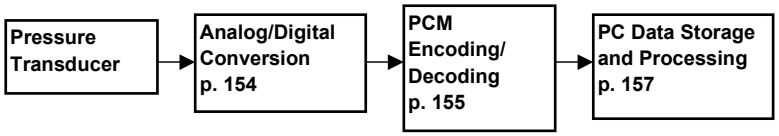

Calibration Procedure (See p. 137)

Pressure Transducers (80% span)

Channel	ID Code	Description
101-151 (odd)	Ptt80ccc Ptt85ccc Ptt90ccc	Surface pressures at 80%, 85%, and 90% span tt = transducer tap number ccc = % chord pressure tap location
153-161 (odd)	5Hx84	Five-hole probe at 84% span x = designation of hole in five-hole probe

Location	Within blade 3 at approximately 80% span
Measurement type and units	Pressure difference between surface or probe and hub
Power Requirement	5 Vdc, ±12 Vdc
Range	±6,894 Pa, (1.0 psi) = ±5 V
Resolution	1,379 Pa / V
Calibration method	Application of known pressures (A2)
Sensor description	32 channel electronic pressure scanner Scan rate: up to 20,000 readings/second Custom made for ±1.0 psi range Pressure Systems Model: ESP-32SL

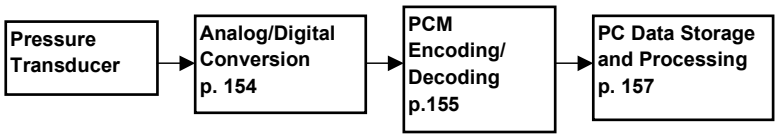

Calibration Procedure (See p. 137)

Pressure Transducers (95% span)

Channel	ID Code	Description
200-250 (even)	Ptt95ccc Ptt92ccc Ptt98ccc	Surface pressures at 95%, 92%, and 98% span tt = transducer tap number ccc = % chord pressure tap location
252-260 (even)	5Hx91	Five-hole probe at 91% span x = designation of hole in five-hole probe

Location	Within blade 3 at approximately 95% span
Measurement type and units	Pressure difference between surface or probe and hub
Power Requirement	5 Vdc, ±12 Vdc
Range	±10,342 Pa (1.5 psi) = ±5 V
Resolution	2,068 Pa / V
Calibration method	Application of known pressures (A2)
Sensor description	32 channel electronic pressure scanner Scan rate: up to 20,000 readings/second Custom made for ±1.5 psi range Pressure Systems Model: ESP-32SL

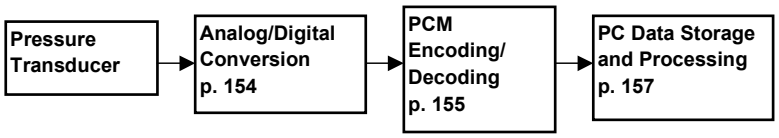

Calibration Procedure (See p. 137)

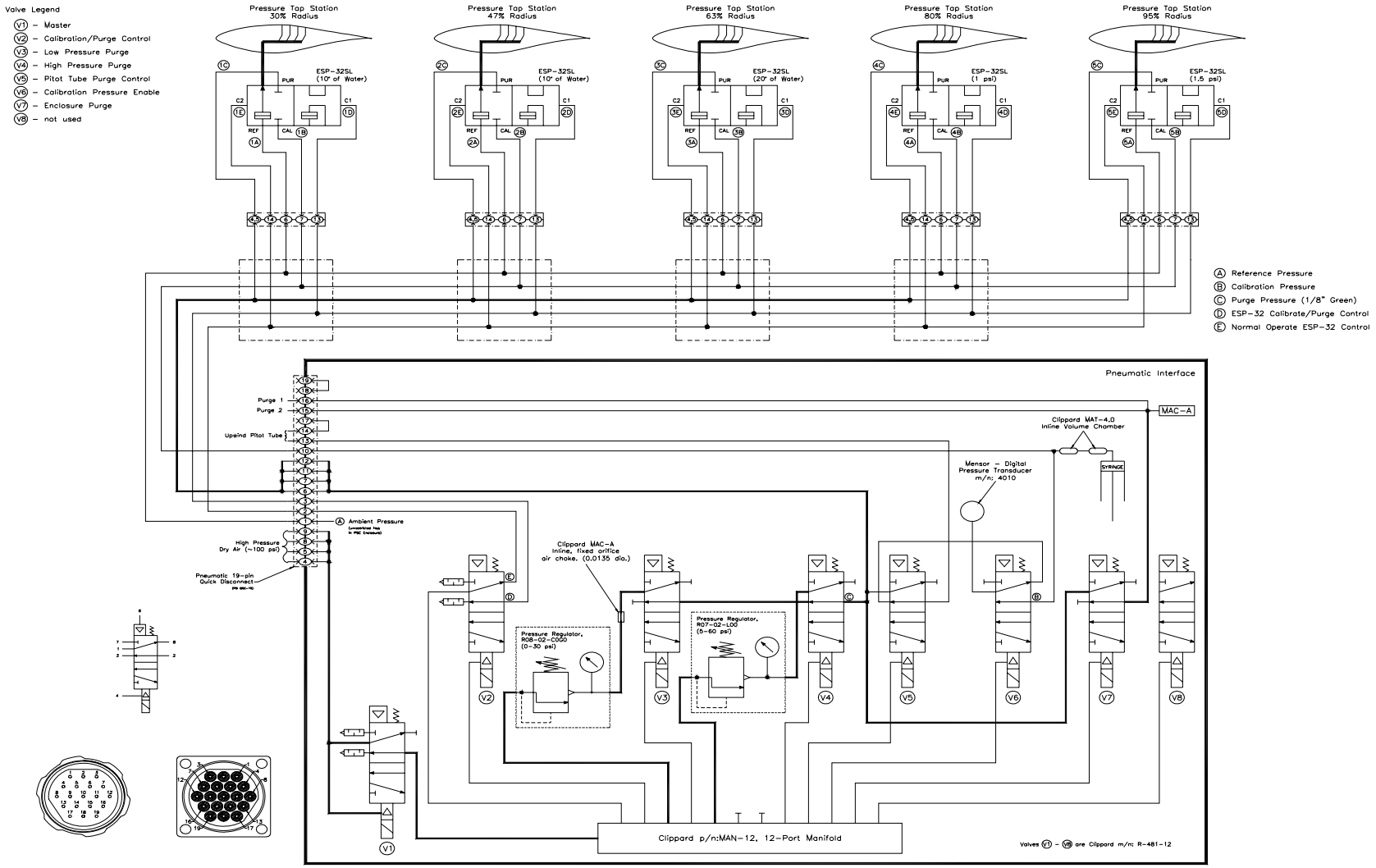

Figure B-30. Pneumatic layout

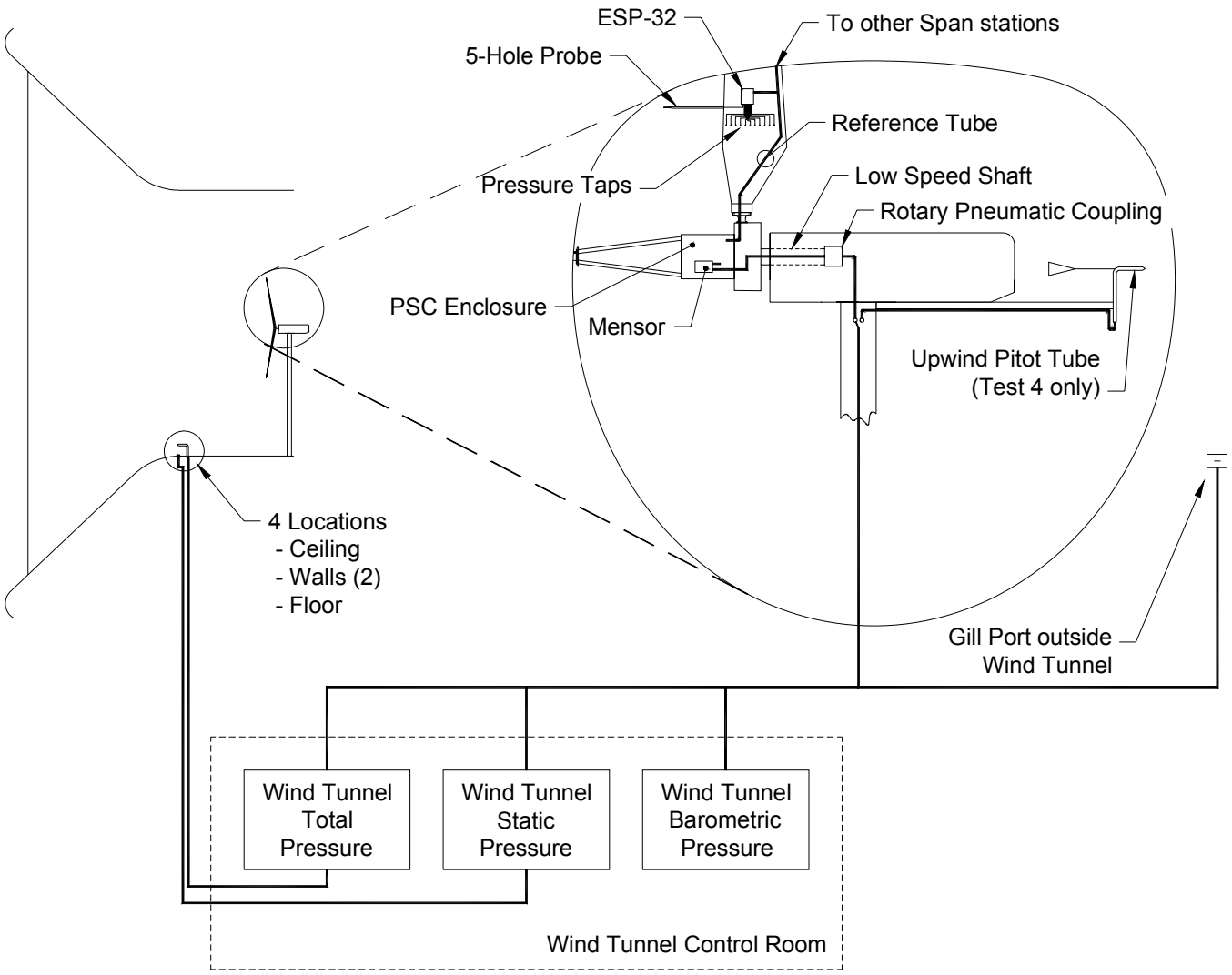

Figure B-31. Pressure system diagram

Digital Differential Reference Pressure

Channel	ID Code	Description
259	MENS1	Digital first 12 bits from Δ pressure
261	MENS2	Digital last 12 bits from Δ pressure

Location	Rotor package, PSC enclosure
Measurement type and units	Calibration reference pressure and static differential pressure, Pa
Power Requirement	12 Vdc
Range	±2 psig (±13,790 Pa)
Resolution	0.42 Pa/bit
Calibration method	Manufacturer (M3)
Sensor description	Digital pressure transducer 16-bit binary output Accuracy: 0.01% full scale Mensor Corporation Model: 4010

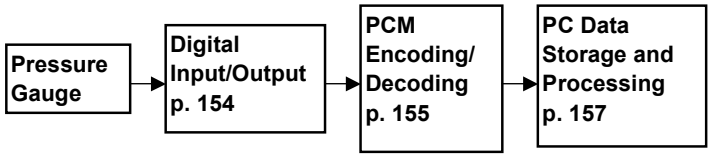

Calibration Procedure

Manufacturer specifications - (M3)

1. Mensor Corporation performed a calibration before installation of either digital pressure transducer.
2. The zero offset was determined by disconnecting the reference pressure tubing, which provided the instrumentation box pressure to both sides of the Mensor. The tare value was adjusted to eliminate the difference.

Calibration frequency

The differential pressure transducers were calibrated by the manufacturer prior to wind tunnel testing. The zero offset was determined daily during the wind tunnel test.

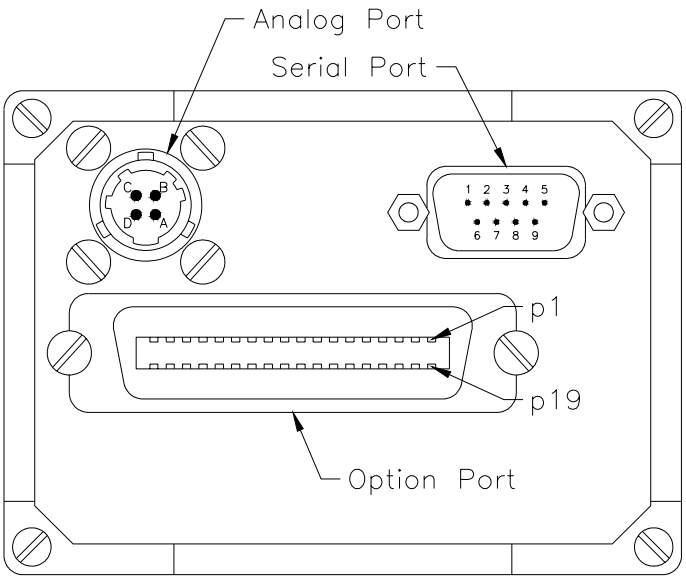

Figure B-32. Mensor electrical ports

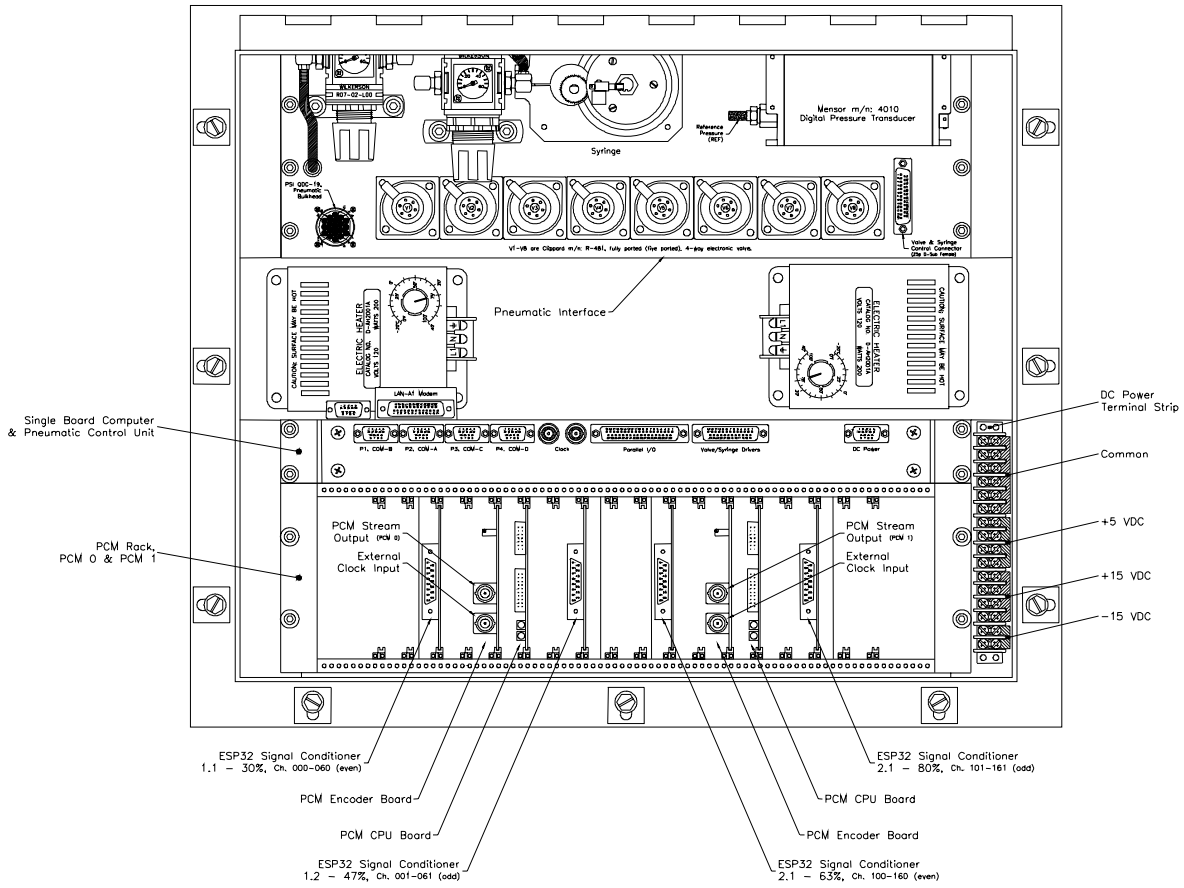

Figure B-33. Pressure system controller (PSC) enclosure

Channel	ID Code	Description
353	DAY	Clock - day
355	HOUR	Clock - hour
357	MINUTE	Clock - minute
359	SECOND	Clock - second
361	MILLISEC	Clock - millisecond

Location	PCM rack in data shed
Measurement type and units	Time, day, hour, minute, second, and millisecond
Power Requirement	120 V AC
Calibration method	Manufacturer (M2)
Sensor description	Time code generator Formats: IRIG-A, IRIG-B, IRIG-C, IRIG-E, IRIG-H Frequency stability: ±5ppm
	Model: 9310-804

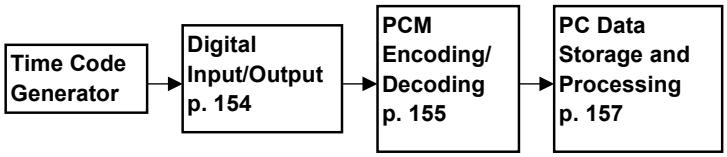

Calibration Procedure

Manufacturer specifications - (M2)

1. A calibration was performed by the manufacturer before installation.

Calibration frequency

The time code generator was calibrated prior to Phase III data collection. However, prior to each series of data collection (or in case of a power failure), the clock was set using atomic clock readings.

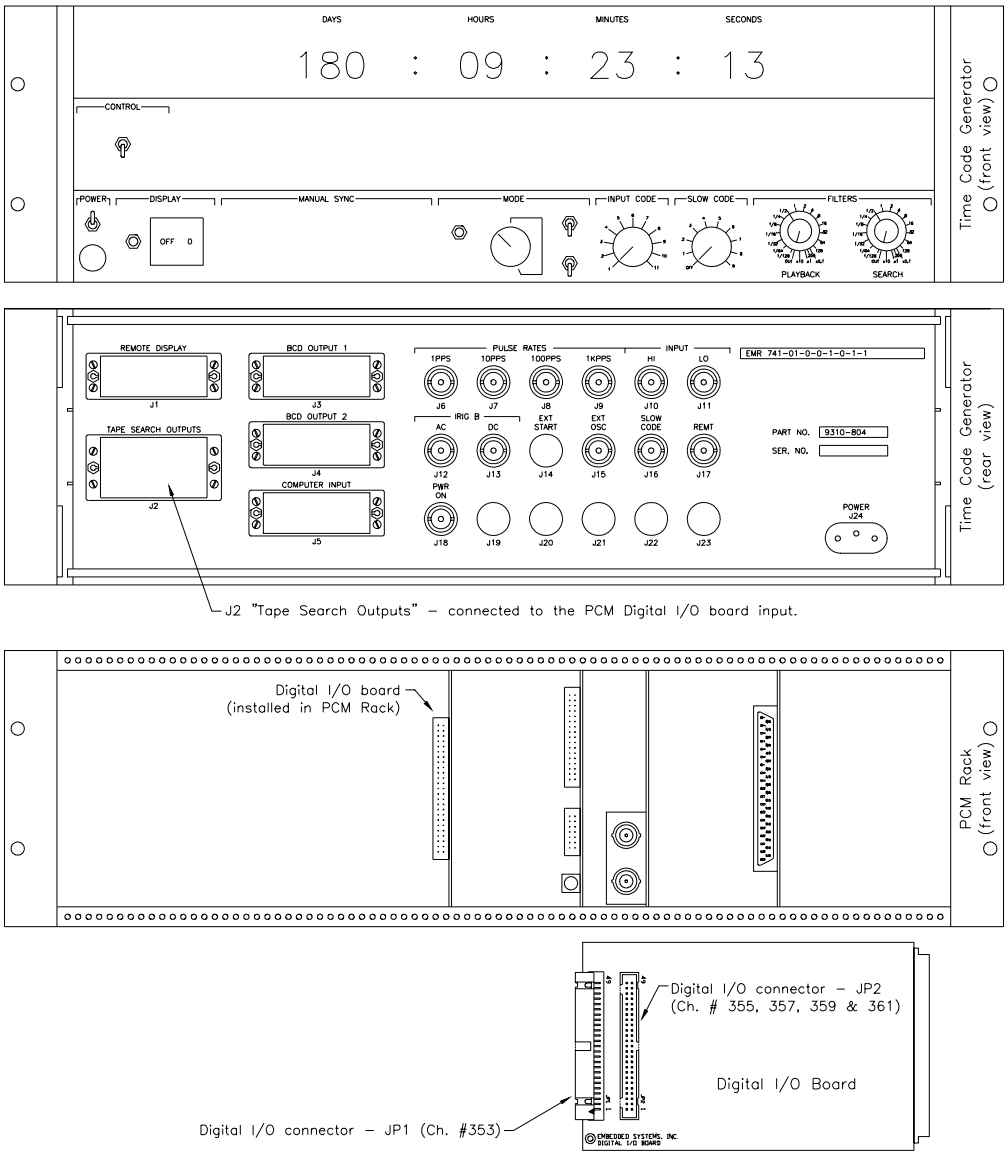

Figure B-34. Time code generator

NASA Channel Signal Conditioning

Channel	Description
300-318 (even), 344-358 (even)	Measurements provided by NASA
Location	Ground-based PCM rack
Input level	± 10 Vdc
Output level	± 5 Vdc
Description	Isolated wide-band voltage input signal conditioning
	Analog Devices, Inc. Model: 5B01 (backplane), 5B41-03 (input module)

Accelerometer Signal Conditioning

Channel	Description
201, 203, 209, 211, 336-340 (even)	Accelerometers in blade tips and nacelle
Location	Rotor package for blade accelerometers; PCM rack for nacelle accelerometers
Input level	± 1 Vdc
Output level	± 5 Vdc
Description	Isolated wide-band voltage input signal conditioning
	Analog Devices, Inc. Model: 5B01 (backplane), 5B41-01 (input module)

Power Transducer Signal Conditioning

Channel	Description
332	Generator power
334	Barometric pressure (field test only)
Location	PCM rack in data shed
Input level	± 5 Vdc
Output level	± 5 Vdc
Description	Isolated wide-band voltage input signal conditioning
	Analog Devices, Inc. Model: 5B01 (backplane), 5B41-02 (input module)

Channel	Description
215-241 (odd)	Blade root, yaw moment, hub shaft, and low-speed shaft strain gauges; teeter damper and teeter link load cells
Location	Rotor package
Input level	Isolated strain gauge input
Output level	± 5 Vdc
Description	Analog Devices, Inc. Model: 5B01 (backplate), 5B38-01 (input module)

Channel	Description
243, 247	Blade1 and Blade 3 pitch rate
Location	Rotor package
Input level	± 10 Vdc
Output level	± 5 Vdc
Description	Isolated wide-band voltage input signal conditioning
	Analog Devices, Inc. Model: 5B01 (backplane), 5B41-03 (input module)

Butterworth Filter

Channel	Description
300-334 (even), 342	Low-pass, 6th order, Butterworth 10-Hz filter
Location	PCM rack
Description	Differential low-pass filter 5V power requirement Pass band remains flat until 0.7 of Fc (-3 dB frequency), and then rolls off monotonically at a rate of 36 dB/oct
	Frequency Devices Model: 5BAF-LPBU6-10Hz

Bessel Filter

Channel	Description
336-340 (even), 344-358 (even)	Low-pass, 6th order, Bessel 100-Hz filter
Location	PCM rack; rotating instrumentation package
Description	Differential low-pass filter 5V power requirement Pass band remains flat until 0.1 Fc and then rolls off monotonically to 20 dB at 2.5 Fc
	Frequency Devices Model: 5BAF-LPBE6-100Hz

Note: Yaw moment (342) channel uses a Butterworth filter, but all other strain gauges use a Bessel filter.

Analog / Digital Conversion

Channel	Description
000-061, 100-161, 200-260 (even), 201-241 (odd), 300-358 (even)	All analog channels
Location	PCM rack; rotating instrumentation package
Description	Instrumentation amplifier gain 0.9 Sample and hold capability 7 µs, 12-bit analog-to-digital conversion 4.250 V reference with 10 ppm accuracy that is adjusted within ±2mV
	Custom built by Embedded Systems

Digital Input / Output

Channel	Description
251-261 (odd), 349-361 (odd)	Position encoders, time code generator
Location	PCM rack; rotating instrumentation package
Description	Digital parallel
	Custom built by Embedded Systems

Channel	Description
All channels	Encode/decode digital data
Location	PCM rack in data shed; rotating instrumentation package
Encode	CPU encoder board with 400 kbits/s capability Encodes 24 bits at one time; no storage capacity Bi-Phase L Filtered at 400 kHz Signal level ±2.5 V
	Custom built by Embedded Systems
Decode	Phase lock loop Software set buffer size, which uses direct memory access (DMA) to place data in computer memory when the buffer is full Number of buffers is also variable
	Custom built by Apex Systems

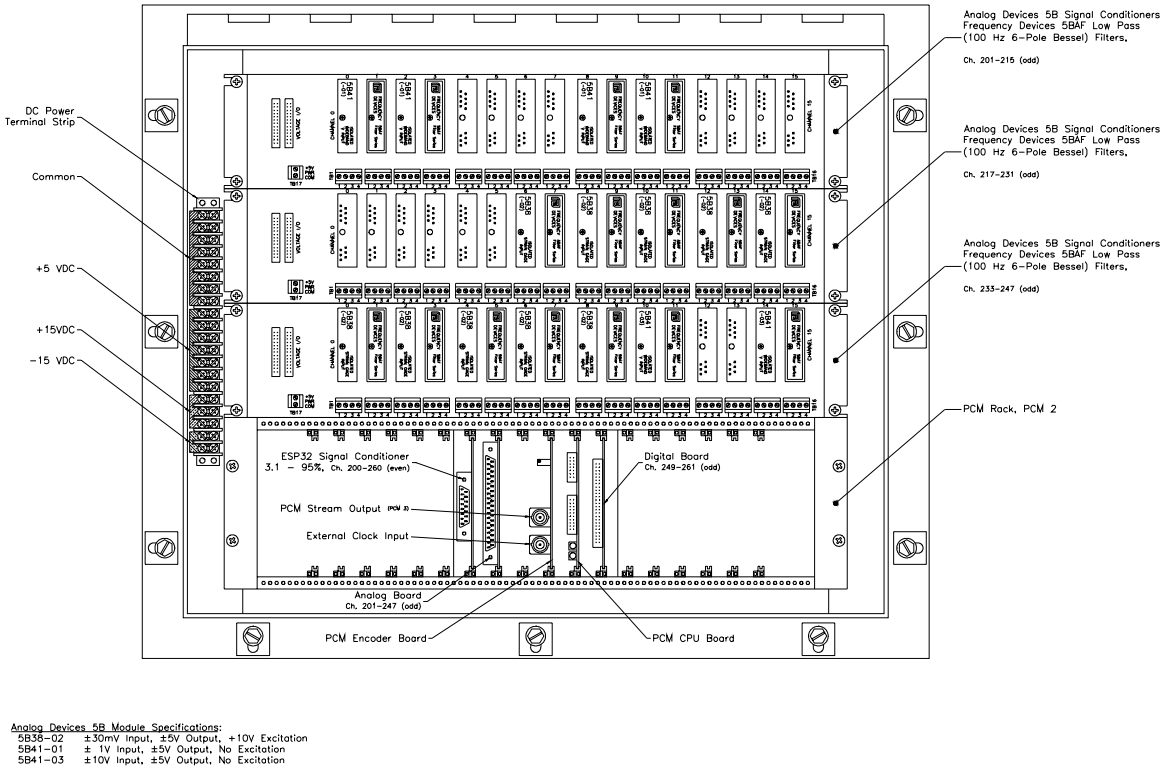

Figure B-35. Rotor-based PCM enclosure

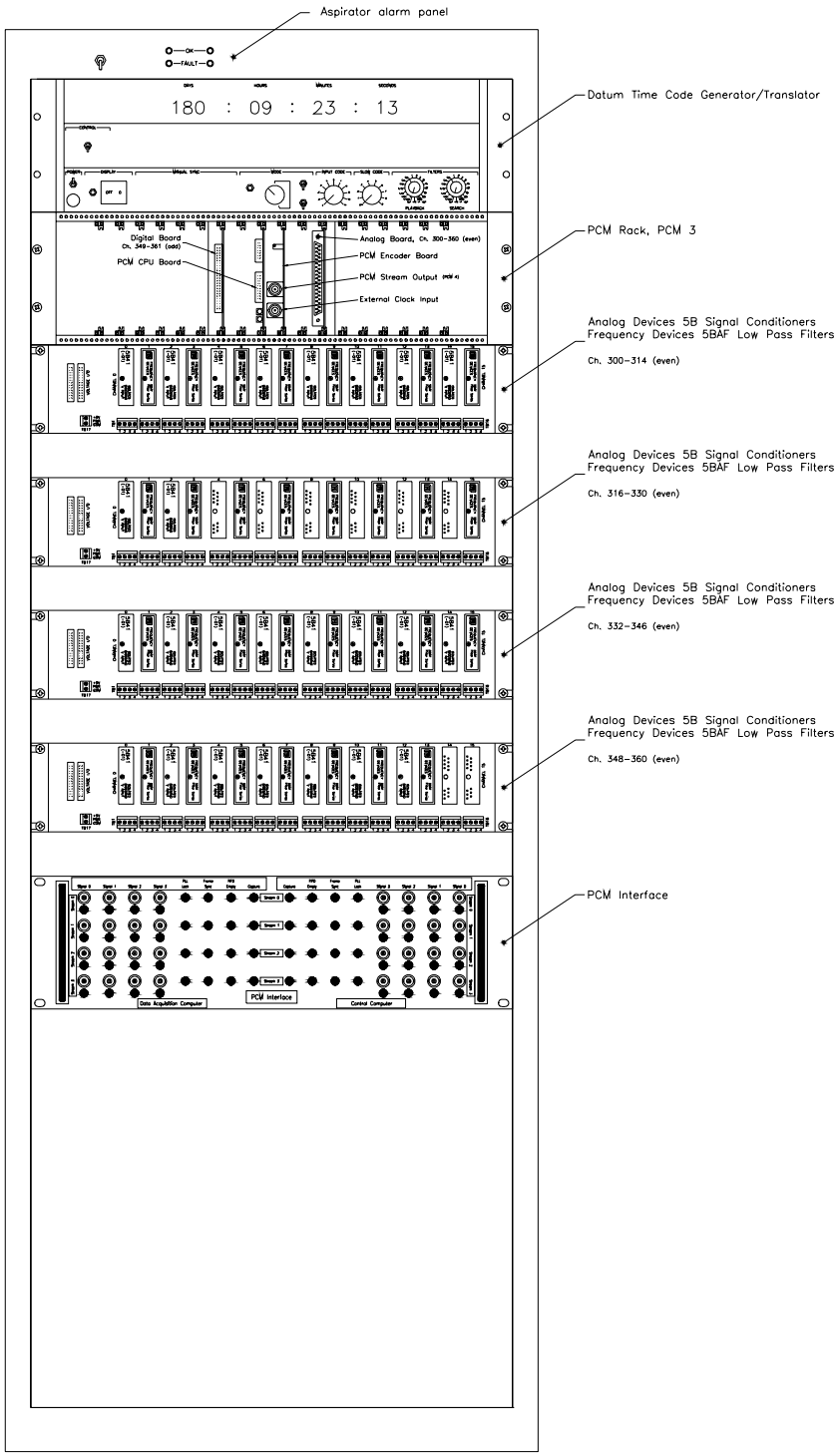

Figure B-36. Ground-based PCM rack

Data Collection and Storage

1. Complete calibrations, and build *master.hdr*. If there is no new calibration data, use the current *master.hdr* file.
2. Allow turbine to run at least 30 minutes before initiating data collection procedure. This allows temperature variations on the blades to stabilize.
3. Run *pcal.bat* [pcal cal-folder]. The following procedures are contained in this batch file:
    a. Initiate pressure calibration sequence (*psc.exe*) or use post-calibration from the previous campaign depending upon user selection.
    b. Update *master.hdr* with new pressure calibration coefficients (*hupdate.exe*).
4. Run *go.bat* [go cal-folder file name].
    a. Record 30 seconds of data to optical disk under file name specified when calling the batch file (*collect.exe*).
    b. Continue for approximately 30 minutes until next pressure calibration required.
5. Run *pcal.bat* [pcal cal-folder] for a post-calibration.
6. Repeat steps 3-5 until approximately 25 data files have been stored to optical disk.
    a. Run *finish.bat* [finish disklabel]. This copies all calibration files and collection files to optical disk.

Data Post-Processing

1. Run *munch.exe* to convert raw PCM data to engineering units and calculate derived channels.
2. Write CD-ROM using the following file structure:
    CALIB\ (contains all programs and files related to calibrations)
    COLLECT\ (contains all programs and files related to data collection)
    PROCESS\ (contains all processing input files)
    **.dat* (raw binary data file)
    **.eng* (binary engineering unit file)
    **.hd1* (header file listing each channel, calibration coefficients, and statistics).

Other Post-Processing Options

1. View data graphically (*replay.exe*).
2. Extract data subsets (*pdis.exe*).
3. Compare pre- and post-calibrations of pressure channels (*drift.exe*).
4. Extract time series of specified cycles (*wtscrunch.exe*).

Data Real-Time Display

1. View data graphically (*viewat2.exe*).
2. Bar graph showing all four PCM streams (*barsall.exe*).
3. Single bar chart (*onebar.exe*).
4. Time-averaged series of user specified channel (*strip.exe*).

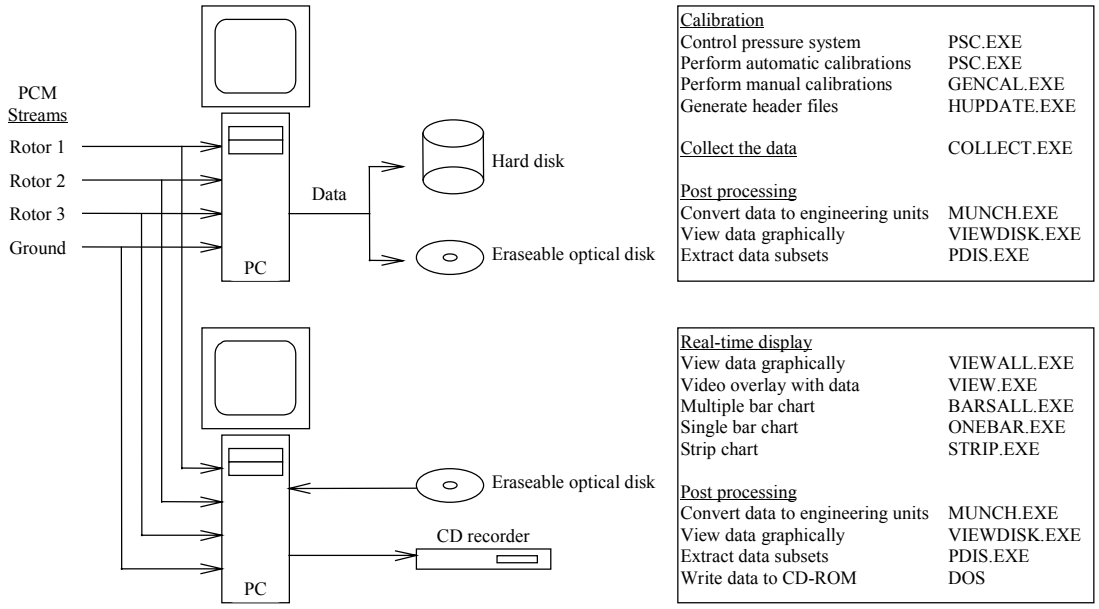

Figure B-37. Signal path from PCM streams to useable data

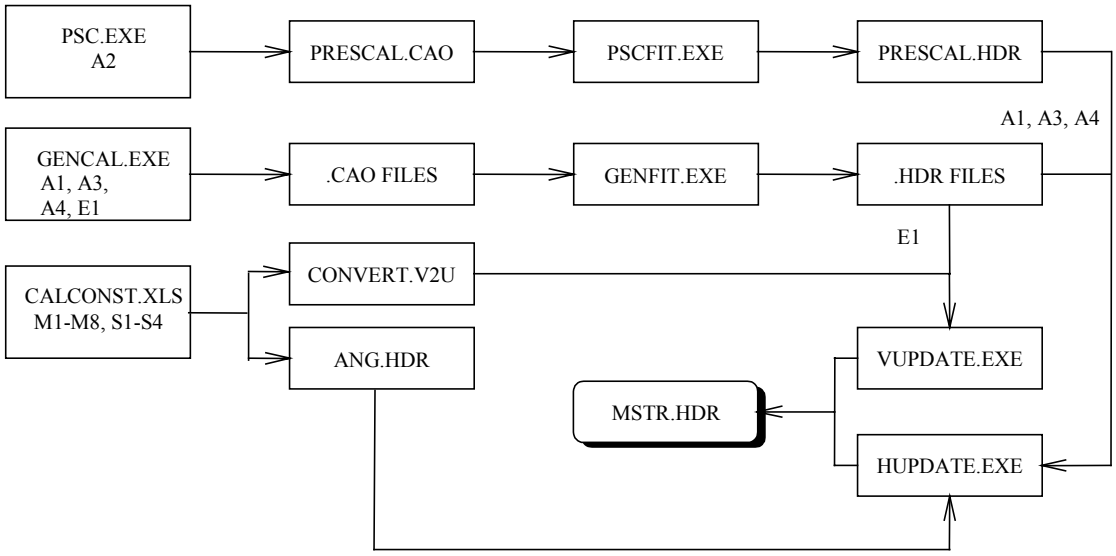

Figure B-38. Production of calibration and header files (calibration procedures are summarized on p. 160)

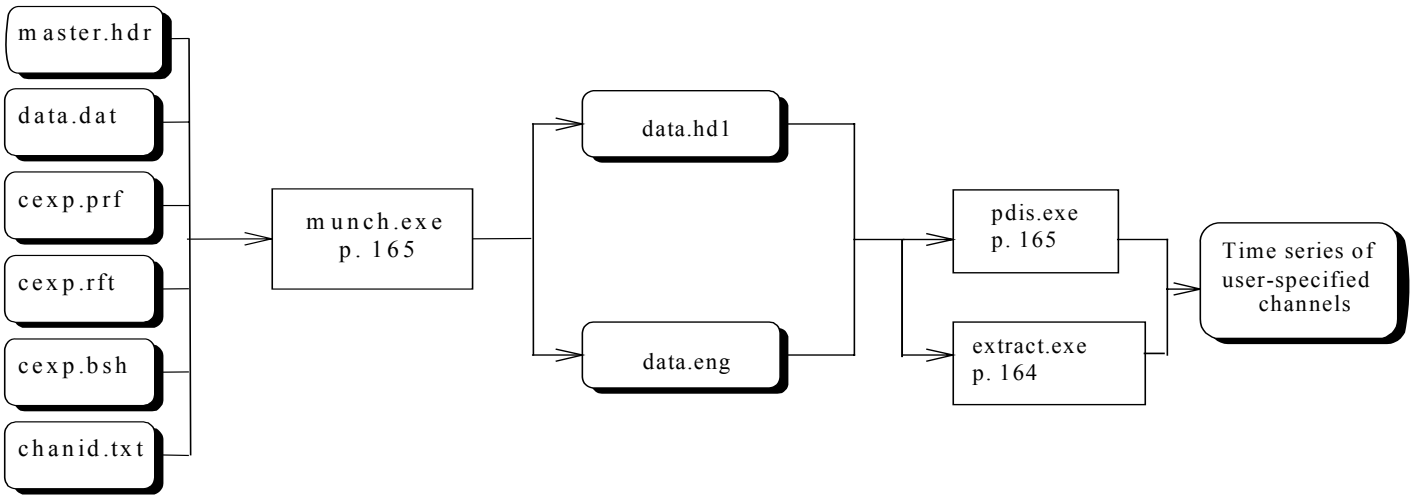

Figure B-39. Data processing flow chart

Applied load calibration - (A1-A3)

The pressure transducers, strain gauges, and load cells were calibrated using this method. Known loads were applied and the results recorded in **.cao* files. Linear regression provided slopes, and the offsets were determined under zero-load conditions. These values are stored in temporary header files, **.hdr*. The *buildhdr.bat* process incorporates these values in the *master.hdr* file.

Table B-2. Applied Load Calibration File Names

Channel Number	ID Code	File Name*	Calibration Range	Increment
225	B1RFB	*b1fpu.cao, b1fnu.cao* *b1fpd.cao, b1fnd.cao*	0 – 120 lb 120 – 0 lb	20 lb
227, 241	B1REB, LSSTQ	*b1epu.cao, b1enu.cao* *b1epd.cao, b1end.cao*	0 – 120 lb 120 – 0 lb	20 lb
233	B3RFB	*b3fpu.cao, b3fnu.cao* *b3fpd.cao, b3fnd.cao*	0 – 120 lb 120 – 0 lb	20 lb
235, 241	B3REB, LSSTQ	*b3epu.cao, b3enu.cao* *b3epd.cao, b3end.cao*	0 – 120 lb 120 – 0 lb	20 lb
237, 239	LSSXXB, LSSYYB	*lsspu.cao, lssnu.cao,* *lsspd.cao, lssnd.cao*	0 – 100 lb 100 – 0 lb	20 lb
342	NAYM	*b3ympu.cao, b3ymnu.cao,* *b3ympd.cao, b3ymnd.cao*	0 – 120 lb 120 – 0 lb	20 lb
225, 227, 233, 235, 237, 239, 241	B1RFB, B1REB, B3RFB, B3REB, LSSXXB, LSSYYB, LSSTQ	*zero1.cao, zero2.cao*	0 – 330°	30°
229, 231	B1TDAMPF, B3TDAMPF	*b1tdamp.cao, b3tdamp.cao*	0 – 10,000 lb	2,000 lb
223	TLINKF	*tl115994.cao*	-10,000 lb to 10,000 lb	2,500 lb

* p indicates load in positive direction; n indicates load in negative direction; u indicates increasing load; d indicates decreasing load; zero1 or zero2: because *gencal* is limited to 20 samples, the samples were split in two files for the zero offset determination.

Pseudo applied load calibration - (A4)

The upwind sonic anemometers were calibrated using this method. Serial signals corresponding to wind speeds were applied and the results recorded in **.cao* files. Linear regression provided slopes and offsets. These values are stored in temporary header files, **.hdr*. The *buildhdr.bat* process incorporates these values in the *master.hdr* file.

Table B-3. Pseudo Applied Load Calibration File Names

Channel Number	ID Code	File Name*	Calibration Range	Increment
320, 322, 326, 328	LESU8M, LESV8M, LWSU8M, LWSV8M	*esonicuv.cao, wsonicuv.cao*	-45 to 45 m/s	10 m/s
324, 330	LESW8M, LWSW8M	*esonicw.cao, wsonicw.cao*	-13.5 to 13.5 m/s	3 m/s

Manufacturer specifications - (M1-M8)

Instrument calibrations were performed by the manufacturer according to accepted practices. The resulting slope and offset values were entered in *calconst.xls*. The macros *Write ang.hdr* and *Write convert.v2u* convert the information in the Excel spreadsheet to text file formats. Using the *buildhdr.bat* batch file, these values were then combined with the results from the electronic path calibration producing the slope and offset values stored in *master.hdr*.

Single point offset determination - (S1-S3)

Each transducer was oriented with a known position using a jig or by line of sight. The associated count value was recorded in *calconst.xls*. The equation of the line for the manufacturer-supplied slope and the manually determined offset was found. These slope and offset values were transferred to *ang.hdr* in the case of the digital channels, and the analog channel calibration coefficients were combined with the electronic path calibration coefficients using *vupdate.exe*. The *buildhdr.bat* batch file then collected all of this information in the *master.hdr* file.

Electronics path calibration - (E1)

All of the NASA-supplied channels, the accelerometers, and the power transducer use data were provided by the manufacturer due to off-site calibrations. The electronics path used by each of these devices is then calibrated by injecting voltages and determining slope and offset values. The precision voltage generator is inserted in the electronic path as near the transducer as possible. The *gc.bat* batch file uses *gencal.exe* to collect 20 samples at 520.83 Hz at each voltage level specified by the user. The *genfit.exe* program performs a linear curve fit and outputs the slope and offset values in **.hdr* files. The files are used during the *buildhdr.bat* process to convert manufacturer supplied calibration coefficients to units of engineering unit/count. The calibration voltage ranges for the various transducers are listed below.

Table B-4. Electronics Path Calibration File Names and Voltage Ranges

Channel Number	ID Code	File Name	Calibration Range	Voltage Increment
243, 247	B1PRATE, B3PRATE	*Prate.cao*	-9.0 to 9.0 V	2.0 V
201, 203, 205, 207, 209, 211	B1ACFL, B1ACED, B2ACFL, B2ACED, B3ACFL, B3ACED	*Bladeacl.cao*	-0.9 to 0.9 V	0.2 V
336, 338, 340	NAACYW, NAACFA, NAACPI	*Grndacl.cao*	-0.9 to 0.9 V	0.2 V
300, 302, 304, 306, 308, 310, 312, 314	OMWS18M, OMWS32M, OMWD18M, OMWD32M, OMT4M, WTBARO, WTSTAT, WTTOTAL	*Ground1.cao*	0.0 to 9.0 V	1.0 V
316, 318	WTDPT, WTT18M	*Ground2.cao*	0.0 to 9.0 V	1.0 V
344, 346, 348, 350, 352, 354, 356	WTLFLIFT, WTRFLIFT, WTLRLIFT, WTRRLIFT, WTFSFORC, WTRSFORC, WTDRAG, YAWTABLE	*Balance.cao*	0.0 to 9.0 V	1.0 V
332	GENPOW	*Power.cao*	-4.5 to 4.5 V	1.0 V

*Master header file compilation (*buildhdr.bat*)*

Once each of the above calibration sequences is completed, the *master.hdr* file containing slope and offset values for every channel is created. Macros (*Write ang.hdr* and *Write convert.v2u*) in *calconst.xls* create text files in the same format as the **.hdr* files output by *genfit.exe*. These two files, *ang.hdr* and *convert.v2u* contain the slope and offset values that were stored in *calconst.xls*. The *buildhdr.bat* batch file then compiles all of the calibration coefficients from the manufacturer, the electronics path calibration, and applied load calibrations into one file that is input in the post-processing software, *munch*. The program *vupdate.exe* converts the manufacturer data in *convert.v2u* from units of engineering unit/V to engineering unit/count using information in the **.hdr* files from the electronics calibrations. These new values are stored in *master.hdr*. Calibration coefficients for the digital position encoders, pressure channels, and strain gauges are transferred, using *hupdate.exe*, from their respective **.hdr* files to the master header file, *master.hdr*.

Other Calibrations

Angle star

The zero was determined by placing the Angle Star on a machinist's surface plate. The surface plate was leveled with a machinist's level accurate to 0.0005 in/ft. The slope was determined by placing the device on precision ground angles on the surface plate at 5°, 10°, 15°, 20°, and 30°. The Angle Star was adjusted until the proper readings were attained.

Precision voltage generator

Two devices are available to use during the electronic path calibrations. The HP 3245A Universal Source was calibrated by the manufacturer on July 10, 1990. The Fluke 743B Documenting Process Calibrator was calibrated by the manufacturer on November 29, 1999.

Scale

Two scales were used to weigh the blades, and they were calibrated with known weights prior to weighing. One scale was used on the root end of the blade, and the other scale was used on the tip end of the blade. The combined reading provided the total weight of the blade.

barsall.exe
Input: **.cap, *.cfg, *.stm*
Output: None
Description: Bar graphs display each of the four PCM streams in real time. This is a useful program for determining if a channel is railed or not operating. This program was written in C.

calconst.xls
Input: Manufacturer supplied slope and offset values, and single point offsets
Output: *ang.hdr*, *convert.v2u*
Description: This spreadsheet contains all manufacturer specified slope and offset values. The single point offsets determined during calibration are also inserted in the spreadsheet. The offset value is used in conjunction with the manufacturer specified slope to determine the equation of the line representing each sensor. Two macros are run to create two files that contain slope and offset values in the format output by *genfit.exe* (**.hdr*). The calibration coefficients for the digital channels that measure angles are contained in *ang.hdr*, and all of the other calibration coefficients are contained in *convert.v2u*.

collect.exe
Input: **.cap, *.cfg, *.stm*
Output: **.dat*
Description: Decoded PCM data is stored directly to erasable optical disk. This program is written in C.

drift.exe
Input: **.cao* (both the pre- and post-calibration files are required)
Output: *drift.txt*
Description: A comparison between pre- and post-calibration of pressure transducers is done. The maximum and minimum drift for each pressure channel is recorded. The maximum and minimum drift overall is also recorded. This program is written in C.

extract.exe
Input: channel list file, **.eng* file, **.hd1* file
Output: user specified file name
Description: This program writes the time series values, decimated by 10, for an entire data file. The channels are listed in a file specified by the user. This program is written in FORTRAN.

gencal.exe
Input: *gencal.cap, vbl.lst*
Output: **.cao*
Description: This program was developed to automate sample collection. All of the strain gauge and electronic path calibrations are performed using this software (Scott 2001). This program is written in C.

1. Create *gencal.exe* input file (**.cao*) by copying the channel(s) to be calibrated from *vbl.lst* to the new input file. Insure the first line indicates the number of channels in the file, and the appropriate PCM stream is listed in *gencal.cap*.
2. Apply load or voltage and collect samples according to user key-stroke input. The software is hardwired to collect 20 samples at 520 Hz when the user signals beginning of collection.
3. Repeat until samples are collected under up to 20 desired load or voltage conditions. This can be done until the user exits the data

collection portion of the program. The **.cao* input file is modified to contain the x and y values created using this program.

genfit.exe
Input: **.cao* (with modifications from *gencal.exe*)
Output: **.hdr, *.rpt, *.res*
Description: This program was developed to perform a linear regression analysis on samples collected using *gencal.exe*. All of the strain gauge and electronic path calibrations are performed using this software. The resulting slopes and offsets are recorded in **.hdr* according to the channels contained in the input file (Scott 2001). This program was written in C.

go.bat
Input: user-specified pressure calibration folder and file name of data to be collected (i.e., go cal1 B0500000)
Description: This batch file initiates data collection and places the appropriate pressure calibration files in the specified folder.

hupdate.exe
Input: **.hdr* files corresponding to channels with calibration coefficients in units of engineering unit/count and counts.
Output: **.hdr* updated
Description: The slope and offset calibration coefficients are transferred from **.hdr* files to *master.hdr*. This program is written in C.

munch.exe
Input: **.hdr*, **.dat, cexp.rft, cexp.bsh, cexp.prf, *.stp, chanid.txt*, *s1pit.tbl, s1tpsph.tbl, s1yaw.tbl…s5pit.tbl, s5tpsph.tbl, s5yaw.tbl.*
Output: **.hd1, *.arc, *.eng, pdiserr.log*
Description: Raw PCM data is converted to engineering units using the calibration coefficients listed in *master.hdr*. In addition to the measured channels, several derived channels are calculated. These include aerodynamic force coefficients, upwash corrected angles of attack, normalized pressure coefficients, and stagnation point pressures. Formulae describing each of these calculations are described in the final report. The output file, **.hd1*, contains the mean, maximum, minimum, and standard deviation of each channel over the 10-minute campaign. One output file, **.arc*, is an archive file essentially copying **.dat*, and the engineering unit conversions are stored in **.eng*. Any errors encountered during processing are indicated in *pdiserr.log*. The additional input files provide information about the record format (*cexp.rft*), blade shape (*cexp.bsh*), pressure profiles (*cexp.prf*), eight-letter codes corresponding to each channel (*chanid.txt*), and look-up tables for each of the five-hole probes (*s1pit.tbl, s1tpsph.tbl, s1yaw.tbl…s5pit.tbl, s5tpsph.tbl, s5yaw.tbl*). These file formats are discussed in the program's documentation (Scott 2001). This program is written in C.

onebar.exe
Input: **.cfg, *.cap, *.stm, master.hdr*, # of desired PCM stream
Output: none
Description: One of the PCM streams is selected, and a horizontal bar chart displays each of the channels on that stream. The spacebar highlights a particular channel, and it's count value and engineering unit value is displayed at the bottom of the screen. This program is useful during calibration of the digital position encoders and observing Ni tank pressure and digital reference pressure channels. This program is written in C.

pdis.exe
Input: **.eng*, **.hd1*
Output: **.hd2, *.en2*

Description: The user may select specific channels and specific frame numbers to be extracted. A new header file is created consisting only of the selected channels, and another file contains all of the selected data. This program is written in C.

psc.exe
Input: *rampcal.cai*
Output: *prescal.cao*
Description: The syringe is used to apply pressures to each of the transducers according to the ramp values indicated in *rampcal.cai*. The count value associated with each applied pressure is recorded to the *prescal.cao* file. This program is written in C.

pscfit.exe
Input: *prescal.cao, t2c.dat*
Output: *prescal.hdr, prescal.res, prescal.rpt*
Description: A linear regression analysis is performed using the applied pressures and associated count values resulting from *psc.exe*. A slope and offset is determined for each channel at each transducer. These slopes and offsets are recorded in *prescal.hdr*. The file *t2c.dat* provides correlation between transducer tap numbers and pressure channel numbers. This program is written in C.

replay.exe
Input: **.eng*, **.hd1*
Output: None
Description: A previously recorded campaign is displayed graphically in the same format as the real-time software *viewall.exe*. The user may speed up or slow down the display or jump to a specific frame number. This program is written in C.

strip.exe
Input: *chanfile.txt, master.hdr*
Output: none
Description: User-specified channels are displayed as a moving time average. The time interval is specified by the user. This program is generally left running overnight to get a feel for the wind speed variations or for diagnostic purposes. This program is written in C.

viewat2.exe
Input: *master.hdr*, **.cfg, *.cap, *.stm*, incoming decoded PCM streams
Output: None
Description: A graphical depiction of various channels is displayed in real time. Pressure distributions for each span location are displayed on the left. The instrumented blade azimuth angle and rotational speed are included. Wind speeds are shown on a vertical graph to provide a visual indication of vertical wind shear. Horizontal wind shear is depicted similarly. Wind direction is shown in relation to turbine angle to provide an indication of yaw error. Other values such as time, temperature, and blade pitch angle are presented as text at the top of the screen. This program is written in C.

vupdate.exe
Input: *convert.v2u*, **.hdr* files corresponding to electronic path calibrations.
Output: **.hdr*
Description: All of the slope and offset values that were stored in *calconst.xls* are contained in the text file *convert.v2u*, and the slopes are in units of engineering unit/V. The electronic path calibrations performed using *gencal.exe* and *genfit.exe* produced slope and offset coefficients in units of V/count for the electronic pathways. This program converts the calibration coefficients to units of engineering unit/count, and these values are recorded in **.hdr*. This program is written in C.

ang.hdr contains the manufacturer-supplied slope and single point offsets for the position encoders. This file is created by the macro *Write ang.hdr* in the spreadsheet *calconst.xls*. The first line indicates the number of channels contained in the file. The following lines list the channel number, description, units, number of calibration coefficients, offset, slope, and other values consistent with the format specified by Scott (unpublished). The turntable angle slope was kept at zero, and the offset was manually adjusted to the actual turntable position. This was zero for all tests except Tests E, 6, 8, and 9.

```
6
349,"Azimuth","deg",2,-110.126953125,.087890625,0,0,0,0,-99999,99999,0,"M"
351,"Yaw","deg",2,225.818359375,.087890625,0,0,0,0,-99999,99999,0,"M"
251,"Flap 1","deg",2,22.093505859375,-.010986328125,0,0,0,0,-99999,99999,0,"M"
253,"Pitch 1","deg",2,2.197265625,.087890625,0,0,0,0,-99999,99999,0,"M"
255,"Flap 3","deg",2,22.60986328125,-.010986328125,0,0,0,0,-99999,99999,0,"M"
257,"Pitch 3","deg",2,-.3515625,.087890625,0,0,0,0,-99999,99999,0,"M"
358,"Turntable angle","deg",2,0,0,0,0,0,0,-99999,99999,0,"M"
```

calconst.xls is a spreadsheet containing all of the manufacturer-supplied slope and offset values. The offsets determined by the single point offset calibration are also entered in this spreadsheet. The NASA channel manufacturer calibration coefficients are in USCS units. These are converted to metric in the Coefficients columns.

Name	Single point			Slope		Coefficients			Channel	Units
Azimuth	180°=	795	counts	0.087890625	° / count	-110.1269531	0.087890625	*counts	349	deg
Yaw	0°=	1527	counts	0.087890625	° / count	-134.2089844	0.087890625	*counts	351	deg
Flap 1	0°=	2010	counts	-0.01098633	° / count	22.08251953	-0.01098633	*counts	251	deg
Pitch 1	0°=	-25	counts	0.087890625	° / count	2.197265625	0.087890625	*counts	253	deg
Flap 3	0°=	2053	counts	-0.01098633	° / count	22.55493164	-0.01098633	*counts	255	deg
Pitch 3	0°=	5	counts	0.087890625	° / count	-0.439453125	0.087890625	*counts	257	deg
Turntable angle	0°=	0	counts	0	° / count	0	0	*counts	358	deg
Blade 1 pitch rate	0 deg/s=	0	volts	10	deg/s /V	0	10	*volts	243	dps
Blade 3 pitch rate	0 deg/s=	0	volts	10	deg/s /V	0	10	*volts	247	dps
wind speed 18.29 m	0 mph=	0	volts	10	mph / V	0	4.4704	*volts	300	mps
wind speed 32.81 m	0 mph=	0	volts	10	mph / V	0	4.4704	*volts	302	mps
wind direction 18.29 m	0°=	0	volts	36	° / V	0	36	*volts	304	deg
wind direction 32.81 m	0°=	0	volts	36	° / V	0	36	*volts	306	deg
Outside air temperature 4.	10°F=	0	volts	10	°F / V	-12.22222222	5.555555556	*volts	308	degC
Wind tunnel barometric pr	0 psi=	0	volts	10	psi / V	0	68949.7	*volts	310	Pa
Wind tunnel static pressur	-0.0062 psf=	0	volts	5.2	psf / V	-0.296857612	248.977352	*volts	312	Pa
Wind tunnel total pressure	-0.0068 psf=	0	volts	2.09	psf / V	-0.325585768	100.0697434	*volts	314	Pa
Wind tunnel dew point tem	12.44°F=	0	volts	6.28	°F / V	-10.86666667	3.488888889	*volts	316	degC
Wind tunnel air temperatu	-0.76°F=	0	volts	9.925	° F/ V	-18.20112222	5.513888889	*volts	318	degC
Generator power	0 kW=	0	volts	8	kW / V	0	8	*volts	332	kW
Blade 1 Flap Accel	0 g=	0	volts	199.1	mV/g	0	49.22149674	*volts	201	mps2
Blade 1 Edge Accel	0 g=	0	volts	199.6	mV/g	0	-49.0981964	*volts	203	mps2
Blade 3 Flap Accel	0 g=	0	volts	196.1	mV/g	0	-49.9745028	*volts	209	mps2
Blade 3 Edge Accel	0 g=	0	volts	197.8	mV/g	0	49.54499494	*volts	211	mps2
Nacelle Yaw Accel	0 g=	0	volts	201	mV/g	0	48.75621891	*volts	336	mps2
Nacelle Fore-Aft Accel	0 g=	0	volts	200.9	mV/g	0	48.7804878	*volts	338	mps2
Nacelle Pitch Accel	0 g=	0	volts	201	mV/g	0	48.75621891	*volts	340	mps2
WT left front lift (#1)	0 lb=	0.002	volts	11804	lb/V	-109.1091073	52506.78888	*volts	344	N
WT right front lift (#2)	0 lb=	-0	volts	11807	lb/V	100.3134551	52520.13354	*volts	346	N
WT left rear lift (#3)	0 lb=	-0	volts	11804	lb/V	237.3306857	52506.78888	*volts	348	N
WT right rear lift (#4)	0 lb=	0.005	volts	11895	lb/V	-250.2717587	52911.5769	*volts	350	N
WT front side force (#5)	0 lb=	-0	volts	11960	lb/V	189.3945319	53200.7112	*volts	352	N
WT rear side force (#6)	0 lb=	6E-05	volts	11915	lb/V	-2.968030313	53000.5413	*volts	354	N
WT drag force (#7)	0 lb=	-0	volts	12203	lb/V	37.67145029	54281.62866	*volts	356	N

convert.v2u contains the manufacturer-supplied slope and offsets in units of e.u./V and V respectively. This file is created by the macro *Write convert.v2u* in the spreadsheet *calconst.xls*.

The first line indicates the number of channels contained in the file. The following lines list the channel number, description, units, number of calibration coefficients, offset, and slope.

```
28
243,"Blade 1 pitch rate","dps",2,0,10
247,"Blade 3 pitch rate","dps",2,0,10
300,"wind speed 18.29 m ","mps",2,0,10
302,"wind speed 32.81 m ","mps",2,0,10
304,"wind direction 18.29 m ","deg",2,0,36
306,"wind direction 32.81 m ","deg",2,0,36
308,"Outside air temperature 4.57 m ","degC",2,10,10
310,"Wind tunnel barometric pressure ","Pa",2,0,10
312,"Wind tunnel static pressure ","Pa",2,-.0062,5.2
314,"Wind tunnel total pressure ","Pa",2,-.0068,2.09
316,"Wind tunnel dew point temperature","degC",2,12.44,6.28
318,"Wind tunnel air temperature ","degC",2,-.76202,9.925
332,"Generator power","kW",2,0,8
201,"Blade 1 Flap Accel","mps2",2,0,49.2214967353089
203,"Blade 1 Edge Accel","mps2",2,0,-49.0981963927856
209,"Blade 3 Flap Accel","mps2",2,0,-49.9745028046915
211,"Blade 3 Edge Accel","mps2",2,0,49.5449949443883
336,"Nacelle Yaw Accel","mps2",2,0,49.0245122561281
338,"Nacelle Fore-Aft Accel","mps2",2,0,48.7804878048781
340,"Nacelle Pitch Accel","mps2",2,0,48.7562189054726
344,"WT left front lift (#1) ","N",2,5,11804
346,"WT right front lift (#2) ","N",2,5,11807
348,"WT left rear lift (#3) ","N",2,5,11804
350,"WT right rear lift (#4) ","N",2,5,11895
352,"WT front side force (#5)","N",2,5,11960
354,"WT rear side force (#6) ","N",2,5,11915
356,"WT drag force (#7) ","N",2,5,12203
```

gencal.cap contains the PCM stream capture information necessary for *gencal.exe* to obtain the required channels. For the channels specified in a given **.cao* file, the corresponding PCM stream must be specified in the line 'USE SIGNAL *;'.

CAPTURE INFORMATION:

```
CARD 0:
  SIGNAL 0 = PCM STREAM 4;
  SIGNAL 1 = PCM STREAM 4;
  SIGNAL 2 = PCM STREAM 4;
  SIGNAL 3 = PCM STREAM 4;
  USE SIGNAL 3;
  CAPTURE CHANNELS 1-62;
```

ground2.cao is an example of the file input to *gencal*. This file was used to calibrate the electronic path for two of the ground-based meteorological channels. The first line indicates the number of channels contained in the file. The following lines are copied from *vbl.lst*. The line of text containing a date begins the modification that occurs when *gencal* is run. The following x and y coordinates were obtained on the date specified. The first two columns correspond to voltages injected and count values read from the "Wind tunnel dew point" channel. The next two columns correspond to the "Wind tunnel air temperature" channel.

```
NV 2
9,316,"Vbl 9","Wind tunnel dew point","V",1,"M",0.000000,1.000000
10,318,"Vbl 10","Wind tunnel air temperature","V",1,"M",0.000000,1.000000
Wed Aug 18 11:43:30 1999
 -9.500 3973  -9.500 3974
 -9.500 3974  -9.500 3973
 -7.500 3572  -7.500 3572
 -7.500 3572  -7.500 3572
 -5.500 3165  -5.500 3165
```

```
-5.500 3166  -5.500 3165
-3.500 2758  -3.500 2757
-3.500 2758  -3.500 2758
-1.500 2351  -1.500 2351
-1.500 2351  -1.500 2352
 1.500 1742   1.500 1742
 1.500 1742   1.500 1742
 3.500 1335   3.500 1335
 3.500 1335   3.500 1335
 5.500  928   5.500  929
 5.500  927   5.500  929
 7.500  521   7.500  521
 7.500  522   7.500  521
 9.500  113   9.500  113
 9.500  112   9.500  113
```

ground2.hdr is an example of the file output from *genfit*. A linear regression was performed on the data added to *ground2.cao* during the *gencal* program. The resulting slope and offset are inserted in the appropriate locations of the **.hdr* file. This file is then used in conjunction with *convert.v2u* during the *vupdate* program to create the *master.hdr* file.

```
002
316,"Wind tunnel dew point","V",2,1.0063e+001,-4.9189e-003,,,,0,0,0,0,"M"
318,"Wind tunnel air temperature","V",2,1.0065e+001,-4.9197e-003,,,,0,0,0,0,"M"
```

master.hdr is a portion of the file containing all calibration coefficients. This file is input to the *munch* processing software. The first line indicates the number of lines of text in the file, and each channel is represented with text on one line. Each line consists of the channel number, description, units, number of calibration coefficients, offset, slope, and dummy values for the mean, maximum, minimum, and standard deviation. The last entry indicates the type of measurement (Scott 2001).

```
248
000,"Pressure #1, 30% span, trailing ","Pascal",2,-2734.899902,1.370700,,,,0.000000,-
999999.000000,999999.000000,0.000000,"M"
001,"Pressure #1, 47% span, trailing ","Pascal",2,-2632.800049,1.384200,,,,0.000000,-
999999.000000,999999.000000,0.000000,"M"
002,"Pressure #4, 30% span, 80% upper ","Pascal",2,-2711.000000,1.371200,,,,0.000000,-
999999.000000,999999.000000,0.000000,"M"
003,"Pressure #4, 47% span, 80% upper ","Pascal",2,-2632.300049,1.432500,,,,0.000000,-
999999.000000,999999.000000,0.000000,"M"
004,"Pressure #6, 30% span, 68% upper ","Pascal",2,-2609.600098,1.362100,,,,0.000000,-
999999.000000,999999.000000,0.000000,"M"
005,"Pressure #6, 47% span, 68% upper ","Pascal",2,-2762.100098,1.413400,,,,0.000000,-
999999.000000,999999.000000,0.000000,"M"
006,"Pressure #8, 30% span, 56% upper ","Pascal",2,-2609.100098,1.388300,,,,0.000000,-
999999.000000,999999.000000,0.000000,"M"
007,"Pressure #8, 47% span, 56% upper ","Pascal",2,-2837.100098,1.424600,,,,0.000000,-
999999.000000,999999.000000,0.000000,"M"
```

****.hd1*** is a portion of the header file produced by the post-processing software, *munch.* This file contains statistics for the 10-minute campaign. The second line lists the number of channels, the number of records in the corresponding **.eng* file, and the time step between records. Next, each channel is represented by one line of text beginning with the channel number. The channel description, units, number of calibration coefficients, offset, slope, mean, maximum, minimum, and standard deviation follow. The last entries are the channel type (Scott 2001), location of maximum, location of minimum, and number of frames in which an error occurred.

```
UAE-P3 HD1 FILE
277,15625,0.001920
000,"P0130100","Pressure #1, 30% span, trailing ","Pascal",2,-
2685.699951,1.364700,,,,0.193445,0.479885,-0.347185,0.081983,"M",8899,8055,1027
```

```
001,"P0147100","Pressure #1, 47% span, trailing ","Pascal",2,-
2564.500000,1.376800,,,,0.081538,0.463605,-1.143663,0.117867,"M",1368,1981,8838
002,"P043080U","Pressure #4, 30% span, 80% upper ","Pascal",2,-
2656.500000,1.365200,,,,0.097054,0.472285,-0.957444,0.100060,"M",8360,8038,1027
003,"P044780U","Pressure #4, 47% span, 80% upper ","Pascal",2,-2577.600098,1.425600,,,,-
0.052411,0.345408,-0.760674,0.104249,"M",13775,2683,8838
004,"P063068U","Pressure #6, 30% span, 68% upper ","Pascal",2,-
2560.399902,1.355900,,,,0.026744,0.500615,-1.302401,0.112997,"M",14650,8024,1027
```

.eng files contain the calibrated data parameters in engineering units along with all of the derived parameters. These binary files contain a series of 32-bit floating point real numbers and one 8-bit byte for each frame of data. A 30-second campaign consists of 15,625 records for 277 channels. Each line is one time step of 1.92 ms.

Channel 000	Channel 001	Channel 002	Channel 003	...	Channel 981	Error Byte
FLOAT	FLOAT	FLOAT	FLOAT	...	FLOAT	BYTE
FLOAT	FLOAT	FLOAT	FLOAT	...	FLOAT	BYTE
FLOAT	FLOAT	FLOAT	FLOAT	...	FLOAT	BYTE

...

References

Scott, G.N. (2001). *PDIS Pressure Display Program Technical Description.* Unpublished.

Appendix C: Test Matrix

Table C-1. Sequence B, Downwind Baseline (F), 197 files of 30-second duration

Uw	Yaw Angle																						Actual WS
(m/s)	0	5	10	20	30	45	60	75	90	135	180	-135	-90	-75	-60	-50	-45	-40	-30	-20	-10	-5	m/s
5.0	1,2	0	0	0	0	0	0	0	0	0	0	0	1	0	0		0		0	0	0	0	**5.0**
6.0	0,1		0		0														0		0		**5.7**
7.0	0,1	0	0	0	0	0	0	0	0	0	1	0	0	1	0	0	0	1	0	0	0	0	**6.7**
8.0	0,1		0		0														0		0		**7.7**
9.0	0,1		0		0										0	0		0	0	0	0		**9.3**
10.0	0,1	0	0	0	0	0	0	0	0	0	0	0	0	0	0		0		0	0	0	0	**10.3**
11.0	2,3		1		1										1	1		1	1	1	1		**11.0**
12.0	0,1		0		0														0		0		**12.0**
13.0	0,1		0		0										0	0		0	0	0	0		**13.0**
14.0	0,1		0		0														0		0		**14.2**
15.0	0,1	0	0	0	0	1							0	0	0	0	0	0	0	0	0	0	**15.2**
16.0	0,1		0		0														0		0		**15.7**
17.0	0,1		0		0														0	0	0		**18.0**
18.0	0,1		0		0														0		0		**19.0**
19.0	0,3		0		0														0	0	0		**19.6**
20.0	0,1	0	0	1	0														0	0	0	0	**20.7**
21.0	0,1		0																	0	0		**21.5**
22.0	0,1		0																		0		**22.5**
23.0	0,1		0																	0	0		**23.6**
24.0	0,1		0																		0		**24.5**
25.0	0,1	0	0																	0	0	0	**25.6**

Table C-1. (continued)

File Name Convention: BWWYYYYR where WW corresponds to the wind speed, Uw; YYYY corresponds to the yaw angle (M030=-30); R corresponds to the repetition digit. Each entry in the above table represents the repetition digit of the filename corresponding to that wind speed and yaw angle.

Data problems in NREL files:

Nominal wind speed did not match actual wind speed. See Actual WS column.
East sonic anemometer not operable for files B1700000, B1700100, and B1700300.
Potential fouling of blade surface pressure measurements due to insects impinging on blade.
Scale measurements questionable (See Table E.2 in Appendix E).

Data problems in NASA files (See Table E.2 in Appendix E).

East wall pressure transducer not connected.
Digital pressure transducers not zeroed for wind speeds 6-10 m/s and 14-25 m/s.
Scale measurements questionable.

NREL/NASA file synchronization issues:

NASA system late for files B05M0750 and B1600300.
NASA system early for file B1500000.

Table C-2. Sequence C7, Downwind Low Pitch (F), 95 files of 30-second duration

Uw	Yaw Angle																			Actual WS
(m/s)	0	5	10	20	30	45	60	75	90	135	180	-135	-90	-75	-60	-45	-30	-20	-10	-5	m/s
5.0	0		0		0												0		0		**5.0**
6.0	0		0		0												0		0		**5.7**
7.0	0		0		0												1		1		**6.7**
8.0	0		0		0												0		0		**7.7**
9.0	0		1		0												0		0		**9.3**
10.0	0		0		0												0		0		**10.3**
11.0	1		1		1												1		1		**11.0**
12.0	0		0		0												0		0		**12.0**
13.0	0		0		0												0		0		**13.0**
14.0	0		0		0												0		0		**14.2**
15.0	0		0		0												0		0		**15.2**
16.0	0		0		0												0		0		**15.7**
17.0	1		0		0												0		0		**18.0**
18.0	0		0		0												0		0		**19.0**
19.0	0		0		0												0		0		**19.6**
20.0	0		0		0												0		0		**20.7**
21.0	0		0																0		**21.5**
22.0	0		0																0		**22.5**
23.0	0		0																0		**23.6**
24.0	0		0																0		**24.5**
25.0	0		0																0		**25.6**

Table C-2. (continued)

File Name Convention: CWWYYYYR where WW corresponds to the wind speed, Uw; YYYY corresponds to the yaw angle (M030=-30); R corresponds to the repetition digit. Each entry in the above table represents the repetition digit of the filename corresponding to that wind speed and yaw angle.

Data problems in NREL files:

Nominal wind speed did not match actual wind speed. See Actual WS column.
East sonic anemometer not operable for files C1700100 and C1700300.
Potential fouling of blade surface pressure measurements due to insects impinging on blade.
Scale measurements questionable (See Table E.2 in Appendix E).

Data problems in NASA files (See Table E.2 in Appendix E).

East wall pressure transducer not connected.
Digital pressure transducers not zeroed for wind speeds 6-10 m/s and 14-25 m/s.
Scale measurements questionable.

Table C-3. Sequence D, Downwind High Pitch (F), 93 files of 30-second duration

Uw	Yaw Angle																			Actual WS
(m/s)	0	5	10	20	30	45	60	75	90	135	180	-135	-90	-75	-60	-45	-30	-20	-10	-5	m/s
5.0	0		0		0												0		0		**5.0**
6.0	0		0		0												0		0		**5.7**
7.0	0		0		0												0		0		**6.7**
8.0	0		0		0												0		0		**7.7**
9.0	0		0		0												0		0		**9.3**
10.0	0		0		0												0		0		**10.3**
11.0	1		1		1												1		2		**11.0**
12.0	0		0		0												0		0		**12.0**
13.0	0		0		0												0		0		**13.0**
14.0	0		0		0												0		0		**14.2**
15.0	0		0		0												0		0		**15.2**
16.0	0		1		0												0		0		**15.7**
17.0	0		0		0												0		0		**18.0**
18.0	0		0														0		1		**19.0**
19.0	1		0		0												0		0		**19.6**
20.0	0		0														0		0		**20.7**
21.0	0		0																0		**21.5**
22.0	0		0																0		**22.5**
23.0	0		0																0		**23.6**
24.0	0		0																0		**24.5**
25.0	0		0																0		**25.6**

Table C-3. (continued)

File Name Convention: DWWYYYYR where WW corresponds to the wind speed, Uw; YYYY corresponds to the yaw angle (M030=-30); R corresponds to the repetition digit. Each entry in the above table represents the repetition digit of the filename corresponding to that wind speed and yaw angle.

Data problems in NREL files:

Nominal wind speed did not match actual wind speed. See Actual WS column.
East sonic anemometer not operable for files D1700000, D1700100, and D1700300.
Potential fouling of blade surface pressure measurements due to insects impinging on blade.
Scale measurements questionable (See Table E.2 in Appendix E).

Data problems in NASA files (See Table E.2 in Appendix E).

East wall pressure transducer not connected.
Digital pressure transducers not zeroed for wind speeds 6-10 m/s and 14-25 m/s.
Scale measurements questionable.

Table C-4. Sequence E, Yaw Releases (P), 181 files of 30-second duration

Uw	Initial Yaw Angle																
(m/s)	0	5	10	20	30	45	60	90	135	180	-135	-90	-45	-30	-20	-10	-5
5.0																	
6.0																	
7.0	A,B, C		A,0,2 ,3,4,5	A,0,1 ,2,3,4		A,0,1 ,2,3,4		A,0,1 ,2,3,4				A,0,1 ,2,3,4	A,0,1, 2,3,4		A,0,2 ,3,4,5	A,0,1 ,3,4,5	
8.0																	
9.0																	
10.0	A,B, C		A,0,1 ,2,3,4	A,0,1 ,2,3,4		A,0,1 ,2,3,4		A,0,1 ,2,3,4				A,0,1 ,2,3,4	A,1,2, 3,4,5		A,0,1 ,2,3,5	A,0,1 ,2,3,4	
11.0																	
12.0	A,B					A,1,2 ,4,5,6							A,0,2, 4,5,6				
13.0																	
14.0																	
15.0	A		A,0,1 ,2,3,4	A,0,1 ,2,3,4		A,1,2 ,3,4,5		A,0,1 ,2,3,4				A,0,1 ,2,3,4	A,0,1, 2,3,4		A,1,2 ,3,4,5	A,0,1 ,2,3,4	
16.0																	
17.0	A,B			A,0,1 ,2											A,0,1 ,2,3,4		
18.0																	
19.0																	
20.0																	

Table C-4. (continued)

File Name Convention: EWWYYYYR where WW corresponds to the wind speed, Uw; YYYY corresponds to the yaw angle (M030=-30); R corresponds to the repetition digit. Each entry in the above table represents the repetition digit of the filename corresponding to that wind speed and yaw angle. A letter indicates that the yaw brake remained engaged. Additional files were collected where the yaw brake was released at 0° yaw, and the turbine naturally reached its equilibrium yaw angle at wind speeds of 10, 12, 15, and 17 m/s respectively: E10XXXX0, E12XXXX0, E15XXXX0, E17XXXX0.

Data problems in NREL files:

Scale measurements questionable (See Table E.2 in Appendix E).

Data problems in NASA files (See Table E.2 in Appendix E).

East wall pressure transducer not connected.

Scale measurements questionable.

Other considerations:

Yaw brake released early in E0700900.

Pitch system remained in manual mode rather than automatic mode: E070000A, E0700100, E0700102, E0700103, E0700104, E0700105, E0700200, E070020A, E120000A, E12M0450, E12M0452, E12M045A, E1500452, E1500453, E1500454, E1500455, E1500900, E1500901, E1500902, E1500903, E1500904, E150090A, E15M0100, E15M0101, E15M0102, E15M0103, E15M0104, E15M010A.

Pitch system switched from manual mode to automatic mode during campaign: E0700201.

Table C-5. Sequence F, Downwind High Cone (F), 49 files of 30-second duration

Uw	Yaw Angle																			
(m/s)	0	5	10	20	30	45	60	75	90	135	180	-135	-90	-75	-60	-45	-30	-20	-10	-5
5.0																				
6.0																				
7.0																				
8.0																				
9.0																				
10.0	0,1																			
11.0	0,1																			
12.0	0,1																			
13.0	0,1		0																0	
14.0	0,1		0																0	
15.0	0,1	0	0	0															0	0
16.0	0,1		0																0	
17.0	0,1		0																0	
18.0	0,1		0																0	
19.0	0,1	0	0	0														0	0	0
20.0	0,1	0	0	0														0	0	0
21.0																				
22.0																				
23.0																				
24.0																				
25.0																				

Table C-5. (continued)

File Name Convention: FWWYYYYR where WW corresponds to the wind speed, Uw; YYYY corresponds to the yaw angle (M030=-30); R corresponds to the repetition digit. Each entry in the above table represents the repetition digit of the filename corresponding to that wind speed and yaw angle. A letter indicates that the yaw brake remained engaged.

Data problems in NREL files:
Scale measurements questionable (See Table E.2 in Appendix E).

Data problems in NASA files (See Table E.2 in Appendix E).
East wall pressure transducer not connected.
Scale measurements questionable.

NREL/NASA file synchronization issues:

NASA system late for F1900000.

Table C-6. Sequence G, Upwind Teetered (F), 160 files of 30-second duration

Uw	Yaw Angle																			
(m/s)	0	5	10	20	30	45	60	75	90	135	180	-135	-90	-75	-60	-45	-30	-20	-10	-5
5.0	0,1,3,4	0	0	0	0	0	0	0	0	0	0	3	1	1	1	1	1	1	1	1
6.0	0,1		0		0												0		0	
7.0	0,2,3,4	0	0	0	0	0	0	0	0	0	0	0	0	0	0	0	0	0	0	0
8.0	2,3		1		1												1		1	
9.0	2,3		1		1												1		1	
10.0	0,1	0	0	0	0	0	0	0	0	0	0	0	0	1	0	0	0	0	1	0
11.0	0,1		0		0												1		0	
12.0	0,1		0		0												0		0	
13.0	0,1		0																0	
14.0	0,1		0																0	
15.0	3,4,5	1,2	1	1														1	1	1
16.0	2,3		1																1	
17.0	2,3		1																1	
18.0	2,3		1																1	
19.0	0,1		0																0	
20.0	2,3	2	1	1															1	1
21.0	2,3		1																1	
22.0	0,1		0																0	
23.0	0,1		0																0	
24.0	0,1		0																0	
25.0	0,1	0	0																0	0

Table C-6. (continued)

File Name Convention: GWWYYYYR where WW corresponds to the wind speed, Uw; YYYY corresponds to the yaw angle (M030=-30); R corresponds to the repetition digit. Each entry in the above table represents the repetition digit of the filename corresponding to that wind speed and yaw angle.

Data problems in NREL files:
Scale measurements questionable (See Table E.2 in Appendix E).

Data problems in NASA files (See Table E.2 in Appendix E).
East wall pressure transducer not connected.
Scale measurements questionable.

Other considerations:
Pitch system remained in manual mode rather than automatic mode during G0800002.
Yaw brake engaged during G20000051.

Table C-7. Sequence H, Upwind Baseline (F), 161 files of 30-second duration, 2 files of 6-minute duration

Uw	Yaw Angle																								
(m/s)	0	2	3	4	5	10	20	30	40	45	50	60	75	90	135	180	-135	-90	-75	-60	-45	-30	-20	-10	-5
5.0	0,1,M0,M1	0	0		0	0	0	0		0		0	0	0	0	0						0		0	0
6.0	0,1					0		0																	
7.0	0,1,M0,M1	0	0	0	0	0	0	0	0	0	0	0	0	0	0	0						0		0	0
8.0	0,1					0		0																	
9.0	0,1					0	0	0	0		0	0													
10.0	0,1,M0,M1	0	0	0	0	0	0	0		0		0	0	0	0	0						0		0	0
11.0	0,1					0	0	0	0		0	1													
12.0	0,2					0		0																	
13.0	0,1					0	0	0	0		0	0													
14.0	0,1					0		0																	
15.0	0,1,M0	0	0	0	0	0	0	0	0	0	0	0	0	0	0	0						0		0	0
16.0	0,1					0		0																	
17.0	0,1					0	0	0																	
18.0	0,1					0																			
19.0	3,4					1	1																		
20.0	2,3,M0,M1	1	1	1	1	2																		0	0
21.0	0,1					0																			
22.0	0,1					0																			
23.0	0,1																								
24.0	0,1																								
25.0	0,1																								

File Name Convention: HWWYYYYR where WW corresponds to the wind speed, Uw; YYYY corresponds to the yaw angle (M030=-30); R corresponds to the repetition digit. Each entry in the above table represents the repetition digit of the filename corresponding to that wind speed and yaw angle. An 'M' in the 0° yaw column indicates that the yaw angle is represented by 'M000'. The repetition digit follows. Two additional files representing 6-minute duration, 360° yaw sweeps at 7 and 10 m/s respectively are H07YS000 and H10YS000.

Data problems in NREL files:

Scale measurements questionable (See Table E.2 in Appendix E).

Data problems in NASA files (See Table E.2 in Appendix E).

East wall pressure transducer not connected.

Scale measurements questionable.

Table C-8. Sequence I, Upwind Low Pitch (F), 49 files of 30-second duration, 2 files of 6-minute duration

Uw	Yaw Angle																		
(m/s)	0	5	10	20	30	45	60	75	90	135	180	-135	-90	-75	-60	-45	-30	-20	-10	-5
5.0	0		0		0															
6.0	0		0		0															
7.0	0		0		0															
8.0	0		0		0															
9.0	0		0		0															
10.0	0		0		1															
11.0	0		0		0															
12.0	0		0		0															
13.0	0		0		0															
14.0	0		0		0															
15.0	0		0		0															
16.0	0		0		0															
17.0	0		0																	
18.0	0		0																	
19.0	1		1																	
20.0	1		2																	
21.0	0		0																	
22.0	0																			
23.0	0																			
24.0	1																			
25.0																				

File Name Convention: IWWYYYYR where WW corresponds to the wind speed, Uw; YYYY corresponds to the yaw angle (M030=-30); R corresponds to the repetition digit. Each entry in the above table represents the repetition digit of the filename corresponding to that wind speed and yaw angle. Two additional files representing 6-minute duration, 360° yaw sweeps at 7 and 10 m/s respectively are I07YS000 and I10YS000.

Data problems in NREL files:

Scale measurements questionable (See Table E.2 in Appendix E).

Data problems in NASA files (See Table E.2 in Appendix E).

East wall pressure transducer not connected.

Scale measurements questionable.

Table C-9. Sequence J, Upwind High Pitch (F), 53 files of 30-second duration, 2 files of 6-minute duration

Uw	Yaw Angle																		
(m/s)	0	5	10	20	30	45	60	75	90	135	180	-135	-90	-75	-60	-45	-30	-20	-10	-5
5.0	0		0		0															
6.0	0		0		0															
7.0	0		0		0															
8.0	0		0		0															
9.0	0		0		0															
10.0	0		0		0															
11.0	0		0		0															
12.0	0		0		0															
13.0	0		0		0															
14.0	0		0		0															
15.0	0		0		0															
16.0	0		0		0															
17.0	0		0		0															
18.0	0		0																	
19.0	1		1																	
20.0	1		1																	
21.0	0		0																	
22.0	0		0																	
23.0	0		0																	
24.0	0																			
25.0	0																			

Table C-9. (continued)

File Name Convention: JWWYYYYR where WW corresponds to the wind speed, Uw; YYYY corresponds to the yaw angle (M030=-30); R corresponds to the repetition digit. Each entry in the above table represents the repetition digit of the filename corresponding to that wind speed and yaw angle. Two additional files representing 6-minute duration, 360° yaw sweeps at 7 and 10 m/s respectively are J07YS000 and J10YS000.

Data problems in NREL files:
Scale measurements questionable (See Table E.2 in Appendix E).

Data problems in NASA files (See Table E.2 in Appendix E).
East wall pressure transducer not connected.
Scale measurements questionable.

Table C-10. Sequence K, Step AOA, Probes (P), 18 files of varying duration

Uw (m/s)	Yaw (deg)	Initial Tip Pitch (deg)	0.30R AOA at Initial Pitch (deg)	0.95R AOA at Initial Pitch (deg)	Final Tip Pitch (deg)	0.30R AOA at Final Pitch (deg)	0.95R AOA at Final Pitch (deg)	Pitch Rate (deg/s)	Pitching	Number of records	Filename
6.0	0.0	32.0	-16.0	-20.1	-15.0	20.0	20.1	0.180	continuous ramp	139,502	K0600RU0
6.0	0.0	-15.0	20.0	20.1	32.0	-16.0	-20.1	-0.180	continuous ramp	139,502	K0600RD0
6.0	0.0	32.0	-16.1	-20.1	-15.0	20.0	20.1	step up then step down	5.0 deg step, 8 second hold	159,502	K0600ST0
6.0	30.0	32.0	-16.1	-20.1	-15.0	20.0	20.1	step up then step down	5.0 deg step, 8 second hold	159,502	K0630ST0
6.0	0.0				3.0			0.0	test points	9,502	K30002, K0003
10.0	0.0	37.0	-9.0	-2.0	-15.0	36.0	26.8	0.180	continuous ramp	154,502	K1000RU0
10.0	0.0	-15.0	36.0	26.8	37.0	-9.0	-2.0	-0.180	continuous ramp	154,502	K1000RD0
10.0	0.0	37.0	-9.0	-2.0	-15.0	36.0	26.8	step up then step down	5.0 deg step, 8 second hold	174,502	K1000ST0
10.0	30.0	37.0	-9.0	-2.0	-15.0	36.0	26.8	step up then step down	5.0 deg step, 8 second hold	174,502	K1030ST0
10.0	0.0				3.0			0.0	test points	9,502	K0000, K30001
15.0	0.0	40.0	-1.6	-16.3	-15.0	48.2	34.0	0.180	continuous ramp	164,502	K1500RU0
15.0	0.0	-15.0	48.2	34.0	40.0	-1.6	-16.3	-0.180	continuous ramp	164,502	K1500RD0
15.0	0.0	40.0	-1.6	-16.3	-15.0	48.2	34.0	step up then step down	5.0 deg step, 8 second hold	189,502	K1500ST1
20.0	0.0	44.0	1.3	-14.4	28.0	14.7	-0.8	0.180	continuous ramp	49,502	K2000RU0
20.0	0.0	28.0	14.7	-0.8	44.0	1.3	-14.4	-0.180	continuous ramp	49,502	K2000RD0
20.0	0.0	44.0	1.3	-14.4	28.0	14.7	-0.8	step up then step down	5.0 deg step, 8 second hold	64,502	K2000ST0

Table C-10. (continued)

The column titled ‘Pitching” describes how the blade was pitched to acquire static data. The entry ‘continuous ramp’ indicates that pitching was carried out at 0.180 degrees per second through the range indicated in the columns to the left. The entry ‘5.0 deg step, 8 second hold’ indicates that, through the range indicated in the columns to the left, the blade was stepped in pitch to each angle and then held for 8 seconds.

Other consideration:

Operator may not have waited 15 seconds before first pitching motion for K0600ST0.

Table C-11. Sequence L, Step AOA Parked (P), 6 files of varying duration

Uw	Initial Tip Pitch (deg)	0.30R AOA at Initial Pitch (deg)	0.95R AOA at Initial Pitch (deg)	Final Tip Pitch (deg)	0.30R AOA at Final Pitch (deg)	0.95R AOA at Final Pitch (deg)	Pitch Rate (deg/s)	Pitching	Number of records	Filename
20.0	90.0	-16.1	-0.3	-15.0	88.9	104.7	0.180	continuous ramp	309,997	L2000RU0
20.0	-15.0	88.9	104.7	90.0	-16.1	-0.3	-0.180	continuous ramp	309,997	L2000RD0
20.0	90.0	-16.1	-0.3	-15.0	88.9	104.7	step up then step down	5.0 deg step, 8 second hold	174,997	L2000ST0
30.0	90.0	-16.1	-0.3	0.0	73.9	89.7	0.180	continuous ramp	309,997	L3000RU0
30.0	0.0	73.9	89.7	90.0	-16.1	-0.3	-0.180	continuous ramp	309,997	L3000RD0
30.0	90.0	-16.1	-0.3	0.0	73.9	89.7	step up then step down	5.0 deg step, 8 second hold	174,996	L3000ST0

The column titled ‘Pitching” describes how the blade was pitched to acquire static data. The entry ‘continuous ramp’ indicates that pitching was carried out at 0.180 degrees per second through the range indicated in the columns to the left. The entry ‘5.0 deg step, 8 second hold’ indicates that, through the range indicated in the columns to the left, the blade was stepped in pitch to each angle and then held for 8 seconds.

Data problems in NREL files:

Scale measurements questionable (See Table E.2 in Appendix E).

Data problems in NASA files (See Table E.2 in Appendix E).

Scale measurements questionable.

Table C-12. Sequence M, Transition Fixed (P), 46 files of 30-second duration, 3 files of 90-second duration

Uw	Yaw Angle																			
(m/s)	0	5	10	20	30	45	60	75	90	135	180	-135	-90	-75	-60	-45	-30	-20	-10	-5
5.0	0,1		0		0				0											
6.0	0,1		0		0															
7.0	0,1		0		0				0											
8.0	0,1		0		0															
9.0	0,1		0		0															
10.0	0,1		0		0				0											
11.0	0,1		0		0															
12.0	0,1		0		0															
13.0	0,1		0		0															
14.0	0,1		0		0															
15.0	0,1		0		0															
16.0																				
17.0																				
18.0																				
19.0																				
20.0																				
21.0																				
22.0																				
23.0																				
24.0																				
25.0																				

Table C-12. (continued)

File Name Convention: MWWYYYYR where WW corresponds to the wind speed, Uw; YYYY corresponds to the yaw angle (M030=-30); R corresponds to the repetition digit. Each entry in the above table represents the repetition digit of the filename corresponding to that wind speed and yaw angle. Two additional files representing 90-second duration, 90° yaw sweeps at 7 and 10 m/s respectively are M07YSU00 and M10YSU00.

Data problems in NREL files:
Scale measurements questionable (See Table E.2 in Appendix E).

Data problems in NASA files (See Table E.2 in Appendix E).
East wall pressure transducer not connected.
Scale measurements questionable.

Other considerations:
File M0700001 accidentally 90 seconds in duration.
Yaw angle approximately 0.5° for M0900000.

Table C-13. Sequence N, Sin AOA, Rotating (P), 121 files of varying duration

Span Station	Chord (m)	Total Local U (m/s)	Local Re	Local K	Mean AOA (deg)	Omega AOA (deg)	Freq (Hz)	Tip Min Pitch (deg)	Tip Max Pitch (deg)	Number of Records	Filename
Test Files					3.00			3.00	3.00	9,502-70,000	N30000, N30001, N30002, N30003, N30004, N30005, N30006, N30007, N30008, N30009, N3000A, N3000B
1	0.711	19.01	872,914	0.1000	10.00	4.00	0.8543	21.02	31.02	24,429	N30020
1	0.711	18.91	868,322	0.1000	24.00	5.00	0.8496	4.25	14.93	24,429	N30030
1	0.711	19.00	872,455	0.1000	38.00	7.00	0.8496	-12.27	2.69	24,429	N30040
1	0.711	18.86	866,026	0.1250	11.00	2.00	1.0636	22.42	27.24	19,194	N30060
1	0.711	18.88	866,944	0.1250	27.00	5.00	1.0636	1.08	11.88	19,194	N30071
1	0.711	18.77	861,893	0.1500	7.00	4.00	1.2637	25.10	34.42	16,577	N30090
1	0.711	18.81	863,730	0.1500	21.00	5.00	1.2621	6.99	18.49	16,577	N30100
1	0.711	18.90	867,863	0.1500	35.00	5.00	1.2621	-7.04	3.80	16,577	N30110
1	0.711	18.89	867,403	0.1750	11.00	3.00	1.4808	21.34	28.32	13,960	N30130
1	0.711	18.91	868,322	0.1750	28.00	3.00	1.4744	2.14	8.72	13,960	N30140
1	0.711	19.00	872,455	0.2000	15.00	2.00	1.6944	17.34	21.96	12,215	N30160
1	0.711	18.76	861,434	0.2125	3.00	1.00	1.7868	33.73	35.71	11,343	N30220
1	0.711	18.75	860,975	0.2125	3.00	2.00	1.7868	32.54	36.90	11,343	N30240
1	0.711	18.86	866,026	0.025	8.00	5.50	0.213	21.68	35.30	97,710	N30250
1	0.711	18.86	866,026	0.025	14.00	5.50	0.213	14.52	27.98	97,709	N30260
1	0.711	18.96	870,618	0.025	20.00	5.50	0.213	7.92	20.22	97,532	N30270
1	0.711	18.90	867,863	0.025	8.00	10.00	0.213	15.99	40.41	97,532	N30280
1	0.711	18.80	863,271	0.025	14.00	10.00	0.213	9.46	33.50	97,532	N30290
1	0.711	18.86	866,026	0.025	20.00	10.00	0.213	3.48	25.78	97,532	N30302
1	0.711	18.85	865,567	0.050	8.00	5.50	0.415	21.71	35.27	49,728	N30310
1	0.711	18.86	866,026	0.050	14.00	5.50	0.415	14.16	27.82	49,728	N30320
1	0.711	18.97	871,077	0.050	20.00	5.50	0.420	7.83	20.19	49,728	N30333
1	0.711	18.75	860,975	0.050	14.00	10.00	0.412	9.39	33.53	50,600	N30350
1	0.711	18.84	865,108	0.050	20.00	10.00	0.415	3.43	25.93	49,728	N30360
1	0.711	18.88	866,944	0.075	8.00	5.50	0.640	21.62	35.36	32,280	N30370
1	0.711	18.89	867,403	0.075	14.00	5.50	0.640	14.26	27.88	32,280	N30380
1	0.711	18.99	871,995	0.075	20.00	5.50	0.640	7.75	20.11	32,280	N30390
1	0.711	18.93	869,240	0.075	20.00	10.00	0.640	3.07	25.55	32,280	N30420
1	0.711	18.83	864,648	0.100	8.00	5.50	0.850	21.58	35.24	24,429	N30430
1	0.711	18.82	864,189	0.100	14.00	5.50	0.850	14.15	27.49	24,429	N30440
1	0.711	18.80	863,271	0.100	20.00	5.50	0.850	7.71	20.23	24,429	N30450
1	0.711	18.80	863,271	0.100	20.00	10.00	0.850	2.71	25.53	24,429	N30470

Table C-13. Sequence N, Sin AOA, Rotating (P), 121 files of varying duration (continued)

Span Station	Chord (m)	Total Local U (m/s)	Local Re	Local K	Mean AOA (deg)	Omega AOA (deg)	Freq (Hz)	Tip Min Pitch (deg)	Tip Max Pitch (deg)	Number of Records	Filename
2	0.627	23.19	939,048	0.0625	3.00	2.00	0.7431	28.72	33.22	27,918	N47020
2	0.627	23.42	948,362	0.0625	12.00	4.00	0.732	15.64	24.82	28,791	N47030
2	0.627	23.47	950,386	0.0750	9.00	2.00	0.9015	21.52	26.02	22,684	N47050
2	0.627	23.50	951,601	0.0750	23.00	5.00	0.8932	3.20	13.78	23,556	N47060
2	0.627	23.30	943,502	0.0750	37.00	6.00	0.8774	-12.01	0.43	23,556	N47070
2	0.627	23.21	939,858	0.1000	-4.00	2.00	1.1731	36.63	40.89	17,449	N47080
2	0.627	23.47	950,386	0.1000	9.00	2.00	1.1935	21.46	26.08	17,449	N47090
2	0.627	23.49	951,196	0.1000	23.00	2.00	1.1949	6.31	10.67	17,449	N47100
2	0.627	23.35	945,527	0.1000	37.00	4.00	1.1865	-9.98	-1.60	17,449	N47110
2	0.627	23.08	934,594	0.1250	-2.00	1.00	1.4754	35.69	37.73	13,960	N47130
2	0.627	23.30	943,502	0.1250	5.00	1.00	1.4778	27.65	29.77	13,960	N47140
2	0.627	23.34	945,122	0.1250	13.00	1.00	1.4838	18.19	20.31	13,960	N47150
2	0.627	23.31	943,907	0.025	8.00	5.50	0.294	18.60	31.36	70,666	N47160
2	0.627	23.36	945,932	0.025	14.00	5.50	0.307	12.12	24.36	68,048	N47170
2	0.627	23.39	947,147	0.025	20.00	5.50	0.307	5.95	17.53	68,048	N47180
2	0.627	23.25	941,478	0.025	8.00	10.00	0.294	13.50	36.46	70,666	N47190
2	0.627	23.34	945,122	0.025	14.00	10.00	0.296	7.38	29.92	70,666	N47200
2	0.627	23.17	938,238	0.025	20.00	10.00	0.294	1.47	22.71	70,666	N47210
2	0.627	23.35	945,527	0.050	8.00	5.50	0.584	18.60	31.36	35,770	N47220
2	0.627	23.34	945,122	0.050	14.00	5.50	0.584	11.95	24.53	35,770	N47230
2	0.627	23.39	947,147	0.050	20.00	5.50	0.584	5.77	17.59	35,770	N47240
2	0.627	23.30	943,502	0.050	20.00	10.00	0.584	1.19	22.45	35,770	N47270
2	0.627	23.32	944,312	0.075	8.00	5.50	0.899	18.60	31.36	23,556	N47280
2	0.627	23.34	945,122	0.075	14.00	5.50	0.899	11.65	24.33	23,556	N47290
2	0.627	23.37	946,337	0.075	20.00	5.50	0.899	5.55	17.43	23,556	N47300
2	0.627	23.40	947,552	0.075	20.00	10.00	0.883	0.81	22.53	23,556	N47330
2	0.627	23.27	942,288	0.100	14.00	5.50	1.187	11.85	24.19	17,449	N47350
2	0.627	23.29	943,098	0.100	20.00	5.50	1.194	5.61	17.43	17,449	N47360
3	0.542	28.17	986,065	0.0375	-7.00	1.00	0.6091	36.00	38.04	34,025	N63010
3	0.542	28.10	983,615	0.0375	-1.00	1.00	0.6091	29.19	31.31	34,025	N63020
4	0.457	33.68	994,049	0.0250	-5.00	1.00	0.5785	28.94	31.06	35,770	N80010
4	0.457	33.86	999,362	0.0250	5.00	1.00	0.6121	17.32	19.44	34,025	N80020
4	0.457	33.70	994,639	0.0250	15.00	3.00	0.5841	4.81	11.17	35,770	N80030
4	0.457	33.95	1,002,018	0.0250	16.00	11.00	0.5785	-4.23	18.53	35,770	N80040
4	0.457	33.68	994,049	0.0375	-5.00	1.00	0.8677	28.94	31.06	24,429	N80050
4	0.457	34.05	1,004,970	0.0375	10.00	2.00	0.8677	10.86	15.08	24,429	N80060
4	0.457	33.87	999,657	0.0375	26.00	2.00	0.8677	-5.11	-1.13	24,429	N80071
4	0.457	33.63	992,573	0.0375	15.00	10.00	0.8677	-2.50	18.48	24,429	N80081
4	0.457	33.79	997,296	0.0500	-4.00	1.00	1.1744	27.89	30.01	17,449	N80090
4	0.457	34.09	1,006,150	0.0500	13.00	1.00	1.1744	8.91	10.87	17,449	N80100
4	0.457	34.08	1,005,855	0.0500	30.00	2.00	1.1744	-9.18	-5.20	17,449	N80110
4	0.457	33.98	1,002,904	0.0500	4.00	2.00	1.1744	17.31	21.67	17,449	N80120
4	0.457	34.04	1,004,674	0.0500	12.00	2.00	1.1744	8.92	13.12	17,449	N80130
4	0.457	33.96	1,002,313	0.0500	25.00	2.00	1.1744	-4.25	0.11	17,449	N80140
4	0.457	34.12	1,007,036	0.0500	10.00	3.00	1.1744	9.79	16.15	17,449	N80150

Table C-13. Sequence N, Sin AOA, Rotating (P), 121 files of varying duration (continued)

Span Station	Chord (m)	Total Local U (m/s)	Local Re	Local K	Mean AOA (deg)	Omega AOA (deg)	Freq (Hz)	Tip Min Pitch (deg)	Tip Max Pitch (deg)	Number of Records	Filename
4	0.457	34.07	1,005,560	0.0500	27.00	3.00	1.1744	-7.35	-0.99	17,449	N80160
4	0.457	34.05	1,004,970	0.025	8.00	5.50	0.584	9.25	21.17	35,770	N80170
4	0.457	34.08	1,005,855	0.025	14.00	5.50	0.584	3.46	14.70	35,770	N80180
4	0.457	33.62	992,278	0.025	20.00	5.50	0.600	-2.73	8.63	34,897	N80190
4	0.457	33.78	997,001	0.025	8.00	10.00	0.584	4.83	26.41	35,770	N80200
4	0.457	33.92	1,001,133	0.025	14.00	10.00	0.584	-1.21	19.61	35,770	N80210
4	0.457	33.83	998,476	0.025	20.00	10.00	0.567	-7.31	13.21	36,642	N80220
4	0.457	33.98	1,002,904	0.050	8.00	5.50	1.175	9.05	21.21	17,449	N80230
4	0.457	33.96	1,002,313	0.050	14.00	5.50	1.175	3.13	14.79	17,449	N80240
4	0.457	34.05	1,004,970	0.050	20.00	5.50	1.175	-2.84	8.74	17,449	N80250
5	0.381	38.98	959,150	0.0125	-4.00	1.00	0.4329	24.31	26.99	47,983	N95010
5	0.381	39.22	965,055	0.0125	5.00	1.00	0.4329	13.59	15.71	47,983	N95020
5	0.381	39.10	962,102	0.0125	15.00	4.00	0.4329	0.12	8.36	47,983	N95030
5	0.381	39.15	963,333	0.0125	6.00	7.00	0.4329	5.97	21.55	47,983	N95040
5	0.381	39.07	961,364	0.0125	13.00	8.00	0.4329	-1.93	14.69	47,983	N95050
5	0.381	39.15	963,333	0.0125	22.00	11.00	0.4329	-14.41	8.41	47,983	N95060
5	0.381	39.23	965,301	0.0125	16.00	15.00	0.4329	-12.34	19.26	47,983	N95070
5	0.381	38.94	958,165	0.0250	-4.00	1.00	0.826	24.41	26.89	25,301	N95080
5	0.381	39.18	964,071	0.0250	16.00	2.00	0.826	1.04	5.22	25,301	N95090
5	0.381	39.90	981,787	0.0250	10.00	8.00	0.826	0.71	17.99	25,301	N95100
5	0.381	39.57	973,667	0.0250	22.00	8.00	0.826	-11.49	5.49	25,301	N95110
5	0.381	39.19	964,317	0.0375	-3.00	1.00	1.2252	22.89	25.37	16,577	N95120
5	0.381	39.39	969,238	0.0375	9.00	1.00	1.2588	9.19	11.31	16,577	N95130
5	0.381	39.47	971,207	0.0375	9.00	2.00	1.2588	8.12	12.38	16,577	N95140
5	0.381	39.17	963,825	0.0375	21.00	2.00	1.2252	-4.03	0.33	16,577	N95150
5	0.381	39.49	971,699	0.025	8.00	5.50	0.826	5.38	17.48	25,301	N95160
5	0.381	39.40	969,484	0.025	14.00	5.50	0.826	-0.55	10.97	25,301	N95171
5	0.381	39.55	973,175	0.025	20.00	5.50	0.826	-6.75	4.77	25,301	N95181
5	0.381	39.83	980,065	0.025	8.00	10.00	0.826	0.70	22.72	25,301	N95190
5	0.381	39.72	977,358	0.025	14.00	10.00	0.826	-5.41	15.83	25,301	N95200
5	0.381	39.57	973,667	0.025	20.00	10.00	0.826	-11.56	9.42	25,301	N95210
5	0.381	39.46	970,961	0.050	20.00	5.50	1.627	-6.91	4.77	13,087	N95230

Wind speed = 15 m/s and yaw angle = 0° throughout this sequence. Data was acquired for 40 successive sinusoidal blade pitch cycles.

Rows for each span station are divided into two sets, and are separated by a heavy horizontal line. The first set of rows consists of combinations of K, mean AOA, and omega AOA that the blades would likely experience during routine operation. The second set of rows contains combinations of K, mean AOA, and omega AOA corresponding to those tested at Ohio State University using an S809 airfoil section under two-dimensional conditions (Reuss Ramsay et al. 1995).

Other considerations:

Blade pitching stopped early due to software glitch for N30250 and N30260.
Software glitch that caused pitch sequence to end early fixed for N30270.
Aborted due to excessive loads: N30350, N47280, N80250, N95100, N95200.
NASA data system early for N47220.

Table C-14. Sequence O, Sin AOA, Parked (P), 131 files of varying duration

Span Station	Chord (m)	Uw (m/s)	Local Re	Local K	Mean AOA (deg)	Omega AOA (deg)	Blade Pitch Freq (Hz)	Tip Min Pitch (deg)	Tip Max Pitch (deg)	Number of Records	Filename
Test Points					3.00			3.00	3.00	9,997-25,000	O30000, O30001, O30002, O30003, O30004, O30005, O47000, O47001, O47002, O80000, O80001, O95000, O95001
1	0.711	18.90	867,863	0.1000	-4.00	4.00	0.846	73.88	81.88	25,118	O30010
1	0.711	18.90	867,863	0.1000	10.00	4.00	0.846	59.88	67.88	25,118	O30020
1	0.711	18.90	867,863	0.1000	24.00	5.00	0.846	44.88	54.88	25,118	O30030
1	0.711	18.90	867,863	0.1000	38.00	7.00	0.846	28.88	42.88	25,118	O30040
1	0.711	18.90	867,863	0.1000	52.00	7.00	0.846	14.88	28.88	25,118	O30050
1	0.711	18.90	867,863	0.1250	11.00	2.00	1.058	60.88	64.88	20,194	O30060
1	0.711	18.90	867,863	0.1250	27.00	5.00	1.058	41.88	51.88	20,194	O30070
1	0.711	18.90	867,863	0.1250	44.00	7.00	1.058	22.88	36.88	20,194	O30080
1	0.711	18.90	867,863	0.1500	7.00	4.00	1.269	62.88	70.88	16,911	O30090
1	0.711	18.90	867,863	0.1500	21.00	5.00	1.269	47.88	57.88	16,911	O30100
1	0.711	18.90	867,863	0.1500	35.00	5.00	1.269	33.88	43.88	16,911	O30110
1	0.711	18.90	867,863	0.1750	11.00	3.00	1.481	59.88	65.88	14,566	O30120
1	0.711	18.90	867,863	0.1750	28.00	3.00	1.481	42.88	48.88	14,566	O30130
1	0.711	18.90	867,863	0.2000	-4.00	2.00	1.692	75.88	79.88	12,807	O30140
1	0.711	18.90	867,863	0.2000	15.00	2.00	1.692	56.88	60.88	12,807	O30150
1	0.711	18.90	867,863	0.2000	10.00	4.00	1.692	59.88	67.88	12,807	O30160
1	0.711	18.90	867,863	0.2000	-4.00	4.00	1.692	73.88	81.88	12,807	O30170
1	0.711	18.90	867,863	0.2000	5.00	3.00	1.692	65.88	71.88	12,807	O30180
1	0.711	18.90	867,863	0.2000	15.00	3.00	1.692	55.88	61.88	12,807	O30191
1	0.711	18.90	867,863	0.2125	-3.00	1.00	1.798	75.88	77.88	12,083	O30200
1	0.711	18.90	867,863	0.2125	3.00	1.00	1.798	69.88	71.88	12,083	O30210
1	0.711	18.90	867,863	0.2125	-3.00	2.00	1.798	74.88	78.88	12,083	O30220
1	0.711	18.90	867,863	0.2125	3.00	2.00	1.798	68.88	72.88	12,083	O30230
1	0.711	18.90	867,863	0.0250	8.0	5.5	0.212	60.38	71.38	98,983	O30240
1	0.711	18.90	867,863	0.0250	14.0	5.5	0.212	54.38	65.38	98,983	O30250
1	0.711	18.90	867,863	0.0250	20.0	5.5	0.212	48.38	59.38	98,983	O30260
1	0.711	18.90	867,863	0.0250	8.0	10.0	0.212	55.88	75.88	98,983	O30270
1	0.711	18.90	867,863	0.0250	14.0	10.0	0.212	49.88	69.88	98,983	O30280
1	0.711	18.90	867,863	0.0250	20.0	10.0	0.212	43.88	63.88	98,983	O30290
1	0.711	18.90	867,863	0.0500	8.0	5.5	0.423	60.38	71.38	49,740	O30300
1	0.711	18.90	867,863	0.0500	14.0	5.5	0.423	54.38	65.38	49,740	O30310
1	0.711	18.90	867,863	0.0500	20.0	5.5	0.423	48.38	59.38	49,740	O30320
1	0.711	18.90	867,863	0.0500	8.0	10.0	0.423	55.88	75.88	49,740	O30330
1	0.711	18.90	867,863	0.0500	14.0	10.0	0.423	49.88	69.88	49,740	O30341

Table C-14. Sequence O, Sin AOA, Parked (P), 131 files of varying duration (continued)

Span Station	Chord (m)	Uw (m/s)	Local Re	Local K	Mean AOA (deg)	Omega AOA (deg)	Blade Pitch Freq (Hz)	Tip Min Pitch (deg)	Tip Max Pitch (deg)	Number of Records	Filename
1	0.711	18.90	867,863	0.0500	20.0	10.0	0.423	43.88	63.88	49,740	O30350
1	0.711	18.90	867,863	0.0750	8.0	5.5	0.635	60.38	71.38	33,325	O30360
1	0.711	18.90	867,863	0.0750	14.0	5.5	0.635	54.38	65.38	33,325	O30370
1	0.711	18.90	867,863	0.0750	20.0	5.5	0.635	48.38	59.38	33,324	O30380
1	0.711	18.90	867,863	0.0750	8.0	10.0	0.635	55.88	75.88	33,325	O30390
1	0.711	18.90	867,863	0.0750	14.0	10.0	0.635	49.88	69.88	33,325	O30400
1	0.711	18.90	867,863	0.0750	20.0	10.0	0.635	43.88	63.88	33,325	O30410
1	0.711	18.90	867,863	0.1000	8.0	5.5	0.846	60.38	71.38	25,118	O30420
1	0.711	18.90	867,863	0.1000	14.0	5.5	0.846	54.38	65.38	25,118	O30430
1	0.711	18.90	867,863	0.1000	20.0	5.5	0.846	48.38	59.38	25,118	O30440
1	0.711	18.90	867,863	0.1000	8.0	10.0	0.846	55.88	75.88	25,118	O30450
1	0.711	18.90	867,863	0.1000	14.0	10.0	0.846	49.88	69.88	25,118	O30460
1	0.711	18.90	867,863	0.1000	20.0	10.0	0.846	43.88	63.88	25,118	O30470
2	0.627	23.30	943,502	0.0625	3.00	2.00	0.739	78.62	82.62	28,676	O47010
2	0.627	23.30	943,502	0.0625	12.00	4.00	0.739	67.62	75.62	28,676	O47020
2	0.627	23.30	943,502	0.0750	9.00	2.00	0.887	72.62	76.62	23,980	O47030
2	0.627	23.30	943,502	0.0750	23.00	5.00	0.887	55.62	65.62	23,980	O47040
2	0.627	23.30	943,502	0.0750	37.00	6.00	0.887	40.62	52.62	23,980	O47050
2	0.627	23.30	943,502	0.0750	52.00	6.00	0.887	25.62	37.62	23,980	O47060
2	0.627	23.30	943,502	0.1000	9.00	2.00	1.183	72.62	76.62	18,109	O47070
2	0.627	23.30	943,502	0.1000	23.00	2.00	1.183	58.62	62.62	18,109	O47080
2	0.627	23.30	943,502	0.1000	37.00	4.00	1.183	42.62	50.62	18,109	O47090
2	0.627	23.30	943,502	0.1000	7.00	6.00	1.183	70.62	82.62	18,109	O47100
2	0.627	23.30	943,502	0.1250	5.00	1.00	1.479	77.62	79.62	14,586	O47110
2	0.627	23.30	943,502	0.1250	13.00	1.00	1.479	69.62	71.62	14,586	O47120
2	0.627	23.30	943,502	0.0250	8.0	5.5	0.296	70.12	81.12	70,946	O47130
2	0.627	23.30	943,502	0.0250	14.0	5.5	0.296	64.12	75.12	70,946	O47140
2	0.627	23.30	943,502	0.0250	20.0	5.5	0.296	58.12	69.12	70,946	O47150
2	0.627	23.30	943,502	0.0250	8.0	10.0	0.296	65.62	85.62	70,946	O47160
2	0.627	23.30	943,502	0.0250	14.0	10.0	0.296	59.62	79.62	70,946	O47170
2	0.627	23.30	943,502	0.0250	20.0	10.0	0.296	53.62	73.62	70,946	O47180
2	0.627	23.30	943,502	0.0500	8.0	5.5	0.591	70.12	81.12	35,721	O47190
2	0.627	23.30	943,502	0.0500	14.0	5.5	0.591	64.12	75.12	35,721	O47201
2	0.627	23.30	943,502	0.0500	20.0	5.5	0.591	58.12	69.12	35,721	O47210
2	0.627	23.30	943,502	0.0500	8.0	10.0	0.591	65.62	85.62	35,721	O47220
2	0.627	23.30	943,502	0.0500	14.0	10.0	0.591	59.62	79.62	35,721	O47230
2	0.627	23.30	943,502	0.0500	20.0	10.0	0.591	53.62	73.62	35,721	O47241
2	0.627	23.30	943,502	0.0750	8.0	5.5	0.887	70.12	81.12	23,980	O47250
2	0.627	23.30	943,502	0.0750	14.0	5.5	0.887	64.12	75.12	23,980	O47260
2	0.627	23.30	943,502	0.0750	20.0	5.5	0.887	58.12	69.12	23,980	O47270
2	0.627	23.30	943,502	0.0750	8.0	10.0	0.887	65.62	85.62	23,980	O47280
2	0.627	23.30	943,502	0.0750	14.0	10.0	0.887	59.62	79.62	23,980	O47290
2	0.627	23.30	943,502	0.0750	20.0	10.0	0.887	53.62	73.62	23,980	O47300
2	0.627	23.30	943,502	0.1000	8.0	5.5	1.183	70.12	81.12	18,109	O47311
2	0.627	23.30	943,502	0.1000	14.0	5.5	1.183	64.12	75.12	18,109	O47320

Table C-14. Sequence O, Sin AOA, Parked (P), 131 files of varying duration (continued)

Span Station	Chord (m)	Uw (m/s)	Local Re	Local K	Mean AOA (deg)	Omega AOA (deg)	Blade Pitch Freq (Hz)	Tip Min Pitch (deg)	Tip Max Pitch (deg)	Number of Records	Filename
2	0.627	23.30	943,502	0.1000	20.0	5.5	1.183	58.12	69.12	18,109	O47330
4	0.457	33.90	1,000,542	0.0250	5.00	1.00	0.590	82.56	84.56	35,788	O80010
4	0.457	33.90	1,000,542	0.0250	15.00	3.00	0.590	70.56	76.56	35,789	O80020
4	0.457	33.90	1,000,542	0.0250	16.00	11.00	0.590	61.56	83.56	35,789	O80030
4	0.457	33.90	1,000,542	0.0250	28.00	13.00	0.590	47.56	73.56	35,789	O80040
4	0.457	33.90	1,000,542	0.0375	10.00	2.00	0.885	76.56	80.56	24,025	O80050
4	0.457	33.90	1,000,542	0.0375	26.00	2.00	0.885	60.56	64.56	24,025	O80060
4	0.457	33.90	1,000,542	0.0375	42.00	3.00	0.885	43.56	49.56	24,025	O80070
4	0.457	33.90	1,000,542	0.0375	15.00	10.00	0.885	63.56	83.56	24,025	O80080
4	0.457	33.90	1,000,542	0.0375	28.00	10.00	0.885	50.56	70.56	24,025	O80090
4	0.457	33.90	1,000,542	0.0375	42.00	10.00	0.885	36.56	56.56	24,025	O80100
4	0.457	33.90	1,000,542	0.0500	13.00	1.00	1.181	74.56	76.56	18,143	O80110
4	0.457	33.90	1,000,542	0.0500	30.00	2.00	1.181	56.56	60.56	18,143	O80120
4	0.457	33.90	1,000,542	0.0500	4.00	2.00	1.181	82.56	86.56	18,143	O80131
4	0.457	33.90	1,000,542	0.0500	12.00	2.00	1.181	74.56	78.56	18,143	O80140
4	0.457	33.90	1,000,542	0.0500	25.00	2.00	1.181	61.56	65.56	18,143	O80150
4	0.457	33.90	1,000,542	0.0500	10.00	3.00	1.181	75.56	81.56	18,143	O80160
4	0.457	33.90	1,000,542	0.0500	27.00	3.00	1.181	58.56	64.56	18,143	O80170
4	0.457	33.90	1,000,542	0.0250	8.0	5.5	0.590	75.06	86.06	35,789	O80180
4	0.457	33.90	1,000,542	0.0250	14.0	5.5	0.590	69.06	80.06	35,789	O80190
4	0.457	33.90	1,000,542	0.0250	20.0	5.5	0.590	63.06	74.06	35,789	O80200
4	0.457	33.90	1,000,542	0.0250	8.0	10.0	0.590	70.56	90.56	35,789	O80210
4	0.457	33.90	1,000,542	0.0250	14.0	10.0	0.590	64.56	84.56	35,789	O80220
4	0.457	33.90	1,000,542	0.0250	20.0	10.0	0.590	58.56	78.56	35,789	O80230
4	0.457	33.90	1,000,542	0.0500	14.0	5.5	1.181	69.06	80.06	18,143	O80240
4	0.457	33.90	1,000,542	0.0500	20.0	5.5	1.181	63.06	74.06	18,143	O80250
4	0.457	33.90	1,000,542	0.0750	14.0	5.5	1.771	69.06	80.06	12,261	O80260
4	0.457	33.90	1,000,542	0.0750	20.0	5.5	1.771	63.06	74.06	12,261	O80270
5	0.381	39.30	967,024	0.0125	5.00	1.00	0.410	83.65	85.65	51,258	O95011
5	0.381	39.30	967,024	0.0125	15.00	4.00	0.410	70.65	78.65	51,257	O95020
5	0.381	39.30	967,024	0.0125	13.00	8.00	0.410	68.65	84.65	51,258	O95030
5	0.381	39.30	967,024	0.0125	22.00	11.00	0.410	56.65	78.65	51,258	O95040
5	0.381	39.30	967,024	0.0250	16.00	2.00	0.821	71.65	75.65	25,877	O95080
5	0.381	39.30	967,024	0.0250	37.00	3.00	0.821	49.65	55.65	25,877	O95090
5	0.381	39.30	967,024	0.0375	9.00	1.00	1.231	79.65	81.65	17,417	O95130
5	0.381	39.30	967,024	0.0375	9.00	2.00	1.231	78.65	82.65	17,417	O95140
5	0.381	39.30	967,024	0.0375	21.00	2.00	1.231	66.65	70.65	17,417	O95151
5	0.381	39.30	967,024	0.0250	8.0	5.5	0.821	76.15	87.15	25,877	O95160
5	0.381	39.30	967,024	0.0250	14.0	5.5	0.821	70.15	81.15	25,877	O95170

Table C-14. (continued)

Yaw angle = 0° throughout this sequence. Data was acquired for 40 successive sinusoidal blade pitch cycles.

Rows for each span station are divided into two sets, and are separated by a heavy horizontal line. The first set of rows consists of combinations of K, mean AOA, and omega AOA that the blades would likely experience during routine operation. The second set of rows contains combinations of K, mean AOA, and omega AOA corresponding to those tested at Ohio State University using an S809 airfoil section under two-dimensional conditions (Reuss Ramsay et al. 1995).

Data problems in NREL files:

Scale measurements questionable (See Table E.2 in Appendix E).

Five-hole probe inboard port is plugged at 67% span for points designed for 30% span station (O30000-O30470).

Data problems in NASA files (See Table E.2 in Appendix E).

Scale measurements questionable.

Table C-15. Sequence P, Wake Flow Vis. Upwind (P), 19 files of 3-minute duration

Uw	Yaw Angle																
(m/s)	0	5	10	20	30	45	60	90	135	180	-135	-60	-45	-30	-20	-10	-5
5.0	0											0	0,1	0	0	0	
6.0																	
7.0	0											0	0	1	0	0	
8.0																	
9.0																	
10.0	0,A0													0	0	0	
11.0																	
12.0																	
13.0																	
14.0																	
15.0	0																
16.0																	
17.0																	
18.0																	
19.0																	
20.0																	

File Name Convention: PWWYYYYR where WW corresponds to the wind speed, Uw; YYYY corresponds to the yaw angle (M030=-30); R corresponds to the repetition digit. Each entry in the above table represents the repetition digit of the filename corresponding to that wind speed and yaw angle. The entry ‘A0’ indicates file P10000A0, which was 10 m/s, 0° yaw, and 3° pitch.

Data problems in NREL files:

Scale measurements questionable (See Table E.2 in Appendix E).
Pressure calibration malfunction.

Data problems in NASA files (See Table E.2 in Appendix E).

East wall pressure transducer not connected.
Scale measurements questionable.

Other considerations:

Blade pitch angle = 12° for P1000000; pitch angle = 3° for all other campaigns.
File P1000000 was 2 minutes in duration instead of 3 minutes.
Smoke candle extinguished early for P05M0450.
Yaw brake released during P07M0301 (yaw drive still engaged).

Table C-16. Sequence Q, Dynamic Inflow (P), 12 files of varying duration

Uw (m/s)	Initial Tip Pitch (deg)	Final Tip Pitch (deg)	Pitch Rate (deg/s)	Delay Time (s)	Hold Time (s)	Number of Pitches	Number of Records	Filename
5.0	-6.0	10.0	66.0	15.0	15.0	20	312,502	Q0500000
5.0	-6.0	10.0	66.0	15.0	15.0	20	312,502	Q0500001
8.0	0.0	18.0	66.0	10.0	10.0	20	208,502	Q0800000
8.0	0.0	18.0	66.0	10.0	10.0	20	208,502	Q0800001
10.0	6.0	24.0	66.0	8.0	8.0	20	167,502	Q1000000
10.0	6.0	24.0	66.0	8.0	8.0	20	167,502	Q1000001
15.0	18.0	36.0	66.0	5.0	5.0	40	25,424	Q1500000 (aborted)
5.0	3.0		0.0			Test point	9,502	Q05REF0
8.0	3.0		0.0			Test point	9,502	Q08REF0, Q08REF1
10.0	3.0		0.0			Test point	9,502	Q10REF0, Q10REF1

'Initial Tip Pitch' column entries indicate the tip pitch angle prior to pitching, and 'Final Tip Pitch' column entries denote tip pitch after pitching. 'Delay Time' is the time period allowed to elapse prior to initiating the next pitch motion. 'Hold Time' is the time allowed to elapse before pitching back to the initial pitch angle. Data was acquired during the entire series of pitches specified in the column titled 'Number of Pitches.'

Table C-17. Sequence R, Step AOA, No Probes (P), 21 files of varying duration

Uw (m/s)	Yaw (deg)	Initial Tip Pitch (deg)	0.30R AOA at Initial Pitch (deg)	0.95R AOA at Initial Pitch (deg)	Final Tip Pitch (deg)	0.30R AOA at Final Pitch (deg)	0.95R AOA at Final Pitch (deg)	Pitch Rate (deg/s)	Pitching	Number of records	Filename
6.0	0.0	32.0	-16.0	-20.1	-15.0	20.0	20.1	0.180	continuous ramp	139,502	R0600RU0
6.0	0.0	-15.0	20.0	20.1	32.0	-16.0	-20.1	-0.180	continuous ramp	139,502	R0600RD0
6.0	0.0	32.0	-16.1	-20.1	-15.0	20.0	20.1	step up then step down	5.0 deg step, 8 second hold	159,502	R0600ST0
6.0	30.0	32.0	-16.1	-20.1	-15.0	20.0	20.1	step up then step down	5.0 deg step, 8 second hold	159,502	R0630ST0
6.0	0.0	3.0						0.0	test point	9,502	R0004, R0005
10.0	0.0	37.0	-9.0	-2.0	-15.0	36.0	26.8	0.180	continuous ramp	154,502	R1000RU0
10.0	0.0	-15.0	36.0	26.8	37.0	-9.0	-2.0	-0.180	continuous ramp	154,502	R1000RD0
10.0	0.0	37.0	-9.0	-2.0	-15.0	36.0	26.8	step up then step down	5.0 deg step, 8 second hold	174,502	R1000ST1
10.0	30.0	37.0	-9.0	-2.0	-15.0	36.0	26.8	step up then step down	5.0 deg step, 8 second hold	174,502	R1030ST0
10.0	0.0	3.0						0.0	test point	9,502	R0002, R0003
15.0	0.0	40.0	-1.6	-16.3	-15.0	48.2	34.0	0.180	continuous ramp	164,502	R1500RU0
15.0	0.0	-15.0	48.2	34.0	40.0	-1.6	-16.3	-0.180	continuous ramp	164,502	R1500RD0
15.0	0.0	40.0	-1.6	-16.3	-15.0	48.2	34.0	step up then step down	5.0 deg step, 8 second hold	189,502	R1500ST1
15.0	30.0	40.0	-1.6	-16.3	-15.0	48.2	34.0	step up then step down	5.0 deg step, 8 second hold	189,502	R1530ST0
15.0	0.0	3.0						0.0	Test point	9,502	R0000, R0001
20.0	0.0	44.0	1.3	-14.4	28.0	14.7	-0.8	0.180	continuous ramp	49,502	R2000RU0
20.0	0.0	28.0	14.7	-0.8	44.0	1.3	-14.4	-0.180	continuous ramp	49,502	R2000RD0
20.0	0.0	44.0	1.3	-14.4	28.0	14.7	-0.8	step up then step down	5.0 deg step, 8 second hold	64,502	R2000ST0

The column titled 'Pitching' describes how the blade was pitched to acquire static data. The entry 'continuous ramp' indicates that pitching was carried out at 0.180 degrees per second through the range indicated in the columns to the left. The entry '5.0 deg step, 8 second hold' indicates that, through the range indicated in the columns to the left, the blade was stepped in pitch to each angle and then held for 8 seconds.

Table C-18. Sequence S, Upwind, No Probes (F), 104 files of 30-second duration, 2 files of 6-minute duration

Uw	Yaw Angle																		
(m/s)	0	5	10	20	30	45	60	75	90	135	180	-135	-90	-75	-60	-45	-30	-20	-10	-5
5.0	0,1	0	0	0	0	0	0	0	0	0	0									
6.0	0,1		0		0															
7.0	0,1	0	0	0	0	0	0	0	0	0	0									
8.0	0,1		0		0															
9.0	0,1		0		0															
10.0	0,1	0	0	0	0	0	0	0	0	0	0									
11.0	0,1		0		0															
12.0	0,1		0		0															
13.0	0,1		0		0															
14.0	0,1		0		0															
15.0	0,1	0	0	0	0	0	0	0	0	0	0									
16.0	0,1		0		0															
17.0	0,1		0		0															
18.0	0,1		0		0															
19.0	0,1		0		0															
20.0	0,1	0	0	0																
21.0	0		0																	
22.0	0		0																	
23.0	0																			
24.0	2																			
25.0	1																			

File Name Convention: SWWYYYYR where WW corresponds to the wind speed, Uw; YYYY corresponds to the yaw angle (M030=-30); R corresponds to the repetition digit. Each entry in the above table represents the repetition digit of the filename corresponding to that wind speed and yaw angle. Two additional files representing 6-minute duration, 360° yaw sweeps at 7 and 10 m/s respectively are S07YSU00 and S10YSU00.

Table C-19. Sequence T, Upwind, 2° Pitch (F), 21 files of 30-second duration

Uw	Yaw Angle																			
(m/s)	0	5	10	20	30	45	60	75	90	135	180	-135	-90	-75	-60	-45	-30	-20	-10	-5
5.0	0																			
6.0	0																			
7.0	0																			
8.0	0																			
9.0	0																			
10.0	0																			
11.0	0																			
12.0	0																			
13.0	0																			
14.0	0																			
15.0	0																			
16.0	0																			
17.0	0																			
18.0	0																			
19.0	0																			
20.0	0																			
21.0	0																			
22.0	0																			
23.0	0																			
24.0	2																			
25.0	1																			

File Name Convention: TWWYYYYR where WW corresponds to the wind speed, Uw; YYYY corresponds to the yaw angle (M030=-30); R corresponds to the repetition digit. Each entry in the above table represents the repetition digit of the filename corresponding to that wind speed and yaw angle.

Table C-20. Sequence U, Upwind, 4° Pitch (F), 21 files of 30-second duration

Uw	Yaw Angle																			
(m/s)	0	5	10	20	30	45	60	75	90	135	180	-135	-90	-75	-60	-45	-30	-20	-10	-5
5.0	0																			
6.0	0																			
7.0	0																			
8.0	0																			
9.0	0																			
10.0	0																			
11.0	0																			
12.0	0																			
13.0	0																			
14.0	0																			
15.0	0																			
16.0	1																			
17.0	0																			
18.0	0																			
19.0	0																			
20.0	0																			
21.0	0																			
22.0	0																			
23.0	0																			
24.0	2																			
25.0	1																			

File Name Convention: UWWYYYYR where WW corresponds to the wind speed, Uw; YYYY corresponds to the yaw angle (M030=-30); R corresponds to the repetition digit. Each entry in the above table represents the repetition digit of the filename corresponding to that wind speed and yaw angle.

Table C-21. Sequence V, Tip Plate (F), 21 files of 30-second duration

Uw	Yaw Angle																			
(m/s)	0	5	10	20	30	45	60	75	90	135	180	-135	-90	-75	-60	-45	-30	-20	-10	-5
5.0	0																			
6.0	0																			
7.0	0																			
8.0	0																			
9.0	0																			
10.0	0																			
11.0	0																			
12.0	0																			
13.0	0																			
14.0	0																			
15.0	0																			
16.0	0																			
17.0	0																			
18.0	0																			
19.0	0																			
20.0	0																			
21.0	0																			
22.0	0																			
23.0	0																			
24.0	0																			
25.0	0																			

File Name Convention: VWWYYYYR where WW corresponds to the wind speed, Uw; YYYY corresponds to the yaw angle (M030=-30); R corresponds to the repetition digit. Each entry in the above table represents the repetition digit of the filename corresponding to that wind speed and yaw angle.

Table C-22. Sequence W, Extended Blade (F), 17 files of 30-second duration

Uw	Yaw Angle																			
(m/s)	0	5	10	20	30	45	60	75	90	135	180	-135	-90	-75	-60	-45	-30	-20	-10	-5
5.0	0																			
6.0	0																			
7.0	0																			
8.0	0																			
9.0	0																			
10.0	0																			
11.0	0																			
12.0	0																			
13.0	0																			
14.0	0																			
15.0	0																			
16.0	0																			
17.0	0																			
18.0	0																			
19.0	0																			
20.0	0																			
21.0	0																			
22.0																				
23.0																				
24.0																				
25.0																				

File Name Convention: WWWYYYYR where WW in the second and third positions corresponds to the wind speed, Uw; YYYY corresponds to the yaw angle (M030=-30); R corresponds to the repetition digit. Each entry in the above table represents the repetition digit of the filename corresponding to that wind speed and yaw angle.

Table C-23. Sequence X, Elevated RPM (F), 45 files of 30-second duration

Uw	Yaw Angle																			
(m/s)	0	5	10	20	30	45	60	75	90	135	180	-135	-90	-75	-60	-45	-30	-20	-10	-5
5.0	3,4	2	1	1	1												1	1	1	1
6.0	0		0		0															
7.0	1,2	0	0	0	0												0	0	0	0
8.0	2		1		0															
9.0	1		0		0															
10.0	1,2	0	0	0	0												0	0	0	0
11.0	0		0		0															
12.0	0		0		0															
13.0																				
14.0																				
15.0																				
16.0																				
17.0																				
18.0																				
19.0																				
20.0																				
21.0																				
22.0																				
23.0																				
24.0																				
25.0																				

File Name Convention: XWWYYYYR where WW in the second and third positions corresponds to the wind speed, Uw; YYYY corresponds to the yaw angle (M030=-30); R corresponds to the repetition digit. Each entry in the above table represents the repetition digit of the filename corresponding to that wind speed and yaw angle.

Table C-24. Sequence 3, Tower Wake, 39 files of 30-second duration

Wind Speed (m/s)	Yaw Angle (deg)	Pitch Angle (deg)	Filename
7.0	-9.2	78.9	30700010
7.0	-7.1	76.8	30700020
7.0	-5.1	74.8	30700030
7.0	-3.0	72.7	30700040
7.0	-0.9	70.6	30700050
7.0	1.1	68.6	30700060
7.0	3.3	66.4	30700070
7.0	5.3	64.4	30700080
7.0	7.4	62.3	30700090
7.0	9.5	60.2	30700100
7.0	11.7	58.0	30700110
7.0	13.7	56.0	30700120
7.0	15.9	53.8	30700130
15.0	-9.2	78.9	31500010
15.0	-7.1	76.8	31500020
15.0	-5.1	74.8	31500030
15.0	-3.0	72.7	31500040
15.0	-0.9	70.6	31500050
15.0	1.1	68.6	31500060
15.0	3.3	66.4	31500070
15.0	5.3	64.4	31500080
15.0	7.4	62.3	31500090
15.0	9.5	60.2	31500100
15.0	11.7	58.0	31500110
15.0	13.7	56.0	31500120
15.0	15.9	53.8	31500130
20.0	-9.2	78.9	32000010
20.0	-7.1	76.8	32000020
20.0	-5.1	74.8	32000030
20.0	-3.0	72.7	32000040
20.0	-0.9	70.6	32000050
20.0	1.1	68.6	32000060
20.0	3.3	66.4	32000070
20.0	5.3	64.4	32000080
20.0	7.4	62.3	32000090
20.0	9.5	60.2	32000100
20.0	11.7	58.0	32000110
20.0	13.7	56.0	32000120
20.0	15.9	53.8	32000130

Data problems in NREL files:

Scale measurements questionable (See Table E.2 in Appendix E).

Data problems in NASA files (See Table E.2 in Appendix E).

East wall pressure transducer not connected.

Scale measurements questionable.

Table C-25. Sequence 4, Static Pressure Calibration (F,P), 31 files of 30-second duration

Uw	Yaw Angle																			
(m/s)	0	5	10	20	30	45	60	75	90	135	180	-135	-90	-75	-60	-45	-30	-20	-10	-5
5.0	0		0		0															
6.0	0																			
7.0	0		1		1															
8.0	0																			
9.0	0																			
10.0	0		0		0															
11.0	0																			
12.0	0																			
13.0	0																			
14.0	0																			
15.0	0		0		0															
16.0	0																			
17.0	0																			
18.0	0																			
19.0	0																			
20.0	0		0		0															
21.0	0																			
22.0	0																			
23.0	0																			
24.0	0																			
25.0	0		0																	

Table C-25. (continued)

File Name Convention: 4WWYYYYR where WW corresponds to the wind speed, Uw; YYYY corresponds to the yaw angle (M030=-30); R corresponds to the repetition digit. Each entry in the above table represents the repetition digit of the filename corresponding to that wind speed and yaw angle.

Data problems in NREL files:

Scale measurements questionable (See Table E.2 in Appendix E).

West sonic anemometer malfunction during 42200000, 42300000, 42400000, 42500000, and 42500100.

Data problems in NASA files (See Table E.2 in Appendix E).

East wall pressure transducer not connected.

Scale measurements questionable.

NREL/NASA file synchronization issues:

NASA system early for file 41000000.

Table C-26. Sequence 5, Sweep Wind Speed, 6 points of 6-minute duration

Wind Speed (m/s)	Yaw Angle (deg)	Pitch Angle (deg)	5-Hole Pressure Probes	Filename
5.0 to 25.0	0.0	3.0	Yes	5UP00000
25.0 to 5.0	0.0	3.0	Yes	5DN00001
5.0 to 25.0	0.0	6.0	Yes	5UP00001
25.0 to 5.0	0.0	6.0	Yes	5DN00002
5.0 to 25.0	0.0	3.0	No	5UP00003
25.0 to 5.0	0.0	3.0	No	5DN00003

Data problems in NREL files:

Scale measurements questionable (See Table E.2 in Appendix E) for files 5UP00000, 5DN00001, 5UP00001, 5DN00002.

Data problems in NASA files (See Table E.2 in Appendix E).

East wall pressure transducer not connected for files 5UP00000, 5DN00001, 5UP00001, 5DN00002.

Scale measurements questionable for files 5UP00000, 5DN00001, 5UP00001, 5DN00002.

Other consideration:

File 5DN00002 less than 6 minutes in duration.

Table C-27. Sequence 6, Shroud Wake, 49 files of 30-second duration

Wind Speed (m/s)	Turntable Angle (deg)	Yaw Angle Relative to Table (deg)	Pitch Angle (deg)	Filename
7.0	-20.0	15.9	73.8	60700010, 60700011
7.0	-20.0	22.2	67.5	60700020
7.0	-20.0	28.5	61.2	60700030
7.0	-10.0	5.9	73.8	60700040
7.0	-10.0	12.2	67.5	60700050
7.0	-10.0	18.5	61.2	60700060
7.0	0.0	-4.1	73.8	60700071
7.0	0.0	2.2	67.5	60700081, 60700082
7.0	0.0	8.5	61.2	60700090
7.0	10.0	-14.1	73.8	60700100
7.0	10.0	-7.8	67.5	60700110
7.0	10.0	-1.5	61.2	60700120
7.0	20.0	-24.1	73.8	60700130
7.0	20.0	-17.8	67.5	60700140
7.0	20.0	-11.5	61.2	60700150
15.0	-20.0	15.9	73.8	61500010
15.0	-20.0	22.2	67.5	61500020
15.0	-20.0	28.5	61.2	61500030
15.0	-10.0	5.9	73.8	61500040
15.0	-10.0	12.2	67.5	61500050
15.0	-10.0	18.5	61.2	61500060
15.0	0.0	-4.1	73.8	61500070
15.0	0.0	2.2	67.5	61500080, 61500081
15.0	0.0	8.5	61.2	61500090
15.0	10.0	-14.1	73.8	61500100
15.0	10.0	-7.8	67.5	61500110
15.0	10.0	-1.5	61.2	61500120
15.0	20.0	-24.1	73.8	61500130
15.0	20.0	-17.8	67.5	61500140
15.0	20.0	-11.5	61.2	61500150
20.0	-20.0	15.9	73.8	62000010
20.0	-20.0	22.2	67.5	62000022
20.0	-20.0	28.5	61.2	62000032
20.0	-10.0	5.9	73.8	62000040
20.0	-10.0	12.2	67.5	62000050
20.0	-10.0	18.5	61.2	62000060
20.0	0.0	-4.1	73.8	62000070
20.0	0.0	2.2	67.5	62000080, 62000081
20.0	0.0	8.5	61.2	62000090
20.0	10.0	-14.1	73.8	62000100
20.0	10.0	-7.8	67.5	62000110
20.0	10.0	-1.5	61.2	62000120
20.0	20.0	-24.1	73.8	62000130
20.0	20.0	-17.8	67.5	62000140
20.0	20.0	-11.5	61.2	62000150

Table C-2. (continued)

Data problems in NREL files:
Scale measurements questionable (See Table E.2 in Appendix E).

Data problems in NASA files (See Table E.2 in Appendix E).
East wall pressure transducer not connected.
Scale measurements questionable.

NREL/NASA file synchronization issues:
NASA system early for file 60700082

Table C-28. Sequence 7, Shroud Operating (P), 26 files of 30-second duration

Wind Speed (m/s)	Turntable Angle (deg)	Yaw Angle Relative to Table (deg)	Pitch Angle (deg)	Filename
5.0	0.0	0.0	3.0	70500010, 70500011
5.0	10.0	-10.0	3.0	70500020
5.0	20.0	-20.0	3.0	70500030
7.0	0.0	0.0	3.0	70700010, 70700011
7.0	10.0	-10.0	3.0	70700020
7.0	20.0	-20.0	3.0	70700030
10.0	0.0	0.0	3.0	71000010, 71000011
10.0	10.0	-10.0	3.0	71000020
10.0	20.0	-20.0	3.0	71000030
15.0	0.0	0.0	3.0	71500010, 71500011
15.0	10.0	-10.0	3.0	71500020
15.0	20.0	-20.0	3.0	71500030
20.0	0.0	0.0	3.0	72000010, 72000011
20.0	10.0	-10.0	3.0	72000020
20.0	20.0	-20.0	3.0	72000030
25.0	0.0	0.0	3.0	72500010, 72500011
25.0	10.0	-10.0	3.0	72500020
25.0	20.0	-20.0	3.0	72500030
10.0	0.0	20.0	3.0	71000200
10.0	0.0	-20.0	3.0	710M0200

Data problems in NREL files:

Scale measurements questionable (See Table E.2 in Appendix E).

Data problems in NASA files (See Table E.2 in Appendix E).

East wall pressure transducer not connected.

Scale measurements questionable.

Table C-29. Sequence 8, Downwind Sonics (F,P),153 files of 30-second duration

Uw	Yaw Angle																			
(m/s)	0	5	10	15	20	25	30	40	50	60	180	-135	-90	-75	-60	-45	-30	-20	-10	-5
5.0	0,1	0	0	0	0	0	0	0	0	0										
6.0	0	0	0	0	0	0	0	0	0	0										
7.0	0,1	0	0	0	0	0	0	0	0	0										
8.0	0	0	0	0	0	0	0	0	0	0										
9.0	0,1	0	0	0	0	0	0	0	0	0										
10.0	0,1	0	0	0		0	0	0	0	0										
11.0	0,1	0	0	0	0	0	0	0	0	0										
12.0	0	0	0	0	0	0	0	0	0	0										
13.0	0,2	0	0	0	0	0	0	0	0	0										
14.0	0	0	0	0	0	0	0	0	1	1										
15.0	0,1	0	0	0	0	0	0	0	0	0										
16.0	0	0	0	0	0	0	0													
17.0	0,1	0	0	0	0	0	0													
18.0	0	0	0	0	0															
19.0	0	0	0	0	0															
20.0	0	0	0																	
21.0	0	0	0																	
22.0	0	0	0																	
23.0	0																			
24.0	0																			
25.0	1																			

File Name Convention: 8WWYYYYR where WW corresponds to the wind speed, Uw; YYYY corresponds to the yaw angle (M030=-30); R corresponds to the repetition digit. Each entry in the above table represents the repetition digit of the filename corresponding to that wind speed and yaw angle.

Other consideration:

Pitch system in manual mode rather than automatic mode for 81000000 and 81000001.

Table C-30. Sequence 9, Sonic Validation (P), 6 files of 30-second duration

Uw	Yaw Angle																			
(m/s)	0	5	10	20	30	45	60	75	90	135	180	-135	-90	-75	-60	-45	-30	-20	-10	-5
5.0	0																			
6.0																				
7.0	0																			
8.0																				
9.0																				
10.0	0																			
11.0																				
12.0																				
13.0																				
14.0																				
15.0	0																			
16.0																				
17.0																				
18.0																				
19.0																				
20.0	0																			
21.0																				
22.0																				
23.0																				
24.0																				
25.0	0																			

File Name Convention: 9WWYYYYR where WW corresponds to the wind speed, Uw; YYYY corresponds to the yaw angle (M030=-30); R corresponds to the repetition digit. Each entry in the above table represents the repetition digit of the filename corresponding to that wind speed and yaw angle.

Other consideration:

Pressure transducers not calibrated.

References

Reuss Ramsay, R.; Hoffman, M.J.; Gregorek, G.M. (1995). *Effects of Grit Roughness and Pitch Oscillations on the S809 Airfoil*. NREL/TP-442-7817. Golden, CO: National Renewable Energy Laboratory.

Appendix D: NASA Software Requirements Document

UNSTEADY AERODYNAMIC EXPERIMENT

Software Requirements Document

September 20, 1999

Hardware Check Req'd: Jan 18, 1999

Real-Time Comp Ready: Jan 24, 1999

Data Acquisition Program Complete: Jan 24, 1999

Originally prepared By: Robert M Kufeld 9-23-99
Robert Kufeld, Project Director

Reviewed By: Janet E Beegle 9/21/99
Janet Beegle, Test Director

Approved By: Betty Silva
Betty Silva, NPRIME Project Manager

Concurrence: Allan D Levin
Al Levin, FOI Computation Group Leader

Concurrence:
Mike Liu, FOI Development Group Leader

Table of Contents

A. Introduction

B. Objectives

C. Factor Table

D. Test Dependent Constants

E. Measurement Channels

F. Data Reduction for Wind Tunnel Parameters

G. Tares for Wind Tunnel Scales

H. Wind Tunnel Scale Loads

I. Data Presentation

J. References

A. Introduction

This test will use the NASA Ames 80 by 120- foot wind tunnel and NREL's "Unsteady Aerodynamics" 10-m (32.8-ft) diameter instrumented research turbine installed in a 2-bladed configuration. Previous atmospheric turbine testing has demonstrated the extremely complex dynamic nature of a typical wind turbine-operating environment. Highly turbulent wind and sheared inflow conditions are major factors that contribute to the complexity. Testing in a controlled wind tunnel environment will eliminate these factors. Resulting data will provide information from which a significant portion of the complex inflow-induced operating environment is removed. This will enable researchers to isolate and characterize specific dynamic stall responses and 3-D rotational effects under benign steady-state operating conditions.

The Unsteady Aerodynamics research turbine is instrumented for structural loads and aerodynamic response measurements. It includes a pressure-tapped blade with 5 radial stations of aerodynamic pressure profile characterization, and local angle-of-attack and spanwise flow angle measurements.

The test objectives for the NREL Wind Turbine Test in the 80-Foot by 120-Foot Wind Tunnel are as follows:

To acquire high quality aerodynamic, loads, performance, boundary layer and turbine wake information for steady test condition similar to the atmospheric test condition experienced in field-testing. The results will be used to validate comprehensive turbine design codes and highly complex CFD models. To acquire this information the test will use turbine installed pressure transducers, strain gages and turbine state parameters (supplied and acquired by NREL) along with high quality tunnel flow conditions, including wall pressure, outside meteorological conditions turn table yaw and balance conditions and video cameras mounted in the 80x120 ceiling.

This test requires the tunnel to operate at very low airspeeds (5 meter/sec). This requires two special operating considerations: the measurement of the low wind speed and operating during outside calm conditions. NREL will mount two sonic anemometers on provided microphone stands to measure the low wind speed and current plans call for operations during the graveyard shift to get the most of outside calm conditions.

This test requires the use of the turn table yaw capability and the measurement of turbine drag using measurements from tunnel scale. NREL has requested all tunnel data be fed to their data acquisition system via analog channels so that they may process and store the data in their database. Appropriate weight and aero tare will be required.

Portion of the test will include the measurement of the turbine wake and blade boundary layers of the blade. To measure the turbine wake two ceiling mounted video cameras are required. NREL will inject smoke into the airflow with a special rotor tip design to hold a smoke generator and release the smoke through a hole in the tip. The cameras will be calibrated by NREL and data recorded on the NREL data processing equipment.

NREL's data acquisition system will serve as the primary acquisition system. All tunnel measurement will be provided to NREL in analog format and the data processing equation also be provided. NIDS will essentially be used to set up Real Time monitors to display test conditions for NREL engineers, the Test Director and the Tunnel Operator. NIDS data will be required to cross-check NREL computations.

B. Objectives

The objectives of this document are to specify

1. The measurement channels
2. The derived equations
3. The format for real-time display
4. The printout format
5. The format of data files acquired by NIDS (the NFAC data acquisition system) and provided to NREL post-test.

NOTE: The software item numbers are specified on the left, followed by the variable names. If the variables are measured parameters, Measurement Numbers (MN) from the Instrumentation Test Plan will be specified. For easy look-up, the software item numbers in the derived parameters are placed in brackets. Although all angle variables are measured or have units in *degree*, proper care must be taken to convert *degree* into *radian* before trigonometric calculation (SIN, COS, TAN, etc.) are performed.

Related documents can be found in Guidelines for Preparation of Software Test Requirements.

C. Factor Table

Factor table parameters must be entered prior to each run.

100TEST_NAME
Alphanumeric description of NREL test name

101TURBINE_YAW
Yaw angle of wind turbine (deg)

103 FMODEL
Wind turbine configuration.

```
= 1,      tower only (no nacelle, no blades)
= 2,      tower + nacelle (no blades)
= 3,      upwind turbine
= 4,      downwind turbine
```

110 TARE,W_S
Weight tare set number for the tunnel scale loads.

111 TARE,A_S
Aero tare set number for the tunnel scale loads.

D. Test Dependent Constants

The following constants are model dependent. Actual values will be measured and entered at the beginning of the test.

Wind Tunnel Constants

The moment center diagram for the 80 x 120 test section can be found in figure 24 of ref [1].

201 HV_DIST
Vertical distance from drag link elevation to midpoint between strut tip ball center, [ft, positive up]
= 55.917/verify/

202 J_DIST
Lateral distance from tunnel centerline to midpoint between strut tip ball centers, [ft, positive starboard]
= 0.0

203 K_DIST
Streamwise distance from lift wire to the model pivot axis, [ft, positive downstream]
= 18.382/verify/

204 XS_DIST
Streamwise distance from the model pivot axis to the model moment center, for zero angle of attack, [ft, positive Downstream]
= 0.0

205 YV_DIST
Vertical distance from midpoint between strut tip ball centers to model moment center, for zero angle of attack, [ft, positive up]
= 0.0

206ZL_DIST
Distance West from Semispan turntable centerline to moment center, [ft,]
= 0.0

207 PSI_PIVOT_DIST
Horizontal distance from turntable center of rotation to model's angle-of-attack pivot when model has zero sideslip, [ft]
= 0.0 (PSIRAD in software)

209 DH
Height from BARO transducer to tunnel centerline (measured 3/6/95 [ft])
= 61.00 ft./verify/

210 CSP (0:3)
Correction coefficients for static plate
(in database)

This test will be run as a full span model orientation.

Constants

211 **PI**
Mathematical constant, [rad]
= 3.141593

212 **CROSS_SECTION_AREA**
Wind tunnel cross-section area for the 80 x120 with acoustic treatment, [ft^2]
= 9401

216 **QLIM**
Dynamic pressure limiting low and high speed aerodynamic tares, [psf]
= /TBD

217 **PBPSI**
Base position of turntable yaw angle, [deg]
= 0.0

E. Measurement Channels

Standard Wind Tunnel Measurements

302 **ATEMP (MN 302)**
Atmospheric temperature from 15' weather station, [°F]

303B **AVEL60 (MN 303B)**
Atmospheric wind speed, [knot], from 60’ weather station

304B **AWDR60 (MN 304B)**
Atmospheric wind direction, [deg], from 60’ weather station

303C **AVEL100 (MN 303C)**
Atmospheric wind speed, [knot], from 100’ weather station

304C **AWDR100 (MN 304C)**
Atmospheric wind direction, [deg], from 100’ weather station

The above measurements are acquired from the Met Tower. They are NOT used in the computation of wind tunnel test conditions.

305A **BARO_DIG (MN 305A)**
Barometric Pressure digital, [psia]

305B **BARO_ANA (MN 305B)**
Barometric Pressure analog, [psia]

306 **PSI (MN 306)**
Wind tunnel turntable yaw angle, [deg, positive starboard], from facility control system

307 **DPT (MN 307)**
Dew point temperature from relative humidity probe, [°F]

308 **TTF (MN 308)**
Tunnel total temperature, [°F]
TTF = TTF_ANA (TTF_ANA from the IMR)

308A **TTF_DIG (MN 308A)**
Tunnel total temperature, [°F]

310 **PSREF_BAR (MN 310)**
Tunnel static pressure at contraction, $(P_S - P_a)$, [psfg]

310A **PSREF_BAR_DIG (MN 310A)**
Tunnel static pressure at contraction, $(P_S - P_a)$, [psfg]

311 **PT_BAR (MN 311)**
Tunnel total pressure at ring $(P_t - P_a)$, [psfg]

311A **PT_BAR_DIG (MN 311A)**
Tunnel total pressure at ring $(P_t - P_a)$, [psfg]

312 **LFL (MN 312)**
Wind tunnel left front lift (scale #1), [lb, positive up]

313 **RFL (MN 313)**
Wind tunnel right front lift (scale #2), [lb, positive up]

314 **LRL (MN 314)**
Wind tunnel left rear lift (scale #3), [lb, positive up]

315 **RRL (MN 315)**
Wind tunnel right rear lift (scale #4), [lb, positive up]

316 **FSF (MN 316)**
Wind tunnel front side force (scale #5), [lb, positive starboard]

317 **RSF (MN 317)**
Wind tunnel rear side force (scale #6), [lb, positive starboard]

318 **DRAG (MN 318)**
Wind tunnel drag force (scale #7), [lb, positive downstream]

Wall Pressure

321 **W1 (MN 321)**
West Wall pressure 1 [psid, positive up]

322 **W2 (MN 322)**
West Wall pressure 2 [psid, positive up]

323 **W3 (MN 323)**
West Wall pressure 3 [psid, positive up]

324 **W4 (MN 324)**
West Wall pressure 4 [psid, positive up]

325 **W5 (MN 325)**
West Wall pressure 5 [psid, positive up]

326 **W6 (MN 326)**
West Wall pressure 6 [psid, positive up]

327 **W7 (MN 327)**
West Wall pressure 7 [psid, positive up]

328 **W8 (MN 328)**
West Wall pressure 8 [psid, positive up]

329 **W9 (MN 329)**
West Wall pressure 9 [psid, positive up]

330 **W10 (MN 330)**
West Wall pressure 10 [psid, positive up]

331 **W11 (MN 331)**
West Wall pressure 11 [psid, positive up]

332 **W12 (MN 332)**
West Wall pressure 12 [psid, positive up]

333 **W13 (MN 333)**
West Wall pressure 13 [psid, positive up]

334 **W14 (MN 334)**
West Wall pressure 14 [psid, positive up]

335 **W15 (MN 335)**
West Wall pressure 15 [psid, positive up]

336 **W16 (MN 336)**
West Wall pressure 16 [psid, positive up]

337 **W17 (MN 337)**
West Wall pressure 17 [psid, positive up]

338 **W18 (MN 338)**
West Wall pressure 18 [psid, positive up]

339 **W19 (MN 339)**
West Wall pressure 19 [psid, positive up]

340 **W20 (MN 340)**
West Wall pressure 20 [psid, positive up]

341 **W21 (MN 341)**
West Wall pressure 21 [psid, positive up]

342 **E1 (MN 342)**
East Wall pressure 1 [psid, positive up]

343 **E2 (MN 343)**
East Wall pressure 2[psid, positive up]

344 **E3 (MN 344)**
East Wall pressure 3 [psid, positive up]

345 **E4 (MN 345)**
East Wall pressure 4 [psid, positive up]

346 **E5 (MN 346)**
East Wall pressure 5 [psid, positive up]

347 **E6 (MN 347)**
East Wall pressure 6 [psid, positive up]

348 **E7 (MN 348)**
East Wall pressure 7 [psid, positive up]

349 **E8 (MN 349)**
East Wall pressure 8 [psid, positive up]

350 **E9 (MN 350)**
East Wall pressure 9 [psid, positive up]

351 **E10 (MN 351)**
East Wall pressure 10 [psid, positive up]

352 **E11 (MN 352)**

East Wall pressure 11 [psid, positive up]

353 **E12 (MN 353)**
East Wall pressure 12 [psid, positive up]

354 **E13 (MN 354)**
East Wall pressure 13 [psid, positive up]

355 **E14 (MN 355)**
East Wall pressure 14 [psid, positive up]

356 **E15 (MN 356)**
East Wall pressure 15 [psid, positive up]

357 **E16 (MN 357)**
East Wall pressure 16 [psid, positive up]

358 **E17 (MN 358)**
East Wall pressure 17 [psid, positive up]

359 **E18 (MN 359)**
East Wall pressure 18 [psid, positive up]

360 **E19 (MN 360)**
East Wall pressure 19 [psid, positive up]

361 **E20 (MN 361)**
East Wall pressure 20 [psid, positive up]

362 **E21 (MN 362)**
Ceiling pressure 21 [psid, positive up]

363 **C1 (MN 363)**
Ceiling pressure 1 [psid, positive up]

364 **C2 (MN 364)**
Ceiling pressure 2[psid, positive up]

365 **C3 (MN 365)**
Ceiling pressure 3 [psid, positive up]

366 **C4 (MN 366)**
Ceiling pressure 4 [psid, positive up]

367 **C5 (MN 367)**
Ceiling pressure 5 [psid, positive up]

368 **C6 (MN 368)**
Ceiling pressure 6 [psid, positive up]

369 **C7 (MN 369)**
Ceiling pressure 7 [psid, positive up]

370 **C8 (MN 370)**
Ceiling pressure 8 [psid, positive up]

371 **C9 (MN 371)**
Ceiling pressure 9 [psid, positive up]

372 **C10 (MN 372)**

Ceiling pressure 10 [psid, positive up]

373 **C11 (MN 373)**
Ceiling pressure 11 [psid, positive up]

374 **C12 (MN 374)**
Ceiling pressure 12 [psid, positive up]

375 **C13 (MN 375)**
Ceiling pressure 13 [psid, positive up]

376 **C14 (MN 376)**
Ceiling pressure 14 [psid, positive up]

377 **C15 (MN 377)**
Ceiling pressure 15 [psid, positive up]

378 **C16 (MN 378)**
Ceiling pressure 16 [psid, positive up]

379 **C17 (MN 379)**
Ceiling pressure 17 [psid, positive up]

380 **C18 (MN 380)**
Ceiling pressure 18 [psid, positive up]

381 **C19 (MN 381)**
Ceiling pressure 19 [psid, positive up]

382 **C20 (MN 382)**
Ceiling pressure 20 [psid, positive up]

383 **C21 (MN 383)**
Ceiling pressure 21 [psid, positive up]

NREL-Supplied Measurements

None of the NREL data will be acquired by NIDS.

F. Data Reduction for Wind Tunnel Parameters

Standard Tunnel Parameters

401A **QU**
Uncorrected dynamic pressure at total and static rings, [psf]

```
= PT_BAR - PSREF_BAR
  [311]    [310]
```

401B **DQSP**
Static plate correction, [psf]

```
= f (QU, CSP) curve fit
  [401A] [210]
```

401C **QCLU**
Corrected dynamic pressure at tunnel centerline, [psf]

```
= QU - DQSP
[401A] [401B]
```

402 **PA**
Atmospheric pressure at tunnel centerline, [psfa]

```
= BARO_ANA * 144 - (0.07285 * DH)
  [305B]                   [209]
```

403 **PT**

Total pressure at tunnel centerline, [psfa]

```
=  PA  +  PT_BAR
  [402]   [311]
```

404A **PS**
Static pressure at tunnel centerline, [psfa]

```
=  PT  -  QCLU
  [403]  [401C]
```

404B **MTUN**
Tunnel Mach number (Note: This equation is exact for air and accounts for compressibility)

```
= SQRT(5*((PT / PS)**(2/7)-1))
         [403] [404A]
```

404C **Q**
Corrected tunnel dynamic pressure, [psf] number (Note: This equation is exact for air and accounts for compressibility)

```
= 0.7 * PS * MTUN**2
      [404A] [404B]
```

405A **TTR**
Tunnel total temperature, [°R]

```
= TTF + 459.67
  [308]
```

405B **TSR**
Tunnel static temperature, [°R]

```
TTR / (1.0 + (0.20) * MTUN**2)
```

```
 [405A]                    [404B]
```

405C **TSF**

Tunnel static temperature, [°F]

```
= TSR – 459.67
  [405B]
```

405D **VPDP**

Test section dew point vapor pressure, [psf]

```
=(2.0901 + 3.46E-6 * PA) *
                        [402]
6.1121*e [(17.502 * DPT - 560.064) /(401.62 + DPT)]
              [307]              [307]
```

405E **VPDB**

Test section dry bulb vapor pressure, [psf]

```
=(2.0901 + 3.46E-6 * PA) *
                        [402]
6.1121*e [(17.502 * TSF - 560.064) /(401.62 + TSF)]
              [405C]              [405C]
```

406 **RHO**

Air density, [slug/ft^3]

```
= 0.000582560 * (PS – (0.38 * VPDP)) / TSR
                [404A]       [405D]  [405B]
```

407 **VFPS**

Tunnel speed, [ft/s]

```
= SQRT (2.0 * Q / RHO)
           [401] [406]
```

408 **VKTS**

Tunnel speed, [knt]

```
= VFPS * 0.5925
  [407]
```

409A **REYN**

Reynolds number, millions per foot

```
= (RHO * VFPS / VISC) / 1.0E+06
  [406] [407]  [409C]
```

409B **RH**

Test section relative humidity, [%]

```
= VPDP / VPDB * 100
 [405D] [405E]
```

409C **VISC**

Tunnel air viscosity, [slug/ft-sec]

```
= 2.27E-8 * (TSR**1.5/(TSR + 198.6))
           [405B]    [405B]
```

410 **CSND**

Tunnel speed of sound, [ft/s]

```
49.0223 * SQRT(TSR)
             [405B]
```

421 **QU_DIG**

Uncorrected dynamic pressure at total and static rings, [psf]

```
= PT_BAR_DIG - PSREF_BAR_DIG
  [311A]          [310A]
```

422 **DQSP_DIG**

Static plate correction, [psf]

```
= f (QU_DIG, CSP) curve fit
    [421] [210]
```

423 **QCLU_DIG**

Corrected dynamic pressure at tunnel centerline, [psf]

```
= QU_DIG - DQSP_DIG
   [421]   [422]
```

425 **PA_DIG**

Atmospheric pressure at tunnel centerline, [psfa]

```
= BARO_DIG * 144 - (0.07285 * DH)
  [305A]                    [209]
```

430 **PT_DIG**

Total pressure at tunnel centerline, [psfa]

```
=  PA_DIG  +  PT_BAR_DIG
   [425]       [311A]
```

435 **PS_DIG**

Static pressure at tunnel centerline, [psfa]

```
=  PT_DIG  -  QCLU_DIG
    [430]     [423]
```

436 **MTUN_DIG**

Tunnel Mach number (Note: This equation is exact for air and accounts for compressibility)

```
= SQRT(5*((PT_DIG / PS_DIG)**(2/7)-1))
           [430]    [435]
```

440 **Q_DIG**

Corrected tunnel dynamic pressure, [psf] number (Note: This equation is exact for air and accounts for compressibility)

```
= 0.7 * PS_DIG * MTUN_DIG**2
        [435]    [436]
```

441 **TTR_DIG**

Tunnel total temperature, [°R]

```
= TTF_DIG + 459.67
   [308A]
```

442 **TSR_DIG**

Tunnel static temperature, [°R]

```
TTR_DIG / (1.0 + (0.20) * MTUN_DIG**2)
```

[441] [436]

443 TSF_DIG

Tunnel static temperature, [°F]

= TSR_DIG – 459.67

[442]

444 VPDP_DIG

Test section dew point vapor pressure, [psf]

=(2.0901 + 3.46E-6 * PA_DIG) *

[425]

6.1121*e [(17.502 * DPT - 560.064) /(401.62 + DPT)]

[307] [307]

445 RHO_DIG

Air density, [slug/ft^3]

= 0.000582560 * (PS_DIG – (0.38 * VPDP_DIG)) / TSR_DIG

[435] [444] [442]

450 VFPS_DIG

Tunnel speed, [ft/s]

= SQRT (2.0 * Q_DIG / RHO_DIG)

[440] [445]

G. Tares for Wind Tunnel Scales

The sequences of acquiring tare sets and their applications are outlined in the following order.
Acquire scale loads as weight tare with blades and nacelle installed and locked in the zero yaw position.
Rotate turntable over full range and record scale data.
Return turntable to zero position and rotate nacelle over full range and record data

1. Curve-fit weight tare as function of turntable angle obtained in (1) and a function of turn table and nacelle angle obtained in (2).
2. Acquire scale loads with blades off with turntable angle sweep and with nacelle locked in the zero yaw position at each tunnel dynamic pressure.
3. Calculate aero tare at each specified value of dynamic pressure (point by point subtraction):
4. Aero tares w/o blade = Aero load w/o blade in (5) – weight tare blade in (1)
5. Repeat (5) and (6) to obtain aero tares at different tunnel dynamic pressures.
6. Curve-fit aero tare obtained in (5)

$$\texttt{aerotare} = C_o + C_1\alpha_c + C_2\alpha_c^2 + C_3\alpha_c^3 + C_4 q_c + C_5 q_c^2 + C_6\Psi + C_7\Psi^2$$

Weight Tares

Weight tares measure the change in moments due to a change in angle of yaw. Weight tare data are acquired with no wind. The model is moved through a series of yaw angles that cover the test envelope.

Two sets of tunnel scale weight tares will be recorded: 1) blades off, and 2) blades on. Both tare sets are acquired when the wind turbine is not rotating. The coefficients (S1 to S4) depend on the weight tare set as specified in TARE,W_S (item 110). Section 6.1.20 of ref. [1] shows two sets of weight-tare equations for curve fitting. The coupled weight-tare equations will be used here.

501 **S1,S2,S3,S4**
Curve fit coefficients for pitch and roll weight tares. The coefficients depend on the weight tare set number to be used, as specified by variable TARE,W_S, item [110].
(computed)

502 **PITCH_WT**
Tunnel weight tare for pitching moment (6.1.20), [ft-lb]
= S1*(1-COS(ALPH)*COS(PSI)) - S2*SIN(ALPH)*COS(PSI) + S3*SIN(PSI) + S4*(1-COS(PSI))

503 **ROLL_WT**
Tunnel weight tare for rolling moment (6.1.20), [ft-lb]
= S1*COS(ALPH)*SIN(PSI) + S2*SIN(ALPH)*SIN(PSI) + S3*(COS(PSI)-1) + S4*SIN(PSI)

```
S1 to S4  Item 215
ALPH      Item 102
PSI       Item 101            (PSI == PSI_FAC)
```

Aerodynamic Tares

Aerodynamic tares measure the effect of dynamic pressure on the model supports and on that part of the model not of interest to the researcher. Aerodynamic tare data are acquired with wind on. The model is

moved through a series of yaw angles that cover the test envelope. For each yaw angle, dynamic pressure is varied over the full range anticipated. See section 6.1.23 of ref. [1]. The aero tare set numbers are stored in TARE,A_S (item 111).

504 **LIFT_AT**
Tunnel aerodynamic tare for lift force, [lb]

505 **DRAG_AT**
Tunnel aerodynamic tare for drag force, [lb]

506 **SIDE_AT**
Tunnel aerodynamic tare for side force, [lb]

507 **PITCH_AT**
Tunnel aerodynamic tare for pitching moment, [ft-lb]

508 **ROLL_AT**
Tunnel aerodynamic tare for rolling moment , [ft-lb]

509 **YAW_AT**
Tunnel aerodynamic tare for yawing moment, [ft-lb]

H. Wind Tunnel Scale Loads

Tunnel Scale Moment Arms

Moment arm length and direction are depicted in figure 24 of ref. [1].

601 **K0**
Tunnel scale moment arm, [ft]
```
= XS_DIST*COS(ALPH) + YV_DIST*SIN(ALPH)
```

602 **K1**
Tunnel scale moment arm, [ft]
```
= 18.382 - PSI_PIVOT_DIST*COS(PSI+PBPSI) + K0*COS(PSI)
+ J_DIST*SIN(PSI)
```

603 **K3**
Tunnel scale moment arm, [ft]
```
= -HV_DIST - YV_DIST*COS(ALPH) + XS_DIST*SIN(ALPH)
```

604 **K6**
Tunnel scale moment arm, [ft]
```
= -PSI_PIVOT_DIST*SIN(PSI+PBPSI) + K0*SIN(PSI) -
J_DIST*COS(PSI)
```

```
HV_DIST         Item 201
J_DIST          Item 202
K_DIST          Item 203
XS_DIST         Item 204
YV_DIST         Item 205
Z_DIST          Item 206
PSI_PIVOT_DIST  Item 207
DH              Item 209
PBPSI           Item 217
ALPH            Item 102
PSI             Item 101
```

Uncorrected Scale Loads (Wind Axes)

The uncorrected scale loads in wind axis are same as those in 6.5.1 of ref. [1].

605 **LIFT,U_S**
Scale lift force, (positive up) [lb]
```
= LFL + RFL + LRL + RRL
 [312] [313] [314] [315]
```

606 **DRAG,U_S**
Scale drag force, (positive downstream) [lb]
```
= DRAG
[318]
```

607 **SIDE,U_S**
Scale side force, (positive starboard) [lb]
```
= FSF + RSF
 [316] [317]
```

608 **PTCH,U_S**

Scale pitching moment, (positive nose up) [ft-lb]

```
= K1*LIFT,U_S - 36.764*(LRL+RRL) + K3*DRAG,U_S
  [602][605]          [314][315]  [603][606]
```

609 **ROLL,U_S**

Scale rolling moment, (positive right-side down) [ft-lb]

```
= 18.382*(LFL-RFL+LRL-RRL) - K6*LIFT,U_S + K3*SIDE,U_S
  [602][312 to 315]      [604][605]   [603][607]
```

610 **YAW,U_S**

Uncorrected scale yawing moment, (positive right-side downstream) [ft-lb]

```
= K1*SIDE,U_S + 7.618*FSF - 44.382*RSF +  K6*DRAG,U_S
 [602][607]          [316]        [317]   [604][606]
```

Weight and Aero Tare Corrected Scale Loads (Tunnel or Wind Axis)

Note: Weight Tare correction for pitch and roll Moments only. Lift, drag, and side force, and yaw moment are not effected by model psi changes.

611 **LIFT,W_S**

Scale lift force Aero tare corrected, (positive up)[lb]

```
= LIFT,U_S - LIFT_AT
  [605]        [503]
```

612 **DRAG,W_S**

Scale drag force Aero tare corrected, (positive downstream) [lb]

```
= DRAG,U_S - DRAG_AT
   [606]       [504]
```

613 **SIDE,W_S**

Scale side force, Aero tare corrected (positive starboard) [lb]

```
= SIDE,U_S - SIDE_AT
   [607]       [505]
```

614 **PTCH,W_S**

Scale pitching moment, weight and Aero tare corrected (positive nose up) [ft-lb]

```
= PTCH,U_S - PITCH_WT - PITCH_AT
    [608]    [501]       [506]
```

615 **ROLL,W_S**

Scale rolling moment, Weight and Aero tare corrected (positive right-side down) [ft-lb]

```
= ROLL,U_S - ROLL_WT - ROLL_AT
[609]          [502]          [507]
```

616 **YAW,W_S**

Scale Yawing moment Aero tare corrected, (positive right-side downstream) [ft-lb]

```
= YAW,U_S - YAW_AT
    [610]      [508]
```

Normalization Constants

None; wind turbine rpm not available to NIDS. Force and Moment coefficients not computed.

I. Data Presentation

Real-Time Display

The Real-Time Display (RTD) formats are shown in figure 1.

Format 1 will be displayed on two large monitors above the control console.

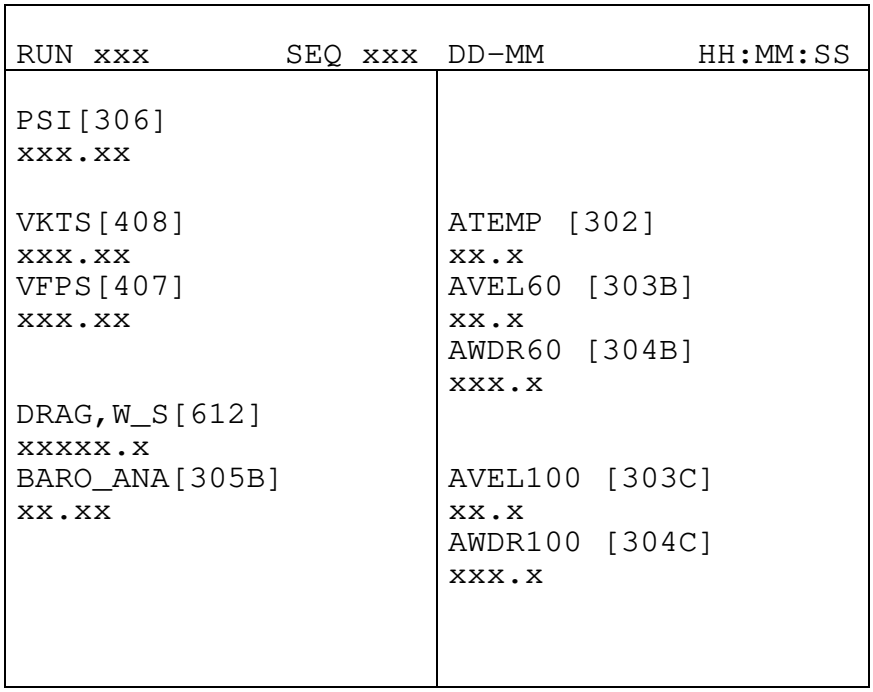

Format 1

Figure 1. Real-Time Display Formats

Data File Configuration

In addition to a hard copy printout an ASCI file of tab limited data will be provided to NREL to be merged with their electronic database.

J. References

1. National Full-Scale Aerodynamics Complex, "Guidelines for Preparation of Software Requirements," AOI-SG-DOC-06, October 1994.

2. Shinoda, P., "Wall Interaction Effects for a Full-Scale Helicopter Rotor in the NASA Ames 80- by 120- foot Wind Tunnel," Paper No. 20, 73rd AGARD Fluid Dynamics Panel Meeting and Symposium on Wall Interference, Support Interference, and Flow Field Measurements, Brussels, Belgium, October 1993.

3. Zell, P., "Dynamic Pressure, Velocity and Reference Pressures - 80- by 120- foot Wind Tunnel," NFAC memo, November 1994.

Appendix E: NASA Instrumentation and File Format

Wall Pressure Channels (*.WP)

Ports along the walls and ceiling of the wind tunnel are instrumented to measure differential pressures between the wall surface and the gill port atmospheric pressure, to which all other pressure measurements are referenced. The mean, standard deviation, maximum, and minimum for each pressure port for each data point are contained in tab-delimited ASCII files using 'WP' for an extension. The first column contains the Julian day and time when the data sample was collected. The second column contains the NASA run and sequence number. The third column contains the duration of the data point in seconds. The fourth column contains the test name using the NREL file name conventions. The next columns represent each of the wall and ceiling pressure ports. Taps on the west wall are labeled W1-W21; the east wall taps are E1-E21; and the ceiling taps are C1-C21. The data format is such that for each day/time entry corresponding to one NREL time series file, four rows of data exist for each measurement. The first row contains mean values followed by standard deviation, maximum, and minimum values over the specified duration. These data files were named such that the first character corresponds to the NREL test sequence. The next three numbers correspond to the NASA run number. Thus, each NREL test sequence may be contained within several NASA data files due to the change in NASA run number. However, all *.WP files beginning with 'B' contain all data points collected during NREL test sequence B. Note that the units for all wall pressure measurements are psid, not Pascals. Specifications for the pressure transducers and the pressure tap locations are included in the Wall Pressure instrumentation sheet that follows.

Additional NASA Channels (*.DAT)

In addition to the wall pressure measurements, NASA provided tab-delimited ASCII files with a *.DAT extension. The naming convention is identical to that for the wall pressure files. The first character represents the NREL test sequence, and the following digits represent the NASA run number. These files contain all additional NASA measurements as well as computed parameters as shown in Table E-1. The analog measurements that were integrated in the NREL data system were included for corroboration with the NREL measurements and are noted in Table A. The digital pressure measurements that could not be integrated in the NREL data system are also included. Again, the first column contains the Julian day and time when the data sample was collected. The second column contains the NASA run and sequence number. The third column contains the duration of the data point in seconds. The fourth column contains the test name using the NREL file name conventions. The next columns are in order of the channels listed in Table E-1. The first row contains the column headings; the second row contains the NASA channel number as specified in Appendix D, Software Requirements Document. The equations for the computed channels can be found in Appendix D using the NASA channel number. The third row contains the units. Note that all NASA measurements use the U.S. Customary System (USCS) of units rather than the International System of Units (SI) that was used by NREL. The data format is such that for each day/time entry corresponding to one NREL time series file, four rows of data exist for each measurement. The first row contains mean values followed by standard deviation, maximum, and minimum values over the specified duration.

Table E-1. NASA Channels Other Than Wall Pressures

NREL Channel Description	NASA Channel Number from Appendix D	Units	Time Series in NREL data stream	Description
OMWS18M	303B	mph	x	Outside met wind speed 18.29 m (60')
OMWS32M	303C	mph	x	Outside met wind speed 32.81 m (100')
OMWD18M	304B	deg	x	Outside met wind direction 18.29 (60')
OMWD32M	304C	deg	x	Outside met wind direction 32.81 m (100')
OMT4M	302	degF	x	Outside met air temperature 4.57 m (15')
WTBARO	305B	psia	x	Wind tunnel barometric pressure (analog transducer)
BARO_DIG	305A	psia		Wind tunnel barometric pressure (digital transducer)
WTSTAT	310	psfg	x	Wind tunnel static pressure (analog transducer)
PSREF_DIG	310A	psfg		Wind tunnel static pressure (digital transducer)
WTTOTAL	311	psfg	x	Wind tunnel total pressure (analog transducer)
PT_DIG	311A	psfg		Wind tunnel total pressure (digital transducer)
WTDPT	307	degF	x	Wind tunnel dew point temperature
WTATEMP	308	degF	x	Wind tunnel air temperature (analog transducer)
TTF_DIG	308A	degF		Wind tunnel air temperature (digital transducer)
WTLFLIFT	312	lb	x	Wind tunnel left front lift (#1)
WTRFLIFT	313	lb	x	Wind tunnel right front lift (#2)
WTLRLIFT	314	lb	x	Wind tunnel left rear lift (#3)
WTRRLIFT	315	lb	x	Wind tunnel right rear lift (#4)
WTFSFORC	316	lb	x	Wind tunnel front side force (#5)
WTRSFORC	317	lb	x	Wind tunnel rear side force (#6)
WTDRAG	318	lb	x	Wind tunnel drag (#7)
YAWTABLE	306	deg	x	Turntable angle
VTun	407	ft/s	x	Tunnel velocity (computed with analog transducer signals)
VFPS_DIG	450	ft/s		Tunnel velocity (computed with digital transducer signals)
QTun	404C	psf	x	Tunnel dynamic pressure (computed with analog transducer signals)
Q_DIG	440	psf		Tunnel dynamic pressure (computed with digital transducer signals)
RhoTun	406	slug/ft^3	x	Tunnel air density (computed with analog transducer signals)
RHO_DIG	445	slug/ft^3		Tunnel air density (computed with digital transducer signals)
PtTun	403	psfa	x	Tunnel total pressure (computed with analog transducer signals)
PT_DIG	430	psfa		Tunnel total pressure (computed with digital transducer signals)
PsTun	404A	psfa	x	Tunnel static pressure (computed with analog transducer signals)
PS_DIG	435	psfa		Tunnel static pressure (computed with digital transducer signals)
QU	401A	psf		Intermediate parameter for computation of dynamic pressure
DQSP	401B	psf		Intermediate parameter for computation of dynamic pressure
QCLU	401C	psf		Intermediate parameter for computation of dynamic pressure
PA	402	psfa	x	Tunnel centerline pressure (computed with analog transducer signals)
PA_DIG	425	psfa		Tunnel centerline pressure (computed with digital transducer signals)
MTUN	404B			Tunnel Mach number
TTR	405A	degR		Tunnel total temperature
TSR	405B	degR		Tunnel static temperature
TSF	405C	degF*		Tunnel static temperature (°F)
VPDP	405D	psf		Test section dew point vapor pressure
VPDB	405E	psf		Test section dry bulb vapor pressure
VKTS	408	knt		Tunnel speed, knots
REYN	409A	million/ft		Reynolds number
RH	409B	%		Test section relative humidity

Table E-1. NASA Channels Other Than Wall Pressures (continued)

NREL Channel Description	NASA Channel Number from Appendix D	Units	Time Series in NREL data stream	Description
VISC	409C	slug/ft-sec		Tunnel air viscosity
CSND	410	ft/s		Tunnel speed of sound
LIFT,W_S	611	lb	x	Scale lift force, no weight or aero tare applied
DRAG,W_S	612	lb	x	Scale drag force, no weight or aero tare applied
SIDE,W_S	613	lb	x	Scale side force, no weight or aero tare applied
PTCH,W_S	614	lb	x	Scale pitching moment, no weight or aero tare applied
ROLL,W_S	615	lb	x	Scale rolling moment, no weight or aero tare applied
YAW,W_S	616	lb	x	Scale yawing moment, no weight or aero tare applied
DPRS_DIG		psf		Wind tunnel dynamic pressure (digital transducer)

* The units in the NASA data files incorrectly state degR instead of degF.

Some changes were made after the Software Requirements Document was completed. For instance, the static plate correction (401B) was deemed unnecessary based on tunnel flow quality measurements obtained by NASA prior to testing NREL's wind turbine (Zell 2000). The computed force and moment channels from the *T*-frame scales listed in the ASCII files correspond to NASA channels 611-616. Weight and aero tares were not computed and subtracted from the measured channels during post-processing as was originally planned. The channels in the ASCII files are better represented by NASA channels 605-610. Lastly, an additional digital pressure transducer measurement corresponding to the wind tunnel dynamic pressure was added in the last column (DPRES_DIG). This pressure measurement was used to establish the desired wind tunnel speed during testing.

Data Collection Procedures

The NREL and NASA data systems were not time synchronized. The NREL turbine operator positioned the turbine; the NREL data acquisition person entered the file name for the specified condition; the NASA data acquisition person entered the wind turbine yaw angle and the NREL file name for the specified condition. On the count of three, both operators would begin data acquisition. Since the NASA system was only supplying statistical values instead of time series, the lack of time synchronization was not perceived as an issue. During the non-standard duration tests, those shorter or longer than 30 seconds, the NASA system was set to collect data for similar duration. For the longer tests (on the order of minutes), the NASA system would collect 30-second samples repeatedly until the NREL system finished. The duration for each NASA point is included in each file.

Instrumentation

The NASA data acquisition computer, NIDS, used Labview software to sample digital signals. The analog signals were wired directly to a 16-bit A/D card in the chassis of this computer, which converted the analog signals to digital signals. The outside wind speeds and directions at two levels as well as the outside air temperature were obtained on a meteorological tower near the inlet. These signals were sent as digital signals via a short-haul modem to another computer in the control room. The digital signals were sent to a local display panel and converted back to analog signals before transmission to the A/D card in the NIDS computer. The analog pressure measurements were wired directly to the A/D card in the NIDS computer. The analog scales signals were filtered with 1-Hz Bessel filters, then wired to the A/D card in the NIDS computer. The wind tunnel temperature and dew point temperature were obtained as both analog and digital signals. The analog signals were wired directly to the NIDS computer for A/D conversion. The

digital signal was held at the server computer in the control room. The dew point digital signal was only available to the display in the control room. The digital pressure measurements, including the wall pressures, were maintained at the server computer. The NIDS computer sampled the digital signals from the server computer. Table E-2 lists instrumentation problems that occurred during the wind tunnel test along with the affected data.

Table E-2. NASA Instrumentation Problems

NREL channel descriptor	NASA channel descriptor	Test Sequences	NASA Run Number	Problem
N/A	E01-E16	B, C, D, 4, E, F, 3, 6, 7, G, H, I, J, P, 5 (Test 5 w/ 5-hole probes)	11, 12, 13, 14, 15, 16, 17, 18, 19, 20, 31, 32, 33, 34, 38, 39, 40, 41, 42, 43	Wall pressure transducer not connected
N/A	BARO_DIG (305A), PSREF_DIG (310A), PT_DIG (311A), DPRS_DIG	B, C, D (except wind speeds 5, 11, 12, 13 m/s)	11, 12, 13	Digital pressure transducers not zeroed
WTLFLIFT	WTLFLIFT (312)	B, C, D, 4, E, F, 3	11, 12, 13, 14, 15, 16, 17, 18	Left front lift filter set improperly resulting in noisy signal
WTLFLIFT	WTLFLIFT (312)	B, C, D, 4, E, F, 3, 6, 7	11, 12, 13, 14, 15, 16, 17, 18, 19, 20	Possible ground loop causing noisy signal for left front lift
WTDRAG	WTDRAG (318)	B, C, D, 4, E, F, 3, 6, 7, G (except G wind speeds 15, 16, 17, 18 m/s)	11, 12, 13, 14, 15, 16, 17, 18, 19, 20, 31, 32, 33, 34	Drag scale discrepancy due to NIDS software bug
WTLFLIFT, WTRFLIFT, WTLRLIFT, WTRRLIFT, WTFSFORC, WTRSFORC, WTDRAG	WTLFLIFT (312), WTRFLIFT (313), WTLRLIFT (314), WTRRLIFT (315), WTFSFORC (316), WTRSFORC (317), WTDRAG (318)	B, C, D, 4, E, F, 3, 6, 7, G, H, I, J, P, 5 (Test 5 with 5-hole probes), O, L	11, 12, 13, 14, 15, 16, 17, 18, 19, 20, 31, 32, 33, 34, 38, 39, 40, 41, 42, 43, 44, 45, 46, 47, 48	Scale snubber contact potentially fouling scale measurements

The following sheets describe the measurement path, calibration procedures, and instrumentation specifications for each NASA channel. The format is similar to that used for the NREL channels in Appendix B.

NASA Locator	NREL ID Code	Description
E1-E21	N/A	East wall taps
W1-W21	N/A	West wall taps
C1-C21	N/A	Ceiling taps
Location		Control room
Measurement type and units		Pressure, psid
Range		± 10" H_2O
Resolution		0.032" H_2O / bit
Accuracy		0.03% FS
Sensor Description		Pressure Systems Inc., ESP-32BP

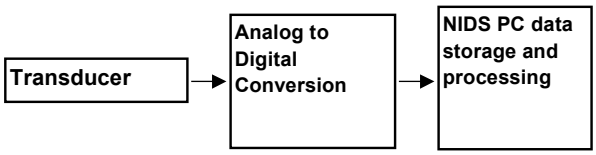

Calibration procedures

1. A pressure ramp of 5 pressures is applied to the transducers. A linear regression provides slope and offset values that are entered in the NIDS data system.

Calibration frequency

The transducers were calibrated daily.

The pressure ports extend longitudinally through the test section, and the location of the wall pressure ports is shown in Table E-3. Positive distances are towards the inlet (upwind) and negative distances are toward the fans (downwind). The zero reference is the center of the turntable to which the wind turbine tower was mounted. The wall pressure taps are at a height of 12.2 m (40'), which is the tunnel centerline. The ceiling pressure taps are aligned with the tunnel centerline as well.

Table E-3. Wall and Ceiling Pressure Port Locations

Module 1				Module 2			
Port Number	Description	Location (ft)	Location (m)	Port Number	Description	Location (ft)	Location (m)
1	West 01	125.7	38.3	1	East 01	119.7	36.5
2	West 02	101.7	31.0	2	East 02	101.7	31.0
3	West 03	75.7	23.1	3	East 03	78.0	23.8
4	West 04	59.7	18.2	4	East 04	61.8	18.8
5	West 05	43.7	13.3	5	East 05	42.5	13.0
6	West 06	35.7	10.9	6	East 06	34.5	10.5
7	West 07	27.7	8.4	7	East 07	26.5	8.1
8	West 08	19.7	6.0	8	East 08	18.5	5.6
9	West 09	11.7	3.6	9	East 09	10.5	3.2
10	West 10	3.7	1.1	10	East 10	3.5	1.1
11	West 11	-4.3	-1.3	11	East 11	-3.5	-1.1
12	West 12	-12.3	-3.7	12	East 12	-10.5	-3.2
13	West 13	-20.3	-6.2	13	East 13	-18.5	-5.6
14	West 14	-28.3	-8.6	14	East 14	-26.5	-8.1
15	West 15	-36.3	-11.1	15	East 15	-34.5	-10.5
16	West 16	-44.3	-13.5	16	East 16	-42.5	-13.0
Module 3				Module 4			
Port Number	Description	Location (ft)	Location (m)	Port Number	Description	Location (ft)	Location (m)
1	Ceiling 01	120.0	36.6	1	West 17	-52.3	-15.9
2	Ceiling 02	100.0	30.5	2	West 18	-68.3	-20.8
3	Ceiling 03	68.7	20.9	3	West 19	-84.3	-25.7
4	Ceiling 04	48.7	14.8	4	West 20	-113.3	-34.5
5	Ceiling 05	38.7	11.8	5	West 21	-144.3	-44.0
6	Ceiling 06	28.7	8.7	6	East 17	-50.5	-15.4
7	Ceiling 07	18.7	5.7	7	East 18	-57.6	-17.6
8	Ceiling 08	8.7	2.7	8	East 19	-73.9	-22.5
9	Ceiling 09	-1.3	-0.4	9	East 20	-108.9	-33.2
10	Ceiling 10	-8.8	-2.7	10	East 21	-139.2	-42.4
11	Ceiling 11	-13.8	-4.2	11	Ceiling 17	-51.3	-15.6
12	Ceiling 12	-18.8	-5.7	12	Ceiling 18	-71.3	-21.7
13	Ceiling 13	-23.8	-7.3	13	Ceiling 19	-100.0	-30.5
14	Ceiling 14	-28.8	-8.8	14	Ceiling 20	-120.0	-36.6
15	Ceiling 15	-33.8	-10.3	15	Ceiling 21	-144.0	-43.9
16	Ceiling 16	-41.3	-12.6	16			

NASA Locator	NREL ID Code	Description
303B	OMWS18M	Outside met wind speed 18.29 m (60')
303C	OMWS32M	Outside met wind speed 32.81 m (100')
304B	OMWD18M	Outside met wind direction 18.29 m (60')
304C	OMWD32M	Outside met wind direction 32.81 m (100')

Location	Meteorological tower 700' from tunnel inlet
Measurement type and units	Wind speed, mph; wind direction, degrees
Range	0-125 kt, 0-360º (0.1 mph, 0.1 degrees)
Resolution	10 mph/V; 36º/V
Accuracy	0.1 mph; 0.1º
Sensor Description	Handar sonic anemometer 14-25A

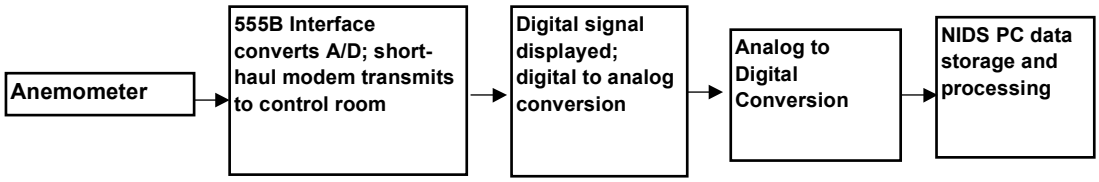

Note: Wind direction is positive clockwise from magnetic north.

Calibration procedures

1. NASA personnel arranged a calibration with the appropriate manufacturer.
2. Enter the slope and the offset in the NIDS data system.

Calibration frequency

The anemometers were calibrated February 1999 prior to installation on the tower.

NASA Wind Tunnel Pressures (Analog)

NASA Locator	NREL ID Code	Description
305B	WTBARO	Wind tunnel barometric pressure
310	WTSTAT	Wind tunnel static pressure
311	WTTOTAL	Wind tunnel total pressure

Location	Control room
Measurement type and units	Pressure, psia (WTBARO); psfg (WTSTAT, WTTOTAL)
Range	11-15 psi (WTBARO); 10" H_2O (WTSTAT); 10 mb (WTTOTAL)
Resolution	10 psi/V (WTBARO); 5.2 psf/V (WTSTAT); 2.09 psf/V (WTTOTAL)
Accuracy	0.05% FS
Sensor description	Edwards 590DF (WTSTAT, WTTOTAL) Edwards 590A (WTBARO)

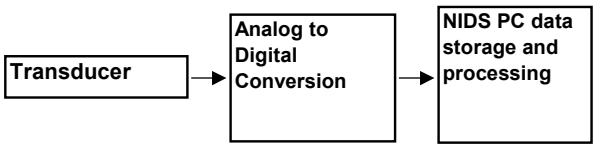

Calibration procedures

1. A calibration was performed according to manufacturer specification at the NASA calibration laboratory (WTBARO: MFR Sec4; WTTOTAL and WTSTAT: NA 17-20MX-157).
2. The zero is verified upon installation using the zero switch on the instrument.
3. Enter the slope and the offset in the NIDS data system.

Calibration frequency

The pressure transducers were calibrated in November 1999 with an expiration of November 2000.

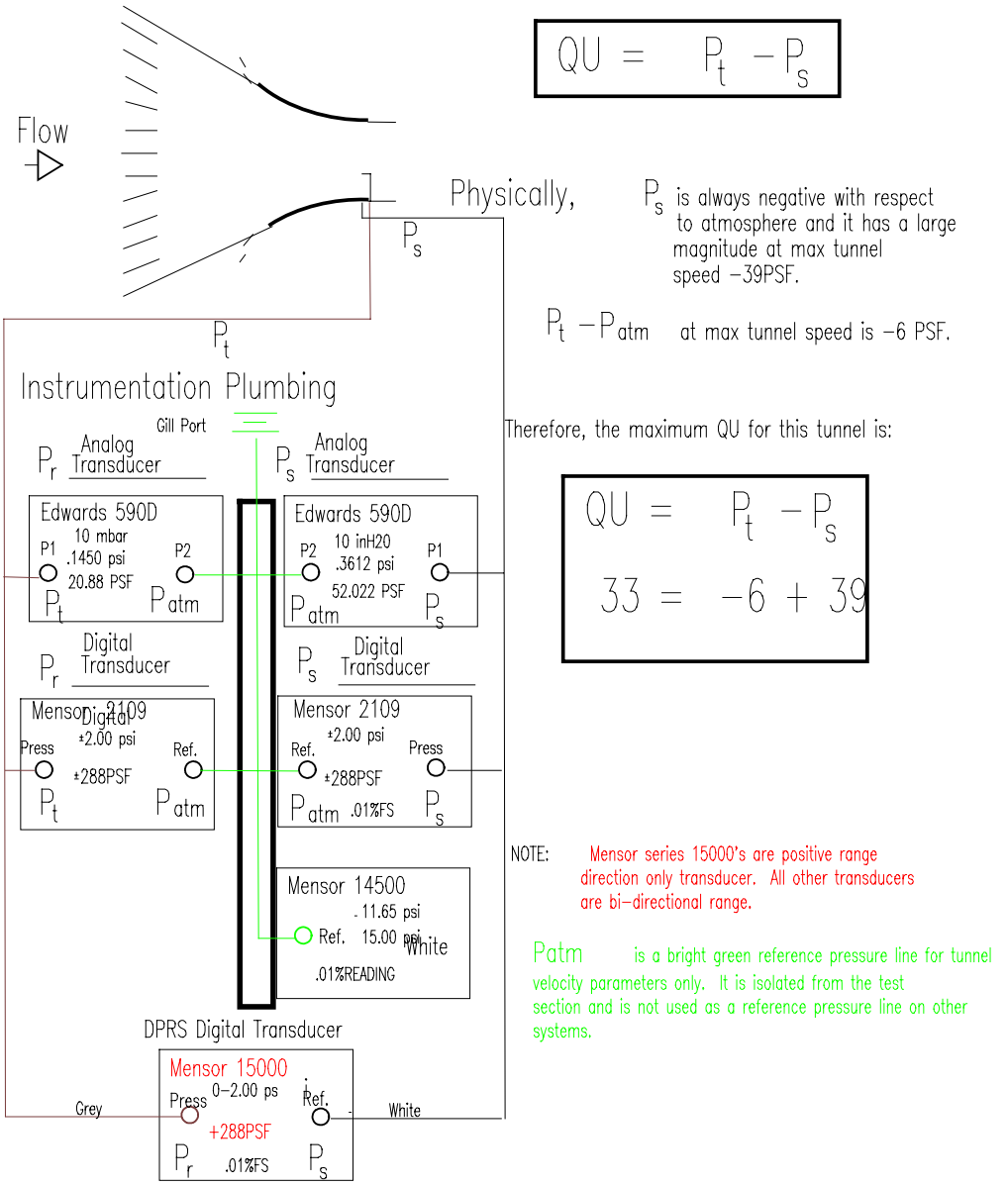

Joe Sacco/Art Silva

Figure E-1. NASA pressure system

NASA Wind Tunnel Pressures (Digital)

NASA Locator	NREL ID Code	Description
305A	BARO_DIG	Wind tunnel barometric pressure
310A	PSREF_DIG	Wind tunnel static pressure
311A	PT_DIG	Wind tunnel total pressure
	DPRS_DIG	Tunnel dynamic pressure

Location	Control room
Measurement type and units	Pressure, psia (BARO_DIG); psfg (PSREF_DIG, PT_DIG, DPRS_DIG)
Range	11-15 psi (BARO_DIG); ± 2 psi (PSREF_DIG, PT_DIG, DPRS_DIG)
Resolution	0.25 psi/bit
Accuracy	0.01 psi (BARO_DIG); 0.05% FS (PSREF_DIG, PT_DIG, DPRS_DIG)
Sensor description	Mensor 2109 (PSREF_DIG, PT_DIG, DPRS_DIG) Mensor 15500 (BARO_DIG)

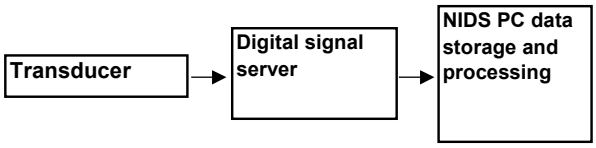

Calibration procedures

1. NASA personnel arranged a calibration with the appropriate manufacturer.
2. The zero is verified by disconnecting the device from the system and using the zero switch on the instrument.

Calibration frequency

The transducers were calibrated November 1999 with an expiration of November 2000. The zero was verified daily during testing.

See Figure E-1.

NASA Turntable Angle

NASA Locator	NREL ID Code	Description
306	YAWTABLE	Turntable angle
Location		Turntable
Measurement type and units		Angular position, degrees
Sensor description		Kearfott 2R982-004

Note: The slope and offset were input in *ang.hdr* to match the turntable angle reading at the wind tunnel controller's station. The turntable was used for Tests 6, 7, 8, and 9 only. The measurement convention is such that positive turntable angle results from clockwise rotation.

NASA Locator	NREL ID Code	Description
312	WTLFLIFT	Tunnel balance left front lift (#1)
313	WTRFLIFT	Tunnel balance right front lift (#2)
314	WTLRLIFT	Tunnel balance left rear lift (#3)
315	WTRRLIFT	Tunnel balance right rear lift (#4)
316	WTFSFORC	Tunnel balance front side force (#5)
317	WTRSFORC	Tunnel balance rear side force (#6)
318	WTDRAG	Tunnel balance drag force (#7)

Location	Lift tubes below *T*-frame
Measurement type and units	Force, lb
Range	-50,000 to 100,000 lb (#1-#4); -50,000 to 50,000 lb (#5-#7)
Resolution	11,804 lb/V (#1, #3); 11,807 lb/V (#2); 11,895 lb/V (#4); 11,960 lb/V (#5); 11,915 lb/V (#6); 12,203 lb/V (#7)
Accuracy	0.06% FS (#1-#4); 0.01% FS (#5-#7)
Sensor description	ACME custom designed system

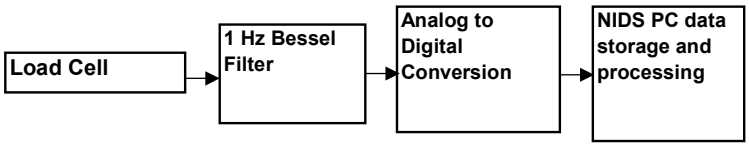

Calibration procedures

3. NASA personnel arranged a calibration with the manufacturer. Weights are applied to pans near the load cell. The slope is computed from a linear regression.
4. A data sample was collected while the turntable was clear to provide offset values for each load cell.
5. Enter the slope and the offset in the NIDS system.

Calibration frequency

The transducers were calibrated April 2000. A zero was determined daily during testing.

Channel	ID Code	Description
302	OMT4M	Outside met air temperature 4.57 m
308	WTATEMP	Wind tunnel air temperature
308A	TTF_DIG	Wind tunnel air temperature (digital)
307	WTDPT	Wind tunnel dew point temperature

Location	Meteorological tower 700' from inlet (OMT4M); Tunnel inlet, 100' from ground level (WTATEMP); Tunnel wall adjacent to turntable center, 10' from floor (WTDPT)
Measurement type and units	Ambient temperature, °F
Range	0-300ºF (OMT4M); 32-100ºF (WTATEMP); -40-80ºC within 45ºC to 65ºC depression at 25ºC (WTDPT)
Resolution	10ºF/V (OMT4M); 9.925ºF/V (WTATEMP); 6.28ºF/V (WTDPT)
Accuracy	0.1% FS (OMT4M); 0.1ºF (WTATEMP); 0.2ºC (WTDPT)
Sensor description	Handar 435A (OMT4M) Hart Scientific thermistor 5610 (WTATEMP) Protimeter RSO (WTDPT)

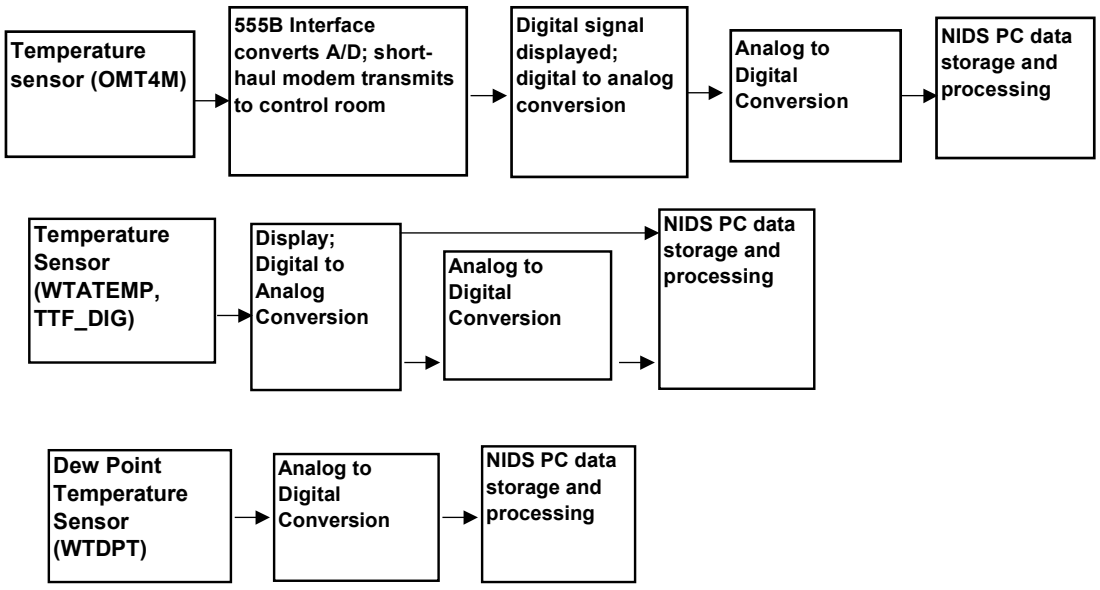

Calibration procedures

3. NASA personnel arranged a calibration with the respective manufacturers.
4. Enter the slope and the offset in the NIDS system.

Calibration frequency

The wind tunnel temperature transducer was calibrated July 1999 with an expiration date of July 2000. The dew point transducer was calibrated November 1999 with an expiration date of August 2000. The outside temperature transducer was calibrated in 1997 prior to installation.

Appendix F: Hydrostatic Pressure Correction

Abstract

The pressure transducers located within the blade translate in altitude as the rotor circulates 360°. The Mensor digital pressure transducer located in the PSC enclosure also translates in altitude. This change in altitude is evident in the measurements obtained for each pressure tap, each port of the five-hole probes, and the measurement obtained for the Mensor. This hydrostatic pressure change is removed from these measurements by adding a sinusoidal wave. The sinusoidal correction is obtained by measuring the hydrostatic change in the reference pressure tube at each blade-mounted pressure transducer. Then a sinusoid that forces the measurement to behave as the ideal hydrostatic correction is determined. The correction sinusoid for the Mensor is obtained by measuring the hydrostatic change it sees during rotation and fitting a sinusoid to the measurement.

Introduction

The pressure transducers are located within the instrumented blade (Blade 3) at five span locations. The reference pressure port of each transducer is connected to a common tube that extends into one of the instrumentation enclosures, the PSC enclosure, mounted on the hub. All three instrumentation enclosures are connected to each other with tubes to provide a large, stable volume of air to serve as the reference pressure for the pressure transducers. As the blade rotates, the hydrostatic pressure inside the reference pressure tube changes as a function of blade azimuth and rotor speed. If the tube were infinitely fast, the reference side of each transducer would appear as a sine wave with the highest amplitude of 11.97 Pa/m (air density of 1.22 kg/m^3 and gravity of 9.81 m/s^2) at 180°, and the lowest amplitude at 0°. This "ideal" sine wave represents the hydrostatic pressure variation caused by the altitude change each transducer experiences over a complete rotation of the instrumented blade. Because field testing was not performed at sea level, the "ideal" sine wave amplitude varied as 10 Pa/m.

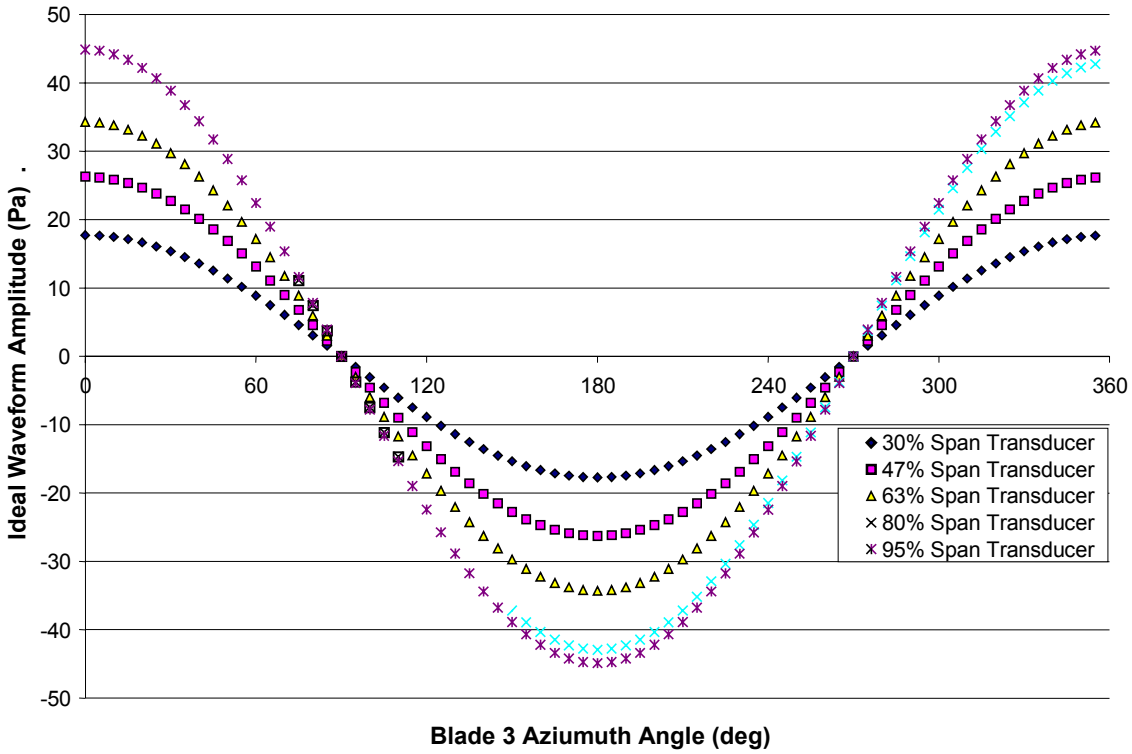

Figure F-1. Ideal representation of reference pressure line hydrostatic correction for pressure transducers within the instrumented blade

The UAE pressure system is not infinitely fast due to the size of the reference pressure tube and the various connections along its length. Thus, the hydrostatic change in the reference tube was measured to determine the correction. The pressure transducers were placed in calibration mode by sliding a plate over the pressure transducers on the pressure tap side. The pressure transducers then measure the difference in pressure between the stable, trapped volume on the pressure tap side and the hydrostatic variation on the reference pressure side. In an ideal situation, this measurement would be the ideal wave shown in Figure F-1. In this case, the air trapped on the pressure tap side of the transducer does not fluctuate with altitude change. However, the air in the reference pressure side does fluctuate. Thus, the "ideal" wave is the negative of the wave obtained when the tap side of the transducer is open as described above. The difference between the measured wave and the ideal wave is the correction that should be applied to each pressure tap measurement and each five-hole probe pressure measurement.

In addition to the pressure transducers inside the blade, we used a Mensor digital differential pressure transducer. The Mensor is mounted in the PSC enclosure on the hub and measures the differential pressure between a static pressure reference (NASA pressure system atmospheric pressure at the Gill port or the upwind static probe) and the ambient pressure inside the PSC enclosure. Once again, the reference pressure side of the transducer, the ambient enclosure pressure, changes as a function of blade 3 azimuth angle and rotor speed. The hydrostatic variation was measured by operating the turbine in zero-wind conditions for both configurations: Mensor connected to the Gill port and Mensor connected to the upwind static probe. A sinusoid was fit to the measured pressure variation. The negative of this waveform is the correction.

Method

To measure the hydrostatic pressure change in the reference pressure tube, we needed a constant pressure on the tap side of the transducer. Three pressure transducer configurations were tested. For one method, the transducer was placed in calibration mode (sliding plate blocked tap side of transducer), and the calibration pressure line was removed from the transducer so only the reference pressure line extended to the instrumentation enclosure. A tube capped with a barb with a screw plug was then placed over the calibration line port of the transducer. This was repeated at all five span locations at once. The second configuration consisted of placing electrical tape over the pressure taps on the blade and running the turbine with the transducer slide in normal operation mode. The volume of air between the tape and the pressure transducer fluctuated with blade rotation to such an extent that this method was deemed unacceptable. The third method was to place a tube capped by a barb with a screw plug on the ports of five pressure taps. This method produced corrections similar to that obtained by blocking the taps with the transducer slide in calibration mode, and it is probably the most direct method for measuring the hydrostatic variation in the reference pressure line. However, the increased difficulty required to disconnect and reconnect pressure taps at each span location was too labor intensive. Thus, we used the first method for both upwind and downwind turbine hydrostatic correction development. Another advantage to this method is that a correction could be obtained for each of the 31 pressure ports although only five were used.

Once the transducers were in the appropriate measurement configuration, the turbine was powered to operate at its normal speed of 72 RPM. Three 30-second data campaigns were collected and processed with the MUNCH program. We then computed the sine wave required to force the measured wave to behave like the ideal wave in Figure F-1 using Microsoft Excel as follows.

First, the measured C_p values output by MUNCH were multiplied by the normalization value corresponding to that span location (QNORM), and the centrifugal force correction was removed as shown in Equation 1.

$$P = C_p * q - \frac{1}{2}\rho * (r * \omega)^2 \tag{1}$$

where,
P = measured pressure, Pa
C_p = pressure coefficient for a given pressure tap
q = normalization pressure for specified span location, QNORM, Pa
ρ = air density, RHOTUN, kg/m3
r = radial distance to pressure tap, m
ω = rotor speed, RPM, converted to radians/second

This was done for four pressure taps and one five-hole probe port at each of the five span locations. Note that the five-hole probe port was not normalized, so subtracting the centrifugal force correction yielded the measured pressure. This results in the actual pressure measured by each transducer for a given pressure tap or five-hole probe port.

An equation describing the desired, corrected pressure is shown in Equation 2.

$$Pcorr = P - \overline{P} + A\cos(Az - \phi) \tag{2}$$

where,
P_{corr} = corrected pressure, Pa
P = measured pressure, Pa
$\overline{P}$ = mean pressure, Pa
A = amplitude of correction sinusoidal wave, Pa
Az = Blade 3 azimuth angle, B3AZI, converted to radians
ϕ = phase angle of correction sinusoidal wave, radians

The correction would be a sinusoidal wave that forced the amplitude and phase of the measured pressure to fit the ideal, corrected waveform for that span location. Subtracting the average pressure at a tap from the instantaneous pressure provided the fluctuation due to hydrostatic variations.

The ideal waveform shown in Equation 3 uses the constant hydrostatic variation of 10 Pa/m. We minimized the sum squared error of the ideal waveform and the corrected waveform by changing A and ϕ in the Excel solver. The resulting A and ϕ represent the values required to force the measured hydrostatic variation to match the ideal hydrostatic correction.

$$P_{ideal} = 10 * (r + r_{trans}) * \cos(Az) \tag{3}$$

where,
P_{ideal} = ideal pressure, Pa
r = radius to nearest inboard pressure tap, m
r_{trans} = radius from pressure tap to transducer, m
Az = Blade 3 azimuth angle, B3AZI, converted to radians

An example of measured pressure and corrected pressure is shown in Figure F-2. This data was obtained by running the turbine at 72 RPM under zero wind conditions. We determined a different correction for each of the five pressure transducers. Different corrections were obtained for both the downwind and upwind turbine configurations. In the upwind configuration, the rotor rotates in the opposite direction, and the instrumentation boxes then rotate in opposite directions. Because all three boxes are connected with pressure tubing, the flow between the boxes differs depending on the direction of rotation. The various corrections for the pressure transducers within the blade are included in Table F-1.

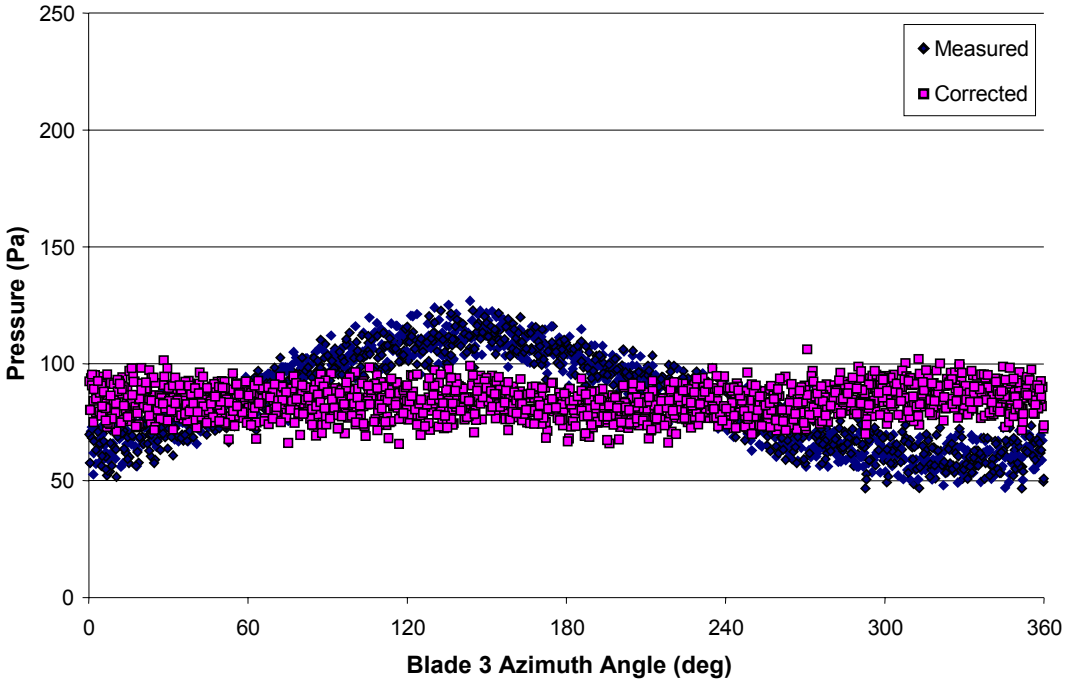

Figure F-2. Example of measured pressure and pressure corrected for hydrostatic variation obtained with turbine running in zero-wind condition

Table F-1. Hydrostatic Corrections for Various Turbine Configurations

	Upwind Turbine		Downwind Turbine		Field Test	
	Amplitude (Pa)	Phase (radians)	Amplitude (Pa)	Phase (radians)	Amplitude (Pa)	Phase (radians)
30% Span Transducer	15.57	-0.50	27.74	-0.60	24.95	-0.68
47% Span Transducer	-32.51	-3.43	-39.50	-3.42	-34.56	-3.47
63% Span Transducer	-43.88	-3.40	-48.25	-3.35	-41.67	-3.39
80% Span Transducer	-52.37	-3.39	-55.58	-3.33	-47.31	-3.36
95% Span Transducer	-47.31	-3.42	-50.47	-3.35	-41.85	-3.39
Mensor connected to upwind static probe, Filter=90%, Window=7	---	---	-6.27	2.94	-5.92	2.93
Mensor connected to NASA Pa, Filter=90%, Window=7 (Not in database)	-5.61	2.09	-5.92	2.93		
Mensor connected to NASA Pa, Filter=92%, Window=7 (Sequence G: wind speeds 19-25 m/s)	-4.41	2.11	---	---		
Mensor connected to NASA Pa, Filter=94%, Window=7 (All upwind configurations; Sequence G wind speeds 5-18 m/s)	-3.26	2.14	---	---		

The Mensor digital pressure transducer was mounted inside the PSC enclosure, and it underwent a hydrostatic variation as well. The Mensor was used to determine the pressure difference between the outside atmospheric pressure and the instrumentation box pressure for most test configurations. During one test, the Mensor measured the differential pressure between the instrumentation box and a static probe mounted on a vane upwind of the turbine. The Mensor is programmable with several filter and windowing options. Different corrections were obtained for both pressure system configurations as well as all variations in filter and window settings. The ideal curve for the Mensor signal required no variation (i.e., a flat line as a function of azimuth). The fluctuation in the Mensor measurement was fit with a sinusoidal curve. This waveform represented the correction that must be subtracted from the measured value to remove hydrostatic variation. We used the Excel solver to minimize the difference between the measured value and a sinusoidal wave by changing the amplitude and phase.

Conclusion

We removed the hydrostatic variations in all pressure measurements caused by the altitude change in the rotating blade and instrumentation enclosures. Corrections were determined by measuring the hydrostatic fluctuation in the reference pressure tube for the blade pressure transducers. A sinusoidal waveform that forced this measurement to behave in an ideal hydrostatic variation was determined. The Mensor hydrostatic variation was also measured and fit with a sinusoid. We determined various corrections for the upwind and downwind configurations and for all filter and window options used during testing.

We did not obtain any data during Sequence X, 90 RPM, which would permit similar derivation of a hydrostatic correction for these data points. The hydrostatic correction developed for the 72 RPM case was used during all processing of Sequence X data.

Appendix G: Wake Measurements: Sequences 8 and 9

Introduction

This appendix describes airflow measurements made of the wake behind the Unsteady Aerodynamics Experiment (UAE) in the NASA Ames 80- by 120-ft wind tunnel. The measurements were made in support of the Department of Energy's (DOE) Small Wind Turbine Program to study airflow in the area of a tail vane. Previous work in the area of wind turbine wake measurements is discussed. The measurements were made at 0.58 diameters downwind of the UAE 10-m diameter turbine at two radial positions. Sonic anemometers were used to measure the three components of wind velocity. The turbine was yawed up to 60º to simulate turbine furling. The data time series at 10-Hz was acquired during a 30-second period and matched to the UAE standard data set.

Background

Small Wind Turbine Program

DOE has embarked on a program to advance technology in the small wind turbine market (Forsyth 1997), paying particular attention to the analytical modeling of small turbines. Manufacturers have used an empirical approach to design the turbine geometry, usually by scaling previous models. As manufacturers design larger turbines, the financial risks of an unsuccessful design increase.

The National Renewable Energy Laboratory (NREL), working with analysts at RANN, Inc., of Palo Alto, California, are working on furling models of small wind turbines (Eggers et al. 2000). One area of uncertainty in the modeling is the nature of the airflow about the tail. The tail is used as a passive yaw control by aligning the turbine into the wind. The tail must remain approximately aligned to the undisturbed wind direction for the rotor to yaw or furl out of the wind at increasing wind speeds.

Currently, RANN has approximated the flow about the tail by assuming far wake conditions. This experiment will investigate the flow near a tail vane to improve the current state of small wind turbine models.

Wake Measurements

Figure G-1 shows wake visualization behind a propeller. The photo shows the tip- and root-edge vortices along with the interaction from a spherical nacelle.

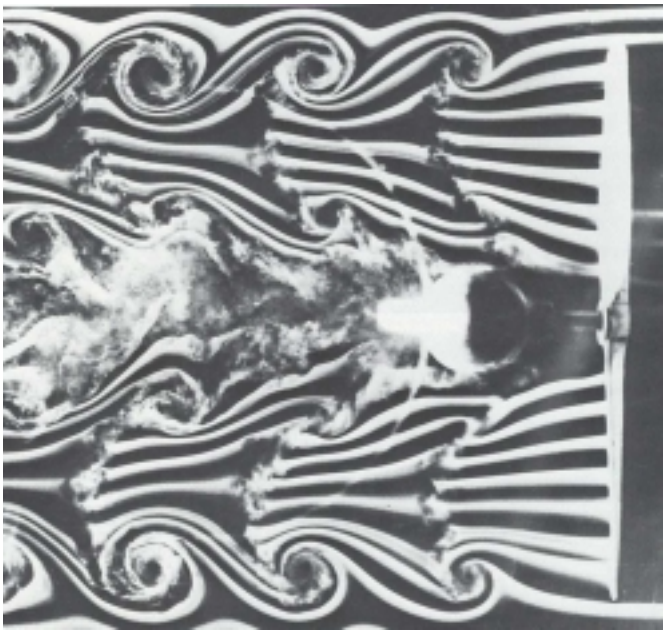

Figure G-1. Propeller wake visualization (Van Dyke 1988)

In the past, wind turbine wake measurement experiments were conducted either to study wind farm wake effects or to advance aerodynamic codes that rely on wake models. No experiments found in the literature have been made to study small-turbine tail aerodynamics. Table G-1. shows a listing of references and pertinent information related to the current experiment. The literature does not show measurements made in the region of tail vanes (approximately 0.5 to 0.67 diameters downwind of the rotor). The data usually is shown as wake deficit—the ratio of downwind to upwind longitudinal velocity. The data shows an increasing wake deficit with increasing tip-speed ratio, as predicted in actuator disk theory.

Table G-1. Wake Measurement Literature

Paper	Model	Axial Measurement	Radial Measurement	TSR	Instrument	Comments
(Balcerak 1980)	3-m diameter, 1 kW, Constant Velocity Testing	0.6 D	0.7 r/R	4-5.5	RM Young anemometer (prop vane?)	Shows velocity ratio 1.0 to 0.5.
(Hansen 1981)	3-m diameter, 1 kW, Constant Velocity Testing	1.85 D- 13.9 D	Centerline to 1.5 D	4.7	Kaijo-Denki Sonic	Shows velocity ratio 0.2 to 0.5 at 1.85 D centerline
(Wentz, Ostowari et al. 1985)	0.5-m wind tunnel model, and flat disk	1D	1D	3.5-7.9 and 21.1	Hot film and scanning total press. probe	Show flow reversals at TSR>6
(Helmis, Whale et al. 1994)	19-m, 100-kW turbine and wind tunnel model	1.1D	Centerline	2-4.4	Cup anemometer (field), Particle Image Velocimetry (tunnel)	Field test of turbine, velocity ratio of 0.7, comparison to wind tunnel measurements

Wake Measurement Test Objectives

The objective of the Wake Measurement Test was to measure the average and time-varying three-dimensional velocity components in the wake of a wind turbine rotor in the locations representative of tail vane positions for small turbine rotors. The experimental uncertainty in the measurements is expected to be less than 5%.

Measurement Layout

Measurement Locations

The wake was measured at two locations downwind of the rotor, with the rotor operating in an upwind configuration. Figure G-2 shows the wake measurement installation in the wind tunnel. Figures G-3 and G-4 show top- and front-view line drawings of the measurement locations. Turbine yaw is positive clockwise from the top view. Rotor rotation is counterclockwise from the front view. Figure G-5 shows a drawing of the sonic anemometer. Both anemometers were located with the center of the U measurement (velocity aligned with tunnel longitudinal direction) positioned 0.58 diameters (5.84 m) downwind from the rotor with the rotor upwind and at zero yaw. Anemometer 1 is closest to the hub shaft centerline with the center of the U measurements at 0.02 radius (0.08 m) higher than shaft centerline. Anemometer 2 is placed 2 m laterally from Anemometer 1. Anemometer 2 is at 0.49 radius. This position was chosen to approximate the position of the wake center with the turbine yawed at 45°.

Figure G-2. Full view of UAE turbine and wake measurement tower in (80 x 120) test section

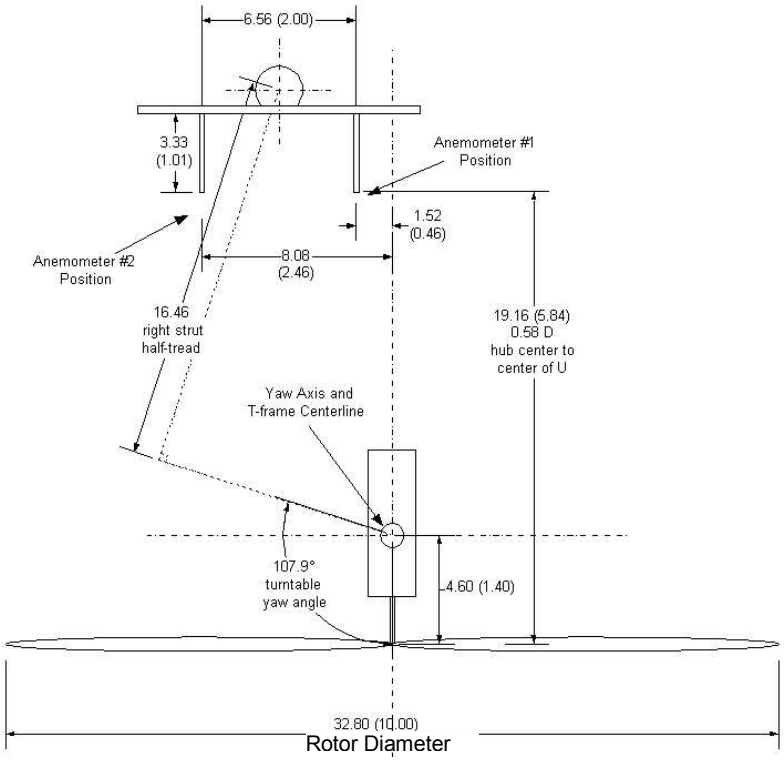

Figure G-3. Top view of wake measurement set-up [ft (m)]

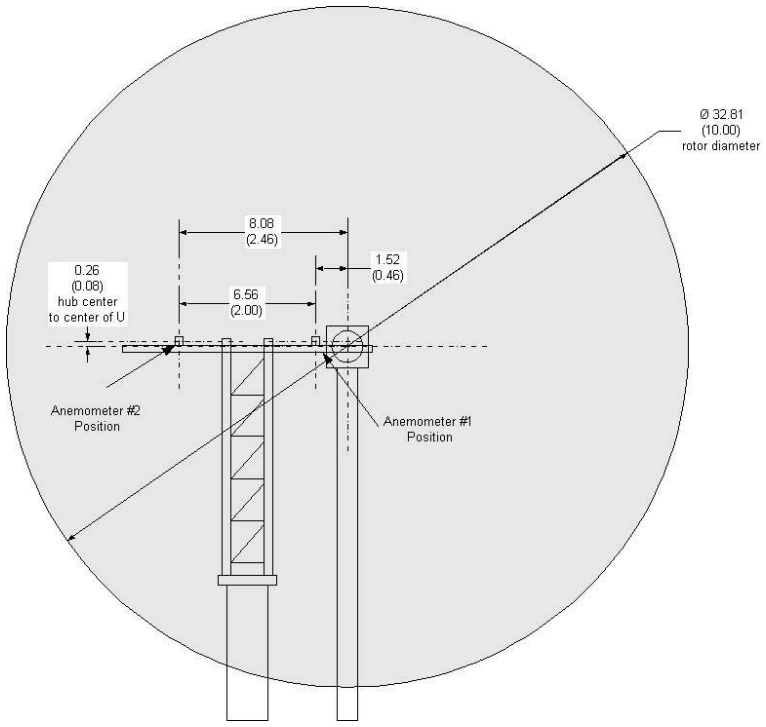

Figure G-4. Front view of wake measurement set-up

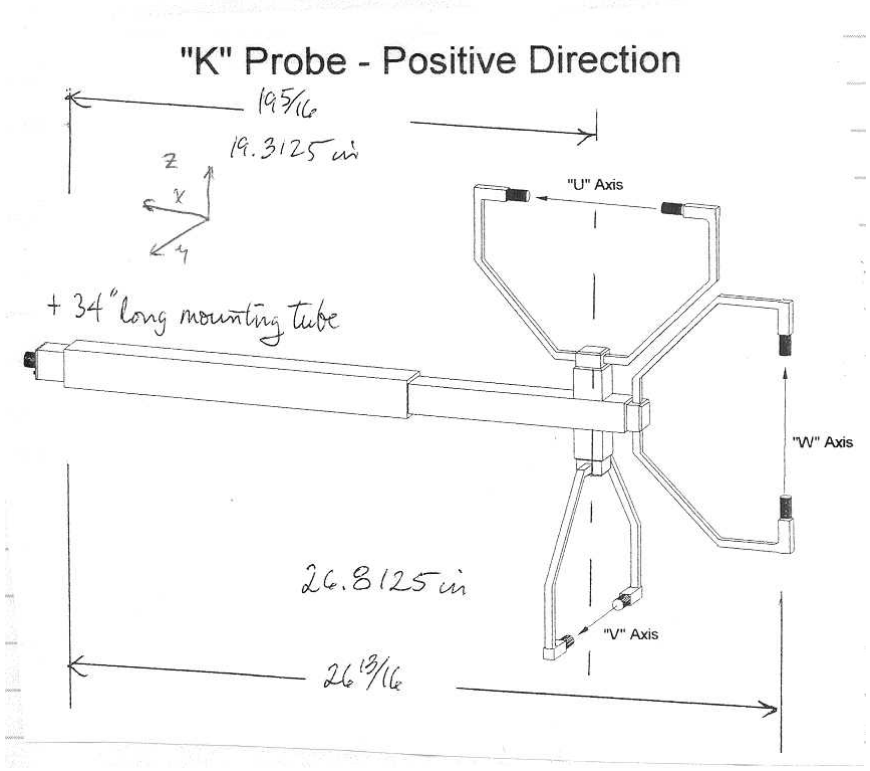

Figure G-5. Line drawing of ATI K-probe

Tower Configuration

The anemometers were placed upon a 9.75-m standard wind tunnel strut. The strut carriage was placed at 5.02 m from the *T*-frame center, and the turntable was yawed to 107.9º. A strut adapter was installed on the strut and torqued to the torque mark. An NREL-supplied adapter plate was then bolted to the strut adapter. A 3-m ROHN 65GH-tower section shown in Figure G-6 was then bolted to the adapter plate. The tower section has a 10.16-cm square, 3.7-m long boom installed at the top with NREL-manufactured mounts for the anemometer booms. The anemometers are mounted such that the center of the U-bar measurement was 10 tower diameters (1 m) from the boom. The tower section was aligned with the face upwind. The anemometer boom centers were positioned 1 m from tower center on either side of the tower.

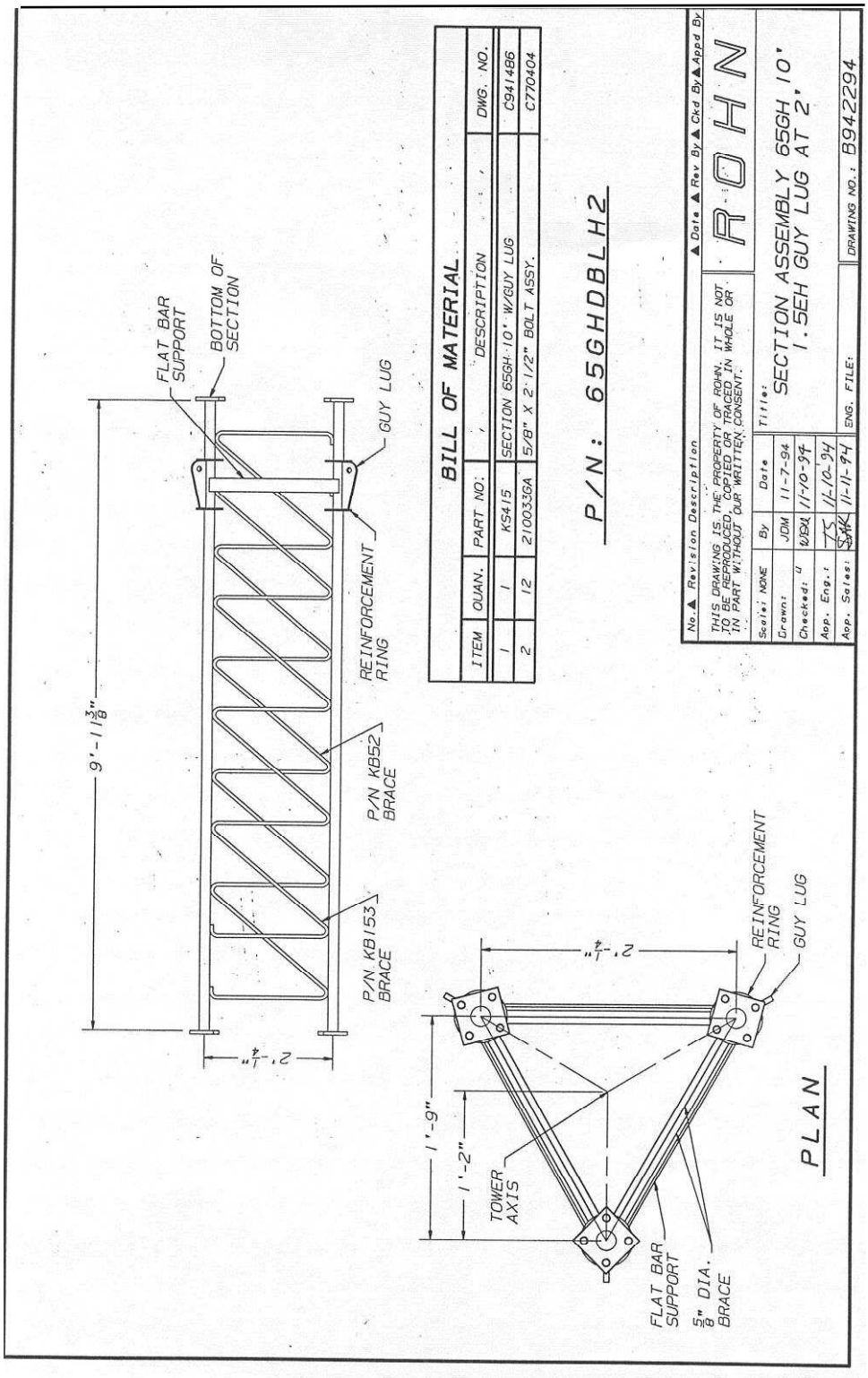

Figure G-6. Rohn 65GH Tower Section Drawing

Positioning the anemometer with respect to the boom has been shown to reduce the tower interference with the measurements (IEA 1999). However, as the turbine is yawed the skew of the wake will change the flow incidence angle to the tower. This angle will affect the tower interference with the wind speed measurements. This potential error could be assessed with the wake measurements.

Additional hardware was added to the turbine tower to restrict turbine yaw in the event of operator error or yaw drive and/or yaw brake failure. The placement of the anemometers was such that there could have been a rotor impact if the turbine was allowed to yaw more than 68º (more in the negative direction—this was checked during assembly). A turbine hard stop was installed for the test to restrict motion to ±65º.

Anemometers

Description

The wake measurements were made with Applied Technologies, Inc., Type K sonic anemometers (Applied Technologies). These were the same instruments that were used to measure the tunnel wind speed. We used these anemometers for this test so we would have spares for the primary wind speed measurements.

Below is a description of the anemometer from the manual:

"The Sonic Anemometer/Thermometer is a solid-state ultrasonic instrument capable of measuring wind velocities in three orthogonal axes (U, V, and W) and provides sonic temperature. The Sonic Anemometer/Thermometer is comprised of a probe array (containing all electronics necessary for operation), and a mounting bar. The probe array's sonic transducers are separated by 10 or 15 cm. Sonic pulses are generated at the transducers and received by opposing transducers. Mathematics derived for these sonic pulses provide a wind velocity measurement in each of the corresponding axes and calculates a sonic temperature, which is generated from the speed of sound measurements in the "W" axis. Temperature measurements are corrected for cross-wind contamination."

The accuracy of the wind speed measurement is claimed by the manufacturer to be 0.05 m/s up to 20 m/s.

Data Acquisition

Below is a description of the built-in anemometer electronics from the manual:

"The Sonic Anemometer/Thermometer uses a microprocessor-based digital electronic measurement system to control the sample rate, and compute the wind speeds and temperature. The standard data output of the Sonic Anemometer/Thermometer is 10Hz, where each output represents the average of 10 discrete measurements. The wind speed from each of the axes and the temperature are presented on the computer screen."

Figure G-7 shows a diagram of the measurement system. The signals from the anemometers were routed to the control room via 525-m cables. The individual signals were connected to the data packer. The data packer provided an RS-232 output to the laptop. The RS-232 connection allowed control of the data packer and separate anemometer electronics, along with transferring the data string to the laptop.

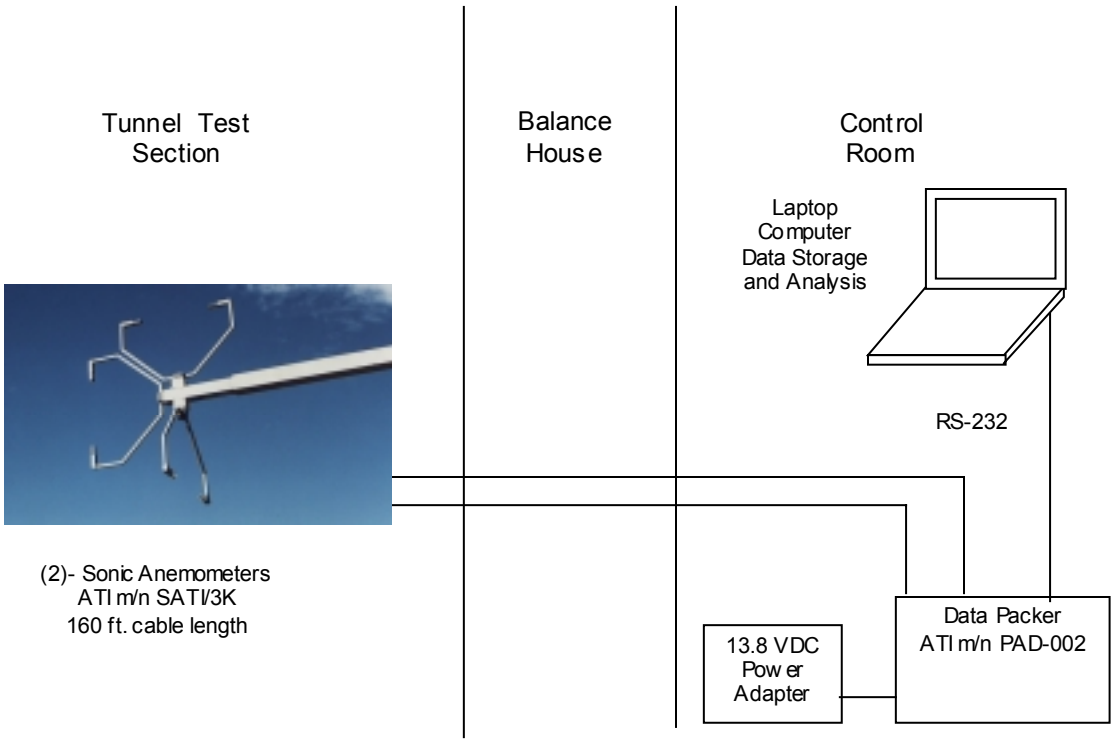

Figure G-7. Data acquisition schematic

An example data string from the data packer is as follows:

"U 00.04 V 00.03 W 00.02 T 19.07 U 00.02 V 00.10 W-00.01 T 19.31"

Anemometer #1's three velocity components are listed (in m/s) with sonic temperature (in ºC). Anemometer #2's is listed after #1 within the same line.

The laptop was running Igor with Very Dumb Terminal (VDT) Extension installed. A procedure was written in Igor to read in the data packer string for a 30-second acquisition period. The data was then saved to disk, with a time stamp for the beginning of the acquisition period, a header of the column names, and a column of relative time in milliseconds. The user can then plot the time series and average for the wind speed (magnitude) and direction (azimuth and elevation) for both anemometers. These are calculated from the data that has been saved to the disk. Figure G-8 shows a plot of some example data with averages shown in the plot legend, and Table G-2 contains an example data file.

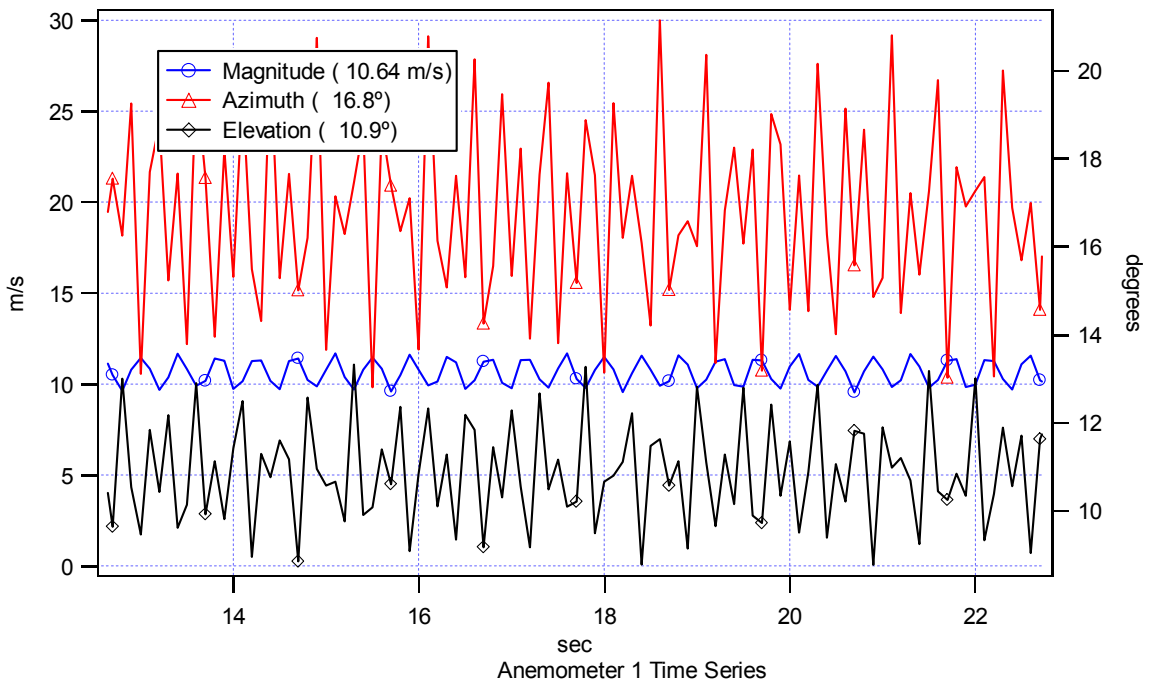

Figure G-8. Wake measurement example time series graph

Table G-2. Example Data File Listing

Start Date =	1/24/00	Start Time =	14:42:07					
relative_time	anem1_U	anem1_V	anem1_W	anem1_T	anem2_U	anem2_V	anem2_W	anem2_T
100	-0.03	0.03	0.03	20.12	0.02	0.08	0	20.26
200	-0.03	0.03	0.04	20.23	0.02	0.09	0.01	20.29
300	-0.01	0.03	0.04	20.27	0.02	0.11	0.01	20.3
400	-0.01	0.04	0.06	20.19	0.02	0.12	0.01	20.3
500	-0.02	0.04	0.04	20.15	0.02	0.12	0.01	20.31
600	-0.02	0.03	0.05	20.18	0.02	0.12	0	20.32
700	-0.02	0.03	0.05	20.22	0.02	0.12	0	20.32
800	-0.03	0	0.04	20.28	0.02	0.12	0	20.32
900	-0.02	0	0.03	20.3	0.02	0.12	0.01	20.33
1000	-0.01	0.01	0.02	20.2	0.03	0.12	0.01	20.34
1100	-0.01	0	0.01	20.18	0.03	0.11	0.02	20.34
1200	-0.01	-0.04	0.01	20.19	0.04	0.11	0.02	20.35
1300	0	-0.05	0.03	20.26	0.04	0.1	0.02	20.35
1400	-0.01	-0.04	0.05	20.29	0.04	0.1	0.02	20.35
1500	-0.02	-0.02	0.05	20.32	0.04	0.1	0.02	20.36
1600	-0.02	0	0.02	20.3	0.04	0.11	0.01	20.37
1700	-0.01	0	0.02	20.3	0.04	0.1	0	20.38
1800	-0.01	-0.01	0.03	20.28	0.04	0.09	0	20.38
1900	-0.01	-0.02	0	20.26	0.03	0.08	0	20.38
2000	0	-0.01	-0.01	20.3	0.03	0.09	0	20.38
2100	0	-0.01	-0.01	20.27	0.03	0.09	0	20.38
2200	0	0	0	20.28	0.03	0.09	0	20.38
2300	0	0	0.02	20.24	0.02	0.1	0	20.37
2400	0	-0.01	0.04	20.2	0.02	0.1	-0.01	20.36
2500	0	0.01	0.06	20.17	0.02	0.1	-0.01	20.35
2600	-0.01	-0.01	0.06	20.12	0.02	0.1	-0.02	20.35
2700	-0.02	-0.01	0.03	20.19	0.02	0.1	-0.02	20.35
2800	-0.02	-0.01	0.06	20.29	0.02	0.09	-0.02	20.35

The filenames match the standard UAE naming convention as follows:

Filename = *TWWYYYYR*.wak

where:

T = test sequence as established by the test matrix- "8" for turbine on, "9" for turbine off
WW = wind speed in m/s (example 05 for 5 m/s)
YYYY = yaw angle in degrees, first digit "M" (for minus) if negative (example 0060 for 60º)
R = repeat number (0, 1, 2 etc).

To reduce the impact on the UAE data acquisition system, we acquired the wake measurements separately. A separate computer was used to acquire the measurements from the anemometer. The data acquisition periods match those of the UAE (30 seconds). Data acquisition began for both systems separately by operator command. *There were no links between the systems.* The filenames for the UAE data match the filenames for the wake measurement data.

Calibration

Below is a description of the calibration process for the anemometers from the manual:

"Calibration of the Sonic Anemometer/Thermometer requires the installation of the 'Zero-Air Chamber' over the axis being calibrated. A measurement of the ambient air temperature to an accuracy of ±1.°C is necessary for calibration. A calibration command is issued from the computer, and the microprocessor automatically calibrates the Sonic Anemometer/Thermometer, compensating for any electronic drift. Enter the temperature and relative humidity at the computer terminal when prompted."

This calibration process was performed after the anemometers were installed and prior to testing.

Noise Documentation

The following steps were taken to determine the noise of the sonic anemometer measurements, and the results are presented in Table G-3:

1. After the initial calibration, a data file was acquired with the zero-air chamber installed. Repeat for each axis.

2. With the zero-air chamber installed, a data file was acquired with the turbine operating. Repeat for each axis. This documents the noise from the turbine generator.

3. During tunnel runs, a data file was acquired with the turbine off and the blades feathered and vertical. The outboard anemometer #2 will be compared to the tunnel velocity. Both anemometers might be influenced by the turbine wake; however, we might be able determine if there is an offset from the tunnel readings. These data points are included in the test matrix under sequence 9.

Table G-3. Sonic Anemometer Noise Quantification

	Anemometer #1		Anemometer #2	
	Mean (m/s)	Standard Deviation (m/s)	Mean (m/s)	Standard Deviation (m/s)
Turbine off, U-axes covered	-0.01	0.02	0.00	0.02
Turbine off, V-axes covered	-0.01	0.01	-0.01	0.01
Turbine off, W-axes covered	0.01	0.01	0.00	0.01
Turbine on, U-axes covered	0.00	0.04	-0.02	0.02
Turbine on, V-axes covered	0.01	0.03	-0.01	0.02
Turbine on, W-axes covered	0.01	0.02	0.00	0.01

Test Matrix

The turbine was in the upwind configuration with a rigid hub and zero cone angle. The rotor speed was the nominal speed of 72 RPM. The blade pitch was 3º. The turbine was restrained to 60º yaw. The five-hole probes were removed from the blades prior to testing. The test matrix in appendix C includes all of the conditions under which data was collected from both the turbine and the downwind sonic anemometers.

As mentioned in the noise documentation section, points were interspersed in the matrix with the turbine not rotating. These points have ordinal number 9 in the file name to distinguish them from the turbine rotating data files.

References

Applied Technologies, Incorporated. *Operator's Manual for a Sonic Anemometer/Thermometer.* Longmont, CO.

Balcerak, J.C. (1980). Controlled Velocity Testing of Small Wind Energy Conversion Systems. Golden, CO, DOE Rocky Flats Wind Systems Program.

Eggers, A.J.; Chaney, K.; Holley, W.E; Ashley, H.; Green, H.J.; Sencenbaugh, J. (2000). "Modeling of Yawing and Furling Behavior of Small Wind Turbines." 38th AIAA Aerospace Sciences Meeting and Exhibit. Reno, NV, American Society of Mechanical Engineers. pp. 1-11.

Forsyth, T.L. (1997). "An Introduction to the Small Wind Turbine Project." AWEA WindPower '97. Austin, TX, American Wind Energy Association, pp. 231-239.

Hansen, A.C. (1981). "Early Results from the SWECS Rotor Wake Measurement Project." Proceedings Small Wind Turbine Systems 1981. Boulder, CO, Solar Energy Research Institute, Golden, CO**,** pp. 185-199.

Helmis, C.G.; Whale, J.; Papadopoulos, K.H.; Anderson, C.G.; Asimakopoulos, D.N.; Skyner, D.J.. (1994). "A Comparative Laboratory and Full-Scale Study of the Near Wake Structure of a Wind Turbine." 5th European Wind Energy Association Conference and Exhibition. 10-14 October 1994. Thessaloniki, Greece, European Wind Energy Association. pp. 465-471.

International Energy Agency (IEA) (1999). *Recommended Practices for Wind Turbine Testing and Evaluation. Wind Speed Measurement and Use of Cup Anemometry*, edited by Raymond S. Hunter, Renewable Energy Systems, Ltd., Scottish Regional Office, 11 Elmbank Street, Glasgow G2 4PB, United Kingdom, p. 50.

Van Dyke, M. (1988). *An Album of Fluid Motion.* Stanford, CA, The Parabolic Press.

Wentz, W.; Ostowari, C.; Manor, D.; Snyder, M. (1985). "Horizontal Axis Wind Turbine Wake and Blade Flow Studies from Model Tests." Windpower '85. 27-30 August 1985. San Francisco, CA. Washington D.C.: American Wind Energy Association. pp. 235-244.

Appendix H: Field Test

Field Test Description

Prior to assembling the wind turbine in the NASA Ames wind tunnel, it was assembled and tested at the NWTC. This facility was used to test previous phases of this experiment (Butterfield et al. 1992, Simms et al. 1999, Hand et al. 2001). From September 24, 1999, through October 29, 1999, the Phase VI configuration was field-tested in preparation for disassembly and transport to the NASA wind tunnel. The configuration was essentially that used during Sequences B and C with additional pitch angles of 8° and -3° to correspond to previous field tests. The turbine operated mostly in free yaw. The variable-speed drive was engaged during some campaigns, but the rotor speed was set to 72 RPM. The hub height of the field turbine was 17.03 m.

In previous experiments, detailed inflow conditions were measured in the predominantly upwind direction of the turbine. This field test used one sonic anemometer mounted at hub height. This anemometer was connected to the channels that were associated with the west anemometer in the wind tunnel (326, 328, 330). All of the NASA channels were collected although no instrumentation was associated with these channels. This appendix mirrors the preceding report highlighting the differences between the field test and the wind tunnel test.

Instrumentation

Atmospheric Conditions

All of the NASA channels were included in the data stream to test processing procedures and file formats. However, there was no instrumentation connected to these channels (300, 302, 304, 306, 308, 316, and 318). The atmospheric temperature at the NWTC was noted in the logbook based on the temperature reported at the site weather station (NREL unpublished). This temperature was then manually inserted as the offset calibration coefficient (the slope calibration coefficient was set to zero) for channel 308, OMT4M. This temperature was used to compute air density. A barometer (channel 334) was mounted in the instrumentation rack inside the data shed as in previous phases of the experiment. The atmospheric pressure was used to compute air density. This barometer was not used during wind tunnel testing.

Wind Speed and Direction

One sonic anemometer of the same type used during the wind tunnel test was installed at hub height on the meteorological tower 1.5 D in the predominantly upwind direction. This anemometer was connected to the channel designated for the west sonic anemometer during wind tunnel testing (326, 328, 330). There was no instrumentation connected to the channels associated with the east sonic anemometer (channels 320, 322, 324). The wind speed and direction were computed. Note that wind speed and direction were computed for the channels associated with the east sonic anemometer as well, although there was no instrumentation connected.

Pressure Measurements

The wind tunnel pressure system channels (310, 312, 314) were not connected to any instrumentation during the field test. However, the pressure transducers in the blade that measured pressures at the pressure taps and the five-hole probes were identical to wind tunnel test configurations. The Mensor digital differential pressure transducer was also installed as in the wind tunnel test. The reference pressure tubing was attached to the upwind static probe as in Sequence 4 as well as run down the tower to the control shed to simulate connection to the gill port. These configurations are noted in Table H-1.

Structural Measurements

The strain gauges and accelerometers used during the wind tunnel test were unchanged during the field test. The load cells for teeter link force and teeter damper forces were also unchanged. The only difference was that the nacelle yaw moment was measured with strain gauges instead of a load cell during field-testing. The strain gauges were installed for previous phases of the experiment as part of the original brake mechanism. The yaw drive and pneumatic brake system that incorporated the load cell was installed after field-testing was completed. The yaw moment strain gauges were calibrated in the same manner as the yaw moment load cell. This channel only registers meaningful data when the yaw brake is applied (noted in Table H-1).

The wind tunnel balance system channels were not connected to instrumentation during the field test (344, 346, 348, 350, 352, 354, 356).

Position Encoders

The turntable angle channel (358) was not connected to any instrumentation during the field test. All other position encoder channels were unchanged from the wind tunnel test.

Data Acquisition and Reduction Systems

The PCM system hardware and software were unchanged from the field test to the wind tunnel test. Calibration procedures were also unchanged. As in previous field tests, campaigns were 10 minutes long.

Derived Channels

The wind tunnel parameter channels were not computed during the field test (channels 880, 881, 882, 883, 884, and 885). The air density was computed as in previous field tests using the barometric pressure (channel 334) and the outside atmospheric temperature (manually inserted in channel 308) as follows:

$$\rho = 0.0034838 * \frac{P_{atm}}{T} \text{ (Smithsonian Institution 1949)} \quad (1)$$

As in previous field measurements, the air density is not included in the output. The hydrostatic corrections were applied to the pressure tap, five-hole probe and Mensor measurements during

field-testing. The pressure measurements were made relative to the instrumentation box (P_{tap}-P_{box}). The Mensor measurement was either P_{atm}-P_{box} or P_{statpr}-P_{box}, but it was not added to the pressure tap and five-hole probe pressure measurements. Therefore, the pressure measurements are not relative to static pressure.

The centrifugal force correction was applied as in the wind tunnel measurements. The dynamic pressure was determined in the same way as the wind tunnel measurements. Because the pressure measurements were not made relative to static pressure, there is an offset between the values listed as dynamic pressure and the true dynamic pressure. The pressure coefficients and aerodynamic force coefficients were also computed as in the wind tunnel test. Rotor thrust and torque computations were unchanged. The flow angle measurements were computed identically. The wind tunnel forces and moments (channels 886, 888, 889, 890, 891) are not included in the output.

The sonic anemometer component channels are used to compute the wind speed and direction. The wind speed computation is unchanged from the wind tunnel test computations, but the wind direction was not computed during the wind tunnel test. The sonic anemometer was oriented with the prevailing wind direction, 292° from true north. The wind direction equation follows, and the angle was restricted to ±180°:

$$LMSWD2 = 292 - \tan^{-1}\left(\frac{LWSV8M}{LWSU8M}\right) \tag{2}$$

Yaw error describes the misalignment of the turbine with the prevailing wind. The channel representing yaw error included in the engineering unit files was calculated by finding the difference between the sonic measured wind direction (LMSWD2) and the turbine angle (YAW). This value is then restricted to ± 180°.

$$YAWERR = YAW - LMSWD2 \tag{3}$$

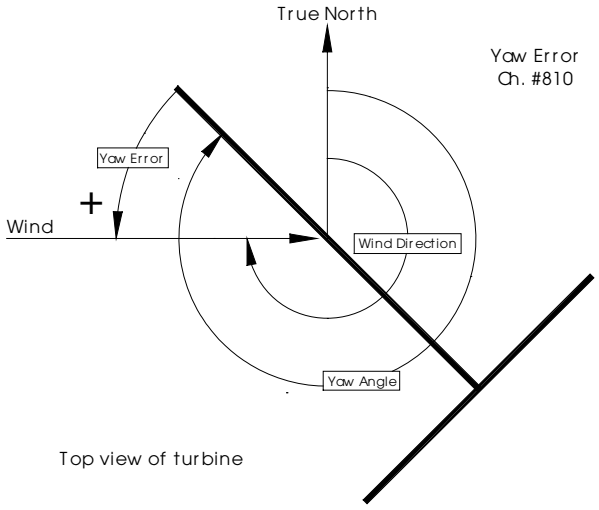

Figure H-1. Yaw error angle convention

Summary of Field Test

The field test provided the opportunity to ascertain functionality of all instrumentation, hardware, and software components. Twenty-six, 10-minute campaigns were collected in procedures similar to previous field tests. The file name convention uses the first two characters, D6, to indicate Phase VI tests. The next two characters specify pitch angle (03=3°, 00=0°, 08=8°, and M3=-3°). The last three characters indicate the sequential order in which the campaigns were collected. The following table summarizes the data collected and the problems encountered.

Instrumentation sheets similar to those in Appendix B illustrate the barometer and yaw moment strain gauges that differ from the wind tunnel test.

References

Butterfield, C.P.; Musial, W.P.; Simms, D.A. (1992). *Combined Experiment Phase I Final Report.* NREL/TP-257-4655. Golden, CO: National Renewable Energy Laboratory.

Hand, M.M.; Simms, D.A.; Fingersh, L.J.; Jager, D.W.; Cotrell. J.R. (2001). *Unsteady Aerodynamics Experiment Phase V: Test Configurations and Available Data Campaigns.* NREL/TP-500-29491. Golden, CO: National Renewable Energy Laboratory.

National Renewable Energy Laboratory (NREL). (1998). *NWTC Site Climatology Test Plan*. Unpublished.

Simms, D.A.; Hand, M.M.; Fingersh, L.J.; Jager, D.W. (1999). *Unsteady Aerodynamics Experiment Phases II-IV: Test Configurations and Available Data Campaigns.* NREL/TP-500-25950. Golden, CO: National Renewable Energy Laboratory.

Table H-1. Summary of Data Collected and Problems Encountered During Field-Testing

Run Order	Campaign	Mean Blade 3 Pitch (deg)	Air Temperature (deg C)	Mean Sonic Wind Speed (m/s)	Mean Sonic Wind Direction (deg)	Mean Yaw Error Angle (deg)	Blade 1 Max. Teeter Damper Force (N)	Blade 3 Max. Teeter Damper Force (N)	Comments	Problems	Calibration History
1	d603001	2.990	18.300	10.365	274.686	-5.192	194.385	245.095	2, 5, 7	A,B,C,E,G	I,II,IV
2	d603002	2.998	18.300	9.070	276.181	-4.899	194.385	245.095	2, 5, 7	A,B,C,E,G	I,III,IV
3	d603003	2.995	18.300	9.945	281.010	-4.508	1360.749	4193.880	2, 5, 7	A,B,C,E,G	I,II,IV
4	d603004	3.003	18.300	6.682	294.184	-6.681	194.385	217.862	2, 5, 7	A,B,C,E,G	I,III,IV
5	d603005	2.998	18.000	8.750	280.199	-6.173	323.981	326.794	2, 5, 8	A,B,C,E,G	I,III,IV
6	d603006	3.000	18.300	8.016	280.649	-5.809	421.178	272.328	2, 5, 8	A,B,C,E,G	I,III,IV
7	d603007	3.002	25.700	7.768	307.652	-3.502	161.986	81.697	2, 6, 7	A,G,J	I,II
8	d603008	3.003	25.700	7.713	306.961	-4.174	194.385	108.930	2, 6, 7	A,G	I,III
9	d603009	2.999	25.700	5.751	301.734	-6.110	161.986	108.930	2, 6, 7	A,G	I,III
10	d603010	3.004	21.900	12.799	273.889	-2.082	2397.517	4221.113	2, 6, 7	A,B,G	I,II
11	d603011	3.019	21.700	9.307	285.204	-5.429	2462.315	5038.103	2, 6, 7	A,B,G	I,III
12	d603012	2.999	15.000	7.970	298.770	-4.613	226.784	245.095	2, 6, 7	A,D	I,II
13	d603013	2.996	15.000	7.775	287.262	-6.822	2721.507	5691.695	2, 6, 7	A,D	I,III
14	d603014	2.997	15.000	8.558	290.887	-4.530	2494.714	3703.686	2, 6, 7	A,D	I,III
15	d603015	2.999	15.000	7.515	291.166	-3.470	194.385	190.629	2, 6, 7	A,D,H	I,III
16	d600001	-0.001	15.000	7.491	295.576	-4.933	194.385	190.629	4, 6, 7	A	I,II
17	d600002	0.002	15.000	8.998	291.499	-6.187	3985.068	6154.656	4, 6, 7	A,H	I,III
18	d603016	3.005	8.200	6.749	295.711	-2.288	161.986	299.561	2, 6, 7	A,D	I,II
19	d603017	3.003	8.200	6.045	274.865	-0.819	161.986	299.561	2, 6, 7	A,D	I,III
20	d6m3001	-2.992	8.300	6.191	280.895	-1.704	161.986	299.561	1, 6, 7	A,I	I,II
21	d6m3002	-2.992	8.200	7.044	289.989	-5.036	161.986	4112.181	1, 6, 7	A,H,I	I,II
22	d608001	7.999	8.200	7.569	288.583	-7.618	161.986	272.328	3, 6, 7	A,I	I,II
23	d608002	7.996	8.200	6.344	284.223	-5.706	161.986	272.328	3, 6, 7	A,I	I,III
24	d603018	3.003	10.900	8.761	279.723	-5.198	161.986	245.095	2, 6, 7	A,I	I, II
25	d603019	3.002	10.900	6.800	275.800	-7.633	161.986	272.328	2, 6, 7	A,I	I, III

Table H-1. Summary of Data Collected and Problems Encountered During Field-Testing (continued)

Suite of problems:

A. 1/2% upper at all span locations
B. 68% upper at 95% span
C. 10%-20% upper at 95% span
D. 1% lower at 80% span may be plugged
E. Possible leak during pressure calibration
F. Transducers at 30%, 47%, 63% span not working
G. Pressure reference not stable
H. Calibration syringe failure
I. Nacelle accelerometer failed
J. File length short

Calibration History:

I. Full system calibration (all non-pressure channels)
II. Pressure channel pre-calibration performed
III. Pre-cal. obtained from post-cal. of previous campaign
IV. Pitch rate output not calibrated.

Suite of comments:

1. -3° pitch
2. 3° pitch
3. 8° pitch
4. 0° pitch
5. Reference tube in building
6. Reference tube to upwind static probe
7. Constant speed operation
8. Variable-speed drive engaged
9. Yaw brake engaged/disengaged during campaign

Channel	ID Code	Description
334	BARO	Barometric pressure
Location		Met rack inside data shed
Measurement type and units		Ambient air pressure, Pa
Excitation		15 Vdc
Range		74,000 to 100,000 Pa = 0 to 5V
Resolution		5,200 Pa/V
Calibration method		Manufacturer specifications and electronic path calibration
Sensor description		Ambient air pressure transducer Atmospheric Instrumentation Research, Inc. Model: AIR-AB-2AX

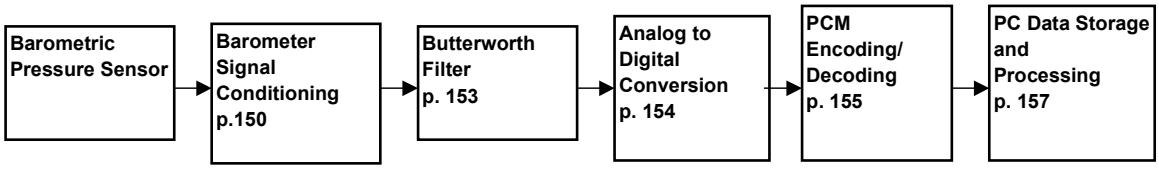

Calibration Procedure

Manufacturer specifications

1. Atmospheric Instrumentation Research performed a calibration before installing either barometer.

2. Enter the nominal slope (5,200 Pa/V) and the nominal offset (74,000 Pa) in the appropriate columns of *calconst.xls*

Electronic path calibration

1. Modify *vbl.lst* so the barometer channel is listed at the top of the file. Set NV in the first line to the number of channels to be calibrated, and insure that the correct PCM stream is specified in *gencal.cap* (all meteorological channels were on stream 3).

2. Connect the precision voltage generator to the barometer output.

3. Run the *gc.bat* batch file, which invokes both *gencal.exe* and *genfit.exe*. Collect samples for voltages ranging from 0 to 4.5 V in 0.5 V increments with two repetitions at each voltage level. The recorded input and output values are stored in the **.cao* input file. *Genfit.exe* computes slopes and offsets of the electronic path from the processor output to the computer in units of V/count and V, respectively. These values are stored in a temporary header file, **.hdr*. These slope and offset values are combined with the manufacturer-provided slope and

offset stored in *calconst.xls* during the *buildhdr.bat* process to obtain units of engineering unit/count and counts, respectively.

Calibration frequency

The barometer was calibrated by the manufacturer prior to Phase VI data collection. The electronic path calibration was performed prior to field-testing.

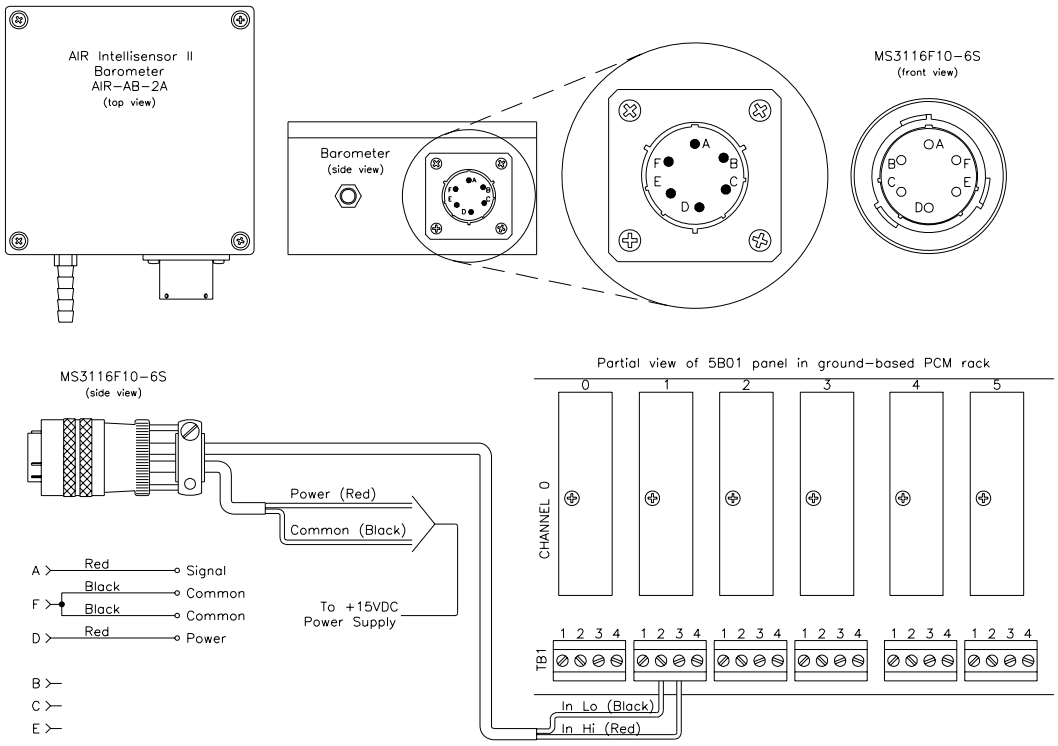

Figure H-2. Barometer wiring diagram

Strain Gauges (Yaw Moment)

Channel	ID Code	Description
342	NAYM	Nacelle yaw moment

Location	Arms of yaw brake mechanism
Measurement type and units	Bending moment, Nm
Excitation	10 Vdc
Range	
Resolution	
Calibration method	Application of known loads (A1)
Sensor description	Resistance = 350.0 ± 0.4% Ω
	Measurements Group, Inc.
	Model:

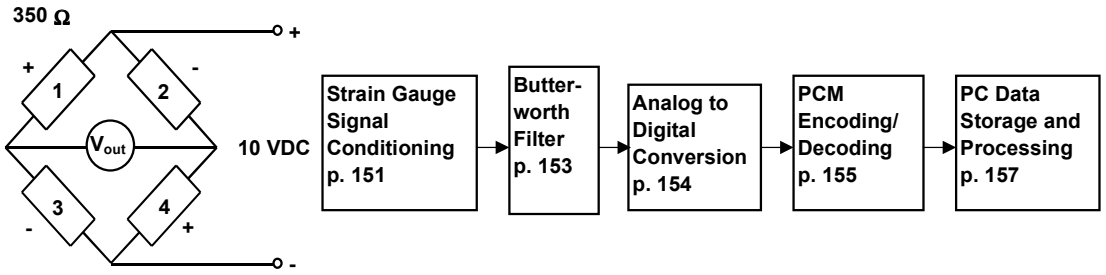

Calibration Procedures (See p. 110)

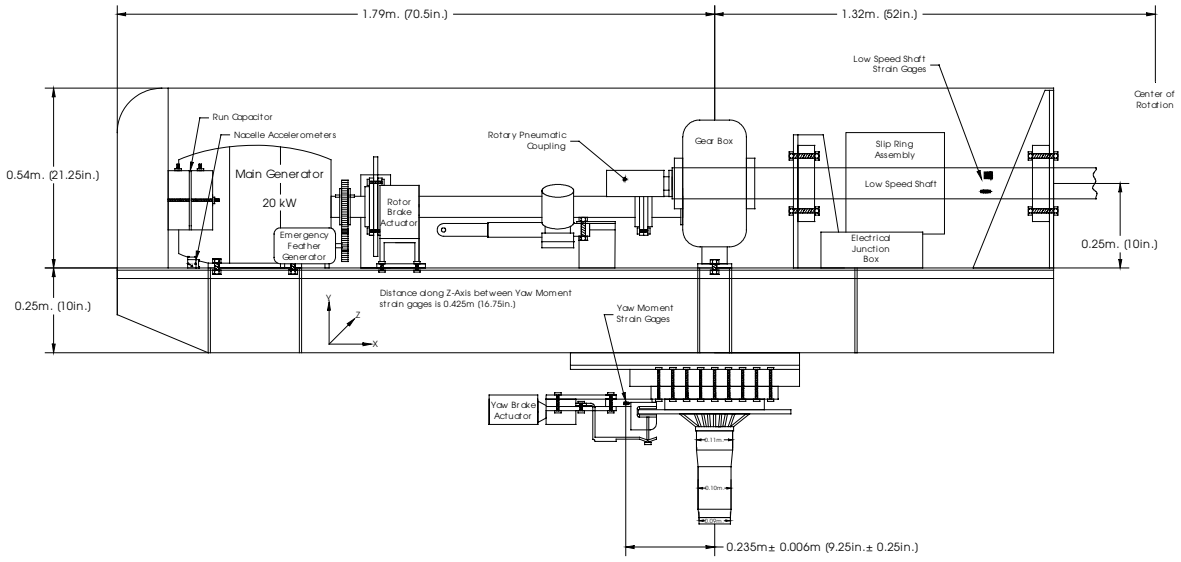

Figure H-3. Yaw moment strain gauge configuration with original yaw shaft and brake mechanism

Appendix I: Tares for Wind Tunnel Scales

The wind tunnel scales provide the capability of resolving three forces and three moments applied to the wind turbine while in operation. The tare coefficients are necessary to remove the effect of the support structure. Weight tare coefficients remove the influence of the rotor overhanging moment from the pitch and roll moments as a function of turbine yaw angle. The aerodynamic drag induced by the tower and/or the nacelle can be eliminated using aerodynamic tare coefficients. The data necessary for computing these tare coefficients is included in this appendix. Because of the ground loop problems associated with the majority of the balance system load cell measurements throughout the wind tunnel test, weight and aerodynamic tare coefficients were not computed and applied to the processed data. The tare data was obtained with the wind turbine in the upwind configuration.

This appendix supplements and clarifies Section G of the NASA Software Requirements Document included in Appendix D. The weight tares were performed with the turbine in the upwind turbine configuration, and it was parked with a blade 3 azimuth angle of 90º. The weight tare with the blades removed specified in the Software Requirements document was not performed. The turntable angle remained at 0º while the turbine was rotated through a full range of yaw angles. Then the turntable was positioned at 180º while the turbine was again yawed through a full range. In the Software Requirements Document, all references to ALPH, Item 102, are to the model angle of attack, which was always zero. The aerodynamic tares were performed with the tower and nacelle (blades removed) as well as tower alone. The turntable angle remained at 0º throughout.

Weight Tare Coefficients

The weight tare was performed when the tunnel was not operating, and the wind turbine was parked with a blade 3 azimuth angle of 90º. Thirty-second data points were obtained at turbine yaw angles from 0º to 180º in 15º increments. This was repeated from -165º to 0. These data are shown in Tables I-1, I-2, and I-3. Weight tare coefficients could be determined by fitting a curve to the pitch and roll moments as a function of turbine yaw angle. These data were obtained during NASA run numbers 031, 032, and 033.

The first column contains the Julian date and time when the data point was collected. The second column contains the point name. The third column of the table contains the turbine yaw angle, which the NASA data system operator input by hand. The rest of the columns contain channels corresponding to NASA data system output as explained in Appendices D and E. The second row of the table contains the number that corresponds to NASA nomenclature in Appendix D. No tare coefficients were applied during post-processing so the forces and moments in Tables I-1, I-2, and I-3 are more representative of channels 605-610 in Appendix D. Note that the data in the table does *not* use SI units.

Table I-1. Weight Tare Run 031 for Upwind Turbine Configuration, Turntable = 0º

DATE/TIME	TEST NAME	TURBINE_YAW	RHO_DIG	Q_DIG	VFPS_DIG	LIFT,W_S	DRAG,W_S	SIDE,W_S	PTCH,W_S	ROLL,W_S	YAW,W_S
			445	440	450	611	612	613	614	615	616
		deg	slug/ft^3	psf	ft/s	lb	lb	lb	lb	lb	lb
118:16:39:22	TURB Y UP1	0.00E+00	2.38E-03	6.15E-02	7.19E+00	2.39E+01	3.68E+00	-7.42E+00	1.48E+02	4.98E+02	1.67E+02
118:16:40:45	TURB Y UP1	1.50E+01	2.38E-03	6.16E-02	7.20E+00	2.58E+01	-5.00E-01	-8.30E+00	2.43E+02	1.66E+03	1.70E+02
118:16:42:45	TURB Y UP1	4.50E+01	2.38E-03	9.93E-02	9.14E+00	2.62E+01	2.52E+00	-9.76E+00	1.32E+03	3.85E+03	2.48E+02
118:16:43:57	TURB Y UP1	1.35E+02	2.38E-03	7.35E-02	7.86E+00	3.20E+01	-6.74E-01	-6.46E+00	7.65E+03	4.21E+03	2.34E+02
118:16:46:30	TURB Y UP1	-1.35E+02	2.38E-03	4.65E-02	6.25E+00	3.22E+01	1.81E+00	-9.00E+00	7.90E+03	-2.27E+03	2.11E+02
118:16:47:39	TURB Y UP1	-4.50E+01	2.38E-03	3.23E-02	5.21E+00	2.55E+01	-3.35E-01	-8.01E+00	1.65E+03	-2.53E+03	1.72E+02
118:16:48:51	TURB Y UP1	0.00E+00	2.38E-03	5.76E-02	6.95E+00	2.29E+01	-6.14E-01	-8.66E+00	1.66E+02	4.55E+02	1.91E+02
118:16:50:13	TURB Y UP1	-9.00E+01	2.38E-03	2.05E-02	4.15E+00	3.06E+01	-1.80E+00	-9.24E+00	4.84E+03	-3.61E+03	2.09E+02
118:16:51:23	TURB Y UP1	-1.80E+02	2.38E-03	5.28E-02	6.66E+00	2.84E+01	-4.41E-01	-1.27E+01	9.12E+03	1.37E+03	2.08E+02
118:16:52:34	TURB Y UP1	9.00E+01	2.38E-03	5.99E-02	7.10E+00	2.52E+01	-3.49E+00	-8.90E+00	4.40E+03	5.34E+03	1.85E+02
118:16:53:47	TURB Y UP1	0.00E+00	2.38E-03	3.14E-02	5.14E+00	2.07E+01	-2.14E-01	-8.80E+00	1.34E+02	5.33E+02	1.83E+02

Table I-2. Weight Tare Run 032 for Upwind Turbine Configuration, Turntable = 0º

DATE/TIME	TEST NAME	TURBINE_YAW	RHO_DIG	Q_DIG	VFPS_DIG	LIFT,W_S	DRAG,W_S	SIDE,W_S	PTCH,W_S	ROLL,W_S	YAW,W_S
			445	440	450	611	612	613	614	615	616
		deg	slug/ft^3	psf	ft/s	lb	lb	lb	lb	lb	lb
118:21:25:49	TURB Y UP2	0.00E+00	2.41E-03	7.00E-03	2.41E+00	5.32E+01	-3.36E+01	-3.55E+01	-8.58E+03	-1.04E+03	-5.34E+01
118:21:26:45	TURB Y UP2	0.00E+00	2.41E-03	0.00E+00	0.00E+00	4.58E+00	1.79E+00	1.05E+00	-1.13E+02	-3.05E+01	-7.31E+00
118:21:28:00	TURB Y UP2	1.50E+01	2.41E-03	9.10E-03	2.75E+00	-4.07E+00	2.24E+00	-3.06E-01	-2.52E+01	1.14E+03	1.16E+01
118:21:28:56	TURB Y UP2	3.00E+01	2.41E-03	3.12E-02	5.09E+00	3.11E+00	4.82E-01	-2.26E+00	4.04E+02	2.54E+03	2.35E+01
118:21:29:53	TURB Y UP2	3.00E+01	2.41E-03	5.69E-03	2.18E+00	1.26E+00	7.02E-01	-1.45E+00	4.38E+02	2.35E+03	4.14E+00
118:21:30:46	TURB Y UP2	4.50E+01	2.41E-03	2.21E-02	4.29E+00	3.76E+00	1.85E+00	-3.63E-02	1.03E+03	3.26E+03	1.27E+01
118:21:31:46	TURB Y UP2	6.00E+01	2.41E-03	4.02E-03	1.83E+00	3.79E+00	-2.32E+00	-8.64E-01	2.04E+03	4.15E+03	2.56E+01
118:21:32:45	TURB Y UP2	7.50E+01	2.41E-03	1.53E-02	3.57E+00	5.62E+00	-1.11E+00	6.06E-01	3.10E+03	4.58E+03	1.07E+01
118:21:33:40	TURB Y UP2	9.00E+01	2.41E-03	2.05E-02	4.13E+00	5.16E+00	-9.81E-01	-1.75E-01	4.23E+03	4.92E+03	2.17E+00
118:21:34:35	TURB Y UP2	1.05E+02	2.41E-03	1.34E-02	3.34E+00	3.24E+00	6.68E-01	-8.70E-03	5.28E+03	4.76E+03	6.89E+00
118:21:35:30	TURB Y UP2	1.20E+02	2.41E-03	2.60E-04	4.65E-01	8.55E+00	1.79E+00	1.99E+00	6.38E+03	4.33E+03	-1.56E+01
118:21:36:25	TURB Y UP2	1.35E+02	2.41E-03	8.35E-03	2.63E+00	1.10E+01	8.25E-01	8.55E-01	7.40E+03	3.73E+03	-1.38E+01
118:21:37:21	TURB Y UP2	1.50E+02	2.41E-03	9.55E-03	2.82E+00	6.86E+00	1.25E+00	2.52E+00	8.14E+03	2.78E+03	-2.64E+01
118:21:38:20	TURB Y UP2	1.65E+02	2.41E-03	1.41E-02	3.43E+00	7.83E+00	5.17E-01	4.94E+00	8.70E+03	1.62E+03	-2.23E+01
118:21:39:20	TURB Y UP2	1.80E+02	2.41E-03	0.00E+00	0.00E+00	1.24E+01	2.26E+00	2.80E+00	8.81E+03	5.43E+02	-2.97E+01
118:21:41:22	TURB Y UP2	-1.65E+02	2.41E-03	4.02E-03	1.83E+00	6.81E+00	1.66E+00	1.43E+00	8.74E+03	-5.92E+02	1.40E+01
118:21:42:22	TURB Y UP2	-1.50E+02	2.41E-03	2.08E-03	1.31E+00	4.40E+00	2.85E-01	1.30E+00	8.50E+03	-1.72E+03	4.02E+00
118:21:43:19	TURB Y UP2	-1.35E+02	2.41E-03	2.82E-02	4.84E+00	2.72E+00	1.08E+00	-5.03E-01	7.67E+03	-2.59E+03	1.83E+01
118:21:44:13	TURB Y UP2	-1.20E+02	2.41E-03	0.00E+00	0.00E+00	4.89E+00	1.12E+00	3.83E-01	6.80E+03	-3.46E+03	-1.88E+01
118:21:45:08	TURB Y UP2	-1.05E+02	2.41E-03	7.57E-03	2.51E+00	5.22E+00	1.41E+00	1.39E+00	5.78E+03	-4.04E+03	-6.29E+01
118:21:46:01	TURB Y UP2	-9.00E+01	2.41E-03	1.72E-02	3.78E+00	4.68E+00	-5.17E-02	2.27E+00	4.62E+03	-4.32E+03	-3.24E+01
118:21:47:30	TURB Y UP2	-7.50E+01	2.41E-03	4.18E-03	1.86E+00	5.04E+00	3.27E-01	3.02E+00	3.48E+03	-4.24E+03	-6.79E+01
118:21:48:23	TURB Y UP2	-6.00E+01	2.41E-03	8.09E-03	2.59E+00	4.93E-01	1.87E-01	3.18E+00	2.40E+03	-3.87E+03	-4.97E+01
118:21:49:21	TURB Y UP2	-4.50E+01	2.41E-03	1.18E-02	3.14E+00	-1.86E+00	2.04E-02	2.94E+00	1.37E+03	-3.20E+03	-5.62E+01
118:21:50:13	TURB Y UP2	-3.00E+01	2.41E-03	2.16E-02	4.23E+00	4.30E-01	-2.20E-01	2.12E+00	6.41E+02	-2.26E+03	-7.76E+00
118:21:51:02	TURB Y UP2	-1.50E+01	2.41E-03	7.47E-03	2.49E+00	1.26E+00	4.69E-02	1.49E+00	2.08E+02	-1.19E+03	-2.02E+01
118:21:51:52	TURB Y UP2	0.00E+00	2.41E-03	1.68E-02	3.73E+00	-8.66E-01	1.26E+00	3.81E+00	-1.34E+02	-9.29E+01	-4.87E+01

Table I-3. Weight Tare Run 033 for Upwind Turbine Configuration, Turntable = 180º

DATE/TIME	TEST NAME	TURBINE_YAW	RHO_DIG	Q_DIG	VFPS_DIG	LIFT,W_S	DRAG,W_S	SIDE,W_S	PTCH,W_S	ROLL,W_S	YAW,W_S
			445	440	450	611	612	613	614	615	616
		deg	slug/ft^3	psf	ft/s	lb	lb	lb	lb	lb	lb
118:22:19:50	TURB Y UP2	0.00E+00	2.41E-03	8.00E-03	2.58E+00	5.76E+02	1.03E+01	-5.98E+01	1.00E+06	-2.48E+05	1.24E+02
118:22:25:57	TURB Y UP3	1.50E+01	2.41E-03	0.00E+00	0.00E+00	1.62E+00	-2.18E+00	1.07E+00	3.69E+02	1.11E+03	-4.18E+01
118:22:27:01	TURB Y UP3	3.00E+01	2.41E-03	9.72E-03	2.84E+00	-1.67E+00	-2.17E+00	2.09E+00	7.54E+02	2.09E+03	2.27E+00
118:22:27:54	TURB Y UP3	4.50E+01	2.41E-03	0.00E+00	0.00E+00	2.87E-02	-3.44E+00	6.58E+00	1.43E+03	2.77E+03	2.95E+01
118:22:29:03	TURB Y UP3	6.00E+01	2.41E-03	7.35E-03	2.47E+00	-4.24E+00	-2.62E+00	1.73E+00	2.23E+03	3.80E+03	-1.05E+01
118:22:30:10	TURB Y UP3	7.50E+01	2.41E-03	9.37E-03	2.79E+00	-7.46E-01	-3.41E+00	1.00E+00	3.39E+03	4.34E+03	-1.40E+01
118:22:31:16	TURB Y UP3	9.00E+01	2.41E-03	1.27E-04	3.24E-01	2.15E+00	-2.99E+00	1.02E+00	4.47E+03	4.62E+03	-2.97E+01
118:22:32:11	TURB Y UP3	1.05E+02	2.41E-03	1.93E-03	1.27E+00	3.03E+00	-1.70E+00	1.43E+00	5.71E+03	4.56E+03	-7.19E+01
118:22:33:03	TURB Y UP3	1.20E+02	2.41E-03	8.87E-03	2.71E+00	1.81E+00	-3.25E+00	3.58E+00	6.79E+03	4.01E+03	-7.27E+01
118:22:34:03	TURB Y UP3	1.35E+02	2.41E-03	1.95E-02	4.02E+00	2.75E-01	-4.20E+00	9.18E-01	7.81E+03	3.51E+03	-8.28E+00
118:22:35:57	TURB Y UP3	1.50E+02	2.41E-03	0.00E+00	0.00E+00	6.75E-01	-2.86E+00	9.55E-01	8.51E+03	2.59E+03	-2.37E+01
118:22:36:51	TURB Y UP3	1.65E+02	2.41E-03	0.00E+00	0.00E+00	4.17E+00	-2.06E+00	1.90E+00	8.98E+03	1.52E+03	-4.55E+01
118:22:37:45	TURB Y UP3	1.80E+02	2.41E-03	0.00E+00	0.00E+00	5.97E+00	-2.79E+00	1.49E+00	9.30E+03	3.77E+02	-6.14E+01
118:22:38:41	TURB Y UP3	-1.65E+02	2.41E-03	7.63E-03	2.52E+00	6.39E+00	-5.20E-01	3.06E+00	9.13E+03	-8.74E+02	-6.12E+01
118:22:39:38	TURB Y UP3	-1.50E+02	2.41E-03	2.39E-02	4.45E+00	5.54E+00	-1.94E+00	1.95E+00	8.79E+03	-1.96E+03	-3.90E+01
118:22:40:35	TURB Y UP3	-1.35E+02	2.41E-03	2.31E-02	4.38E+00	1.47E+00	-5.41E+00	2.23E+00	8.19E+03	-2.94E+03	-6.00E+01
118:22:41:33	TURB Y UP3	-1.35E+02	2.41E-03	1.52E-02	3.55E+00	1.36E+00	-3.44E+00	1.76E+00	8.15E+03	-2.87E+03	-1.28E+01
118:22:42:24	TURB Y UP3	-1.20E+02	2.41E-03	3.91E-03	1.80E+00	2.50E+00	-2.97E+00	1.61E+00	7.27E+03	-3.70E+03	-1.32E+01
118:22:43:24	TURB Y UP3	-1.05E+02	2.41E-03	0.00E+00	0.00E+00	3.19E+00	-5.81E+00	3.20E+00	6.34E+03	-4.22E+03	-5.25E+01
118:22:44:24	TURB Y UP3	-9.00E+01	2.41E-03	0.00E+00	0.00E+00	1.79E+00	-1.74E+00	3.62E+00	5.00E+03	-4.46E+03	-6.70E+01
118:22:45:20	TURB Y UP3	-7.50E+01	2.41E-03	1.14E-02	3.07E+00	3.72E+00	-4.63E+00	4.11E+00	4.00E+03	-4.47E+03	-3.46E+01
118:22:46:13	TURB Y UP3	-6.00E+01	2.41E-03	1.09E-02	3.00E+00	-1.17E+00	-3.57E+00	3.82E+00	2.84E+03	-4.03E+03	-4.82E+01
118:22:47:09	TURB Y UP3	-4.50E+01	2.41E-03	1.03E-03	9.26E-01	5.64E-02	-4.61E+00	5.39E+00	1.96E+03	-3.42E+03	-4.05E+01
118:22:48:04	TURB Y UP3	-3.00E+01	2.41E-03	1.16E-02	3.10E+00	-9.51E-01	-3.97E+00	3.36E+00	1.10E+03	-2.47E+03	-2.12E+01
118:22:48:57	TURB Y UP3	-1.50E+01	2.41E-03	2.48E-02	4.54E+00	-6.09E-01	-2.64E+00	4.71E+00	5.63E+02	-1.54E+03	-1.81E+01
118:22:49:51	TURB Y UP3	0.00E+00	2.41E-03	1.06E-02	2.96E+00	-1.86E+00	-3.58E+00	4.44E+00	3.90E+02	-3.63E+02	-4.13E+01

Aerodynamic Tare Coefficients

Aerodynamic tare coefficients could be determined in order to eliminate aerodynamic effects for two configurations: tower and nacelle (blades removed) or tower alone. Data for the tower and nacelle configuration was obtained by yawing the turbine with the blades removed at several wind speeds. Fifteen-second data points were obtained using the NASA data system at yaw angles of 0º, 5º, 10º, 30º, 45º, 90º, 135º, 150º, 170º, 175º, 180º, -175º, -170º, -150º, -135º, -90º, -45º, -30º, -10º, and -5º. This was repeated for each wind speed, 5 m/s, 7 m/s, 10 m/s, 15 m/s, 20 m/s, and 25 m/s. The turntable angle remained at 0º throughout. Using NASA nomenclature, this data was obtained during run 056.

Table I-4 contains the data necessary for computing aerodynamic tare coefficients for the tower and nacelle (blades removed) configuration. The first column contains the Julian date and time when the data point was collected. The second column contains the point name using a convention similar to that used during the majority of the wind tunnel tests. The first two digits 'AT' indicate aerodynamic tare; the next two digits represent the nominal wind speed in m/s; the next four digits represent the turbine yaw angle; and the last digit is reserved for repeated points. The third column of the table contains the turbine yaw angle, which the NASA data system operator input manually. The rest of the columns contain channels corresponding to NASA data system output as explained in Appendices D and E. The second row of the table contains the number that corresponds to NASA nomenclature in Appendix D. No tare coefficients were applied during post-processing so the forces and moments in Table I-4 are more representative of channels 605-610 in Appendix D. Note that the data in the table does *not* use SI units.

Aerodynamic tare coefficients can be computed by fitting a curve to each force and moment as a function of yaw angle. A separate curve is required for each Q, or wind speed. The value for each force or moment at a given dynamic pressure and yaw angle is subtracted from the measured force or moment during operation.

Once the nacelle was removed from the tower, an aerodynamic tare run (run 058) was performed to determine the aerodynamic effect of the tower alone. In this case, 30-second data points were collected using the NASA data system at wind speeds of 5 m/s, 7 m/s, 9 m/s, 10 m/s, 12 m/s, 14 m/s, 15 m/s, 20 m/s, and 25 m/s. These data are included in Table I-5. In this case, the aerodynamic tare coefficients are a function of dynamic pressure only.

Application of aerodynamic tare coefficients must be done for sequences where the turntable angle remained at 0º. Additionally, the quality of data from the load cells should be ascertained using Table E-2.

Table I-4. Aerodynamic Tare Run 056 with Tower and Nacelle (Blades Removed)

DATE/TIME	TEST NAME	TURBINE_YAW	RHO_DIG	Q_DIG	VFPS_DIG	LIFT,W_S	DRAG,W_S	SIDE,W_S	PTCH,W_S	ROLL,W_S	YAW,W_S
			445	440	450	611	612	613	614	615	616
		deg	slug/ft^3	psf	ft/s	lb	lb	lb	lb	lb	lb
152:08:33:08		0.00E+00	2.37E-03	0.00E+00	0.00E+00	2.16E+00	-1.96E+00	6.06E-01	7.29E+01	-8.37E+00	-2.34E+01
152:08:48:10	AT0500000	0.00E+00	2.36E-03	3.15E-01	1.64E+01	7.24E+00	2.03E+01	2.13E+00	-4.10E+02	-7.87E+01	-7.72E+01
152:08:52:32	AT0500050	5.00E+00	2.36E-03	3.15E-01	1.64E+01	9.38E+00	2.17E+01	-6.19E-01	-3.84E+02	3.74E+02	-3.26E+01
152:08:53:26	AT0500100	1.00E+01	2.36E-03	3.15E-01	1.64E+01	1.15E+01	2.28E+01	-1.17E+00	-4.30E+02	6.59E+02	2.48E+01
152:08:54:14	AT0500300	3.00E+01	2.36E-03	3.11E-01	1.63E+01	1.33E+01	2.45E+01	2.03E+00	-1.38E+02	1.67E+03	4.00E+01
152:08:54:54	AT0500450	4.50E+01	2.36E-03	3.12E-01	1.63E+01	1.83E+01	2.86E+01	2.45E+00	2.83E+02	2.42E+03	1.43E+01
152:08:55:33	AT0500900	9.00E+01	2.35E-03	3.15E-01	1.63E+01	1.68E+01	3.07E+01	-2.78E-01	2.36E+03	3.47E+03	1.91E+01
152:08:56:01	AT0500901	9.00E+01	2.36E-03	3.12E-01	1.63E+01	1.35E+01	3.14E+01	-1.76E-02	2.36E+03	3.44E+03	5.78E+00
152:08:56:54	AT0501350	1.35E+02	2.35E-03	3.14E-01	1.63E+01	1.80E+01	2.99E+01	-5.16E+00	4.61E+03	2.70E+03	3.06E+01
152:08:57:35	AT0501500	1.50E+02	2.35E-03	3.13E-01	1.63E+01	1.52E+01	2.55E+01	-5.36E+00	5.15E+03	2.13E+03	2.53E+01
152:08:58:18	AT0501700	1.70E+02	2.35E-03	3.16E-01	1.64E+01	1.82E+01	2.14E+01	-9.71E-01	5.73E+03	1.06E+03	-2.75E+01
152:08:59:04	AT0501750	1.75E+02	2.35E-03	3.19E-01	1.65E+01	1.78E+01	2.15E+01	-1.01E+00	5.70E+03	8.93E+02	-3.74E+01
152:08:59:38	AT0501800	1.80E+02	2.35E-03	3.16E-01	1.64E+01	1.65E+01	2.17E+01	4.98E-01	5.78E+03	6.38E+02	-2.80E+01
152:09:00:34	AT05M1750	-1.75E+02	2.35E-03	3.23E-01	1.66E+01	1.74E+01	2.18E+01	1.06E+00	5.82E+03	4.15E+02	-4.38E+01
152:09:01:20	AT05M1700	-1.70E+02	2.35E-03	3.19E-01	1.65E+01	1.63E+01	2.33E+01	1.23E+00	5.77E+03	1.79E+02	-3.91E+01
152:09:01:56	AT05M1500	-1.50E+02	2.35E-03	3.18E-01	1.64E+01	1.58E+01	2.62E+01	3.50E+00	5.46E+03	-8.34E+02	-6.01E+01
152:09:02:32	AT05M1350	-1.35E+02	2.35E-03	3.18E-01	1.65E+01	1.75E+01	2.87E+01	5.40E+00	5.03E+03	-1.62E+03	-1.19E+02
152:09:03:17	AT05M0900	-9.00E+01	2.36E-03	3.16E-01	1.64E+01	1.44E+01	3.18E+01	2.85E+00	2.90E+03	-2.84E+03	-5.45E+01
152:09:04:00	AT05M0450	-4.50E+01	2.36E-03	3.16E-01	1.64E+01	1.74E+01	2.87E+01	-3.55E+00	6.51E+02	-2.10E+03	-6.05E+01
152:09:04:36	AT05M0300	-3.00E+01	2.36E-03	3.11E-01	1.63E+01	1.27E+01	2.52E+01	-2.19E+00	1.16E+02	-1.49E+03	-4.64E+01
152:09:05:12	AT05M0100	-1.00E+01	2.36E-03	3.19E-01	1.65E+01	1.13E+01	2.17E+01	-2.40E+00	-2.58E+02	-3.67E+02	-5.35E+01
152:09:05:52	AT05M0050	-5.00E+00	2.36E-03	3.15E-01	1.64E+01	8.16E+00	2.37E+01	1.35E+00	-4.80E+02	-3.16E+02	-5.87E+01
152:09:11:18	AT0700000	0.00E+00	2.35E-03	6.15E-01	2.29E+01	6.87E+00	3.77E+01	7.09E-01	-7.03E+02	7.41E+01	-1.57E+01
152:09:12:00	AT07M0050	-5.00E+00	2.35E-03	6.15E-01	2.29E+01	9.86E+00	3.78E+01	1.16E+00	-6.51E+02	-2.78E+02	-4.18E+01
152:09:12:32	AT07M0100	-1.00E+01	2.35E-03	6.17E-01	2.29E+01	1.32E+01	3.88E+01	1.10E+00	-5.80E+02	-5.89E+02	-7.57E+01
152:09:13:17	AT07M0300	-3.00E+01	2.35E-03	6.14E-01	2.28E+01	2.07E+01	4.44E+01	-3.52E+00	-4.64E+01	-1.60E+03	-4.21E+01
152:09:14:01	AT07M0450	-4.50E+01	2.35E-03	6.17E-01	2.29E+01	2.81E+01	5.11E+01	-4.17E+00	4.10E+02	-2.19E+03	-4.41E+01
152:09:14:47	AT07M0900	-9.00E+01	2.35E-03	6.12E-01	2.28E+01	2.69E+01	5.45E+01	3.55E+00	2.61E+03	-2.80E+03	-1.39E+02
152:09:15:32	AT07M1350	-1.35E+02	2.35E-03	6.15E-01	2.29E+01	2.66E+01	5.09E+01	1.10E+01	4.75E+03	-1.61E+03	-1.01E+02
152:09:16:13	AT07M1500	-1.50E+02	2.35E-03	6.13E-01	2.28E+01	2.23E+01	4.47E+01	1.68E+01	5.24E+03	-1.20E+03	-1.40E+02
152:09:16:51	AT07M1700	-1.70E+02	2.35E-03	6.12E-01	2.28E+01	1.79E+01	3.85E+01	1.15E+01	5.49E+03	-2.12E+02	-1.14E+02

Table I-4. Aerodynamic Tare Run 056 with Tower and Nacelle (Blades Removed) (cont.)

DATE/TIME	TEST NAME	TURBINE_YAW	RHO_DIG	Q_DIG	VFPS_DIG	LIFT,W_S	DRAG,W_S	SIDE,W_S	PTCH,W_S	ROLL,W_S	YAW,W_S
			445	440	450	611	612	613	614	615	616
		deg	slug/ft^3	psf	ft/s	lb	lb	lb	lb	lb	lb
152:09:17:26	AT07M1750	-1.75E+02	2.35E-03	6.08E-01	2.27E+01	1.65E+01	3.68E+01	1.08E+01	5.54E+03	1.66E+01	-1.27E+02
152:09:18:03	AT0701800	1.80E+02	2.35E-03	6.11E-01	2.28E+01	1.79E+01	3.61E+01	1.06E+01	5.52E+03	2.68E+02	-1.44E+02
152:09:18:41	AT0701750	1.75E+02	2.35E-03	6.13E-01	2.28E+01	1.79E+01	3.79E+01	5.26E-01	5.45E+03	7.91E+02	-2.14E+01
152:09:19:11	AT0701700	1.70E+02	2.35E-03	6.14E-01	2.29E+01	1.65E+01	3.87E+01	5.84E-01	5.37E+03	1.00E+03	-6.12E+01
152:09:19:45	AT0701500	1.50E+02	2.35E-03	6.12E-01	2.28E+01	1.89E+01	4.49E+01	-4.58E+00	4.92E+03	1.97E+03	-2.22E+01
152:09:20:25	AT0701350	1.35E+02	2.35E-03	6.18E-01	2.29E+01	2.50E+01	4.93E+01	-8.13E-01	4.46E+03	2.41E+03	-4.01E+01
152:09:21:09	AT0700900	9.00E+01	2.35E-03	6.19E-01	2.29E+01	2.05E+01	5.44E+01	8.44E+00	2.01E+03	3.17E+03	-5.68E+01
152:09:21:54	AT0700450	4.50E+01	2.35E-03	6.18E-01	2.29E+01	2.25E+01	5.00E+01	1.46E+01	3.68E+01	2.20E+03	-1.31E+02
152:09:22:31	AT0700300	3.00E+01	2.35E-03	6.16E-01	2.29E+01	1.17E+01	4.38E+01	1.50E+01	-4.52E+02	1.35E+03	-1.20E+02
152:09:23:15	AT0700100	1.00E+01	2.35E-03	6.12E-01	2.28E+01	8.28E+00	3.92E+01	1.00E+01	-7.26E+02	3.22E+02	-8.86E+01
152:09:24:03	AT0700050	5.00E+00	2.35E-03	6.12E-01	2.28E+01	7.08E+00	3.82E+01	9.02E+00	-7.08E+02	6.25E+01	-1.16E+02
152:09:29:30	AT1000000	0.00E+00	2.35E-03	1.25E+00	3.27E+01	9.58E+00	5.90E+01	2.33E+01	-1.06E+03	-4.37E+02	-2.09E+02
152:09:30:01	AT1000050	5.00E+00	2.35E-03	1.25E+00	3.27E+01	6.13E+00	5.90E+01	2.13E+01	-1.03E+03	1.79E+01	-1.68E+02
152:09:30:40	AT1000100	1.00E+01	2.35E-03	1.25E+00	3.26E+01	6.01E+00	5.94E+01	2.44E+01	-9.67E+02	2.45E+02	-2.18E+02
152:09:31:18	AT1000300	3.00E+01	2.35E-03	1.24E+00	3.25E+01	1.76E+01	7.28E+01	2.96E+01	-8.11E+02	1.39E+03	-2.01E+02
152:09:31:51	AT1000450	4.50E+01	2.35E-03	1.25E+00	3.26E+01	3.72E+01	8.30E+01	3.59E+01	-3.11E+02	1.96E+03	-2.30E+02
152:09:32:36	AT1000900	9.00E+01	2.35E-03	1.25E+00	3.26E+01	3.54E+01	9.20E+01	2.18E+01	1.73E+03	2.90E+03	-1.53E+02
152:09:33:22	AT1001350	1.35E+02	2.35E-03	1.26E+00	3.27E+01	3.39E+01	8.69E+01	3.95E+00	4.01E+03	2.21E+03	-7.96E+01
152:09:34:10	AT1001500	1.50E+02	2.35E-03	1.26E+00	3.27E+01	2.40E+01	7.46E+01	4.50E+00	4.57E+03	1.70E+03	-8.34E+01
152:09:34:47	AT1001700	1.70E+02	2.35E-03	1.26E+00	3.28E+01	1.73E+01	5.97E+01	1.95E+01	5.14E+03	6.30E+02	-2.17E+02
152:09:35:18	AT1001750	1.75E+02	2.35E-03	1.26E+00	3.28E+01	1.81E+01	5.80E+01	2.14E+01	5.18E+03	4.08E+02	-2.00E+02
152:09:35:50	AT1001800	1.80E+02	2.35E-03	1.26E+00	3.28E+01	1.79E+01	5.75E+01	2.30E+01	5.24E+03	7.30E+01	-2.27E+02
152:09:36:32	AT10M1750	-1.75E+02	2.35E-03	1.26E+00	3.28E+01	1.25E+01	5.87E+01	2.65E+01	5.10E+03	-1.34E+02	-2.45E+02
152:09:37:04	AT10M1700	-1.70E+02	2.35E-03	1.26E+00	3.27E+01	1.35E+01	5.83E+01	2.66E+01	5.17E+03	-2.90E+02	-2.65E+02
152:09:37:41	AT10M1500	-1.50E+02	2.35E-03	1.25E+00	3.26E+01	2.27E+01	7.34E+01	3.91E+01	4.75E+03	-1.31E+03	-3.56E+02
152:09:38:15	AT10M1350	-1.35E+02	2.35E-03	1.25E+00	3.26E+01	3.38E+01	8.57E+01	4.15E+01	4.35E+03	-2.08E+03	-3.90E+02
152:09:38:58	AT10M0900	-9.00E+01	2.35E-03	1.26E+00	3.27E+01	3.07E+01	9.31E+01	2.49E+01	2.21E+03	-3.17E+03	-3.06E+02
152:09:39:42	AT10M0450	-4.50E+01	2.35E-03	1.25E+00	3.26E+01	3.55E+01	8.53E+01	4.39E+00	1.53E+01	-2.42E+03	-1.61E+02
152:09:40:16	AT10M0300	-3.00E+01	2.35E-03	1.25E+00	3.26E+01	2.16E+01	7.51E+01	1.03E+01	-5.97E+02	-1.92E+03	-2.23E+02
152:09:40:50	AT10M0100	-1.00E+01	2.35E-03	1.25E+00	3.26E+01	7.78E+00	6.31E+01	1.50E+01	-1.07E+03	-8.42E+02	-1.99E+02
152:09:41:24	AT10M0050	-5.00E+00	2.35E-03	1.25E+00	3.26E+01	8.54E+00	6.22E+01	1.14E+01	-1.04E+03	-5.42E+02	-1.72E+02
152:09:51:30	AT1500000	0.00E+00	2.34E-03	2.83E+00	4.91E+01	1.21E+01	9.28E+01	-7.61E+00	-1.70E+03	1.68E+02	-7.95E+01

Table I-4. Aerodynamic Tare Run 056 with Tower and Nacelle (Blades Removed) (cont.)

DATE/TIME	TEST NAME	TURBINE_YAW deg	RHO_DIG 445 slug/ft^3	Q_DIG 440 psf	VFPS_DIG 450 ft/s	LIFT,W_S 611 lb	DRAG,W_S 612 lb	SIDE,W_S 613 lb	PTCH,W_S 614 lb	ROLL,W_S 615 lb	YAW,W_S 616 lb
152:09:52:29	AT15M0050	-5.00E+00	2.35E-03	2.83E+00	4.91E+01	1.32E+01	9.46E+01	-8.75E+00	-1.67E+03	-2.32E+02	-3.39E+01
152:09:53:04	AT15M0100	-1.00E+01	2.35E-03	2.81E+00	4.90E+01	1.65E+01	9.81E+01	-1.11E+01	-1.58E+03	-6.48E+02	-5.04E+01
152:09:53:57	AT15M0300	-3.00E+01	2.34E-03	2.81E+00	4.90E+01	3.89E+01	1.28E+02	-2.55E+01	-1.19E+03	-1.66E+03	-1.89E+01
152:09:55:02	AT15M0450	-4.50E+01	2.35E-03	2.82E+00	4.91E+01	7.95E+01	1.54E+02	-3.89E+01	-6.72E+02	-2.21E+03	6.00E+01
152:09:55:44	AT15M0900	-9.00E+01	2.34E-03	2.81E+00	4.90E+01	6.16E+01	1.63E+02	-4.14E-01	1.56E+03	-2.84E+03	-2.16E+02
152:09:56:28	AT15M1350	-1.35E+02	2.34E-03	2.82E+00	4.91E+01	6.28E+01	1.51E+02	4.07E+01	3.57E+03	-1.64E+03	-4.01E+02
152:09:57:04	AT15M1500	-1.50E+02	2.34E-03	2.82E+00	4.91E+01	4.59E+01	1.19E+02	3.35E+01	4.12E+03	-1.15E+03	-3.54E+02
152:09:57:45	AT15M1700	-1.70E+02	2.34E-03	2.82E+00	4.91E+01	2.65E+01	9.52E+01	8.94E+00	4.33E+03	-1.39E+02	-2.03E+02
152:09:58:15	AT15M1750	-1.75E+02	2.34E-03	2.81E+00	4.90E+01	2.24E+01	9.11E+01	-2.86E-01	4.48E+03	2.22E+02	-1.48E+02
152:09:58:52	AT1501800	1.80E+02	2.34E-03	2.83E+00	4.92E+01	2.20E+01	9.08E+01	-7.66E+00	4.39E+03	5.59E+02	-5.82E+01
152:09:59:30	AT1501750	1.75E+02	2.34E-03	2.83E+00	4.92E+01	2.26E+01	9.08E+01	-1.07E+01	4.41E+03	6.65E+02	-2.66E+01
152:10:00:04	AT1501700	1.70E+02	2.34E-03	2.83E+00	4.91E+01	2.68E+01	9.47E+01	-1.50E+01	4.32E+03	8.99E+02	-7.90E+00
152:10:00:39	AT1501500	1.50E+02	2.34E-03	2.84E+00	4.92E+01	4.80E+01	1.22E+02	-3.78E+01	3.81E+03	1.84E+03	1.54E+02
152:10:01:21	AT1501350	1.35E+02	2.34E-03	2.82E+00	4.91E+01	7.37E+01	1.52E+02	-4.63E+01	3.26E+03	2.36E+03	2.63E+02
152:10:02:05	AT1500900	9.00E+01	2.34E-03	2.82E+00	4.91E+01	6.37E+01	1.65E+02	-7.56E+00	9.90E+02	3.36E+03	1.76E+02
152:10:02:52	AT1500450	4.50E+01	2.34E-03	2.81E+00	4.90E+01	7.66E+01	1.48E+02	2.66E+01	-1.10E+03	2.34E+03	-1.36E+02
152:10:03:32	AT1500300	3.00E+01	2.34E-03	2.82E+00	4.91E+01	4.01E+01	1.24E+02	1.62E+01	-1.53E+03	1.54E+03	-1.53E+02
152:10:04:08	AT1500100	1.00E+01	2.34E-03	2.83E+00	4.92E+01	2.01E+01	9.83E+01	-9.70E-01	-1.77E+03	5.86E+02	-6.43E+01
152:10:04:38	AT1500050	5.00E+00	2.34E-03	2.82E+00	4.91E+01	1.40E+01	9.40E+01	-3.45E+00	-1.72E+03	3.03E+02	-2.77E+01
152:10:11:36	AT2000000	0.00E+00	2.34E-03	5.06E+00	6.57E+01	2.93E+01	1.79E+02	-2.37E+01	-3.34E+03	1.98E+02	1.05E+02
152:10:12:05	AT2000050	5.00E+00	2.34E-03	5.05E+00	6.57E+01	2.98E+01	1.80E+02	-1.85E+01	-3.33E+03	3.91E+02	6.59E+01
152:10:12:34	AT2000100	1.00E+01	2.34E-03	5.04E+00	6.56E+01	3.09E+01	1.88E+02	-1.27E+01	-3.37E+03	7.22E+02	1.34E+01
152:10:13:07	AT2000300	3.00E+01	2.34E-03	5.05E+00	6.57E+01	6.25E+01	2.33E+02	1.32E+01	-3.23E+03	1.93E+03	-2.76E+01
152:10:13:39	AT2000450	4.50E+01	2.34E-03	5.04E+00	6.56E+01	1.29E+02	2.80E+02	3.63E+01	-2.91E+03	2.53E+03	-1.00E+02
152:10:14:27	AT2000900	9.00E+01	2.34E-03	5.05E+00	6.57E+01	1.12E+02	3.10E+02	-2.30E+01	-8.96E+02	3.45E+03	3.32E+02
152:10:15:08	AT2001350	1.35E+02	2.34E-03	5.05E+00	6.57E+01	1.07E+02	2.84E+02	-1.00E+02	1.47E+03	2.46E+03	6.91E+02
152:10:15:40	AT2001500	1.50E+02	2.34E-03	5.06E+00	6.58E+01	8.24E+01	2.31E+02	-8.49E+01	2.01E+03	1.97E+03	5.73E+02
152:10:16:16	AT2001700	1.70E+02	2.34E-03	5.04E+00	6.56E+01	3.99E+01	1.82E+02	-4.71E+01	2.64E+03	1.33E+03	2.97E+02
152:10:16:48	AT2001750	1.75E+02	2.34E-03	5.04E+00	6.56E+01	3.73E+01	1.77E+02	-3.88E+01	2.64E+03	1.01E+03	2.01E+02
152:10:17:19	AT2001800	1.80E+02	2.34E-03	5.07E+00	6.59E+01	3.41E+01	1.75E+02	-3.04E+01	2.68E+03	6.95E+02	1.92E+02
152:10:17:56	AT20M1750	-1.75E+02	2.34E-03	5.04E+00	6.57E+01	3.63E+01	1.77E+02	-1.63E+01	2.70E+03	3.44E+02	6.20E+01
152:10:18:25	AT20M1700	-1.70E+02	2.34E-03	5.04E+00	6.56E+01	4.37E+01	1.81E+02	-5.01E+00	2.66E+03	2.52E+02	2.40E+01

Table I-4. Aerodynamic Tare Run 056 with Tower and Nacelle (Blades Removed) (cont.)

DATE/TIME	TEST NAME	TURBINE_YAW	RHO_DIG	Q_DIG	VFPS_DIG	LIFT,W_S	DRAG,W_S	SIDE,W_S	PTCH,W_S	ROLL,W_S	YAW,W_S
			445	440	450	611	612	613	614	615	616
		deg	slug/ft^3	psf	ft/s	lb	lb	lb	lb	lb	lb
152:10:19:00	AT20M1500	-1.50E+02	2.34E-03	5.04E+00	6.57E+01	8.21E+01	2.24E+02	3.80E+01	2.38E+03	-5.57E+02	-3.18E+02
152:10:19:38	AT20M1350	-1.35E+02	2.33E-03	5.05E+00	6.58E+01	9.53E+01	2.77E+02	5.39E+01	1.90E+03	-1.31E+03	-4.48E+02
152:10:20:25	AT20M0900	-9.00E+01	2.34E-03	5.05E+00	6.58E+01	1.16E+02	3.07E+02	-1.40E+01	-2.62E+02	-2.76E+03	-2.67E+02
152:10:21:12	AT20M0450	-4.50E+01	2.34E-03	5.03E+00	6.56E+01	1.33E+02	2.86E+02	-7.99E+01	-2.55E+03	-2.24E+03	2.60E+02
152:10:21:45	AT20M0300	-3.00E+01	2.34E-03	5.03E+00	6.56E+01	6.60E+01	2.41E+02	-6.32E+01	-3.06E+03	-1.56E+03	1.87E+02
152:10:22:26	AT20M0100	-1.00E+01	2.34E-03	5.04E+00	6.57E+01	3.33E+01	1.91E+02	-3.76E+01	-3.47E+03	-3.78E+02	1.79E+02
152:10:22:58	AT20M0050	-5.00E+00	2.34E-03	5.07E+00	6.58E+01	2.98E+01	1.85E+02	-3.11E+01	-3.47E+03	-1.17E+02	1.42E+02
152:10:27:26	AT2500000	0.00E+00	2.34E-03	7.86E+00	8.20E+01	3.91E+01	2.98E+02	-4.73E+01	-5.79E+03	7.12E+02	2.73E+02
152:10:28:00	AT25M0050	-5.00E+00	2.34E-03	7.85E+00	8.20E+01	4.00E+01	3.05E+02	-5.46E+01	-5.88E+03	2.01E+02	2.70E+02
152:10:28:30	AT25M0100	-1.00E+01	2.34E-03	7.84E+00	8.19E+01	4.70E+01	3.11E+02	-6.66E+01	-5.80E+03	-2.71E+01	3.17E+02
152:10:29:07	AT25M0300	-3.00E+01	2.33E-03	7.84E+00	8.20E+01	1.03E+02	3.93E+02	-1.08E+02	-5.55E+03	-1.14E+03	4.09E+02
152:10:29:41	AT25M0450	-4.50E+01	2.33E-03	7.84E+00	8.20E+01	2.03E+02	4.62E+02	-1.34E+02	-5.00E+03	-1.90E+03	5.11E+02
152:10:30:25	AT25M0900	-9.00E+01	2.33E-03	7.84E+00	8.20E+01	1.67E+02	4.91E+02	-3.11E+01	-2.70E+03	-2.05E+03	-1.49E+02
152:10:31:11	AT25M1350	-1.35E+02	2.33E-03	7.83E+00	8.20E+01	1.34E+02	4.42E+02	6.91E+01	-6.53E+02	-5.90E+02	-5.67E+02
152:10:31:46	AT25M1500	-1.50E+02	2.33E-03	7.85E+00	8.20E+01	1.16E+02	3.65E+02	4.88E+01	-1.75E+02	-1.68E+02	-3.92E+02
152:10:32:20	AT25M1700	-1.70E+02	2.33E-03	7.83E+00	8.19E+01	5.79E+01	2.95E+02	-1.57E+01	3.30E+02	6.54E+02	7.91E+01
152:10:32:54	AT25M1750	-1.75E+02	2.33E-03	7.84E+00	8.20E+01	5.30E+01	2.88E+02	-3.32E+01	4.50E+02	8.39E+02	1.85E+02
152:10:33:31	AT2501800	1.80E+02	2.33E-03	7.86E+00	8.21E+01	5.09E+01	2.86E+02	-5.51E+01	4.47E+02	1.11E+03	2.91E+02
152:10:35:01	AT2501750	1.75E+02	2.33E-03	7.84E+00	8.20E+01	5.50E+01	2.89E+02	-6.68E+01	3.49E+02	1.45E+03	3.84E+02
152:10:35:34	AT2501700	1.70E+02	2.33E-03	7.87E+00	8.22E+01	6.49E+01	2.99E+02	-8.03E+01	2.30E+02	1.76E+03	4.60E+02
152:10:36:14	AT2501500	1.50E+02	2.33E-03	7.85E+00	8.21E+01	1.27E+02	3.74E+02	-1.38E+02	-3.42E+02	2.38E+03	9.43E+02
152:10:36:52	AT2501350	1.35E+02	2.33E-03	7.87E+00	8.21E+01	1.58E+02	4.56E+02	-1.59E+02	-9.04E+02	2.88E+03	1.19E+03
152:10:37:47	AT2500900	9.00E+01	2.34E-03	7.82E+00	8.18E+01	1.70E+02	4.95E+02	-5.09E+01	-3.34E+03	4.36E+03	7.81E+02
152:10:38:34	AT2500450	4.50E+01	2.33E-03	7.81E+00	8.18E+01	2.01E+02	4.50E+02	4.26E+01	-5.37E+03	3.39E+03	1.13E+02
152:10:39:08	AT2500300	3.00E+01	2.33E-03	7.83E+00	8.20E+01	9.28E+01	3.83E+02	1.09E+01	-5.82E+03	2.52E+03	1.55E+02
152:10:39:41	AT2500100	1.00E+01	2.33E-03	7.85E+00	8.21E+01	4.11E+01	3.11E+02	-3.33E+01	-5.93E+03	1.28E+03	2.37E+02
152:10:40:22	AT2500050	5.00E+00	2.33E-03	7.85E+00	8.21E+01	3.85E+01	3.00E+02	-4.19E+01	-5.93E+03	1.11E+03	3.24E+02

Table I-5. Aerodynamic Tare Run 058 with Tower Only

DATE/TIME	TEST NAME	TURBINE_YAW deg	RHO_DIG 445 slug/ft^3	Q_DIG 440 psf	VFPS_DIG 450 ft/s	LIFT,W_S 611 lb	DRAG,W_S 612 lb	SIDE,W_S 613 lb	PTCH,W_S 614 lb	ROLL,W_S 615 lb	YAW,W_S 616 lb
158:16:09:04		0.00E+00	2.33E-03	0.00E+00	0.00E+00	4.06E+03	-6.26E+01	-6.73E+01	-1.95E+03	3.43E+03	3.94E+02
158:16:15:42	ATT000000	0.00E+00	2.33E-03	3.80E-02	5.71E+00	4.07E+03	-6.16E+01	-6.86E+01	-2.03E+03	3.36E+03	4.51E+02
158:16:32:55	ATT050000	0.00E+00	2.34E-03	3.05E-01	1.62E+01	4.65E+00	1.47E+01	-8.61E-01	-2.82E+02	1.12E+02	-3.79E+00
158:16:38:25	ATT070000	0.00E+00	2.33E-03	5.94E-01	2.26E+01	4.73E+00	2.25E+01	1.36E-01	-3.92E+02	6.14E+01	-2.41E+01
158:16:43:41	ATT090000	0.00E+00	2.33E-03	1.02E+00	2.96E+01	1.09E+01	3.28E+01	5.70E+00	-6.22E+02	5.34E+01	-5.48E+01
158:16:49:15	ATT100000	0.00E+00	2.33E-03	1.23E+00	3.25E+01	1.21E+01	3.16E+01	1.89E+01	-7.63E+02	2.25E+01	-1.02E+02
158:16:55:46	ATT120000	0.00E+00	2.33E-03	1.81E+00	3.94E+01	1.92E+01	3.76E+01	-9.08E+00	-9.37E+02	3.37E+02	5.78E+01
158:17:02:27	ATT140000	0.00E+00	2.34E-03	2.48E+00	4.61E+01	2.21E+01	5.57E+01	-1.43E+01	-1.48E+03	4.10E+02	1.08E+02
158:17:07:30	ATT150000	0.00E+00	2.33E-03	2.81E+00	4.91E+01	2.11E+01	6.31E+01	-1.55E+01	-1.66E+03	3.60E+02	1.10E+02
158:17:13:25	ATT200000	0.00E+00	2.33E-03	4.98E+00	6.54E+01	3.30E+01	1.26E+02	-3.53E+01	-3.19E+03	6.44E+02	2.57E+02
158:17:20:56	ATT250000	0.00E+00	2.33E-03	7.89E+00	8.23E+01	4.21E+01	2.16E+02	-5.28E+01	-5.71E+03	8.38E+02	4.25E+02

Appendix J: Wake Flow Visualization: Sequence P

Introduction

Flow visualization of the UAE horizontal-axis wind turbine (HAWT) wake was carried out to provide characterization of the wake kinematics. To visualize the blade tip vortex, smoke was generated within a modified blade tip attached to the instrumented blade, and ejected into the wake through three ports located on the pressure surface of the blade tip. The helical vortex thus visualized was lighted by the mercury vapor lamps in the ceiling of the wind tunnel. The visualized flow field was recorded using two video cameras situated at approximately orthogonal viewing angles. Images from the two cameras were superimposed on a single video frame. In total, 56 minutes of videotaped smoke visualization was obtained with corresponding wind turbine measurements.

Turbine Configuration

During the wake flow visualization sequence, the turbine was configured so that unnecessary complications to aerodynamics and structural dynamics were avoided, while retaining the elements essential to HAWT operation. As such, the rotor was positioned upwind of the tower, to avoid the complexities inherent in the passage of the blade through the tower wake. Similarly, a rigid hub was employed to exclude the aerodynamic and structural couplings that occur when the teeter degree of freedom is active. Finally, a flat rotor was used to avoid any effects due to coning.

Smoke Generation and Ejection

To inject smoke into the blade tip vortex, and thus visualize the wake, the solid tip normally affixed to the instrumented blade was replaced with a specially modified tip. The external contour of the modified blade tip was identical to the normal solid tip. However, the modified tip was fabricated from aluminum, and was hollow to allow a pyrotechnic chemical smoke-generating cartridge to fit within. The smoke cartridge used for all experiments described herein was the Model 3C Superior Smoke, manufactured by Superior Signal Co. of Spotswood, NJ.

After being installed in the hollow blade tip, the smoke cartridge was ignited remotely at the start of each test, by passing modest currents through resistance wire igniters. Subsequently, the smoke cartridge typically burned for one to two minutes, and provided approximately 1,133 cubic meters of gray-white smoke. Smoke was ejected from the interior of the hollow blade tip and into the tip vortex through three ports (approx. 1 mm in diameter) located on the pressure surface of the blade tip. The hollow aluminum blade tip, with smoke cartridge installed, is shown in Figure J-1.

Figure J-1. Hollow aluminum blade tip with smoke generating cartridge installed

Test Section Lighting

To allow video imaging of the vortex wake thus visualized, the smoke needed to be strongly illuminated against a dimly lit background. Illumination of the visualized wake was provided by the mercury vapor lamps normally present in the ceiling of the wind tunnel test section. Prior to testing, the detritus fouling the lamp lenses was removed, considerably increasing light intensity in the test section. To attenuate background lighting, the mercury vapor lamps in the rows nearest the test section side walls were unplugged, leaving the four central rows of lights to illuminate the test section. In addition, a mercury vapor lamp mounted on a cart was positioned on the tunnel centerline, approximately 21.3 m downstream of the turbine, with the light beam directed downstream and upward at an elevation angle of approximately 45°.

Video Cameras and Lenses

Video images of the illuminated smoke visualization were simultaneously acquired from cameras placed at two locations. One camera was located in the test section ceiling, and was 5.88 m upstream of the tower axis and 2.93 m west of the test section centerline. The other camera was mounted in the east wall of the test section, and was 12.41 m downstream of the tower axis and 1.92 m above the test section centerline.

To facilitate later analyses, the video images from the two cameras were superimposed on the same frame using a video multiplexer. Each camera was aimed to place the wake in the frame such that, when superimposed on the same frame, the two images did not overlap. These camera locations also were advantageous in that the wake was recorded in both the horizontal and vertical planes, and because photogrammetric analyses of the imagery could be carried out at a later time if desired.

The video camera mounted in both the ceiling and wall locations was a Panasonic WV-BL734 ½" CCD black and white video camera. To achieve the wide field of view required, extremely short focal length lenses were employed. The same lens was used on both cameras, a Computar CS

mount 2.6 mm lens (model # H2616FICS-3). Used in conjunction with the WV-BL734, this lens provided a 128° x 98° field of view. However, wide field of view was obtained at the expense of considerable distortion. To enable subsequent removal or compensation for this distortion, the cameras and lenses were calibrated by acquiring video of a planar square grid (1.3 mm (½ in.) grid spacing) at a range of approximately 0.152 m (6 in.).

In addition to the video imagery acquired as described above, video was shot using a hand-held camera with a low distortion lens. Finally, photographs also were taken using a digital still camera, also using a low distortion lens. A typical digital photograph of the turbine wake is shown in Figure J-2.

Figure J-2. Typical photo of wake flow visualization taken with digital still camera

Appendix K: Transition Fixed: Sequence M

During the "Transition Fixed" sequence, boundary layer transition was fixed by applying self-adhesive zigzag turbulator tape of various thicknesses to the upper and lower surfaces of the instrumented blade shown in Figure K-1. The dimensions and placement of the turbulator tape are described by Selle (1999). All turbulator tapes used in this experiment employed a geometry like that shown in Figure K-2, having 60° sweep angles and extending 12 mm from leading edge to trailing edge. The tapes were installed from 25% span (outboard boundary of the blade root cross-section transition), to 98% span (inboard boundary of the blade tip cap). On the upper surface, the trailing edge of the tape was positioned at 2% chord; and on the lower surface, the trailing edge of the tape was located at 5% chord. To avoid influencing pressure measurements at the five full-chord pressure tap locations, application of the tape was interrupted a distance of 6.35 mm as shown in Figure K-3.

Figure K-1. Turbine configuration for sequence M

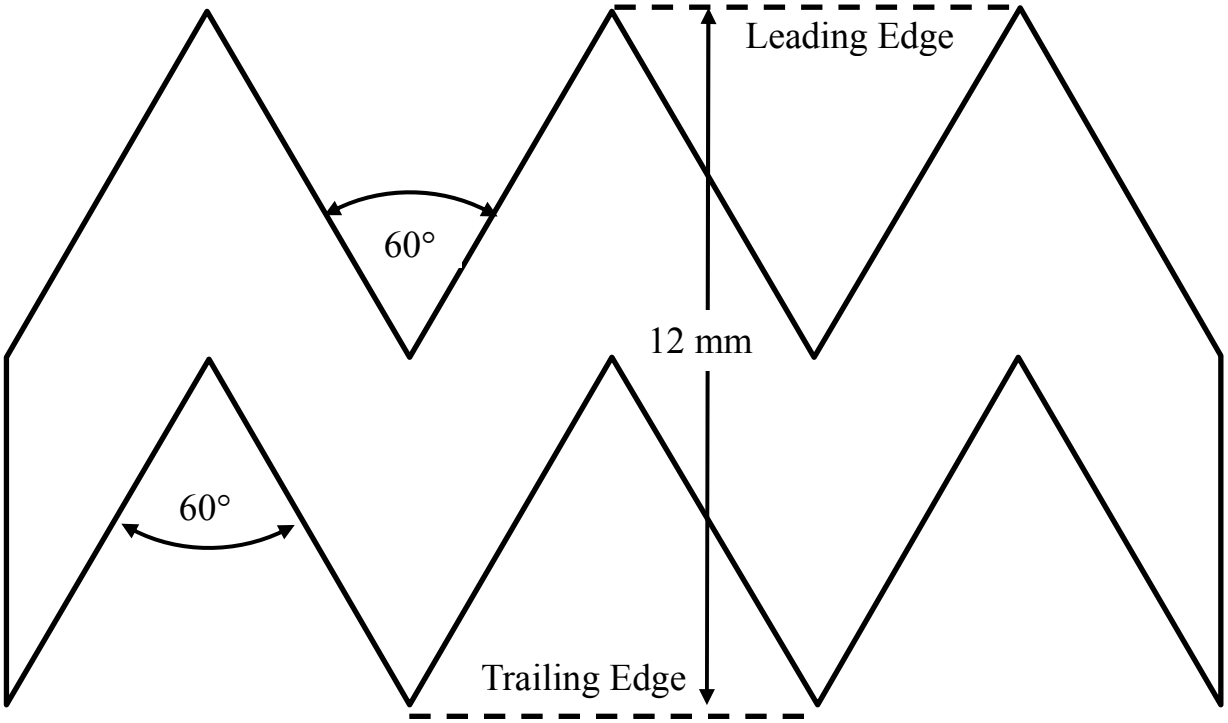

Figure K-2. Zigzag turbulator tape geometry

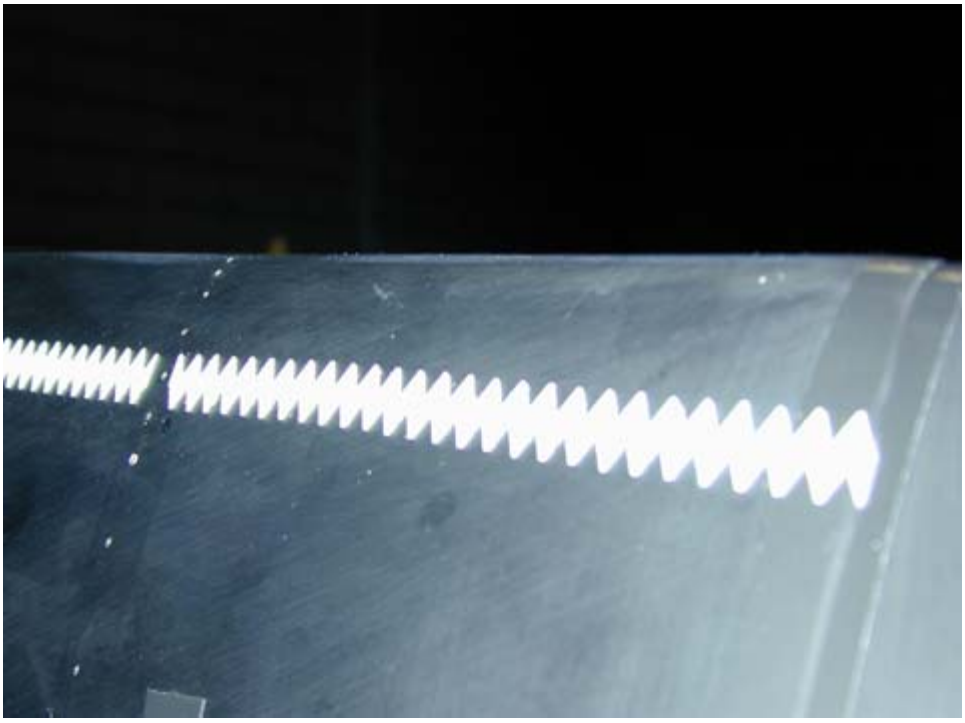

Figure K-3. Zigzag tape installed near pressure ports

Because local boundary layer depth on the blade decreased for span stations farther outboard, zigzag tape thickness decreased in similar fashion. Zigzag tape thicknesses and blade radius

ranges are documented in Table K-1. All zigzag tapes used in these experiments were obtained from Glasfaser-Flugzeug-Service, Hofener Weg, D-72582 Grabenstetten, Germany (http://www.streifly.de).

Table K-1. Zigzag Tape Radial Range and Thickness

Upper Surface	
r/R	**Tape Thickness**
0.25 to 0.40	0.85 mm
0.40 to 0.80	0.51 mm
0.80 to 0.98	0.31 mm

Lower Surface	
r/R	**Tape Thickness**
0.25 to 0.80	0.95 mm
0.80 to 0.98	0.65 mm

References

Selle, J. (1999). *Study on the effectiveness of turbulator tape on boundary-layer transition.* Research Report. Davis, CA: University of California at Davis.

Index

The page number of indexed figures or tables is italicized.

accelerometers, 35, 123, *124*, *125*
  calibration of, 41, 123
  signal conditioning, 149
aerodynamic power. *See* power.
aerodynamic tare, 234, 237, 285
air density, 231, 233, 273
analog / digital conversion, 154
angle of attack. *See* local flow angle.
atmospheric pressure, 26, 44, 96, 272, 278, 279

balance system, *4*, 36, *37*, 59, 99, 226, 236, 237, 251
blade
  airfoil. *See* S809 airfoil
  design & fabrication, 12
  dimensions, *12*, 63, *64*, *66*
  direction of rotation, 8, 62
  extension, 12, 22, 66, *67*, 75
  mass and stiffness, 75, *76*
  smoke tip, 12, 20, 66, *67*, 291
  surface pressure. *See* pressure taps.
  tip plate, 12, *13*, *14*, 21, 66, *68*, 75
blade surface pressure
  normalization of, 33, 47
blockage, 6

calibration, 15, 33, 41, *158*, 160, *161*, 162, 163, 164
  after downwind to upwind configuration transition, 8
  anemometers, 94, 105, 246, 255, 270, 282
  balance system, 99
  barometer for field test, 278
  five-hole probes, 136
  load cells, 108, 110, 112
  Mensor digital differential pressure transducer, 16, 144
  position encoders, 130, 133
  pressure transducers, 26, 32, 96, 137, 244, 247, 249, 253, 256, 258
  servo-electric motor, 127
  strain gauges, 114, *117*
  temperature, 101, 252
  watt transducer, 126
calibration coefficient database, 42, 43, 169
centrifugal force correction, 33, 46, 274
cone angle, *58*
  adjustment of, 8, *10*
  computation of, 57

data acquisition
  hardware, 41
  NASA system, 7, 220
  NREL system, 6, *7*
  procedure, 15
  software, 42
data processing, *159*
data validation, 15
digital input / output, 154
downwind to upwind configuration transition, 8
drivetrain, 10, *11*, 79, *80*
dynamic pressure, *47*
  blade, 46
  five-hold probe, 46
  wind tunnel, 44, 230–232, 241

error byte, 43

file name convention, 15, 269
filters, 41, 153
five-hole probes, 27, *28*, *30*, 75
  calibration of, 136
  dynamic effects of, 32
  flow angles, 55, *56*
  measurement out of range, *49*, *50*
  plugs, 12
flow visualization. *See* wake flow visualization.

Gill port, 16, 33, 45, See also reference pressure.

header file. *See* calibration coefficient database.
hub, 8, 9, *10*, 62
hydrostatic pressure correction, 33, 44, 45, 253–259, 273

load cells, *36*
  calibration of, 42, 108, 110, 112
  teeter damper, 35, 110, *111*
  teeter link, 35, 108, *109*
  yaw moment, 35, *36*, 112, *113*
local flow angle, 55, *56*

low-speed shaft strain gauges. *See* strain gauges

modal frequencies
  blade, 77, *79*
  turbine, 88, *89*, *90*, *91*, *92*

NASA Ames Research Center, 3
NASA data acquisition system, 7, 220, 242
NASA instrumentation, 7, 94, 96, 98, 99, 101, 240, *241*, 242, 249
  signal conditioning, 148
normal force coefficient, *51*, *52, 53*
normalization pressure. *See* blade surface pressure coefficients.

outdoor
  air temperature, *25*, 101, 225, 252, 274
  wind speed and direction, 25, 94, 225, 272, 274

PCM encoding, 34, 41, 155, *156*
pitch control
  blade, 36, 127, *128*
  signal conditioning, 152
pitch shaft, *9*, *12*, 34, *78*
pitching moment coefficient, 51, *52*, *53*
position encoders, *39*
  blade azimuth angle, 37, *38*, *131*, *132*
  blade flap angle, 37, 38, *39*, 133, *134*, *135*
  blade pitch angle, 37, *38*, *131*
  calibration of, 41, 130, 133
  turntable, 39, 98, 250
  yaw, 37, *132*
post-processing, 43, 157, 164
power
  generator, 36, 62, 126, 150
  rotor, 58, *59*
power enclosure, *129*
pressure coefficients, 47
pressure system controller, 34
pressure taps, 29, *30*, *31*, *138*
  dynamic effects of, 32
pressure transducer, 15, *26*, *27*, 32, 33, 45, 136, 139–142
  calibration of, 42, 137, 144, 247, 249
  location of, 26, 27, 29, 33, 34, *142*
  Mensor digital differential,33, 44, *45*,144, *145*, 254, 273
  temperature drift of, 15
  wind tunnel, 26
  wall pressure. *See* wall pressure.
PSC enclosure, 26, 32, 33, *145*, 254

reference pressure, 33, 253
root flap bending moment
  estimated, 54
  strain gauges. *See* strain gauges.
rotor brake, 11
rotor inertia, 80, 81, *82*
rotor lock, 11, 18, 19, 86, *88*
rotor speed, 57, *58*, 62, 272

S809 airfoil, 12, 64, *65*
  2-D wind tunnel aerodynamic coefficients, *69*, *70*, *71*, *72*, *73*, *74*
servo-electric motor. *See* pitch control.
signal conditioning, 41, 148–153
sonic anemometers
  field test, 272
  for test section speed, 5, *6*, 14, 15, 25, *26*, *58*, 103, *104*, *106*, *107*
  for wake measurements, 24, 26, *262*, *263*, 266
spanwise flow angle, 55, *56*
static pressure
  pitot probe mounted to turbine, 22, *29*, 33, 45, 273
  wind tunnel, 44, 45, 96, 225, 230, 232, 247, *248*, 249
strain gauges, *34*
  blade root, 34, 114, *117*, *118*, *119*
  calibration of, 42, 114, *117*
  low-speed shaft, 34, 58, *59*, 120, *121*, *122*
  signal conditioning, 151
  yaw moment
    for field test, 273, *280*

tangential force coefficient, 51, *52*, *53*
teeter angle, 57, *58*
temperature, 25, 101, 225, 230–233, 252, 272
test matrix, 13, *14*, *177–217*
test section speed, 3, *6*, 231, 233
  wind tunnel measurement of, 5, 26, 44
thrust
  estimated aerodynamic, 53, *54*
thrust coefficient, 52, *53*
time code generator, 39, *40*, 146, *147*
torque
  estimated aerodynamic, 53, *54*
torque coefficient, 52

total pressure, 44, 96, 225, 226, 230, 232, 247, 249, *248*
tower, *5*, 11, 86, *87*
  shroud, 86, *88*
tower shroud, 23
tunnel scale system. *See* balance system.
turbine control, *7*, 8
turbine description, 8, *9*, 62
turntable. *See* position encoders.

wake
  flow visualization, *7*, 20, 291–293
  instrumentation boom & enclosures, 47, *48, 49*
  measurements, 260–271
wall pressure, 6, 226–229, 240, 244, *245*
  calibration of
    transducers, 244
weight tare, 234, 237, 281

yaw angle. *See* position encoders.
yaw brake, 10, *11*
yaw drive, 10, *11*, 86
yaw error, 57, *58*, 274
yaw moment, 10, 35, *36*
yaw sweep, 17, 18, 21

zigzag tape, 18, 294, *295*, *296*

REPORT DOCUMENTATION PAGE

Form Approved
OMB NO. 0704-0188

1. AGENCY USE ONLY (Leave blank)	2. REPORT DATE	3. REPORT TYPE AND DATES COVERED
	December 2001	Technical Report

4. TITLE AND SUBTITLE
Unsteady Aerodynamics Experiment Phase VI: Wind Tunnel Test Configurations and Available Data Campaigns

5. FUNDING NUMBERS
WER1.1110

6. AUTHOR(S)
M.M. Hand, D.A. Simms, L.J. Fingersh, D.W. Jager, J.R. Cotrell, S. Schreck, S.M. Larwood

7. PERFORMING ORGANIZATION NAME(S) AND ADDRESS(ES)

8. PERFORMING ORGANIZATION REPORT NUMBER

9. SPONSORING/MONITORING AGENCY NAME(S) AND ADDRESS(ES)
National Renewable Energy Laboratory
1617 Cole Blvd.
Golden, CO 80401-3393

10. SPONSORING/MONITORING AGENCY REPORT NUMBER
NREL/TP-500-29955

11. SUPPLEMENTARY NOTES

12a. DISTRIBUTION/AVAILABILITY STATEMENT
National Technical Information Service
U.S. Department of Commerce
5285 Port Royal Road
Springfield, VA 22161

12b. DISTRIBUTION CODE

13. ABSTRACT *(Maximum 200 words)*
The primary objective of the unsteady aerodynamics experiment was to provide information needed to quantify the full-scale, three-dimensional aerodynamic behavior of horizontal-axis wind turbines. This report is intended to familiarize the user with the entire scope of the wind tunnel test and to support the use of the resulting data.

14. SUBJECT TERMS
Unsteady aerodynamics experiment, NASA Ames Wind Tunnel, horizontal-axis wind turbines

15. NUMBER OF PAGES

16. PRICE CODE

17. SECURITY CLASSIFICATION OF REPORT	18. SECURITY CLASSIFICATION OF THIS PAGE	19. SECURITY CLASSIFICATION OF ABSTRACT	20. LIMITATION OF ABSTRACT
Unclassified	Unclassified	Unclassified	UL